CORA Cork Open Research Archive
Cartlann Taighde Oscailte Chorcaí

Title	The role of regulatory T cells in stroke recovery
Authors	Malone, Kyle
Publication date	2022-06-16
Original Citation	Malone, K. 2022. The role of regulatory T cells in stroke recovery. PhD Thesis, University College Cork.
Type of publication	Doctoral thesis
Rights	© 2022, Kyle Malone. - https://creativecommons.org/licenses/by-nc-nd/4.0/
Download date	2026-11-12 06:21:19
Item downloaded from	https://hdl.handle.net/10468/13665

UCC
University College Cork, Ireland
Coláiste na hOllscoile Corcaigh

mOllscoil na hÈireann, Corcaigh

The National University of Ireland, Cork



University College Cork, Ireland
Coláiste na hOllscoile Corcaigh

The Role of Regulatory T Cells in Stroke Recovery

Thesis presented by

Kyle Malone, BPharm, MPharm

For the degree of

Doctor of Philosophy

Under the supervision of

Professor Christian Waeber and Dr. Anne Moore



School of Pharmacy
University College Cork

Head of School: Prof. Brendan Griffin

June 2022

Table of Contents

Declaration x

Publications and Presentations xii

List of Tables xv

List of Figures xvi

List of Abbreviations xxiv

Acknowledgements xxix

Thesis Abstract 1

Chapter 1 Introduction 3

1.1 Stroke 5

1.1.1 Animal Models of Brain Ischaemia 7

1.2 Stroke and the Immune System 9

1.2.1 Involvement of the Immune System in Acute Ischaemic Stroke 9

1.3 T Cells & Acute Ischaemic Stroke 16

1.3.1 T Cell Responses in Acute Ischaemic Stroke 16

1.3.2 T cell-targeted Immunotherapies in Stroke 19

1.4 Regulatory T Cells 20

1.4.1 Regulatory T Cell Biology 20

1.4.2 Regulatory T Cells in Animal Models of Stroke 23

1.4.3 Regulatory T Cells in Human Stroke 27

1.4.4 Mechanisms of Treg-mediated Neuroprotection in Stroke 28

1.4.5 Treg-targeted Immunotherapies in Stroke 32

1.5 Fingolimod 37

1.5.1 Fingolimod Pharmacology 37

1.5.2 Fingolimod in Animal Models of Stroke 39

1.5.3 Clinical Trials of Fingolimod in Human Stroke 42

1.5.4 The Effect of Fingolimod on Regulatory T Cells 44

1.6 Pregnancy-Specific Glycoproteins (PSGs) 45

1.6.1 PSG Pharmacology 45

1.6.2 The Effect of PSGs on Regulatory T Cells 45

1.7 Thesis Hypothesis, Aims, & Objectives 46

1.7.1 Hypothesis 46

1.7.2 Aims 46

1.7.3 Objectives 46

Chapter 2 The effect of fingolimod on regulatory T cells in a mouse model of brain ischaemia 49

2.1 Introduction 52

2.2 Methods 54

2.2.1 Ethics Statement 54

2.2.2 Mice 55

2.2.3 Ischaemia Model 56

2.2.4 Fingolimod Treatment 57

2.2.5 Neurological Deficit Evaluation 58

2.2.6 Tissue Collection and Processing 58

2.2.7 Flow Cytometric Analysis 59

2.2.8 Immunohistochemistry 60

2.2.9 Statistical Analysis 61

2.3 Results 65

2.3.1 Fingolimod increases Treg frequency in murine spleen and blood post-pMCAO 65

2.3.2 Age has a major impact on peripheral Treg frequencies in lymph nodes at baseline and at 7 days post-pMCAO 66

2.3.3 Extending fingolimod treatment duration from 5 days to 10 days post-pMCAO increased Treg frequencies in lymph nodes 68

2.3.4 Fingolimod increases FoxP3+ cell infiltration into the brain post-pMCAO .. 69

2.3.5 Fingolimod produces profound lymphopenia and causes a re-distribution of T cells in mice post-pMCAO 71

2.3.6 Fingolimod decreases the ratio of CD4+ to CD8+ T cells in mice post-pMCAO 79

2.3.7 Improvement in fingolimod-treated mice at 7 days post-pMCAO correlated with higher CD8+ T cell frequency, lower CD4+T cell frequency, and lower Treg frequency in the periphery. 80

2.4 Discussion 83

2.5 Conclusion 90

Supplementary material related to chapter 2 92

Chapter 3 The Impact of Fingolimod on Treg Function in Brain Ischaemia 101

3.1 Introduction 104

3.2 Methods 106

3.2.1 Materials 106

3.2.2 Mice 106

3.2.3 Ischaemia Model 107

3.2.4 Fingolimod Treatment 108

3.2.5 Neurological Deficit Evaluation 108

3.2.6 Tissue Collection and Processing 108

3.2.7 Flow Cytometric Analysis 109

3.2.8 Isolation of Tregs from Post-Ischaemic Spleen 110

3.2.9 Treg Suppression Assay 112

3.2.10 Statistical Analysis 113

3.3 Results 114

3.3.1 Fingolimod attenuates neurobehavioural deficits post-pMCAO 114

3.3.2 Fingolimod increases the frequency of CCR8+ Tregs in spleen, blood, lymph nodes, and brain post-pMCAO 114

3.3.3 Fingolimod enhances secretion of IFN-γ, IL-17, and IL-10 by CD4+ T cells post-pMCAO 118

3.3.4 Fingolimod treatment rescues Treg suppressive function against saline-treated but not fingolimod-treated Tconv cells. 123

3.4 Discussion 127

3.5 Conclusion 134

Supplementary material related to chapter 3 135

Chapter 4 Recombinant pregnancy-specific glycoprotein-1-Fc reduces functional deficit in a mouse model of permanent brain ischaemia 136

4.1 Introduction 139

4.2 Methods 140

4.2.1 Ethics Statement 140

4.2.2 PSG Protein Production 141

4.2.3 Mice 142

4.2.4 Ischaemia Model 142

4.2.5 Neurological Deficit Evaluation 143

4.2.6 Tissue Collection and Processing 144

4.2.7 Infarct Size Measurement 144

4.2.8 Flow Cytometric Analysis 145

4.2.9 Immunohistochemistry (CD3, FoxP3, ICAM) 146

4.2.10 Immunofluorescence (Iba-1) 148

4.2.11 Determination of TGF-β1 in Spleen by ELISA 149

4.2.12 Statistical Analysis 150

4.3 Results 150

4.3.1 rPSG1-Fc significantly improves neurobehavioural recovery post-pMCAO without impacting infarct size 150

4.3.2 rPSG1-Fc increases circulating CD4+ CD25+ and CD4+ FoxP3+ T cell frequencies but does not increase CD4+CD25+Foxp3+ Treg frequency in the periphery post-pMCAO 151

4.3.3 rPSG1-Fc increases FoxP3+ cell infiltration into the brain post-pMCAO 154

4.3.4 rPSG1-Fc increases the secretion of IL-10 and downregulates the production of IFN-γ and IL-17 154

4.3.5 rPSG1-Fc reduces activated microglia in the infarct core of post-ischaemic mice 157

4.3.6 rPSG1-Fc does not influence ICAM-1 expression in post-pMCAO brain tissue 160

4.3.7 rPSG1-Fc treatment does not increase TGF-β1 expression in spleen post-ischaemia 160

4.4 Discussion 164

4.5 Conclusion 169

Supplementary material related to chapter 4 171

Chapter 5 Regulatory T Cell Frequency is Acutely Increased in Mild Ischaemic Stroke Patients 177

5.1 Introduction 180

5.2 Methods 182

5.2.1 Ethics Statement 182

5.2.2 Patients and Controls 182

5.2.3 PBMC Isolation and Cryopreservation 183

5.2.4 Quantification of Treg Frequency and Function by Flow Cytometry 184

5.2.5 Flow Cytometry Data Analysis 185

5.2.6 Quantification of Plasma Cytokines by Multiplex Assay 186

5.2.7 Statistical Analysis 187

5.3 Results 194

5.3.1 Study Cohort 194

5.3.2 Stroke reduces CD3+ T cell frequency without affecting the relative proportion of CD4+ or CD8+ subsets 195

5.3.3 Stroke increases B cell frequency at 24 hours post-ischaemia 195

5.3.4 Stroke acutely decreases intermediate monocyte frequency while increasing classical monocyte frequency 199

5.3.5 Stroke increases circulating Treg frequency 201

5.3.6 Stroke transiently enhances markers of Treg suppressive activity 201

5.3.7 Stroke increases proliferating Tregs (Ki67+ Tregs) and the frequency of PD-1/CTLA-4+ Ki67+ Tregs at 24 hours post-ischaemia 203

5.3.8 IL-4 and IL-5 are significantly increased at 7 days post-ischaemia 205

5.4 Discussion 207

5.5 Conclusion 213

Supplementary material related to chapter 5 214

Chapter 6 General Discussion 219

6.1 Overview and summary of key findings 220

6.2 Interpretation of key findings 222

6.2.1 Mild stroke acutely increases Treg frequency and function, but these cells do not play a major role in the early stages of recovery 222

6.2.2 Fingolimod and rPSG1-Fc impact Tregs and this mechanism may contribute to improvements in functional recovery 224

6.2.3 The inconsistent neuroprotection observed with fingolimod in experimental stroke may stem from a promotion of both pro and anti-inflammatory T cell phenotypes 226

6.3 Strengths and Limitations 227

6.4 Implications for Future Research 230

6.5 Conclusion 232

Bibliography: 234

Appendix I: Materials & Reagents 268

Declaration

This is to certify that the work I am submitting is my own (except where duly noted and acknowledged) and has not been submitted for another degree, either at University College Cork or elsewhere. All external references and sources are clearly acknowledged and identified within the contents. I have read and understood the regulations of University College Cork concerning plagiarism and intellectual property.

Author Contribution

All work was performed independently by the author, with the following exceptions:

Chapter 2

Ms. Andrea Diaz and Dr. Jennifer Shearer performed permanent brain ischaemia surgery model. Dr. Jennifer Shearer stained and quantified brain tissue histology via H & E/NeuN.

Chapter 3

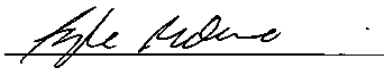
Dr. Jennifer Shearer performed permanent brain ischaemia surgery model. Dr. Jennifer Shearer stained and quantified brain tissue histology via H & E/NeuN.

Chapter 4

Dr. John Williams prepared PSG1-Fc protein Dr. Jennifer Shearer performed permanent brain ischaemia surgery model, stained and quantified brain tissue histology via H & E/NeuN, and assisted in TGF-β1 quantification via ELISA.

Chapter 5

Dr. Aine Merwick recruited study participants and, in the case of stroke in-patients, recorded relevant clinical data. Ms. Deirdre Flynn, Ms. Fionnuala O'Brien, Ms. Amy Stone, and Ms. Jennifer Connolly collected blood samples. Dr. Jennifer Shearer assisted in PBMC isolation.

Signed:  Date: June 16th, 2022

Publications and Presentations

Peer-reviewed publications associated with this thesis

Chapter 1

1. **Malone K**, Amu S, Moore AC, Waeber C. The immune system and stroke: from current targets to future therapy. Immunol Cell Biol. 2018;97(1):5-6.

2. **Malone K**, Amu S, Moore AC, Waeber C. Immunomodulatory Therapeutic Strategies in Stroke. Front Pharmacol. 2019; 10:630.

3. Diaz AC, Shearer JA, **Malone K**, Waeber C. Acute Treatment with Fingolimod Does Not Confer Long-Term Benefit in a Mouse Model of Intracerebral Haemorrhage. Front Pharmacol. 2020; 11:613103.

Chapter 2

4. **Malone K**, Diaz A, Shearer J, Moore AC, Waeber C. The Effect of Fingolimod on Regulatory T Cells in a Mouse Model of Brain Ischaemia. Journal of Neuroinflammation. 2021; 18(1):37.

5. Diaz AC, **Malone K**, Shearer JA, Moore AC, Waeber C. Histological, behavioural and flow cytometric datasets relating to acute ischaemic stroke in young, aged and $ApoE^{-/-}$ mice in the presence and absence of immunomodulation with fingolimod. Data in Brief. 2021; 36:107146.

6. Diaz AC, **Malone K**, Shearer JA, Moore AC, Waeber C. Preclinical Evaluation of Fingolimod in Rodent Models of Stroke with Age or Atherosclerosis as Comorbidities. Frontiers in Pharmacology. 2022; 13:920449.

Chapter 3

7. **Malone K**, Shearer JA, Waeber C, Moore AC. The Impact of Fingolimod on Treg Function in Brain Ischaemia. *Submitted to Journal of Neuroimmune Pharmacology.*

Chapter 4

8. **Malone K**, Shearer JA, Moore AC, Moore T, Waeber C. Recombinant pregnancy-specific glycoprotein-1 reduces functional deficit in a mouse model of permanent brain ischaemia. *Submitted to Brain, Behaviour, and Immunity.*

Chapter 5

9. **Malone K**, Shearer JA, Kelly A, Moore AC, Merwick A, Waeber C. Regulatory T Cell Frequency is Acutely Increased in Mild Ischaemic Stroke Patients. *Draft Publication.*

Other peer-reviewed publications

1. Amu S, **Malone K**. Flow Cytometry and Stroke: From Current Methodology to Future Applications. Neural Regen Res. 2022 Aug;17(8):1748-1750.

2. Trench F, **Malone K**, Waeber C. An analysis of the reporting of flow cytometric results in peer-reviewed research articles. *Draft Publication.*

Conference Presentations

1. **Malone K**, Kruschel R, McCarthy F, Waeber C. A fluorescence-based assay of novel sphingosine kinase inhibitors. Oral presentation at All-Ireland School of Pharmacy Conference, Trinity College Dublin, Ireland, April 17th, 2019.

2. **Malone K**, Diaz A, Shearer J, Moore AC, Waeber C. The Effect of Fingolimod on Regulatory T Cells in a Mouse Model of Brain Ischaemia. Oral Presentation at Irish Association of Pharmacologists Annual General Meeting, National University of Ireland, Galway, November 30th, 2019.

3. **Malone K**, Diaz A, Shearer J, Moore AC, Waeber C. The Effect of Fingolimod on Regulatory T Cells in a Mouse Model of Brain Ischaemia. Oral Presentation at New Horizons Conference, University College Cork, December 5th, 2019.

4. **Malone K**, Diaz A, Shearer J, Moore AC, Waeber C. Fingolimod Increases Regulatory T Cells in a Mouse Model of Brain Ischaemia. Poster Presentation at Irish Institute of Clinical Neuroscience meeting (online), October 1st, 2020.

5. **Malone K**, Diaz A, Shearer J, Moore AC, Waeber C. The Effect of Fingolimod on Regulatory T Cells in a Mouse Model of Brain Ischaemia. Poster Presentation at Stroke Immunology Conference, Munich (online), March 3rd, 2021.

6. **Malone K**, Diaz A, Shearer J, Moore AC, Waeber C. Fingolimod Increases Regulatory T Cells in a Mouse Model of Brain Ischaemia. Poster Presentation at Targeting Therapeutics for Brain Disorders, University College Cork (online), June 2nd, 2021.

7. **Malone K**, Kelly A, Shearer J, Moore AC, Merwick A, Waeber C. Changes in Treg Frequency and Function in Ischaemic Stroke Patients. Poster Presentation at Irish Association of Pharmacologists Annual General Meeting, University Limerick, November 5th, 2021.

List of Tables

Table S2.1: Detailed breakdown of number of mice excluded pre-surgery, mid-surgery for serious uncontrollable haemorrhage, or post-surgery for reaching a humane endpoint.

Table 5.1: Antibodies employed in Treg panel.

Table 5.2: Antibodies employed in PBMC panel.

Table 5.3: Cell Populations evaluated by flow cytometry panels.

Table 5.4: Participant demographics and clinical information.

List of Figures

Figure 1.1: Schematic representation of the blood–brain barrier (BBB) under healthy conditions and during its early breakdown following stroke.

Figure 1.2: Immune response to stroke.

Figure 1.3: A time course of immune targets and proposed immunomodulatory therapies in stroke.

Figure 1.4: Thesis outline.

Figure 2.1: Gating strategy for determination of Treg frequency.

Figure 2.2: Representative immunohistochemistry images of CD3+ and FoxP3+ staining in the infarct core of young mice post-pMCAO.

Figure 2.3: Frequency of CD4+ CD25+ FoxP3+ T cells in the blood and secondary lymphoid tissue across three individual mouse cohorts of brain ischaemia as a result of fingolimod treatment.

Figure 2.4: Effect of pMCAO on the frequency of CD4+ CD25+ FoxP3+ T cells in blood and secondary lymphoid tissue of young and aged mice

Figure 2.5: Frequency of CD4+ CD25+ FoxP3+ T cells in blood and secondary lymphoid tissue in response to short-term and long-term fingolimod treatment post-brain ischaemia in young mice.

Figure 2.6: Total CD3+ and FoxP3+ cell counts in the infarct core and peri-infarct zone of mice post-pMCAO.

Figure 2.7: Frequency of CD3+ T cells in blood and secondary lymphoid tissue at 7 days post-pMCAO in young, aged, and ApoE-/- mice following saline/fingolimod treatment

Figure 2.8: CD3+ T cell frequency, CD4+ T cell frequency, CD8+ T cell frequency, and CD4+/CD8+ ratio in blood and secondary lymphoid tissue in response to short-term and long-term fingolimod (FTY720) treatment post-brain ischaemia in young mice.

Figure 2.9: CD3+ T cell counts at 7 days post-pMCAO in spleen, cervical lymph nodes, blood, and inguinal lymph nodes in young, aged, and ApoE-/- mice following saline/fingolimod treatment, as well as in young mice receiving either short-term (5 days) or long-term (10 days) fingolimod treatment.

Figure 2.10: Correlation matrix between the proportion of T lymphocytes and experimental outcomes.

Figure S2.1: Comparison of neurological deficit score, total checklist neuroscore, and mouse weight between sham, young and aged mice.

Figure S2.2: Comparison of neurological deficit score in young male and female mice, and aged male and female mice.

Figure S2.3: Effect of sex and pMCAO on the frequency of CD4+ CD25+ FoxP3+, CD3+, CD4+, and CD8+ T cells in spleen of young and aged mice.

Figure S2.4: t-Distributed stochastic neighbour embedding (t-SNE) plot showing clusters and annotations of spleen cells obtained from young mice receiving either

saline, low dose (0.5 mg/kg) fingolimod treatment or high dose (1 mg/kg) fingolimod treatment post-pMCAO

Figure S2.5: t-Distributed stochastic neighbour embedding (t-SNE) plot showing clusters and annotations of spleen cells obtained from aged mice and ApoE-/- mice fed a high-fat diet (HFD) receiving either saline or fingolimod treatment post-pMCAO

Figure S2.6: t-Distributed stochastic neighbour embedding (t-SNE) plot showing clusters and annotations of spleen cells obtained from young mice receiving either saline, short-term (5 days) fingolimod treatment, or long-term (10 days) fingolimod treatment post-pMCAO

Figure S2.7: Correlation matrix between the proportion of T lymphocytes and experimental outcomes for young, aged, and ApoE-/- mice.

Figure S2.8: Correlation matrix between the proportion of T lymphocytes and experimental outcomes in young, aged, and ApoE-/- mice receiving either saline or fingolimod.

Figure 3.1: Gating strategy for determination of chemokine expression among Tregs, cytokine expression among CD4+ T cells, and cytokine expression among CD8+ T cells in representative mouse splenocytes post-brain ischaemia.

Figure 3.2: Pseudocolour plots depicting Treg and Tconv cells isolated from spleens of naïve, saline-treated, and fingolimod-treated mice.

Figure 3.3: Neurobehavioural and clinical outcome of mice post-stroke with or without fingolimod treatment.

Figure 3.4: Comparison of lesion size, ipsilateral/contralateral hemispheric volume ratio, and tissue loss between saline and fingolimod-treated mice.

Figure 3.5: Frequency of CD4+ CD25+ FoxP3+ T cells in blood, brain, and secondary lymphoid tissue in response to saline or fingolimod (0.5 mg/kg) treatment post-brain ischaemia in young mice.

Figure 3.6: Frequency of CCR5+, CCR6+, and CCR8+ CD4+CD25+Foxp3+ Treg cells in blood, brain, and secondary lymphoid tissue in response to saline or fingolimod (0.5 mg/kg)) treatment post-brain ischaemia in young mice.

Figure 3.7: Frequency of CD4+ IFN-γ+, CD4+ IL-17+, and CD4+ IL-10+ T cells in blood and secondary lymphoid tissue in mice treated with saline or fingolimod (0.5 mg/kg) post-brain ischaemia in young mice (t = 10 days) or in untreated, naïve, mice.

Figure 3.8: Frequency of CD8+ IFN-γ+, CD8+ IL-17+, and CD8+ IL-10+ T cells in blood and secondary lymphoid tissue in mice treated with saline or fingolimod (0.5 mg/kg) post-brain ischaemia in young mice (t = 10 days) or in untreated, naïve, mice.

Figure 3.9: The percentage of cytokine-producing cells in blood of naïve, saline treated, and fingolimod treated CD4+ and CD8+ T cells stained intracellularly for γγ, IL-17, and IL-10.

Figure 3.10: Suppressive capacity of Tregs and susceptibility of Tconv, isolated from naïve, saline-treated and fingolimod-treated mice.

Figure S3.1: Representative FACS pseudocolour plots depicting CD4+ CD25+ FoxP3+ T cells in spleen, blood, non-draining lymph nodes, draining lymph nodes,

Peyer's patches, and brain in naïve as well as saline and fingolimod-treated post-pMCAO mice.

Figure 4.1: Gating strategy for determination of Tregs, cytokine expression among CD4+ T cells, and cytokine expression among CD8+ T cells in representative mouse splenocytes 5 days post-brain ischaemia.

Figure 4.2: Comparison of ipsilateral/contralateral foot fault ratio as assessed by grid-walking test, total checklist score, and mouse weight between saline and rPSG1-Fc-treated mice.

Figure 4.3: Comparison of lesion size, ipsilateral/contralateral hemispheric volume ratio, and tissue loss between saline and rPSG1-Fc-treated mice as quantified by NeuN staining.

Figure 4.4: Frequency of CD4+ CD25+, CD4+ FoxP3+, and CD4+ CD25+ FoxP3+ T cells in blood and secondary lymphoid tissue in response to either saline or rPSG1-Fc treatment post pMCAO

Figure 4.5: Total CD3+ and FoxP3+ cell counts in the infarct core and peri-infarct zone of saline-treated and rPSG1-Fc -treated mice post-pMCAO

Figure 4.6: Frequency of CD4+ IFN-γ+, CD4+ IL-17+, and CD4+ IL-10+ T cells in blood and secondary lymphoid tissue in response to either saline or rPSG1-Fc treatment post-pMCAO.

Figure 4.7: Frequency of CD8+ IFN-γ+, CD8+ IL-17+, and CD8+ IL-10+ T cells in blood and secondary lymphoid tissue in response to either saline or rPSG1-Fc treatment post-pMCAO.

Figure 4.8: Total numbers of activated microglia and quiescent microglia in the core, peri-infarct zone, healthy ipsilateral tissue, and contralateral tissue of saline-treated and rPSG1-Fc -treated mice post-pMCAO.

Figure 4.9: Total ICAM-1 positive vessel length in the infarct core and peri-infarct zone of saline treated and rPSG1-Fc -treated mice post-pMCAO.

Figure 4.10: Total TGF-β1 in the spleens of saline and rPSG1-Fc-treated mice.

Figure S4.1: Representative images of NeuN stained brain sections from saline and rPSG1-Fc treated mice.

Figure S4.2: Representative immunohistochemistry images of CD3+, FoxP3+, and ICAM-1 staining in the peri-infarct zones of mice post-pMCAO.

Figure S4.3: Representative immunofluorescence images of Iba-1 staining in the core and peri-infarct zones of mice post-pMCAO.

Figure S4.4: Representative standard curve employed for the determination of TGF-β1 in spleen of saline-treated or rPSG1-Fc-treated mice post-pMCAO.

Figure S4.5: Representative FACS pseudocolour plots depicting CD4+ CD25+ FoxP3+ T cells, CD4+ IFN-γ+ T cells, CD4+ IL-17+ T cells, and CD4+ IL-10+ T cells in saline and rPSG1-Fc treated mice.

Figure S4.6: Total CD4+ FoxP3+ T cells in blood in response to either saline or rPSG1-Fc treatment post pMCAO.

Figure 5.1: Gating strategy for determination of Tregs, as well as expression of CTLA-4, PD-1, and CD39 among naïve, memory and proliferating Tregs in blood.

Figure 5.2: Representative FACS pseudocolour plots depicting key results from Treg panel in in stroke patients (at 24 hours (T1) and one week (T2) post-brain ischaemia) and age-matched controls.

Figure 5.3: Gating strategy for determination of immune cell subsets in blood.

Figure 5.4: Representative FACS pseudocolour plots depicting key results from PBMC panel in in stroke patients (n = 12) (at 24 hours (T1) and one week (T2) post-brain ischaemia) and age-matched controls (n = 9).

Figure 5.5: Frequencies of circulating T cells in stroke patients (at 24 hours and one-week post-brain ischaemia) and age-matched controls.

Figure 5.6: Frequencies of circulating CD4+ and CD8+ T cell subsets in in stroke patients (at 24 hours (T1) and one week (T2) post-brain ischaemia) and age-matched controls.

Figure 5.7: Frequencies of non-T cell lymphoid subsets in stroke patients (at 24 hours and one-week post-brain ischaemia) and age-matched controls.

Figure 5.8: Frequencies of monocyte and dendritic cells in stroke patients (at 24 hours and one-week post-brain ischaemia) and age-matched controls.

Figure 5.9: Frequencies of circulating Treg populations in stroke patients (at 24 hours and one-week post-brain ischaemia) and age-matched controls.

Figure 5.10: Frequencies of proliferating Tregs (Ki67+ Tregs), naive Tregs (nTregs) and memory Tregs (mTregs) within Treg population (CD4+CD127-CD25+FOXP3+) in stroke patients (at 24 hours (T1) and one week (T2) post-brain ischaemia) and age-matched controls.

Figure 5.11: Plasma concentrations of 12 cytokines in stroke patients (at 24 hours and one-week post-brain ischaemia) and age-matched control.

Figure S5.1: t-Distributed stochastic neighbour embedding (t-SNE) plot showing clusters and annotations of PBMCs cells obtained from humans (no stroke, stroke at 24 hours, stroke 7 days).

Figure S5.2: t-Distributed stochastic neighbour embedding (t-SNE) plot showing clusters and annotations of PBMCs cells obtained from humans (no stroke, stroke at 24 hours, stroke 7 days).

Figure S5.3: Plasma concentrations of 12 cytokines in stroke patients (at 24 hours and one-week post-brain ischaemia) colour coded by Day 0 Rankin Score.

Figure S5.4: Correlation between plasma concentrations of IL-9 and IL-17 in stroke patients at 24 hours post-brain ischaemia with admission modified Rankin Score.

Figure S5.5: Frequencies of Tregs in male vs. female stroke patients at 24 hours and one-week post-brain ischaemia) and age-matched controls.

List of Abbreviations

AIS	Acute ischaemic stroke
ANOVA	Analysis of variance
ADP	Adenosine diphosphate
APC	Antigen-presenting cells
ARRIVE	Animal Research: Reporting of In Vivo Experiment
ATP	Adenosine triphosphate
BBB	Blood brain barrier
BDNF	Brain derived neurotrophic factor
BMSC	Bone marrow derived stem cell
BSA	Bovine serum albumin
CAR	Chimeric antigen receptor
CCR5	C-C chemokine receptor type 5
CCR6	C-C chemokine receptor type 6
CCR8	C-C chemokine receptor type 8
CD	Cluster of differentiation
CNS	Central nervous system

CRP	C-reactive protein
CSP	Cerebrospinal fluid
CTLA-4	Cytotoxic T lymphocyte antigen 4
DAMP	Damage associated molecular pattern
DC	Dendritic cell
DMSO	Dimethyl sulfoxide
DNA	Deoxyribonucleic acid
EAE	Experimental autoimmune encephalomyelitis
ECM	Extracellular matrix
EDTA	Ethylenediaminetetraacetic acid
EGFR	Epidermal growth factor receptor
ELISA	Enzyme-linked immunosorbent assay
FACS	Fluorescence-activated cell sorting
FDA	Food and drug administration
FITC	Fluorescein isothiocyanate
FOXP3	Forkhead box protein 3
GITR	Glucocorticoid-induced tumour necrosis factor receptor-related receptor

HDAC	Histone deacetylase
HDL	High-density lipoprotein
HFD	High fat diet
ICAM-1	Intracellular adhesion molecule 1
ICH	Intracerebral haemorrhage
IFN	Interferon
IL	Interleukin
IQR `	Interquartile range
IR	Ischaemia-reperfusion
LAP	Latency-associated peptide
LDL	Low-density lipoprotein
LFA-1	Lymphocyte function-associated antigen 1
LPS	Lipopolysaccharide
MBP	Myelin basic protein
MCA	Middle cerebral artery
MCAO	Middle cerebral artery occlusion
MHC	Major histocompatibility complex

MMP-9	Matrix metalloproteinase 9
MS	Multiple sclerosis
NIHSS	National Institutes of Health stroke scale
NK	Natural killer
NO	Nitrous Oxide
PBMC	Peripheral blood mononuclear cell
PBS	Phosphate buffered saline
PD-1	Programmed cell death protein 1
PRR	Pattern recognition receptor
PSG	Pregnancy-specific glycoprotein
ROS	Reactive oxidative species
RT	Room temperature
S1P	Sphingosine-1-phosphate
SIID	Stroke-induced immunodepression
SIV	Simian immunodeficiency viruses
SSRI	Selective serotonin reuptake inhibitor
STAIR	Stroke Therapy Academic Industry Roundtable

TIA	Transient ischaemic attack
TGF	Tumour growth factor
TNF	Tumour necrosis factor
tSNE	t-distributed stochastic neighbour embedding
UV	Ultraviolet
VCAM-1	Vascular cell adhesion molecule 1
VLA-4	Very late antigen-4
WBC	White blood cells

Acknowledgements

I've thought of an ending for my book - "And he lived happily ever after... to the end of his days." – J.R.R. Tolkien

I am extremely grateful to the colleagues, friends, and family who have supported me in my PhD studies since 2017. Truly, I would not have been able to complete this thesis without your advice, encouragement, and generosity. Although I could never name everyone who made this thesis possible, a few people deserve special mention.

Firstly, I would like to thank my supervisors, Professor Christian Waeber and Dr. Anne Moore. From the moment this research was conceived, you have been a tireless source of support and guidance. Thank you for your insights, wisdom, encouragement, and patience. You have inspired me to become a better researcher, educator, and academic. I will always be indebted to you for the opportunities you have afforded me.

Next, I would like to thank my fellow researchers: Dr. Jennifer Shearer, Andrea Diaz, and Rasha Alshaikh. Jennifer, I doubt I could ever convey how grateful I am to you for sharing your technical expertise with me. You are a brilliant researcher, and an even better friend. I will hold onto fond memories of us discussing history, economics, and politics at the lab bench for years to come. Andrea, thank you for acting as a role model to me when I joined the pharmacology team. Your determination was only ever matched by your team spirit (and super-strength cups of coffee!). I wish you the very best of luck with your next adventure stateside. Rasha, thank you for your unending support, particularly over the last year. Although we were not fortunate to share more time together, I will always be grateful for your pointers on cell culture, thesis

structure, and the magical properties of Siponimod! I look forward to one day reading your own thesis.

Research would never be possible without the knowledge and goodwill of talented staff. To Dr. Sylvie Amu, thank you for giving me the best possible start on the flow cytometry path. Not one of these studies would have been achievable without you. To the School of Pharmacy staff, I am humbled to have shared this workplace with you. Since starting my undergraduate degree in 2012, you have supported me at every stage of my career. A special thanks to Aisha, Kathleen, Noreen, Tom, Ken, Áine and Michael for always rescuing me in times of need. Thanks to Linda McGuire, Professor Brendan Griffin, and Dr Rachel Moloney for your help with PT6401. I also owe thanks to the entire staffs of the Department of Pharmacology, Department of Biochemistry, and BSU for research support.

Thank you also to all those who collaborated, or participated, in this work. A special thanks to Dr. Aine Merwick, Dr. Tom Moore, Dr. Mary O'Connell, Dr. Florence McCarthy, Dr. Ryan Kruschel and the nursing team at CUH. I would like to thank the Irish Research Council for funding this work.

A major debt of gratitude is also owed to the students who helped make this research dream a reality. Thank you Stephanie Er, Lucia Pelloni, Graham Shaw, Rida Saqib, Valentina Davi, Eden Debebe, Fionnuala Trench and Adam Kelly. A quick shout out also to all the undergraduate students I had the joy of teaching.

During my write-up, I have also been lucky to work with the amazing staff at Turners Cross Pharmacy. Thank you Thérése, Niamh, Gráinne, Chantelle, Marian, Roarke, Colm, Conor, Julia, and Jean for your understanding and unflinching support.

xxx

I am blessed to have shared my PhD experience with a wonderful group of fellow researchers. Thank you, Kieran, Laura, Cian, Brian, Dominic, Ciarán, Gary, Jacinta, Harriet, Ziad, Conor, Colm, Seif, Emer, Adam, Olivia, Ayse, and all the other postgrads past and present at the SoP for walking the long road by my side.

Beyond the borders of work, I would also like to acknowledge family and friends who motivated me every step of the way. A special thanks to the Deerpark lads, the pharmacy gang, Bolt, Ember, and Paul and Constance for seeing me over the line. A shout out also to my brothers, Craig and Brandon, who've provided the best homegrown competition these last twenty-odd years. Thank you as well Noreen Crowley for all the home-cooked dinners and kind words of encouragement.

My last thanks I reserve for the three people without whom I'd never have reached this destination. To Mom and Dad, thank you for raising me to understand the value of hard work and education, and for always believing I could make it this far. No words can describe the gratitude I have for the support you've given me.

And finally, to Claire. For five years, you've been by my side on this PhD journey. From the day of acceptance, right down to these last moments, where we turn the page to a new chapter in our lives. I will always remember, and be grateful, for the unwavering support you have shown me. And for all the life we fit between these pages. The late-night coffees, the walks round the quad, the lengthy phone calls, and the lazy Sundays. The concerts, the holidays, and the Covid nightmare. The memories made, and the memories missed. Claire, you will not find the words of our story within this thesis, but it is all of it dedicated to you.

Thesis Abstract

Background: Acute ischaemic stroke is a major cause of mortality worldwide. Despite the search for new therapies, tissue plasminogen activator remains the only FDA-approved medication. The immune system is involved in all stages of stroke, from risk factors to pathogenesis and tissue repair. The presence of a lymphocyte subpopulation termed regulatory T cells (Tregs) appears to correlate with improved disease outcome. However, the impact of stroke on Tregs, and the contribution of these cells to stroke recovery remains under debate. Likewise, attempts at developing Treg-targeted immunotherapies have been hampered by high cost, toxicity, and the stability of expanded Tregs. The aim of this thesis was to explore the role Tregs play in ischaemic stroke recovery and evaluate the neuroprotective and immunomodulatory effects of two potential Treg-targeted stroke immunotherapies, namely fingolimod and recombinant pregnancy-specific glycoprotein-1 (rPSG1-Fc).

Methods: The effect of fingolimod on Tregs in a mouse model of permanent brain ischaemia was first investigated using a combination of flow cytometry and immunohistochemistry. Next, the impact of fingolimod on Treg suppressive function was characterised via Treg suppression assay. Following this, the immunomodulatory and neuroprotective properties of rPSG1-Fc in permanent brain ischaemia were determined. Finally, the changes in Treg frequency and function in the peripheral blood of mild stroke patients were quantified.

Results: Fingolimod increased peripheral Treg frequency in the post-ischaemic mouse. Fingolimod augmented brain infiltration of FoxP3+ T cells, possibly via CCR8 signalling. Fingolimod also enhanced the secretion of IFN-γ, IL-17, and IL-10 from

CD4+ T cells. Likewise, fingolimod promoted both suppressive and effector T cell function. rPSG1-Fc improved neurobehavioural recovery in mice post-brain ischaemia, possibly via increased CD4+IL-10+ T cells. Finally, an increased Treg frequency and an increased expression of functional markers of suppression (CTLA-4, PD-1) was observed in stroke patients at 24 hours post-ischaemia, and specifically among proliferating Tregs. However, by 7 days, the expression of PD-1/CTLA-4 among proliferating Treg frequency had returned to baseline.

Conclusions: This thesis has made a number of novel insights. A positive impact of fingolimod on both Treg frequency and function post-ischaemia was revealed. The observed dual effect of fingolimod on regulatory and pro-inflammatory T cell function may explain why the drug fails to consistently improve experimental stroke outcome. The immunomodulatory and neuroprotective effects of rPSG1-Fc post-stroke were also characterised for the first time. Finally, the impact of clinical stroke on Treg frequency and phenotype was comprehensively quantified. Overall, this thesis shows Tregs may not play a major role in the early stages of recovery of mild stroke, but therapies manipulating them can still promote functional recovery in a mouse model. It provides a basis for further study on Tregs in ischaemic stroke. It also illustrates rigorous methods by which researchers should test future Treg-targeted stroke immunotherapies.

Chapter 1

Introduction

In this introduction chapter, an overview of the literature related to regulatory T cells (Tregs) in ischaemic stroke recovery is provided. First, the scale of the morbidity and mortality associated with ischaemic stroke is highlighted. Next, the role of the immune system in post-stroke inflammation and subsequent repair is outlined. Specifically, the role Tregs have been shown to play in both animal and human stroke is explored, including references to potential mechanisms of Treg-mediated neuroprotection. Finally, a background to two potential Treg-targeted stroke immunotherapies (fingolimod, recombinant pregnancy-specific glycoprotein 1) is provided, including known effects these drugs have on Tregs.

Excerpts from this chapter appear in the following publications:

Malone K, Amu S, Moore AC, Waeber C. The immune system and stroke: from current targets to future therapy. Immunol Cell Biol. 2018;97(1):5-6.

Malone K, Amu S, Moore AC, Waeber C. Immunomodulatory Therapeutic Strategies in Stroke. Front Pharmacol. 2019; 10:630.

1.1 Stroke

Stroke is defined as a cerebrovascular disease involving prolonged reduction in blood supply to a part of the brain (1). Approximately 87% are ischaemic in nature, meaning a clot blocks blood flow to the brain. This clot typically forms in a blood vessel serving the brain, usually due to the rupture of a fatty plaque (or "atherosclerotic lesion"). The outcome is referred to as a thrombotic stroke. Conversely, if the clot travels from another place in the body, it is referred to as an embolic stroke. Separately, if a blood vessel in the brain ruptures (normally as a result of a ballooned blood vessel or "aneurysm"), the result is referred to as a haemorrhagic stroke. Haemorrhagic strokes, which can be subdivided into intracerebral haemorrhage (ICH) or subarachnoid haemorrhage, represents only 10-20% of stroke cases, but account for a disproportionately larger number of deaths worldwide (2). This thesis focuses on acute ischemic stroke (AIS).

In 2022, the number of people who died as a result of stroke reached nearly 6.5 million, making it the second-largest cause of death globally (3). It also stands as the most common cause of acquired disability, with roughly 100 million disability-adjusted life years (DALYs) lost annually in survivors (4). Even in the case of so-called "mild" stroke (modified Rankin Score (mRS) of 0-2) (5), 30% of patients have a poor functional outcome (mRS 2-6) at 90 days (6, 7). In the US, a stroke occurs every 40 seconds, and causes a death every 4 minutes (8). Among the 12.6 million survivors in Europe ~~t~~oday, 15-30% remain disabled, and 20% require institutional care after 3 months (3). Statistics are proportionally similar in Ireland, where direct expenditure on stroke accounts for 2-4% of total health costs, with absolute total costs of almost €500 million per year (9, 10). The lifetime risk of stroke has increased from 22.8% in

1990 to 24.9% in 2016 (11, 12). These trends have likely stemmed from a surge in stroke risk factors (13). Conventional non-modifiable risk factors include age, ethnicity, and sex, while modifiable risk factors include hypertension, obesity, diabetes mellitus, hyperlipidaemia, smoking, infection, and substance abuse. For many people, these predisposing factors present together, and overall are estimated to account for 60–80% of the stroke risk in the general population (14, 15). Symptoms of acute ischaemic stroke (AIS) range from loss of speech, to paralysis, to facial numbness and visual disturbances (16). Acute complications usually involve seizures, infection (e.g., pneumonia), or dysphagia. For stroke survivors, longer-term sequalae may include mobility issues, cognitive impairment, pain, fatigue, gastrointestinal disturbances, and poor mental health outcomes (17).

Given the high morbidity and mortality associated with AIS, there has been an intensive search for new therapeutic strategies. To date, however, the options for acute ischaemic stroke treatment are limited. Intravenous recombinant tissue plasminogen activator (rtPA) is the only FDA-approved medication (18). tPA can restore perfusion to the brain via thrombolysis and thereby prevent cell death in the hypoperfused but potentially salvageable area known as the ischaemic penumbra. However, beyond a therapeutic window of 4.5 hours, the benefits of tPA are outweighed by its risks, with the incidence of haemorrhagic transformation increasing dramatically (19). Only a small number of patients (<25%) therefore receive tPA (20, 21). Separately, mechanical thrombectomy is indicated for up to 6 hours after the onset of ischaemic stroke symptoms, though recent trials have allowed for an extension to 24 hours in selected patients (22). However intra-arterial thrombectomy with medical devices is not without its own complications and limitations (23). Additional agents for the

treatment of AIS are therefore urgently required, not only as adjuncts to increase the therapeutic potential of thrombolysis and thrombectomy, but also for patients who, for various reasons, cannot undergo these interventions. Ideally, such therapies, through curtailing damage to the brain post-stroke or contributing to long-term tissue remodelling, would improve patient survival and functional outcomes.

Over the last few decades, neuroprotection, i.e., the ability of a therapy to prevent neuronal cell death by inhibiting the pathogenetic cascade that results in cell dysfunction and eventual death, has been the main focus of proposed treatments in AIS. However, the field of brain-protective medicines remains a therapeutic graveyard, with over 1000 different molecules buried across hundreds of failed clinical trials (24). Yet, despite the poor clinical translation, important lessons have been learned. The role of immunity in all stages of stroke, for instance, is becoming better understood, with animal and human studies highlighting the immune system plays a pivotal and multifaceted role in central nervous system (CNS) injury (25). New candidate therapies have been suggested as a result.

1.1.1 Animal Models of Brain Ischaemia

Models of acute brain ischaemia can be performed in a variety of small and large animals including mice, rats, gerbils, rabbits, cats, dogs, pigs, sheep, and monkeys (26). While larger animals do provide an advantage in terms of being more suitable to receive sophisticated imaging and physiological monitoring during and after surgery, as well as displaying gyrencephalic brains, huge variability in the ischaemic injury itself is noted. As a result, smaller animals (in particular mice and rats) have become the mainstay of pre-clinical stroke research, with added benefits of low cost and genetic homogeneity. As mice have a long history of use in the field of immunology,

all of the animal studies described in this thesis employed mice to study aspects of the immune system in brain ischaemia (27). In mice, brain ischaemia models can be broadly divided into global; involving a reduction in cerebral blood flow throughout most or all of the brain and focal; involving a reduction in blood flow to a specific brain region, subtypes. However, focal brain ischaemia, in which blood vessels are blocked by mechanical occlusion or embolization approaches, is more relevant to the clinical presentation of AIS in humans than its global counterpart (which may be more relevant to, for example, the brain damage caused by cardiac arrest) (28). This thesis will therefore only describe a model of focal ischaemia. At present, such models encompass five subtypes: transcranial occlusion, endovascular filament middle cerebral artery (MCA) occlusion (MCAO), embolic occlusion, endothelin-1 occlusion, and photothrombotic occlusion. As the MCA is routinely implicated in ischaemic stroke (~50% of all cases) (29), almost all of these subtypes involve occluding this vessel, either proximally or distally. Embolic occlusion, which usually involves the injection of autologous blood clots or thrombin into the MCA, best mimics the natural "thromboembolism" that is observed in clinical stroke. Despite this, infarct location and volume can be highly variable. Low survival rates among mice made this model unsuitable for the current thesis (30). Separately, the endothelin-1 model was deemed unsuitable as a previous report in mice demonstrated injection of the peptide alone could not produce infarcted tissue (31). On the other hand, the photothrombotic model, which involves the injection of a photosensitive dye (rose bengal, erythrosin B) into circulation and then irradiation of the area, has low mortality and produces predictable lesions (32). However, the use of this model for studies with a translational interest is limited due to the systemic nature of the dye and the lack of a salvageable area of tissue (or "penumbra") (33).

The most common method of focal ischemic stroke is intraluminal thread occlusion (34). This proximal model involves introducing a filament into the internal carotid artery (ICA) and advancing it until it blocks the MCA. Depending on how long the filament is left in place, the model can produce both permanent and transient ischaemia, although the majority of reported uses (~90%) tend to be transient in nature (35). While well-suited to studies wherein larger lesions are desired, the filament model has severe animal welfare impacts (weight loss, abnormal motility, difficulty eating/drinking) (32). The fact that most patients do not successfully recanalize (36) has also led to the contention among stroke researchers that the use of transient middle cerebral artery occlusion (or "tMCAO") should be secondary to established transcranial models of permanent middle cerebral artery occlusion (pMCAO) (37). For all of these reasons, in this thesis, a permanent electrocoagulation model of distal middle cerebral artery occlusion was selected (38).

1.2 Stroke and the Immune System

1.2.1 Involvement of the Immune System in Acute Ischaemic Stroke

In the past, the brain was thought to be hidden from our immune system. This is in large part due to the lack of an obvious lymphatic system and the presence of a blood brain barrier (BBB). This barrier separates the blood compartment from the CNS at the level of brain endothelial cells and astrocytic end feet, thus rigorously controlling immune cell trafficking between the CNS and the periphery (39). Correspondingly, breakdown of this barrier may underlie the pathophysiology of immune-based CNS disorders. However, while the BBB is indeed compromised in some CNS disorders and brain injury, the recent discovery of meningeal lymphatics suggests that, even under basal conditions, the "immune privilege" of the brain is not as absolute as was

once thought (40). The BBB is composed of specialized endothelial cells in capillaries and postcapillary venules of the brain and spinal cord, characterized by low pinocytotic activity and by complex tight junctions comprised of transmembrane and cytoplasmic adhesion molecules (**Fig. 1.1**) (41). These endothelial cells produce a basement membrane containing embedded pericytes. Another basement membrane, produced by astrocytes, constitutes together with the astrocytic end feet, the glia limitans perivascularis. While these two basement membranes are indistinguishable at the capillary level, they are separate at the level of post-capillary venules, where they form a perivascular space containing cerebrospinal fluid (CSF) and antigen-presenting cells (APCs). Under basal conditions, leukocytes rarely penetrate the glia limitans, but accumulate in this perivascular space (as well as in the leptomeningeal and ventricular spaces). Here they fulfil an immune-surveillance function by interacting with antigen-presenting bone marrow derived macrophages and dendritic cells.

Following the onset of brain ischaemia, a sequence of events involving the CNS, its vasculature, the blood, and lymphoid organs is invoked (**Fig. 1.2**). From an inflammatory point of view, the hyperacute phase of brain ischaemia can be defined as the first 24 hours, wherein the initial ischaemic insult results in coagulation in blood vessels serving the brain, and the production of pro-inflammatory factors in the infarct site. The acute phase can be defined as days 1-7, where pro-inflammatory immune cells ranging from neutrophils to macrophages to lymphocytes infiltrate into the brain in large numbers. The subacute phase (days 7-14) involves the infiltration of more brain-protective immune phenotypes including regulatory T and B cells. Finally, the chronic phase of inflammation in AIS encompasses the long-term processes of brain repair/reconstruction such as neurogenesis and neuronal sprouting.

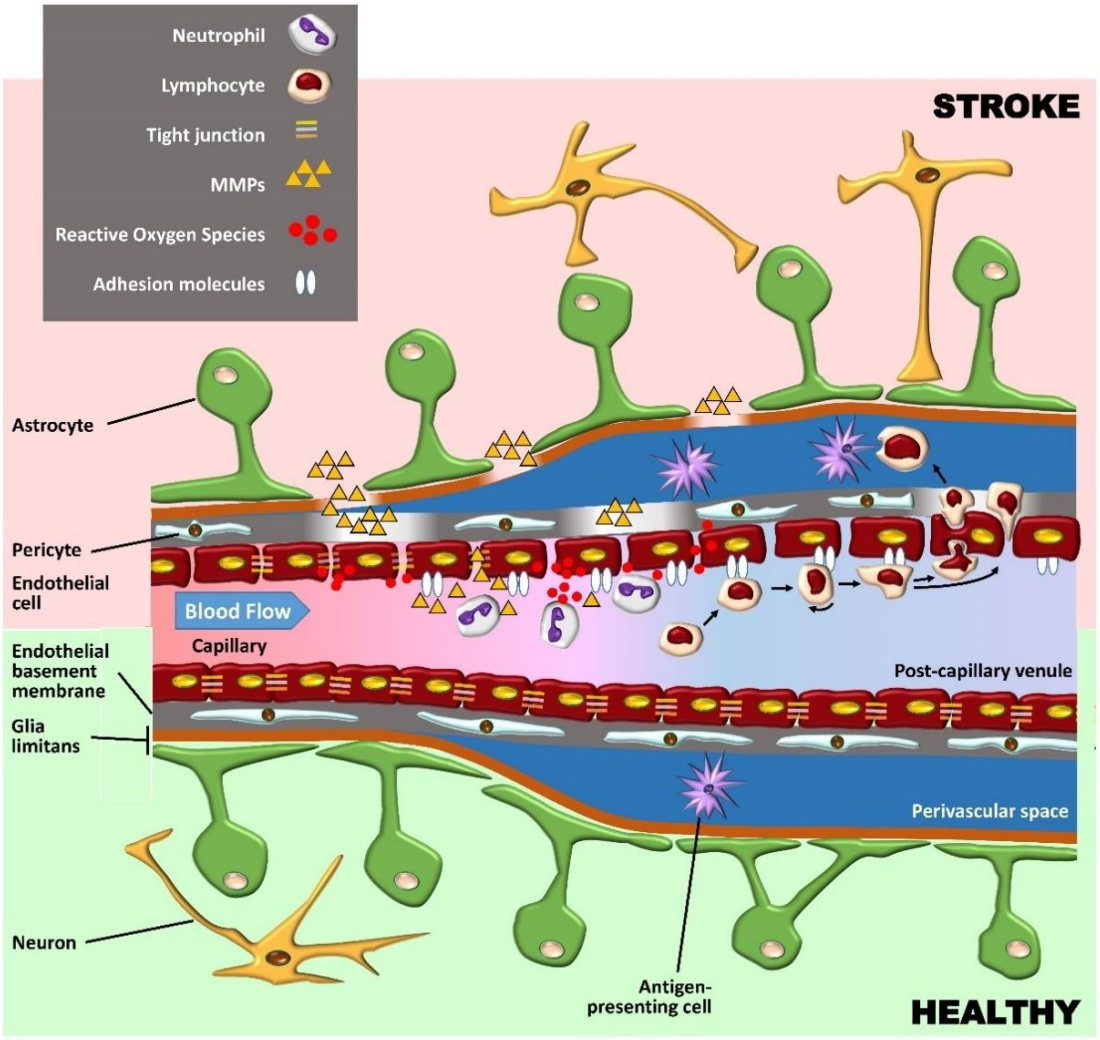


Figure. 1.1: Schematic representation of the blood–brain barrier (BBB) under healthy conditions (bottom part of the figure) and during its early breakdown following stroke (top part). The BBB is composed of a layer of endothelial cells with tight junctions composed of transmembrane and cytoplasmic adhesion molecules. These cells produce a basement membrane containing embedded pericytes. Astrocytes and their end feet constitute the glia limitans perivascularis. At the capillary level (left side of the figure), the endothelial basement membrane and the glia limitans are indistinguishable, but at the level of post-capillary venules (on the right), they are separated by a perivascular space containing cerebrospinal fluid (CSF) and antigen-presenting bone marrow-derived macrophages and dendritic cells. Following reperfusion, reactive oxygen species (ROS) cause an initial breakdown of the BBB by activating matrix metalloproteinases (MMPs) and upregulating inflammatory mediators. Stroke leads to an increased expression of integrin molecules on the leukocyte surface (not shown) and of the corresponding adhesion molecules on the endothelium. Leukocytes tether and roll onto the vascular endothelium before being activated by chemokines (not shown). They then firmly adhere to the endothelium and undergo either transcellular or paracellular diapedesis through the endothelial layer. From Malone et al., 2019.

Ischaemic stroke starts in the blood vessels perfusing the brain, where arterial occlusion results in hypoxia, reactive oxidative species (ROS) production, and changes in shear stress across the lumen wall (42). The coagulation cascade is triggered, resulting in microvascular occlusion (43). Platelet aggregation is exacerbated by the concomitant fall in the bioavailability of nitrous oxide (NO). The combined effect of oxidative stress, inflammatory mediators (e.g. IL-1, TNF-α), downregulated endothelial junction proteins and upregulated leukocyte- or vascular-derived proteases increases blood brain barrier (BBB) permeability (43). A critical point is reached if these processes cause detachment of endothelial cells from the basement membrane, at which stage the unimpeded entry of free water and serum into the brain leads to haemorrhage (44).

Endothelial cell-derived prostaglandins and chemoattractants also drive leukocyte entry into the infarct site (44). The infiltration of neutrophils, macrophages, and other leukocytes is further promoted by the activation of high-avidity integrin molecules on the leukocyte surface and the upregulated expression of corresponding ligands on the endothelium e.g., vascular cell adhesion molecule-1 (VCAM-1) and intracellular adhesion molecule-1 (ICAM-1). Activated leukocytes produce ROS, proteolytic enzymes, leukotrienes, cytokines, and platelet-activating factor which promote vasoconstriction, platelet aggregation, and further neurotoxicity (42). In the perivascular space, activated macrophages secrete a host of pro-inflammatory cytokines, while mast cell degranulation results in the release of histamine, proteases and TNF-α, further degrading BBB integrity.

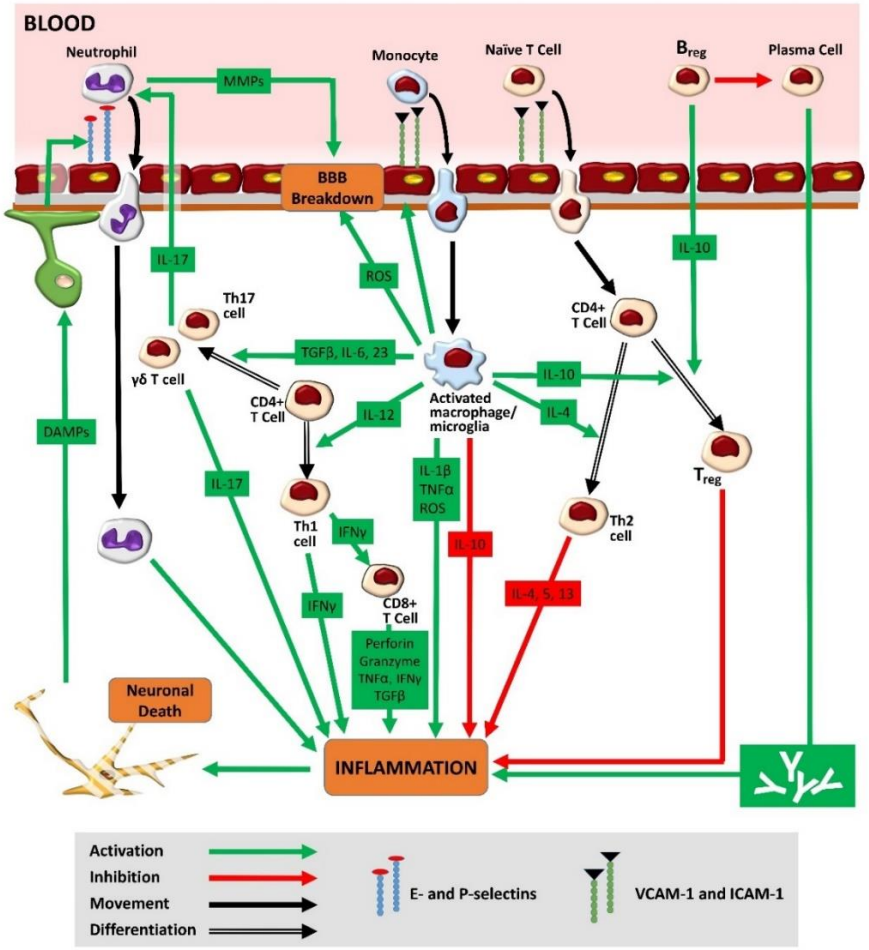


Figure 1.2: Immune response to stroke. Hypoperfusion causes an immediate deprivation of glucose and oxygen to the brain, leading to widespread neuronal cell death. The release of danger/damage-associated molecular patterns (DAMPs) from dying neurons results in the secondary activation of astrocytes and microglia. The release of chemokines/cytokines from glial cells generates an inflammatory environment featuring ROS, activated leukocytes, and the upregulated expression of adhesion molecules on endothelial cell membranes. Adhesion molecules such as E- and P-selectin mediate the initial tethering of circulating leukocytes to the endothelium. Separate surface molecules such as ICAM-1 and VCAM-1 then facilitate firm adhesion and transmigration. Neutrophils, entering the brain as early as 1 h post-stroke, increase BBB permeability via MMPs, further exacerbating ischaemic injury. Monocytes, infiltrating 1–2 days later, function as tissue macrophages. The M1 macrophage/microglia phenotype increases ischaemic injury through the production of ROS and pro-inflammatory cytokines (TNF-α and IL-1β). The M1 subtype also secretes cytokines [IL-12, IL-6, transforming growth factor beta 1 (TGF-β), and IL-23], which encourage the differentiation of infiltrated naïve CD4+ T-cells into pro-inflammatory Th1 and Th17 forms. Th1 cells, through release of interferon gamma (IFN-γ), promote the cytotoxic activity of CD8+ T-cells. Th17 cells (as well as their γδ T-cell counterparts) further increase neutrophilic activity and enhance ischaemic through the production of IL-17. Ultimately, the pro-inflammatory milieu seen in the acute stages of ischaemic stroke gives way to a second, subacute anti- inflammatory phase typified by increased M2 microglial/macrophagic activity. The release of IL-10 from both glial cells and circulating regulatory B cells (Bregs) encourages the generation of Tregs, a cell type that promotes neuroprotection and repair. Bregs may also play a role in the chronic immune response to stroke where they serve to reduce the effect of long-term antibody-mediated neurotoxicity. From Malone et al., 2019.

At the same time that these processes are occurring in the blood vessels and perivascular spaces, ischaemia also impacts the brain parenchyma. Hypoperfusion causes an immediate deprivation of glucose and oxygen, leading to a fall in ATP production. A series of interconnected cytoplasmic and nuclear events then begins (bioenergetic failure, acidotoxicity, excitotoxicity, oxidative stress and inflammation), causing neuronal cell death, commonly termed neurotoxicity (45). The release of danger/damage-associated molecular patterns (DAMPs) from dying and dead neurons precipitates a new phase of the inflammatory response in the brain (46). Activation of pattern-recognition receptors (PRRs) leads to the production of IL-1β and TNF-α. An inflammatory environment emerges as a result, containing IL-17, perforin, granzyme, and increasing concentrations of ROS (45).

The adaptive arm of the immune response is activated as early as 24 hours post-stroke (46). CD4+ T cell subtypes exacerbate neurotoxicity in the early stages of stroke in an antigen-independent manner, possibly via secretion of several cytokines, including IFN-γ and IL-17 (44). Infiltrated gamma-delta (γδ) and CD8+ T cells mediate further neuronal cytotoxicity. Antigen-specific T cells only contribute later (7 days+) to stroke pathophysiology, participating in autoimmune or tolerance reactions in a manner largely dependent on whether they are skewed towards a more damaging (T helper 1 (T_H1), T helper 17 (T_H17)) or protective (T helper 2 (T_H2), T regulatory (T_{reg})) phenotype (47). Lastly, B cells can produce antibodies against brain-derived molecules, resulting in further neuronal damage in the weeks following disease onset and possibly leading to clinical stroke sequelae such as dementia (48).

Initial inflammation is self-limiting and ultimately gives way to structural remodelling and functional reorganisation. The end of the acute phase (day 7) is characterised by

three processes (42): 1) removal of dead cells/tissue debris, 2) creation of an anti-inflammatory milieu, and 3) production of pro-survival factors. The processes of repair and reconstruction, which involves neuronal sprouting, angiogenesis, neurogenesis, and alteration to the cellular matrix, are carried out in concert by many cell types, ranging from immune cells to neurons and astrocytes (49). Together, these cells produce growth factors and proteases, allowing for re-modelling of the ischaemic site (42).

Due to the known involvement of the immune system, a variety of immunotherapies have been trialled at the pre-clinical and clinical levels for the treatment of AIS (**Fig. 1.3**) (25). In the earliest stages (<24 hours), proposed therapeutic targets have focused on inflammatory cytokines (IL-1, TNF-α), matrix metalloproteinases (MMP-9), and adhesion markers (ICAM-1) (50). Immune cells (neutrophils, macrophages) have also been targeted in the acute and subacute stages.

Overall, there has been a significant failure to bridge the gap between experimental and clinical studies for stroke immunotherapies. Notwithstanding the need for further study of the bi-directional communication between the CNS and the immune system, and the requirement to test drugs in more rigorous and more clinically relevant models of the disease, there are several target-linked explanations. For instance, many drugs trialled to date have aimed to manipulate the innate immune response, a fact which would restrict their use to the acute phase of the disease. Likewise, many targets (e.g., microglia) play both beneficial and detrimental roles in ischaemic stroke. However, regulatory T cells (Tregs), a subset of T cells, are an aspect of the adaptive immune system which are suspected to play a largely neuroprotective role in stroke recovery.

Below, a closer examination of the role of T cells in AIS is presented, followed by a detailed look at Tregs in particular.

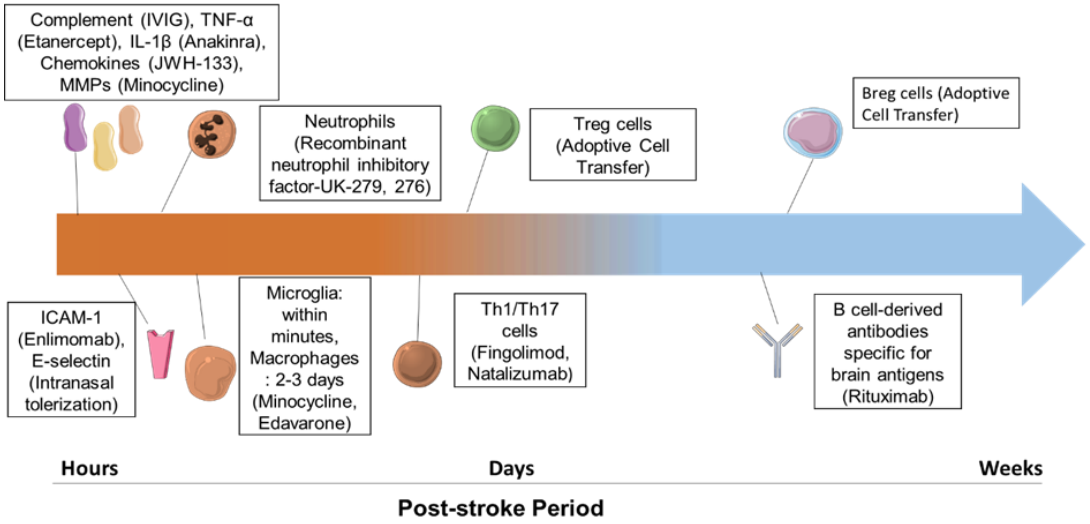


Figure 1.3: A time course of immune targets and proposed immunomodulatory therapies in stroke. Targets are placed according to the predominant role each plays in either neurotoxicity (red) or tissue remodelling and repair (blue). Potential therapies are highlighted in parentheses. (Malone et al., 2018).

1.3 T Cells & Acute Ischaemic Stroke

1.3.1 T Cell Responses in Acute Ischaemic Stroke

T cells (including CD4+, CD8+, natural killer T, γδ, and regulatory subtypes) begin infiltrating into the CNS in significant numbers as early as 24 hours post-ischaemia (51); thereafter they can be detected for at least 30 days (52). T cells predominantly enter through the BBB, meninges, and choroid plexus (53). It is widely accepted T cells have a damaging effect in the acute phase of stroke, as RAG-/- knockout mice lacking all T cells showed smaller infarct size and improved functional outcome (54-56). The fact this neuroprotection is abolished by the re-introduction of CD3+ T cells further corroborates the view that T lymphocytes are involved in a detrimental manner in stroke pathophysiology. Depletion of specific T cell subsets (CD4+, CD8+, γδ)

likewise reduces secondary lesion progression (57-60). The temporal dissociation between early T cell effects in stroke and the period required for antigen recognition suggests antigen-independent mechanisms, such as cytokine secretion, likely mediate initial neurotoxicity (61). Separate research indicates antigen-dependent T cell responses then take over in later stroke stages (59)

γδ T cells are predominantly thought to have deleterious effects in stroke. Depletion of γδ T cells significantly reduced cerebral ischaemia-reperfusion (I/R) injury in an experimental model of stroke (60). The same study found that IL-17 was responsible for the negative impact of γδ T cells on infarct size and neurological function. A separate study demonstrated that, not only are γδ T cells the principal source of IL-17 in the ischaemic brain, but blockade of the IL-17 axis improved stroke outcome through reduced neutrophil invasion (57). Increased production of IFN-γ and perforin by γδ T cells, on the other hand, correlated positively with clinical improvement, possibly due to increased protection against infection (62). However, crosstalk between the immune system and bacteria can also produce deleterious results, as evidenced by the activation of γδ T cells by pro-inflammatory gut microbiotas (63). These γδ T cells traffic to the brain meninges post-ischaemia where they exacerbate stroke injury via IL-17.

Cytotoxic cells such as CD8+ T cells and NKT cells are also known to participate in stroke pathology. CD8+ T cells accumulate in the pan-necrotic area of the ischaemic brain as early as three hours post-stroke, where they mediate many cytotoxic responses, partly through perforin (58). However, NKT cells have garnered interest not for their neurotoxic roles, but for their importance in host immune function (64). It has been shown that stroke can induce behavioural changes in hepatic invariant NKT

(iNKT) cells to an anti-inflammatory phenotype that facilitates infection (65). These changes, brought about by noradrenergic neurotransmitters, can be experimentally reversed through administration of propranolol. Similar results can be achieved through the activation of iNKT cells with α-galactosylceramide in pre-clinical models (65)

CD4+ T cells are also recruited to the ischaemic hemisphere, in even greater numbers than their CD8+ counterparts (66). In stroke, infiltrating CD4+ T cells are predominantly of the Th1 type, while circulating Th17 cells may also contribute to ischaemic injury through pro-inflammatory cytokine secretion (67). Adoptive transfer of Th1 or Th17 CD4+ T cells worsened behavioural outcomes in an experimental model of ischaemic stroke (68). Systemic treatments that promoted the Th2 phenotype on the other hand, e.g., IL-33, were beneficial (69). Autoimmune CD4+ T cells are also implicated in stroke damage. The number of myelin basic protein (MBP)-responsive Th1 cells, for example, act as a marker for poor clinical outcome (70). The fact that many stroke patients display increased concentrations of CNS antigens in lymph nodes, and increased circulating levels of T cells specific for them, strongly indicates the presence of a self-directed immune response (71). Studies have also shown immunization with myelin antigens worsened outcomes in experimental stroke, while systemic inflammation helps prime such deleterious autoimmune responses (70, 72). The production of IL-4 or brain-derived neurotrophic factor (BDNF) by Th2 cells, on the other hand, leads to direct neuroprotection and a tissue-healing phenotype in myeloid cells (73).

1.3.2 T cell-targeted Immunotherapies in Stroke

To date, the T-cell targeted therapies which have come closest to clinical translation have focused on reducing initial T cell trafficking to the infarct site. No drug exemplifies this better than natalizumab.

Natalizumab is a humanized monoclonal antibody that binds to the α4 subunit (CD49d) of the adhesion molecule α4β1 integrin (VLA-4) on lymphocytes and neutrophils (74). By blocking the adhesion of leukocytes to receptors such as VCAM-1, natalizumab prevents trans endothelial leukocyte migration. The drug was approved for the treatment of relapsing-remitting multiple sclerosis in 2004.

In rodent models of stroke, natalizumab reduced the infiltration of T cells into the CNS (58, 75). Decreased brain damage and improved clinical outcomes were also noted, although this was mostly noted in permanent and not transient models of brain ischaemia (58). Nevertheless, a majority of preclinical studies supported natalizumab use (76-78), and the drug was brought forward for clinical trials. Disappointingly, however, results of the phase II clinical trial "ACTION" failed to show a reduction in infarct growth, although improvements in functional outcomes warranted further investigation (88). But the follow-up phase IIb trial ("ACTION2") did not meet its primary or secondary endpoints. As a result, further development of natalizumab in acute ischaemic stroke is not currently being pursued.

Ultimately, the failure of natalizumab to translate from the bench to bedside highlighted fundamental flaws in our understanding of T cells post-ischaemia. A recent study confirmed natalizumab only transiently decreases T cell counts in the infarcted brain, and chronic T cell accumulation ultimately occurs due to local

proliferation of T cells (79). In light of these findings, the approach of targeting T cell trafficking to the brain post-stroke will need to be fundamentally re-evaluated. If we accept that no pharmacological intervention can completely block the recruitment of predominantly pro-inflammatory T cells to the infarct site, the next most obvious therapeutic strategy becomes boosting the frequency and/or function of the anti-inflammatory subtypes. Hence this thesis focuses on regulatory T cells (Tregs), the subtype of CD4+ T cells most widely reported to provide neuroprotection in AIS.

1.4 Regulatory T Cells

1.4.1 Regulatory T Cell Biology

The immune system has evolved several regulatory mechanisms to prevent autoreactivity to self-antigens and control excessive immune reactions after tissue injury. As part of this, naturally occurring CD4+ regulatory T cells (or "Tregs") are indispensable for the maintenance of peripheral immunological self-tolerance as well as homeostasis in a variety of disease states including those involving autologous tumour cells, allergic responses, and organ transplantation (80-83).

The checks and balances concept of immune regulation by specialised lymphocytes has been a doctrine of immunology for several decades (84). Following several findings in the 1970s and 1980s suggesting the existence of a "suppressor T cell" in particular, efforts were made to characterise them by molecular markers (85). In the mid-1990s, a population of CD4+ T cells that constitutively and highly expressed the surface marker CD25 (IL-2 receptor α chain) were labelled Tregs (86). Depletion of these CD4+ CD25+ T cells, which constituted approximately 10% of peripheral CD4+ T cells in mice, induced a variety of autoimmune diseases (e.g., gastritis, thyroiditis,

and type I diabetes). Reconstitution of this population prevented autoimmune disease development. This initial characterisation of CD4+ CD25+ T cells facilitated an exploration of the role that Tregs play in cancer, infection, and transplantation settings. CD4+ CD25+ Tregs in both mice and humans were subsequently found to express forkhead box protein 3 (FoxP3), a transcription factor which controls the expression of a range of genes in Tregs at baseline and during activation (87, 88). FoxP3-mutant Scurfy mice spontaneously succumb to widespread autoimmune disease. Likewise, mutations of the human FOXP3 gene produce multiorgan autoimmunity, referred to as immune dysregulation polyendocrinopathy enteropathy X-linked syndrome (89). However, while Tregs are universally associated with the expression of FoxP3, there is substantial heterogeneity in the phenotype and genetic transcriptome of FoxP3+ T cells. This makes FoxP3 a specific but not outright marker of Treg cells. Indeed, in humans, FoxP3 as well as CD25 can be detected in low amounts in conventional, non-regulatory T cells (90). A higher expression of markers including Helios, CD39, CD73, CTLA-4, LAP/GARP can also be used to identify Tregs and determine activation status (91). Furthermore, a combination of CD45RA and Ki67 can be employed to delineate between naïve, memory, and proliferating Treg phenotypes (91). In humans, lower expression of the IL-7 receptor α chain (CD127) by Tregs also aids in Treg identification; however, this receptor also can be downregulated by conventional T cells. Thus, the study of human Tregs remains more complicated than their mouse counterparts. Similar to other CD4+ T cell phenotypes, there is an ongoing discussion on whether Tregs are functionally stable at inflammatory sites, or whether they are functionally plastic and able to differentiate into pro-inflammatory T cell subsets under certain circumstances (92, 93). This is compounded by the fact that as well as showing lineage instability, Tregs also display functional adaptability,

allowing them to express transcription factors and chemokine receptors normally associated with Th1, Th2, Th17, and T follicular helper cells (94-101). Chemokine receptors endow Tregs with the ability to home to the site of a specific type of inflammation and suppress the corresponding effector T cell subset (102).

Tregs are generated mainly via two different pathways. The majority develop directly from CD4+CD8+ double-positive (DP) precursor T cells in the thymus as a functionally and phenotypically distinct T cell subpopulation. These are called thymus-derived Tregs (tTregs) or naturally occurring Tregs (nTregs) (103). As these tTregs recognise self-antigen–MHC complexes with relatively high avidity, they express a T-cell antigen-receptor (TCR) repertoire with a bias for self and thus are crucial for preventing autoimmunity (104). The second pathway of Treg generation involves the differentiation of naive CD4+ T cells in the periphery upon antigen stimulation amid high levels of cytokines such as interleukin-2 (IL-2) and TGF-β (105). These "peripherally-induced" Tregs are referred to as pTregs, and as they recognise non-self-antigens, they are commonly located at mucosal surfaces exposed to microorganisms, food, and environmental allergens (106). Separately, conventional CD4+ T cells can also be skewed *in vitro* to form induced Tregs (or "iTregs"). However, these cells normally lack the full combination of CpG hypomethylation of Treg signature genes (including Foxp3, Tnfrsf18, Ctla4, Ikzf4) and are functionally unstable (107). Finally, more recent research suggests the existence of tissue-localised Tregs (or "tissue Tregs") in non-lymphoid organs including skin, fat, muscle, lungs, and brain (108). These Tregs play a diverse role in processes ranging from muscle repair to cardiac remodelling to metabolic function (109).

Various cell contact–dependent and -independent mechanisms of Treg suppressive function have been elucidated. These include consumption of IL-2 required by non-Treg T cells for proliferation, secretion of anti-inflammatory cytokines (IL-10, IL-35, TGF-β) which can suppress effector T cell differentiation, inhibition of lymphocyte proliferation, promotion of Treg differentiation, and inhibition of inflammatory activity of other immune cells such as macrophages (110). Tregs can also downregulate costimulatory molecules on antigen-presenting cells via CTLA-4 and induce apoptosis through the release of granzyme (111). Tregs can employ other cell surface receptors such as CD39, CD73, PD-1 and TIGIT to modulate immunity (112). Finally, Tregs have also been shown to play a key role in tissue repair in organs ranging from the gastrointestinal tract to the skin (113). In the CNS, for example, such repair mechanisms can include promoting re-myelination and reducing astrogliosis (114).

1.4.2 Regulatory T Cells in Animal Models of Stroke

The onset of AIS produces profound changes in immune function which impact Tregs both at the site of infarction and in the periphery. In the brain, relatively few (~5%) Tregs infiltrate during the first few days post-ischaemia in transient middle cerebral artery occlusion (tMCAO) (66), the most commonly employed model of cerebral infarction in rodents (36). Indeed, most Tregs detected remain in the cerebral vasculature (115). However, by 7-10 days, this proportion increases to 20% (52), and may reach as high as 40% in the chronic phase (day 14+) (116). Importantly, at this stage, most brain Tregs are expressing markers of proliferation (e.g., Ki67), highlighting the fact that both infiltration and *in situ* proliferation likely contribute to the enhanced Treg frequency (52). Factors such as age and sex may also play a role,

with higher Treg frequencies (21% vs 12.2%) and counts observed in the brains of older aged male mice than in females at 15 days post-tMCAO (117). However, it is crucial to note that both the kinetics and magnitude of Treg cerebral invasion also starkly differ between models of ischaemia. In contrast to the delayed adaptive response in tMCAO, in permanent models of middle cerebral artery occlusion (pMCAO), Tregs constitute approximately 20% of brain-invading T cells within the first week of ischaemia (118). Indeed, these findings echo reports of the manifold higher T cell counts, as well as other immune cells in permanent models (119).

Brain Tregs are characterised by high expression of Treg-specific genes including *Ctla-4, Pd-1, Gitr, Cd103, and Helios* (116). Upregulated expression of serotonin receptor 7 (Htr7), which may facilitate Treg expansion and activity, is also noted (116). Notably, levels of the IL-33 receptor subunit ST2, which can also mediate increased brain Tregs, are also higher (120). Brain Tregs also display heightened expression of chemokine receptors including CCR5, CCR6, and CCR8 (121, 122). These and other receptors are likely involved in Treg trafficking to the infarct site through chemokines such as CCL1, CCL5, CCL20, and CXCL14, all of which are upregulated post-brain ischaemia (123-126). A role for the sphingosine 1-phosphate (S1P) gradient in Treg recruitment to the brain has also been suggested (127)

Peripherally, AIS induces substantial lymphopenia, while Treg frequency is significantly increased (128, 129). Consistently, Treg cells have been shown to be more resistant to ischaemia-induced changes in circulating frequency than effector T cell populations (130). Indeed, even when circulating Tregs were reduced at 24 hours, these levels returned to baseline by 3 days (115). A potential mechanism for this is CNS-induced splenic atrophy, which is accompanied by a drastic reduction in

splenocyte numbers and an increase in the number and activation of IL-10 secreting Tregs (131).

The potential involvement of Tregs in post-stroke recovery has been investigated in animal models of brain ischaemia using both Treg depletion and Treg enhancement. Two commonly employed methods of Treg depletion are antibody-mediated cell depletion, via anti-CD25 antibodies in mice, and depletion using transgenic mice with a diphtheria toxin receptor transgene under control of the Foxp3 promoter (132, 133). Using these Treg-depletion paradigms, several studies have demonstrated an increase in infarct volume, suggesting a protective role for these cells in stroke (128, 134, 135). However, results of other studies demonstrated Treg depletion produced no effect on infarct size, or even reduced it (115, 136). A detailed analysis suggests that differences within (for example different transgenic constructs) as opposed to between methods of Treg depletion are more likely have contributed to this inconsistency. Other factors such as environmental conditions, the specific microbiota, or experimental stressors may also play a role (118).

Separately, several research groups have examined various methods of increasing Treg numbers and/or function post-brain ischaemia. Adoptive transfer of isolated Tregs improves outcome in transient brain ischaemia in both rats and mice (129, 137-139). Similar infarct reduction has been observed with CD28 superagonists, monoclonal antibodies which activate Tregs and enhance their suppressive function (139, 140). Finally, mucosal immunisation with CNS antigens to induce autoantigen specific Tregs also improves functional and histological outcomes in rat models of both tMCAO and pMCAO (141-143). However, neutral or detrimental effects of Treg-boosting strategies, including adoptive transfer and CD28 superagonist, have also been

reported (115, 144, 145). Once more, the discrepancy in these results does not appear to be linked to the method of Treg expansion itself, but rather to experimental and environmental factors such as stroke model and species (118).

In the acute stage of brain ischaemia, it has been argued Tregs likely provide neuroprotection by modulating immune responses from outside the infarct site in an antigen-nonspecific manner, a phenomenon commonly termed "bystander suppression" (146). Tregs may also play a dual role in the peripheral immune system by reducing systemic inflammatory responses while simultaneously ameliorating stroke-induced immunosuppression by correcting lymphopenia (130, 137). Furthermore, Tregs may maintain BBB integrity (129). More recent evidence of a novel gut-brain axis in stroke also points to a mechanism by which Tregs could inhibit the early migration of effector T cells migration from the gut to the infarcted brain (63). Mechanisms by which Tregs may promote stroke recovery at the brain are discussed in more detail below.

Evidence from experimental stroke models predominantly suggests a neuroprotective function of Tregs in AIS. However, many studies conducted to date are small, and have not always adhered to the Stroke Therapy Academic Industry Roundtable (STAIR) recommendations. Potential reasons for inconsistent findings in pre-clinical models may include, for example, the effect variations in the local inflammatory milieu can have on Treg function (147). When comparing stroke models, substantially higher numbers of T and B cells can be seen in permanent MCAO as opposed to transient MCAO as early as 5 days post-ischaemia (119). Differences in microglial activation and the expression of inflammatory markers (e.g., IL-1, TNF-α, IFN-γ, and ICAM-1) are also noted. Overall, independent of infarct size, 50% fewer infiltrating

leukocytes are observed at 24 hours post-tMCAO compared to permanent MCAO (148). Conversely, secondary microthrombosis and endothelial damage due to reperfusion are more apparent post-tMCAO compared to post-pMCAO (149, 150). All of these model differences may impact Treg function. Separately but not entirely unrelated is the effect of infarct size. Given smaller brain lesions induce only a minor immunomodulation, but no immunosuppressive syndrome, Tregs may play a lesser role in the recovery of mild stroke. Finally, the concept of a time-dependent effect of Treg post-brain ischaemia cannot be discounted. It is plausible Tregs could contribute to worsened brain injury, via thromboinflammatory mechanisms, for example, in the acute stages of ischaemic stroke, while also enhancing chronic CNS repair (151). Overall, therefore, there is an urgent need for further research on the role of Tregs in animal models of stroke, especially in milder pMCAO models.

1.4.3 Regulatory T Cells in Human Stroke

To date, relatively few studies have considered the role of Tregs in human stroke compared to rodents. Similar to animal models of the disease, Treg frequency is correlated with better stroke outcome (152-154). However, early research involving these cells suggested a decline in both Treg frequencies and cell counts post-brain ischaemia (67, 155-160). A number of recent papers have also demonstrated an increase in Treg frequency in stroke patients compared to healthy controls (153, 154, 161-164). An increased Treg frequency has been noted in patients with smaller stroke lesions, while a separate study identified a similar negative correlation between infarct volume and Tregs (154, 161). However, previous studies have also shown no relationship between infarct volume (as well as gender, stroke location and post-stroke infection) and Treg frequency, indicating time of Treg quantification may in fact be

the primary determinant influencing circulating Tregs in stroke patients (158, 161). Indeed, regardless of whether Treg frequency increases or decreases in acute ischaemia, Treg frequency tends towards baseline in the subacute stages (67, 152, 154, 161-165). Data on the effect of ischaemic stroke on Treg function is also lacking (162, 165). Results of Treg suppression assays show brain ischaemia acutely ameliorates Treg suppressive capacity (162, 165). The frequency of CD39+ Tregs (a population shown in rodents and humans to be functionally active) is also strongly reduced (165). Several studies have highlighted that AIS can decrease levels of anti-inflammatory cytokines including IL-10 and TGF-β (67, 157). Overall, the caveats of limited sample sizes, the use of differing Treg definitions, and the recruitment of patients with varying stroke classifications, including haemorrhage, must be borne in mind.

1.4.4 Mechanisms of Treg-mediated Neuroprotection in Stroke

Various mechanisms by which Tregs may afford neuroprotection and promote stroke recovery have been evaluated (151). The most compelling are outlined below.

1.4.4.1 Secretion of Anti-Inflammatory Cytokines

As noted previously, perhaps the most well-studied manner in which Tregs could attenuate ischaemic injury as well as enhance tissue repair is via the release of cytokines such as IL-10, TGF-β, and IL-35 (166). In AIS, low levels of IL-10 are correlated with worse outcomes, while exogenous administration of IL-10 improves recovery in preclinical models of the disease (167). From this, it has been verified that IL-10 plays a crucial role in early Treg-afforded neuroprotection, potentially as a means by which these cells downregulate pro-inflammatory cytokine (IFN-γ, TNF-α) secretion from macrophages (128, 140). In later stages, IL-10 may be involved in

Treg-directed neurogenesis (168, 169). Meanwhile, a potentially smaller role for Treg-derived TGF-β and IL-35 has also been described (135).

1.4.4.2 Perforin and Granzyme

As noted above, Tregs may induce the death of pro-inflammatory cell populations via the perforin/granzyme pathway (170). In particular, it appears a combination of granzyme-B and perforin allow Tregs to trigger apoptosis among effector T cells (171). However, the contribution of this mechanism to Treg-mediated neuroprotection remains as yet unevaluated.

1.4.4.3 PD-1/PD-L1

Programmed cell death-1 (PD-1) is an inducible receptor expressed on Tregs that plays a central role in regulating T cell exhaustion (172). By binding to its corresponding ligand (PD-L1) on APCs, Tregs can inhibit T cell activation (173). However, to date, PD-1+ Tregs remain understudied in stroke. Interestingly, Tregs can also express PD-L1, and it has been shown that Tregs can protect the BBB by suppressing the release of matrix metalloproteinase-9 (MMP-9) from neutrophils via its PD-L1 receptor (an interaction which may be facilitated by the expression of CCR5 on Tregs) (138). However, separate research highlighted smaller infarct in PD-L1$^{-/-}$ mice (122, 174). This suggests, like many aspects of the immune system, the PD-1/PD-L1 pathway may have a dual role in stroke-induced inflammation, and its contribution to Treg-mediated neuroprotection requires further investigation.

1.4.4.4 Treg-Microglia Crosstalk

Recent research has focused on the crosstalk Tregs may have with brain-resident cells including neurons, astrocytes, and microglia (175, 176). A lack of Tregs skews microglia and infiltrating macrophages towards a pro-inflammatory M1 phenotype, while boosting Tregs shifts these same cells back towards a protective M2 phenotype (176). This relationship is reciprocal, with microglia-derived IL-10 and TGF-β promoting Treg differentiation (139). Direct interactions between microglia and neurons via CD200-CD200R can also promote M2 polarisation which further attracts Tregs by release of chemokines including CCL2 and CCL5 (177). This Treg-microglia crosstalk not only contributes to better acute stroke outcomes, but also may benefit long-term brain repair via Treg-derived osteopontin, which promotes oligodendrocyte regeneration and remyelination by microglia (178). However, microglia can also downregulate Treg suppressive function post-ischaemia by inducing Sirt2 expression, highlighting a negative component to this crosstalk that deserves further exploration (179).

1.4.4.5 Amphiregulin (AREG)

Amphiregulin (AREG), a ligand of the epidermal growth factor receptor (EGFR), may play a crucial role in post-stroke tissue regeneration (120). AREG appears to regulate the STAT3 and IL-6 pathways in astrocytes and microglia. There is an increased expression of AREG on brain infiltrating Tregs post-brain ischaemia which has been linked to a Treg-mediated reduction in astrogliosis (a general response after brain injury linked with both beneficial and detrimental processes) (116, 180). Given AREG expression by Tregs only begins to increase during the subacute/chronic phase of

stroke, this mechanism could be exploited by immunotherapies aiming to improve long-term recovery (116).

1.4.4.6 CTLA-4

Cytotoxic T lymphocyte antigen 4 (CTLA-4) is a T cell surface receptor that mediates a crucial tolerogenic interaction with dendritic cells (DCs) by binding to its corresponding ligands, CD80 and CD86 (181). Research has shown expression of CTLA-4 is higher on brain-infiltrating Tregs compared to their splenic counterparts (116). Although this alone does not imply the CTLA-4 plays a role in Treg-mediated neuroprotection, it is interesting to note that the cholesterol-lowering agent atorvastatin treatment reduced infarct volume and neurological deficit in a rat model of brain ischaemia while upregulating CTLA-4+ Tregs (182).

1.4.4.7 CD39/73

The dual exoenzymes CD39/CD73 on Tregs convert extracellular ATP sequentially into adenosine, a molecule which among other immunomodulatory effects can inhibit the activity of NK and effector T cells, as well as induce Treg cell differentiation (183). In a mouse model of tMCAO, IL-2/IL-2 complex treatment reduced brain infarct and ameliorated neurological deficit. This was associated with significantly enhanced CD39/73 expression on Treg cells (184).

1.4.4.8 Secondary Microthrombosis

In contrast to previous mechanisms, other research involving Tregs in AIS suggested a possible mechanism by which these cells may exacerbate post-stroke injury. In 2013, Kleinschnitz *et al.* used a DEREG mouse model to show that Treg depletion protected

against brain ischaemia (115). Meanwhile, adoptive transfer of Tregs promoted infarct progression. Increased interaction between Tregs and LFA-1/ICAM-1 on the brain endothelium, resulting in microvascular dysfunction, was proposed as a "non-immunological" mechanism of this Treg-mediated neurotoxicity. These results were confirmed by a second study wherein Tregs were expanded *in vivo* using an anti-CD28 superagonist (145).

1.4.5 Treg-targeted Immunotherapies in Stroke

Already, several clinical studies have trialled Treg-targeted immunotherapies as potential treatments for diseases including a number of autoimmune diseases ranging from type 1 diabetes to hepatitis and Crohn's disease (185, 186). Clinical studies of therapies aiming to increase Treg frequency or function in neuroinflammatory conditions such as Alzheimer's disease, Parkinson's disease, and amyotrophic lateral sclerosis are also ongoing (187). Such Treg-targeted immunotherapies include cell-based therapies (e.g., polyclonal Tregs, autoantigen-specific TCR Tregs, autoantigen-specific CAR Tregs, tolerogenic DCs) and non-cell-based therapies (low-dose IL-2, rapamycin, peptide administration) (188-194).

1.4.5.1 Adoptive Treg Transfer

As noted above, the most intuitive approach yet explored in stroke to expand Tregs is the adoptive transfer of isolated Treg cells. When infused immediately following AIS, adoptively-transferred Tregs have been shown to promote BBB integrity in mice (129). Transferred Tregs may also abrogate tPA-induced intracerebral haemorrhage in stroke by inhibiting the production of MMP-9 and CCL2 (160). From this, transferred Tregs can safely extend the therapeutic window for tPA beyond 4.5 hours. This makes

adoptively transferred Tregs one of the more promising therapies to improve the efficacy and safety of thrombolytic treatment in AIS. Bone marrow-derived stem cell (BMSCs) transplantation also show promise, as Tregs within the BMSC transplant will mediate therapeutic immunomodulation and neuroprotection post-stroke (195).

1.4.5.2 CD28 Superagonist (CD28SA)

CD28 superagonists (CD28SAs), monoclonal antibodies that engage the CD28 costimulatory receptors and in theory induce preferential activation and expansion of Tregs, are another Treg-targeted immunotherapy which have received extensive attention in AIS. CD28SA-expanded Tregs mediate neuroprotection via IL-10, and this beneficial effect lasts at least one month after the onset of AIS (139). However, CD28SA has also been shown to cause vascular lesions and inflammatory thrombosis post-ischaemia (145). Likewise, the clinical history of CD28SA antibodies shows patients displayed unexpected cytokine release syndrome and unexpected severe adverse events, and more extensive dosing studies are required to optimise these drugs for clinical development (196).

1.4.5.3 Histone Deacetylase Inhibitors

The inhibition of histone deacetylase (HDAC) induces Foxp3 expression, a mechanism which could be exploited to convert naïve T cells to a regulatory phenotype (197). In stroke, the HDAC inhibitor trichostatin A has been trialled in mice, where it was noted to increase the number of brain-invading Tregs and the expression of IL-10 while simultaneously reducing infarct volume and behavioural deficits (128). Similar results were obtained with the HDAC6 inhibitor tubastatin. Notably, the neuroprotective effects of HDAC inhibitors post-ischaemia depended on

the presence of Foxp3+ Tregs. Given the ever-expanding list of HDAC inhibitors, coupled to both the development of iso-form selective drugs and an increased understanding of the role of HDACs in AIS, this avenue of Treg expansion may become increasingly attractive going forward (198-200).

1.4.5.4 Induction of Tolerance through Mucosal Immunisation

Mucosal immunisation with brain antigens such as myelin basic protein (MBP) has also been explored as an alternative method of inducing tolerance through development of antigen-specific Tregs (201). In particular, the repetitive administration of low doses of antigen has been shown to generate Tregs and suppress neuroinflammation in pre-clinical models of multiple sclerosis through enhanced TGF-β/IL-10 (202, 203). In stroke, evidence already suggests there is T cell reactivity to MBP (204), with higher concentrations of MBP and other brain antigens associated with worse outcomes (205). Indeed, clinical evidence demonstrates a strong correlation between Th1 responses and poorer stroke outcome up to 3 months later in humans (70). It is unclear if these autoreactive cells are involved in short- or long-term pathogenesis, or instead, act as a severity marker or are associated effects of the stroke. Some studies suggest a role of autoreactive Th1 in poor outcome (206), whereas other studies demonstrate no impact (207). Nonetheless, in theory, immune-based therapies that modulate the T cell phenotype away from a cytotoxic response towards a more tolerised response, possibly mediated by Treg, might have application in stroke. Intranasal or oral application of MBP weeks before stroke onset reduced infarct volume and improved recovery in rats (208) while separately intranasal MBP administration ameliorated the Th1 response in mice/rats (142). Administration of E-selectin can likewise induce Tregs which either suppress activated microglia through

TGF-β and IL-10 or promote neurogenesis (141, 143, 209). Further studies however cast doubt over the long-term involvement of autoreactive T cell responses in stroke, while the safety of induced mucosal tolerance has also been called into question (210, 211).

1.4.5.5 IL-33

As noted above, through its ST2 receptor, IL-33 can promote Foxp3 expression. In a mouse model of brain ischaemia, IL-33 administration enhanced the proliferation and the differentiation of Tregs, as well as the production of TGF-β and IL-10 (120). Further studies confirmed Tregs are an essential component of the anti-apoptotic neuroprotective effect of IL-33 (69, 212). As IL-33 may also improve white matter integrity and restore neurological functions via modulating microglia/macrophage activity through the STAT6 pathway, it represents a promising future stroke immunotherapy (213, 214).

1.4.5.6 IL-2/IL-2 Antibody Complex

While IL-2 induces T cell proliferation, Shevach *et al.*, demonstrated that a complex of IL-2 with a specific anti-IL-2 monoclonal antibody, clone JES6-1, (IL-2/JES6-1) blocked the site on IL-2 that binds to CD122, the IL-2Rβ chain, but did not inhibit binding to CD25. This complex preferentially expanded Treg, that constitutively express CD25, compared to conventional, naïve or effector T cells (215). Injection of the IL-2/JES6-1 complex expands Treg numbers over tenfold in multiple organs (216). This expanded Treg pool is stable for 1-2 weeks and display increased suppressive function. Mice treated with this IL-2/IL-2Ab complex show resistance to experimental autoimmune encephalomyelitis (EAE) induction (216). Administration of IL-2/JES6-

1 complex in mouse tMCAO reduced infarct volume, inhibited neuroinflammation, and improved sensorimotor functions, possibly via enhanced expression of CD39/73 (184). These beneficial effects were eliminated by Treg depletion. Recent *in vitro* research suggests that the adoptive transfer of IL-2/JES6-1 complex-treated Tregs mitigates cell death in both ischemic grey and white matter more effectively than Tregs alone, pointing to a potential combination of IL-2/JES6-1 and isolated Tregs as a future therapy (217).

1.4.5.7 Poly (ADP-ribose) Polymerase-1 (PARP-1) Inhibitors

Poly (ADP-ribose) polymerase (PARP)-1 is an intracellular enzyme which contributes to the pathogenesis of many diseases including ischemic stroke (218). Administration of PARP-1 inhibitors effectively increases Treg frequency through FOXP3 stabilisation (219). Peripheral blood mononuclear cells (PBMCs) isolated from stroke patients and treated with a PARP-1 inhibitor for 24 hours showed significantly increased Treg frequencies alongside higher expression of FoxP3 and CTLA-4 (158). PARP-1 inhibitor treatment also decreased pro-inflammatory cytokines (IFN-γ, TNF-α, and IL-17) and increased anti-inflammatory cytokines (IL-4, IL-10, and TGF-β1). As with IL-33, PARP-1 inhibitors may also alleviate post-ischaemic neuroinflammation via reduced microglial activation (220). However, further work is required to delineate the exact role of PARP-1 post-ischaemia and overcome limitations related to apparent sexual dimorphism (221).

1.4.5.8 Small Molecule Treg Enhancers

A number of more traditional, small molecule drugs have also been demonstrated to enhance Tregs post-ischaemia. These include rapamycin, which has been shown to

attenuate secondary injury and motor deficits in rat tMCAO by enhancing IL-35 and TGF-β among Tregs (135). Rapamycin has the advantage of already being approved for transplantation and a number of autoimmune conditions coupled with a long history of use in the production of Tregs for cell therapy applications (222). Selective serotonin reuptake inhibitors (SSRIs), which also have a strong clinical foundation, can likewise increase the number of brain-infiltrating Tregs and improve functional outcomes in mice (116). However, a recent meta-analysis concluded SSRIs do not reduce disability and dependency after clinical stroke but only improve depression (223). Finally, atorvastatin, a drug commonly prescribed as part of secondary prevention in stroke patients, reduces lesion volume and attenuates neurological deficits in rat tMCAO, possibly by promoting Treg migration to the infarcted brain (182).

Despite the plethora of Treg-targeted therapies available, some disadvantages remain. Broadly, these include the potential toxicity of Treg stimulants, the lead-time for regulatory approval, and the stability of expanded Tregs (224). A novel Treg-targeted therapy for stroke must show a good safety profile and have robust pre-clinical stroke effectiveness. Ideally, it will already exist on the market for another medical condition. It is for this reason that in this thesis we considered the immunomodulator fingolimod.

1.5 Fingolimod

1.5.1 Fingolimod Pharmacology

Fingolimod (FTY720), an analogue of the immunosuppressant myriocin, was first described in 1994 (225). The drug displayed clinical potential after the discovery that it prolonged skin allograft survival in animal models, and subsequently demonstrated

efficacy in several animal models of organ transplantation (226). It was also shown to prevent ischemia-reperfusion (IR) injury in organs such as the liver and kidney (227, 228). Despite these preclinical successes, clinical trial results showed insufficient benefits in renal transplantation, and development for this indication was halted. However, data from pre-clinical models of multiple sclerosis (experimental autoimmune encephalomyelitis) suggested the drug may provide more benefit in the treatment of autoimmune and neurodegenerative diseases (229). Following positive clinical trials, fingolimod was FDA-approved for the treatment of multiple sclerosis (MS) in 2010 under the brand name Gilenya (230, 231).

Administered orally as a pro-drug, fingolimod's absorption is food-independent and slow (maximal plasma concentration reached after 12-16 hours). However, the drug has a high bioavailability of 93% (232). It reaches steady-state concentrations after 1-2 months during daily intake. The half-life of FTY720 in humans averages ~9 days and its pharmacology does not appear to be affected by age, weight, sex, or ethnicity (233). Notable adverse effects include herpetic viral infections, bradycardia, atrioventricular block, and macular oedema (234).

Fingolimod is predominantly phosphorylated into its active metabolite via sphingosine kinase 2 (SphK2), an isoenzyme highly expressed in the brain and brain microvasculature (235). Once activated, the drug displays a high affinity for four of the five sphingosine-1-phosphate receptors (S1P1, S1P3, S1P4, and S1P5), a family of G protein-coupled lipid cell surface receptors which are involved in diverse processes ranging from cell death and proliferation to vascular functions to operation of the nervous system (229).

In total, three main mechanisms have been suggested for the neuroprotective effects of fingolimod. In MS, the principle mechanism of action of fingolimod is thought to involve manipulation of the role sphingosine-1-phosphate, the endogenous bioactive lipid agonist of the S1P receptor, plays in immune cell trafficking. By acting as a functional antagonist of the S1P1 receptor (S1P1R) (inducing receptor internalization and degradation), fingolimod stops the egress of CCR7+ T cells from lymph nodes. This prevents access of pro-inflammatory and neurotoxic cells to the peripheral circulation and the central nervous system (236). Beyond lymphopenia, however, fingolimod also has direct functional agonistic activity involving S1P1 and S1P3 receptors providing pro-survival and anti-inflammatory effects (237, 238). Finally, receptor-independent mechanisms in which fingolimod binds to specific cellular proteins involved in intracellular signalling pathways or epigenetic transcription may also provide neuroprotection (239, 240).

1.5.2 Fingolimod in Animal Models of Stroke

While stroke and multiple sclerosis have a different aetiology, some pathophysiological processes (e.g., role of adaptive immune cells and of inflammation) play a role in both conditions, suggesting the diseases may respond to the same drug treatments, such as natalizumab or fingolimod (241-243).

Several pre-clinical studies suggest fingolimod may be one of the most compelling candidate stroke therapies characterised to date (244-251). The drug has proven effective in various rodent models of stroke at concentrations ranging from 0.25 to 2 mg/kg, normally administered via intraperitoneal injection. Fingolimod provided benefit in both transient and permanent focal ischemia, although results in transient ischaemia appear to be more consistent (252). It has been shown to improve short and

long-term histological and functional outcomes, even when administered several hours after the onset of ischemia (251). In fact, fingolimod is not only effective in an acute or subacute setting, but may also promote repair when administered as late as 24 hrs after stroke (249). As for MS, mechanisms of action for fingolimod in stroke can be broadly divided into three streams, namely: 1) functional antagonist activity (lymphopaenia), 2) functional agonist activity (encompassing vasoprotection, endothelial cell effects, macrophage/microglia effects, direct neuroprotection, etc.,), and 3) receptor-independent activity (233).

Daily administration of 1 mg/kg of fingolimod produces a >80% drop in peripheral lymphocytes within 6 hours of first administration in mice, with cell counts remaining significantly reduced after 7 days of treatment (253). The subsequent reduction in brain-infiltrating T cells is thought to play a pivotal role in fingolimod-mediated neuroprotection in stroke (254).

Furthermore, fingolimod may provide vascular protection post-ischaemia, again in a manner related to immunomodulation. By reducing circulating lymphocytes, fingolimod can decrease interactions between these cells and platelets/endothelial cells, which leads to reduced thrombosis and associated inflammation, improving microvascular function (115). Fingolimod-mediated reductions in adhesion molecule expression (e.g., ICAM-1) likewise ameliorate leukocyte plugging and the associated "no-reflow phenomenon" (249).

Fingolimod can also act at endothelial S1P receptors to regulate the endothelial cell barrier (255). By stimulating S1P1 receptors on endothelial cells, greater amounts of adherens junction proteins are recruited for assembly (256). In this way fingolimod

can enhance cell-to-cell contact at the BBB and limit, for example, post-ischaemic neutrophil infiltration.

The expression of S1P receptors on cells such as neurons, astrocytes, microglia, and oligodendrocytes has also prompted researchers to investigate a potential direct neuroprotective effect of fingolimod (257). However, while research in mice has shown fingolimod agonist activity at S1P receptors can promote neuronal survival (245, 258), other studies show the drug provides no protection against glutamate excitotoxicity or hydrogen peroxide (249), suggesting further investigation of this specific mechanism may be required. Similarly, the ability of fingolimod to promote longer-term stroke recovery through reducing astrogliosis or enhancing oligodendrocyte myelination potential also needs more extensive examination (259-261).

One mechanism which has garnered recent interest is the effect of fingolimod on local microglia and infiltrating macrophages. Fingolimod significantly downregulates expression of key inflammatory mediators released by LPS-stimulated microglial cells (262). Furthermore, whereas brain ischaemia induces pro-inflammatory M1 microglia, fingolimod can re-polarize these cells toward an anti-inflammatory M2 phenotype, potentially via activity at the S1P3 receptor (263). The promotion of the M2 phenotype by fingolimod has also been shown to enhance angiogenesis and improve behavioural recovery in a mouse photothrombotic stroke model (264).

Finally, accumulating evidence also points to receptor-independent mechanism involving fingolimod, most interestingly an epigenetic ability (240). Fingolimod, via inhibition of histone deacetylases, may decrease T cell activation, increase

neurotrophic factor generation, and rescue memory deficit. To date, however, the contribution of these effects to fingolimod-mediated neuroprotection in stroke has not been examined.

In summary, fingolimod is a promising candidate stroke immunotherapy, and a recent systematic review and meta-analysis of fingolimod efficacy in pre-clinical stroke has highlighted the drug both reduces infarct volume and improves neurobehavioral outcomes (265). However, aspects of the STAIR guidelines (266) (e.g., different species, presence of comorbidities) have not yet been addressed. Separately, mechanisms beyond lymphopenia and direct neuroprotection (such as an effect on Tregs) have not been robustly studied in AIS.

1.5.3 Clinical Trials of Fingolimod in Human Stroke

Four pilot clinical trials have been conducted in stroke patients (267-269). The first in 2014 was an open-label, evaluator-blinded, non-randomised study that examined the effectiveness of a three-day course of once daily 0.5mg fingolimod (n = 11) compared to standard care alone (n = 11) (inclusion criteria: age >18 years, admission NIHSS score ≥5, anterior circulation ischemic stroke, and time of onset to admission max 4.5–72 hours) (270). Importantly, use of other immunomodulatory drugs was employed as an exclusion criterion. Patients who received fingolimod displayed reduced circulating lymphocytes, milder neurological deficits, and improved functional recovery. Fingolimod also limited secondary tissue injury from admission to 7 days and decreased microvascular permeability. The rate of adverse drug effects including bradycardia, macular oedema, and infection did not differ between study group and control.

Building on this, in 2015, a second randomised, open-label, evaluator-blinded study assessed the efficacy of fingolimod in combination with tPA (n = 22) versus tPA alone (n = 25) for treating AIS (inclusion criteria: age 18–80 years, first-ever stroke due to anterior or middle cerebral artery occlusion, and admission NIHSS score ≥5) (268). In line with the previous study, a total of three doses of 0.5 mg oral fingolimod were administered on consecutive days. Compared with patients who received tPA alone, patients who received the fingolimod-tPA combination lowered circulating lymphocytes, reduced lesion size and haemorrhagic volume, and improved both short and long-term neurological recovery at day 90. Once more, no serious adverse effects were recorded in fingolimod-treated patients.

In 2018, Tian *et al* also investigated whether a combination of fingolimod (administered as above) and tPA improved clinical stroke outcome versus alteplase alone (n = 23 each) (269). Patients receiving fingolimod exhibited early clinical improvement at 24 hours and a favourable shift of modified Rankin score (mRS) distribution at 90 days. Infarct growth at 24 hours was also suppressed. Mechanistically, Tian *et al.* argued the lymphopaenic effects of fingolimod may preserve microvasculature at this crucial early stage through reduced thromboinflammation.

A positive result at 3 months was also demonstrated by Liantao *et al.* who in 2019 also evaluated the impact of a fingolimod-tPA combination (n = 45) versus alteplase alone (n = 45) (271). While in this study no significant differences in NIHSS score were noted between groups at 14 days, fingolimod did significantly improve neurological recovery at 90 days.

Overall, fingolimod appears promising as a stroke therapeutic as the drug prevents, haemorrhagic transformation and BBB disruption, reduces infarct size and improves functional recovery. A further trial characterising potential combination of fingolimod with mechanical thrombectomy is already in progress (NCT Identifier: NCT04629872). It should be noted most studies of fingolimod in clinical stroke carried out to date have involved small numbers of patients. Likewise, these studies have focused primarily on functional outcomes, and potential mechanisms beyond fingolimod-mediated lymphopaenia remain unexplored.

1.5.4 The Effect of Fingolimod on Regulatory T Cells

Several recent studies have examined the effect of fingolimod on Tregs in humans, rodents, and *in vitro* models (272-276). Co-culturing Tregs with high dose (1000 ng/ml or ~2.9 micromolar) fingolimod has been shown to enhance expression of CD25+ and FoxP3+, while also upregulating levels of associated anti-inflammatory cytokines (TGF-β1) (277). The capacity of Tregs to inhibit effector T cell proliferation is also boosted. In mice, fingolimod administration likewise enhances Treg frequency in disease models ranging from colitis to acute kidney injury (276, 278, 279). In such experiments, fingolimod treatment prominently upregulated expression of FoxP3, IL-10, TGF-β1, and CTLA4, demonstrating a direct effect of the drug on Treg function (278). Separately, depletion and adoptive transfer of Tregs were associated with loss and recovery, respectively, of the beneficial effects of fingolimod (279). Significantly, extensive results from fingolimod-treated MS patients confirm the drug increases Treg frequency alongside functional markers such as CD39 (272, 274, 280, 281). Overall, these observations, combined with the beneficial effects of both fingolimod and Tregs

in ischaemic stroke, discussed above, suggests fingolimod-mediated neuroprotection may be mediated, at least in part, by Tregs.

1.6 Pregnancy-Specific Glycoproteins (PSGs)

1.6.1 PSG Pharmacology

Pregnancy-specific glycoproteins (PSG) are a group of highly homologous proteins synthesized by placental trophoblasts (386). Encoded by at least 11 different genes, the PSG family encompasses 30 different proteins through alternatively spliced mRNAs (282). Detectable in maternal blood as early as 7 days post-implantation, the serum levels of PSGs reach 200–400 μg/ml by the end of gestation, making them the major group of secreted proteins (387). While PSGs are pivotal for successful pregnancy (low levels are associated with spontaneous abortion and intrauterine growth retardation), these proteins have garnered more recent interest for their profound immunomodulatory properties (388, 389). PSG molecules impair T cell proliferation, enhance secretion of anti-inflammatory cytokines (e.g., IL-10) by macrophages, reduce pro-inflammatory factor production, and shift T cell differentiation towards a Th2-type immunity (390-394).

1.6.2 The Effect of PSGs on Regulatory T Cells

Evidence also exists to suggest PSG molecules may be strong promoters of the Treg phenotype, most likely due to the activation of latent TGF-β (395). Increased FoxP3 expression was observed in cells incubated with PSG1 (396). Likewise, mice administered PSG1 showed increased numbers of Tregs in the colonic lamina propria, a response which proved protective in a model of colitis (397). Enhanced numbers of Tregs and improved recovery was also noted in a mouse model of acute graft-versus-

host disease (398). Finally, vector-based expression of PSG1 in a model of rheumatoid arthritis ameliorated clinical symptoms while increasing splenic Treg cells (387). Taken together, these data suggest PSG1 strongly promotes the Treg phenotype and provides marked improvement in disease states characterised by excess inflammation.

1.7 Thesis Hypothesis, Aims, & Objectives

1.7.1 Hypothesis

A review of the stroke immunology literature suggests Tregs may provide neuroprotection post brain-ischaemia. However, to date, this hypothesis has not been robustly tested in all stroke subtypes (such as pMCAO in mice, or mild stroke in humans). Separately, fingolimod and rPSG1-Fc have demonstrated a capacity to increase Treg frequency/function. Whether this mechanism could provide benefit in animal models of stroke, however, has not been investigated. The over-arching hypothesis of this thesis is that regulatory T cells play a pivotal neuroprotective role in ischaemic stroke, and that by administering immunomodulatory drugs which enhance T cell frequency and/or function, recovery can be improved (**Fig. 1.4**).

1.7.2 Aims

The two over-arching aims of this thesis were (a) to explore the overall role of regulatory T cells in ischaemic stroke recovery, and (b) to investigate the neuroprotective and immunomodulatory effects of potential Treg-targeted stroke immunotherapies (fingolimod and rPSG1-Fc).

1.7.3 Objectives

In order to achieve these aims, the following objectives were identified:

- **Objective 1:** to determine whether the small molecule fingolimod increases regulatory T cell frequency in a mouse model of permanent brain ischaemia (**Chapter 2**).
- **Objective 2:** To determine the impact of fingolimod on Treg suppressive function in a mouse model of permanent brain ischaemia (**Chapter 3**).
- **Objective 3:** To investigate whether the recombinant rPSG1-Fc increases regulatory T cell frequency in a mouse model of permanent brain ischaemia and enhances functional recovery (**Chapter 4**).
- **Objective 4:** To quantify the impact of mild ischaemic stroke on Treg frequency and function in stroke patients (**Chapter 5**).

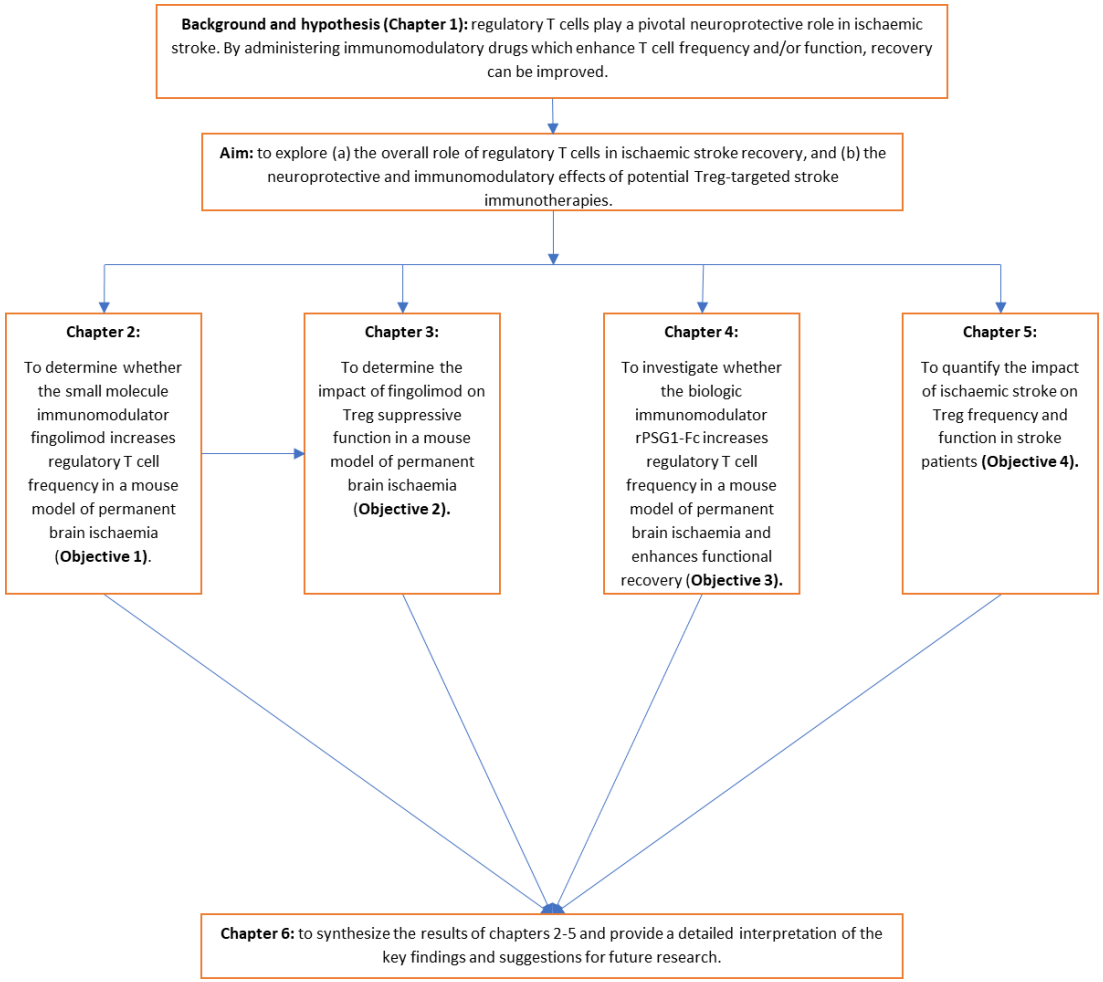


Figure 1.4: Thesis outline.

Chapter 2

The effect of fingolimod on regulatory T cells in a mouse model of brain ischaemia

In the previous chapter, a broad overview of the immune response post-stroke was provided. Notably, the part Tregs may play in stroke recovery was highlighted, and the importance of therapies which could enhance either Treg number or function was stressed. In particular, the possibility of upregulating Treg frequency or suppressive capacity post-stroke via manipulation of the S1P pathway was detailed. In this chapter, the role of Tregs post-stroke is explored through the lens of fingolimod (FTY720), a sphingosine-1-phosphate receptor agonist with known immunomodulatory effects. Specifically, it was investigated whether fingolimod increases regulatory T cell frequency in a mouse model of permanent brain ischaemia.

The text of this chapter has been adapted from the following publications:

Malone K, Diaz A, Shearer J, Moore AC, Waeber C. The Effect of Fingolimod on Regulatory T Cells in a Mouse Model of Brain Ischaemia. Journal of Neuroinflammation. 2021; 18(1):37

Diaz AC, **Malone K**, Shearer JA, Moore AC, Waeber C. Preclinical Evaluation of Fingolimod in Rodent Models of Stroke with Age or Atherosclerosis as Comorbidities. Frontiers in Pharmacology. 2022; 13:920449.

Diaz AC, **Malone K**, Shearer JA, Moore AC, Waeber C. Histological, behavioural and flow cytometric datasets relating to acute ischaemic stroke in young, aged and $ApoE^{-/-}$ mice in the presence and absence of immunomodulation with fingolimod. Data in Brief. 2021; 36:10714.

Abstract

Background*:* The role of the immune system in all stages of stroke is well-recognised. Fingolimod, an immunomodulatory agent licensed for the management of relapsing-remitting multiple sclerosis, has been shown to provide benefit in rodent models of stroke. Its mechanism of action, however, remains unclear. We hypothesised that fingolimod increases the number and/or function of regulatory T cells (Treg), a lymphocyte population known to promote stroke recovery. The primary aim of this study was to rigorously investigate the effect of fingolimod on Tregs in a mouse model of brain ischaemia. The effect of fingolimod in mice with common stroke-related comorbidities (age and hypercholesteremia) was also investigated.

Methods*:* Young (15-17 weeks), aged (72-73 weeks), and $ApoE^{-/-}$ mice fed a high fat diet (20-21 weeks) (all C57BL/6 mice) underwent permanent electrocoagulation of the left middle cerebral artery. Mice received either saline or fingolimod (0.5 mg/kg or 1 mg/kg) at 2-, 24-, and 48-hours post-ischaemia via intraperitoneal injection. Another cohort of young mice (8-9 weeks, 17-19 weeks) received either short-term (5 days) or long-term (10 days) fingolimod (0.5 mg/kg) treatment. Tregs were quantified in blood, spleen, and lymph nodes using flow cytometry. FoxP3+ cell infiltration into the ischaemic brain was quantified with immunohistochemistry.

Results*:* Fingolimod significantly increased the frequency of Tregs within the CD4+ T cell population in blood and spleen post-ischaemia in all three mouse cohorts compared to untreated, ischemic mice. The highest splenic Treg frequency in fingolimod-treated mice was observed in $ApoE^{-/-}$ mice (9.32 ± 1.73% vs. 7.8 ± 3.01% in young, 6.09 ± 1.64% in aged mice). The highest circulating Treg frequency was also noted in $ApoE^{-/-}$ mice (8.39 ± 3.26% vs. 5.43 ± 2.74% in young, 4.56 ± 1.60% in

aged mice). Fingolimod significantly increased the number of FoxP3+ cells in the infarct core of all mice. However, pooled analysis from young, aged, and ApoE$^{-/-}$ mice showed peripheral and brain Tregs showed a negative correlation with functional recovery in fingolimod-treated mice.

Conclusions: Fingolimod increases Treg frequency in spleen and blood post-ischaemia and enhances the number of FoxP3+ cells in the ischaemic brain. The effect of fingolimod on this regulatory cell population could provide neuroprotective activity and may be exploited as part of future stroke therapy.

2.1 Introduction

Fingolimod has proven effective in various rodent models of stroke, including both transient and permanent focal ischaemia (265). The drug significantly reduces both infarct volume and neurological deficits, even when administered several hours after the onset of ischaemia (232). In fact, fingolimod is not only effective in an acute or subacute setting, but also promotes repair in rodents when administered as late as 24 hours post-ischaemia (250). Small-scale pilot studies investigating fingolimod in ischemic stroke patients demonstrated the drug to be safe and effective (267-269). Nevertheless, while considerable evidence supports the future use of fingolimod in stroke therapy, the exact mechanism of action remains unclear. Although, immunomodulation is likely to be involved (233).

Fingolimod administration post-stroke has been associated with reduced levels of inflammatory markers in the brain, improved endothelial function, and decreased incidence of haemorrhagic transformation (283). It is widely accepted that fingolimod reduces neuroinflammation in multiple sclerosis (MS) by abrogating the sphingosine-

1-phosphate (S1P)-dependent egress of naive and central memory T cells from lymph nodes (284). Pre-clinical stroke studies employing lymphocyte-deficient Rag1-/- mice support the involvement of T cells in fingolimod-afforded neuroprotection (246). However, in separate studies fingolimod treatment has failed to significantly reduce infarct volume or neurobehavioural dysfunction despite inducing profound lymphopenia, indicating that other mechanisms may contribute (253).

Regulatory T cells (Tregs) appear to improve disease outcome in stroke, with the only detrimental effects thought to be a role in secondary microthrombosis (134). Tregs, characterised in mice by high and constitutive expression of the alpha subunit of the IL-2 receptor, CD25, and the transcription factor forkhead box P3 (FoxP3), constitute approximately 20% of all CD4+ T cells found in the ischaemic hemisphere in mice (118). Mechanisms of Treg-mediated neuroprotection include secretion of IL-10, production of TGF-β and IL-35, priming of M2 macrophages, and reduced inflammatory cytokine secretion (128, 129, 134, 135, 143). Clinical evidence suggests a reduction in Treg circulating number and function in peripheral blood post-stroke (165). An imbalance between Th17 cells and Tregs has also been shown to occur (67, 157). Several recent studies indicate that fingolimod increases the number of Treg and regulatory properties in humans, rodents, and *in vitro* (272, 274-277). These observations, combined with the beneficial effects of both fingolimod and Tregs in ischaemic stroke, suggest that fingolimod-mediated neuroprotection may be mediated, at least in part, by Tregs.

The principal aim of this study was to test the hypothesis that fingolimod treatment increases Treg frequency and absolute numbers in the blood and secondary lymphoid organs of mice at one-week post-ischaemia. A second objective was to determine

whether fingolimod increases the number of infiltrated FoxP3+ T cells into the infarcted brain. A third objective was to investigate whether the immunomodulatory effects of fingolimod treatment on Treg cells differed in mice with stroke co-morbidities, namely aged mice and ApoE$^{-/-}$ mice fed a high-fat diet (the latter representative of patients suffering from hypercholesteremia). Age and hypercholesteremia were chosen as co-morbidities due to known aberrations in Treg number and function in these states, alongside the increased stroke risk (285, 286). Finally, the general effects of fingolimod on peripheral lymphocyte counts and distribution were characterised.

A three-day course of daily fingolimod treatment was administered in this study, in line with clinical trials of the drug in ischaemic stroke (267, 269). A follow-up study then investigated the effect of short-term (5 days) vs. long-term (10 days) fingolimod administration to test the hypothesis that protracted treatment showed enhanced effects. We used a model of permanent distal middle cerebral artery occlusion (pMCAO) (38). This model is representative of human middle cerebral artery infarction in which cerebral reperfusion does not occur. Similar to most human stroke cases, the infarct is located principally within the cortex (287). Moreover, the model provides high reproducibility and low mortality and has been strongly recommended for studies in which clinical translation is a primary focus (35). As a result, this study was capable of testing fingolimod in a pre-clinical model of brain ischaemia most closely matched to human stroke.

2.2 Methods

2.2.1 Ethics Statement

Animal experiments were carried out in accordance with the European Directive 2010/63/EU, following approval by the Animal Ethics Committee of University College Cork and under an authorization issued by the Health Products Regulatory Authority Ireland (license number AE19130/P042 and AE19130/P075). The study was conducted and its immune-related results reported according to the ARRIVE guidelines (288). The data associated with all outcome measures is summarized in Diaz *et al.* (2021) (289).

2.2.2 Mice

All mice were sourced from Envigo unless otherwise stated. For experiments carried out in designated "young" mice populations, male C57BL/6JOlaHsd (15-17-week old) mice were used unless otherwise stated. For experiments carried out in "aged" mice, C57BL/6NCrl male and female mice were obtained at 58-62 weeks of age (Charles River, UK); procedures were carried out at 72-73 weeks of age. Male ApoE-/- (Apoetm1Unc) mice were received at 4-5 weeks of age and starting at 8 weeks of age were placed on an adjusted calorie high fat diet (TD.88137) for 12 weeks. Subsequent experiments were carried out at 20-21 weeks of age. All mice were acclimatized for at least one week before any procedure took place. Mice were group housed in individually ventilated cages in a specific-pathogen-free facility. Mice were exposed to a 12-hour light/12 hour-dark cycle and kept at a temperature of 20-24°C and a relative humidity of 45-65%. Mice were provided with environmental enrichment and ad libitum access to both food and water. A total of n = 257 mice were included as part of this study. Data from an initial pilot study confirmed n > 3 per group would be sufficient to detect the expected effect of fingolimod on Treg frequency in spleen, while n > 6 per group would be sufficient to detect the expected change of CD3+ T

cells in brain. Notably, for all experiments n = 16 mice were allocated to each group unless otherwise stated. This number was determined by an a priori sample size calculation conducted as part of a larger research project investigating the effect of fingolimod on histological and functional stroke outcomes. Based on a previously published meta-analysis (251), these 16 mice per group were required to detect changes in infarct size and neurological score (significance level set at $\alpha = 0.05$, power of 80%). Where possible, tissue from all mice under study was collected to both maximize power for other measurements and to allow for comparison of immunological results with other outcomes. Pre-determined exclusion criteria included mice with serious uncontrollable haemorrhage as well as mice with thermal or physical damage of the cortex. The number of mice excluded for meeting such criteria or human endpoints are outlined for each cohort in Supplementary Material (**Table S2.1)**.

2.2.3 Ischaemia Model

A permanent distal middle cerebral artery occlusion model was employed, as previously described (38). All mice were randomly allocated to treatment groups using an online pseudo-random number generator (randomizer.org) a few days prior to surgery. Mice were anesthetized by vaporiser with isoflurane (3-4% for induction; 1-2% for maintenance) in O_2/N_2 (30%/70%). Suitable depth of anaesthesia was confirmed by absence of the pedal withdrawal reflex. Body temperature, monitored by rectal probe, was maintained at 37°C with a homeothermic blanket system. Hair removal cream (Veet) was applied to the area between the left ear and left eye. The site was washed repeatedly with saline and iodine. The site was anesthetised topically with 0.5% bupivacaine (0.1ml) before being incised. The temporal muscle was

retracted to expose the temporal and parietal bones. In sham animals, only the skin incision and exposure of the skull was performed. A small craniotomy was performed over the bifurcation of the middle cerebral artery (MCA) and the dura was removed to expose the MCA (including parietal and frontal branches). The distal portion of the MCA, including the branches and the main artery below the bifurcation were occluded using a small vessel bipolar electrocoagulation forceps (Bovie Bantam Pro electrosurgical generator (#A952) /McPherson 3 1/2" straight forceps (#A842) (Symmetry Surgical Inc, USA)). The middle cerebral artery was cut to confirm successful occlusion of the artery and prevent reperfusion. The burr hole was then covered with bone wax and the incision sutured. Anaesthesia was discontinued and mice were allowed to recover in a heated chamber (32°C) for 30 minutes before being returned to their home cage. Recovery of experimental mice was monitored daily through use of a scoresheet which graded weight loss, appearance changes, behaviour, and neurological function.

2.2.4 Fingolimod Treatment

At 2, 24- and 48-hours post-ischaemia, mice received either normal saline, or 0.5 mg/kg or 1 mg/kg fingolimod (Novartis Institutes for Biomedical Research, Basel) via intraperitoneal (i.p.) injection. Aged and $ApoE^{-/-}$ mice received either normal saline or 0.5 mg/kg fingolimod via i.p. injection. For young mice allocated to the treatment duration study, mice received either normal saline, or fingolimod (0.5 mg/kg) for 5 days followed by normal saline, or fingolimod (0.5 mg/kg) for 10 days. A researcher not associated with the surgery prepared treatment solutions (pH 7) for volumes no greater than 250µl per injection.

2.2.5 Neurological Deficit Evaluation

A subset of young and aged mice underwent neurological evaluation 72 hours post-stroke to characterise the effect of age and pMCAO on neurobehavioural recovery. Each mouse was placed in a clear Perspex cylinder (12.5 cm Diameter x 23.5 cm Height) for 5 minutes. The sessions were videoed (Canon Legria HFR706), so that a neurological score could be calculated at a later date. To calculate this score, the number of times the mouse used a paw for weight support against the wall of the cylinder during a rear was counted over a five-minute period (a minimum of 20 contacts were recorded). Specifically, the independent use of the left (L) or right (R) forepaw, or simultaneous use of both (B) forepaws was noted. The 3 numbers were then expressed as a percentage of all paw contacts with the wall to obtain a neurological deficit score (R-L)/(R+L+B). The results of this analysis are presented in Supplementary Material (**Fig. S2.1, S2.2)**.

2.2.6 Tissue Collection and Processing

At 7 days post-ischaemia (or at 10 days in the treatment duration study), mice were culled by anaesthetic overdose (200 mg/ml i.p.; Euthatal; Merial, France). Blood was collected from the descending aorta and transferred into EDTA-coated tubes (Cruinn Diagnostics, #262197) (approximately 500µl). Mice were then perfused transcardially with 20ml cold phosphate buffered saline (PBS) (Sigma-Aldrich, #P4417). The brain was removed from the skull, frozen in isopentane at -42°C and stored at -20°C. Brain sections (20 µm) were cut at 500 µm intervals on a cryostat and stored at -20°C. Cervical and inguinal lymph nodes, and spleen tissue were harvested and stored in PBS until further manipulation. Spleen and lymph node tissues were mechanically dissociated using the back of the plunger of a 3ml syringe (Fischer Scientific,

#14955451) in approximately 3ml PBS in a sterile 6-well plate. The resulting cell suspensions were passed through a 70µm cell strainer (Cruinn Diagnostics, #542070G) and collected in a 50ml conical tube. Wells and strainers were washed twice with 1X Dulbecco's PBS (Sigma-Aldrich, #D8537). Spleen and blood samples were re-suspended in 5ml of 1X red blood cell lysis buffer and incubated for 5 minutes at room temperature (eBioscience, #430054). The lysis reaction was stopped by adding 20ml of 1X PBS. All samples were then washed twice with 1X PBS, re-suspended in an appropriate volume of PBS and counted using trypan blue (Sigma-Aldrich, #T8154) to determine total cell concentration and viability.

2.2.7 Flow Cytometric Analysis

Samples were incubated for 5 minutes with 50µl of anti-mouse CD16/CD32 eBioscience, #14016182) (Clone 93, 1:100). The respective cell suspensions were then stained for anti-mouse CD45 (PerCP-CY5.5, # 45045182) (30-F11, 1:100), CD3 (PE-Cy7, #14003182) (145-2C11, 1:100), CD4 (FITC, #11004282) (RM4-5, 1:800), CD8 (Pacific Blue, #MCD0828) (5H10, 1:100), and CD25 (APC, #17025182) (PC61.5, 1:100) (all eBioscience). A live/dead stain (1:10,000 solution) was also added to each sample (Fixable Viability Dye eFluor 780) (eBioscience, #65086514). Samples were then incubated for 30 minutes at 2-8°C in the dark. Post-incubation, the samples were washed, fixed, permeabilised, and stained intracellularly for anti-mouse FoxP3 (PE, #12577382) (FJK-16s, 1:100,), in accordance with the instructions provided with the Mouse Regulatory T Cell Staining Kit #1 (eBioscience, #88811140). Samples were then re-suspended in an appropriate volume of PBS. Flow cytometric analysis was performed with a LSRII flow cytometer (Becton Dickinson). Compensation control was set using BD CompBead Anti-Rat/Anti-Hamster Particles Set (BD, #552845).

Data was analysed using FlowJo (v10) according to the following gating strategy: live cells (as determined by live/dead stain), lymphocytes (as determined by FSC/SSC), T lymphocytes (as determined by CD3+), CD4+ and CD8+, and regulatory T cells (CD4+ T cells which co-express CD25 and FoxP3). Gates were set according to unstained samples and fluorescent minus one controls. The gating strategy required for the determination of Treg frequency (expressed as CD4+ CD25+ FoxP3+ / CD4+ %) is outlined in **Fig. 2.1**. For spleen samples, high-dimensional cytometry data was also visualised in two dimensions based on the t-distributed Stochastic Neighbour Embedding (t-SNE) algorithm (Iterations = 1000, perplexity = 20) (Supplementary Material, **Fig S2.4 – S2.6**). Absolute cell counts for all tissues were calculated in accordance with the instructions provided with the CountBright Absolute Counting Beads (Molecular Probes, #C36950). All results are reported according to the Minimum Information About a Flow Cytometry Experiment (MIFlowCyt) (290). All data was uploaded to Mendeley Data.

2.2.8 Immunohistochemistry

Immunohistochemical analysis of immune cell infiltration into brain tissue was performed on n = 10 mice per group. Slides were brought from -20°C to room temperature and dried overnight. Sections were fixed with ice cold acetone (-20°C) for 10 minutes, dried for 30 minutes at room temperature and washed twice with PBS. Slides were incubated in blocking solution (5% Rabbit Serum (Vector Laboratories, #S-5000) in 0.01M PBS) for 30 minutes and endogenous biotin was blocked according to the instructions provided with the Avidin/Biotin Blocking Kit (Vector Laboratories, #SP-2001). Sections were incubated with primary antibodies against either CD3 (145-2C11, 1:500, #14003182, eBioscience) or FoxP3 (FJK-16s, 1:300, #14577382,

eBioscience) at room temperature for 60 minutes. Slides were washed twice with PBS then incubated with 3% H_2O_2 (Sigma-Aldrich, #H1009) for 30 minutes. Subsequently, slides were incubated with either a biotinylated goat anti-hamster (1:500, # PA132045, eBioscience) or a donkey anti-rat secondary antibody (1:500, #A18739, eBioscience) for 60 minutes at room temperature. Slides were washed twice with PBS. Immunoreactivity was visualized by the avidin-biotin complex method (Vectastain avidin-biotin complex Kit) (Vector Laboratories, #PK-4000) and developed for 10 minutes with diaminobenzidine (DAB, Vector Laboratories, #SK-4100). Slides were counterstained with eosin and then dehydrated sequentially in graded ethanol (70% for 2 minutes, 95% for 2 minutes, 100% for two minutes). Slides were washed twice in HistoChoice (Sigma-Aldrich, #H2779) for 2 minutes and then mounted with Permount (Fischer Scientific, #SP15-500). Finally, slides were visualized under an Olympus BX51 microscope (**Fig. 2.2**). A single representative image of the ischaemic core, undamaged ipsilateral tissue, and contralateral tissue were taken at the 20X objective lens. Three random representative images of the peri-infarct zone were also taken at this magnification. Positively stained cells were counted in the relevant regions of interest using ImageJ (291).

2.2.9 Statistical Analysis

The Kolmogorov–Smirnov test was used to test normality of all data. Flow cytometric and immunohistochemical data are displayed as 10-90 percentile box-and-whisker plots. The ROUT method (Q = 1%) was used to identify possible outliers, which were then screened for exclusion. Two-sided, independent-samples T tests were employed to investigate differences between two groups. One-way analysis of variance (ANOVA) followed by post-hoc Tukey's multiple comparisons was used to

investigate differences between three or more groups. One-way repeated measures ANOVA with post-hoc Tukey's multiple comparisons was used to investigate neurobehavioural results. Two-way repeated measures ANOVA followed by post-hoc Tukey's multiple comparisons was used to investigate differences between groups when the effect of two independent variables were studied. A p-value <0.05 was considered statistically significant. Statistical analysis was performed using GraphPad Prism 8.0. Correlations between experimental outcomes and lymphocyte subpopulation frequencies were investigated using Pearson's correlation analysis. The heatmap of linear correlation was visualized with GraphPad Prism version 9.0. All investigators remained blinded to treatment groups throughout analysis.

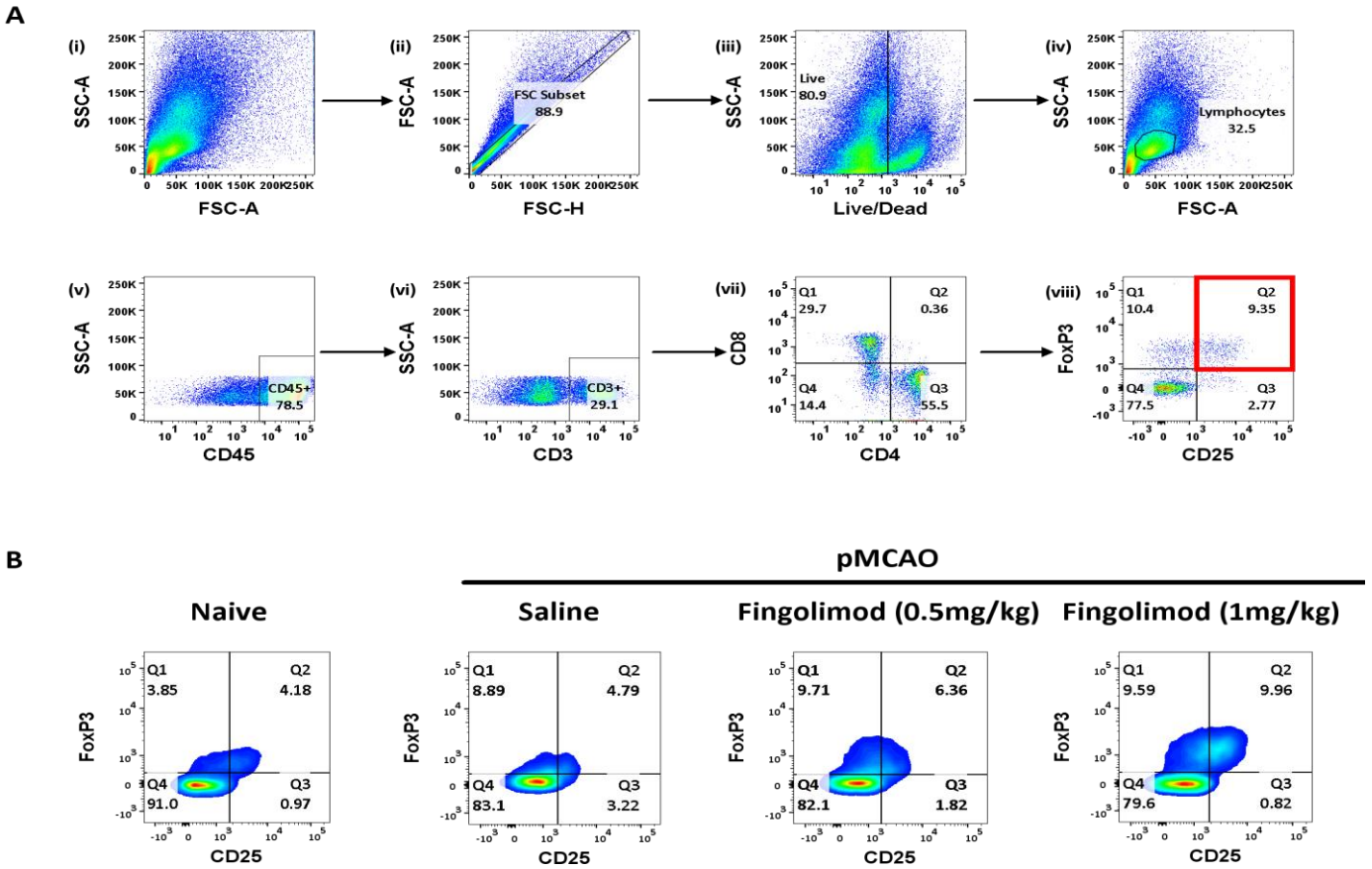


Figure 2.1: A) Gating strategy for determination of Treg frequency (i) Initial population, (ii) singlets, (iii) Live cells, (iv) lymphocytes, (v) CD45hi cells, (vi) CD3+ T cells (T cells), (vii) CD4+ T cells vs. CD8+ T cells, (viii) CD4+ CD25+ FoxP3+ T cells (quadrant in red) designated Tregs. B) Flow cytometric analysis of splenic Treg frequencies in a mouse model of brain ischaemia. 15-17-week-old male, C57BL/6 mice underwent permanent middle cerebral artery occlusion (pMCAO). At 2-, 24-, and 48-hours post-ischaemia, mice received either saline or fingolimod (0.5 mg/kg or 1 mg/kg) by intraperitoneal injection (n=16 mice per group). Age-matched mice who had not undergone pMCAO acted as immunological controls (n = 8). At 7 days post-ischaemia, flow cytometry was used to determine the frequency of splenic Treg cells. All gates were determined by both negative cells and fluorescence minus one controls.

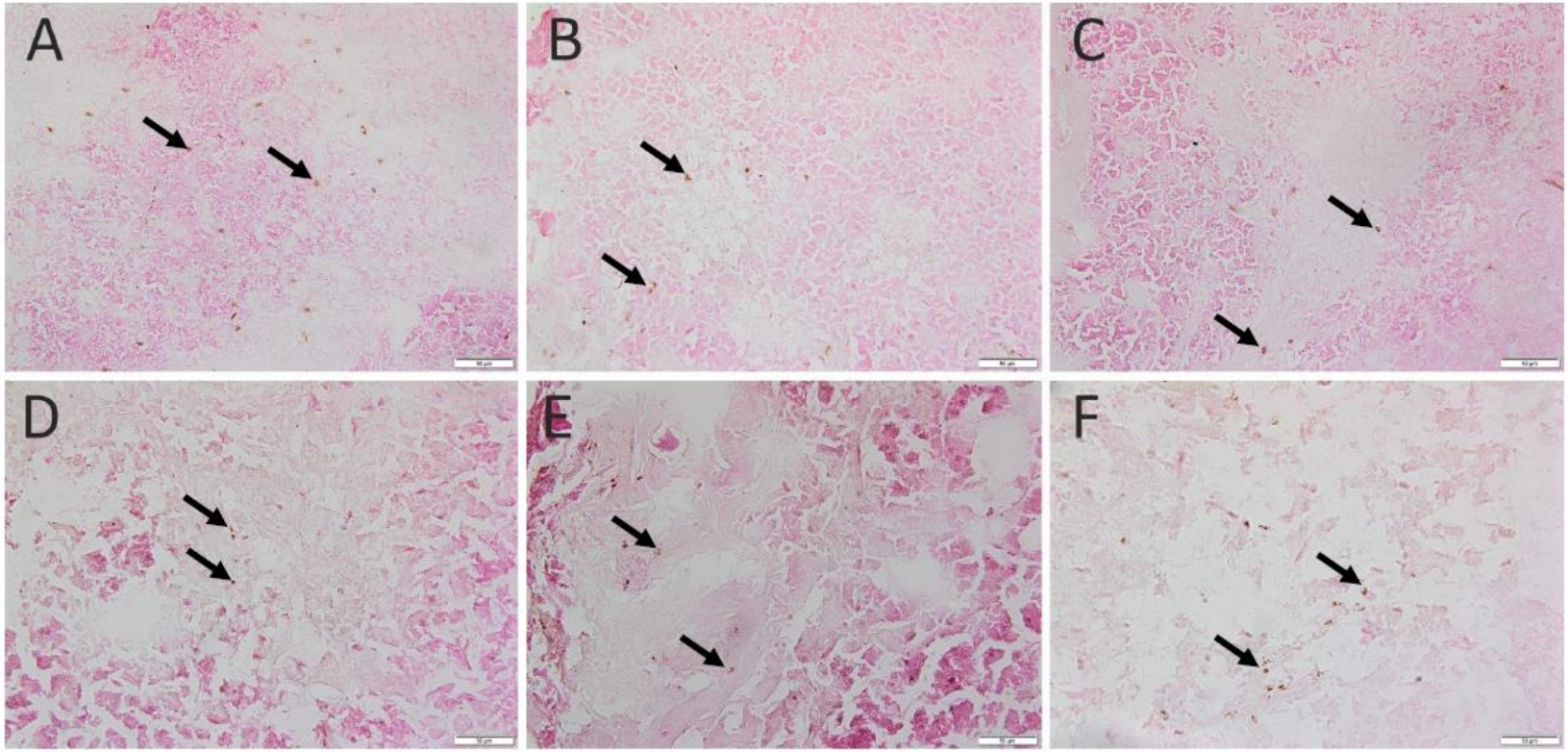


Figure 2.2: Representative immunohistochemistry images of CD3+ (A-C) and FoxP3+ (D-F) staining in the infarct core (A) of young mice post-pMCAO (t = 7 days). CD3+ images acquired with the 20X objective lens of an Olympus BX51 microscope. FoxP3+ images acquired with the 40X objective lens. Positive cells counted using ImageJ. A = CD3 (saline), B = CD3 (fingolimod 0.5 mg/kg), C = CD3 (fingolimod 1 mg/kg). D = FoxP3 (saline), E = FoxP3 (fingolimod 0.5 mg/kg), F = FoxP3 (fingolimod 1 mg/kg). Sample positive staining indicated via black arrows.

2.3 Results

2.3.1 Fingolimod increases Treg frequency in murine spleen and blood post-pMCAO

The impact of fingolimod on the frequency of peripheral Tregs (defined as CD4+ CD25+ Foxp3+ cells) was first established via flow cytometric analysis of blood, spleen, draining lymph nodes (cervical), and non-draining lymph nodes (inguinal) harvested from young mice at 7 days post-ischaemia. Mice received either normal saline, 0.5 mg/kg fingolimod, or 1 mg/kg fingolimod via i.p. injection at two hours post-pMCAO and again 24 and 48 hours later. Age-matched mice (n = 8) that had not undergone either surgery or treatment acted as naïve controls.

In comparison to non-ischaemic controls, stroke caused a significant increase in Treg frequency in both draining (p = 0.0080) and non-draining (p = 0.0019) lymph nodes (**Fig. 2.3**). No significant differences in Treg frequency were observed between ischaemic and non-ischaemic mice in spleen or blood.

Fingolimod significantly increased Treg frequency in the spleens of young mice post-ischaemia in a dose-dependent manner (p <0.0001). The 0.5 mg/kg dose was used for experiments in aged and ApoE-/- mice. In aged and ApoE$^{-/-}$ mice, fingolimod (0.5 mg/kg) also significantly increased splenic Treg frequency (p = 0.0348, 0.0002, respectively). Likewise, this dose of fingolimod was sufficient to increase Treg frequency in blood in all populations under study (Young: p = 0.0195, Aged: p = 0.0011, ApoE$^{-/-}$ mice: p = 0.0003). In draining lymph nodes, fingolimod (0.5 mg/kg) only boosted Treg frequency in young mice (p = 0.0140). In non- draining lymph nodes, only the higher dose (1 mg/kg) produced a significant

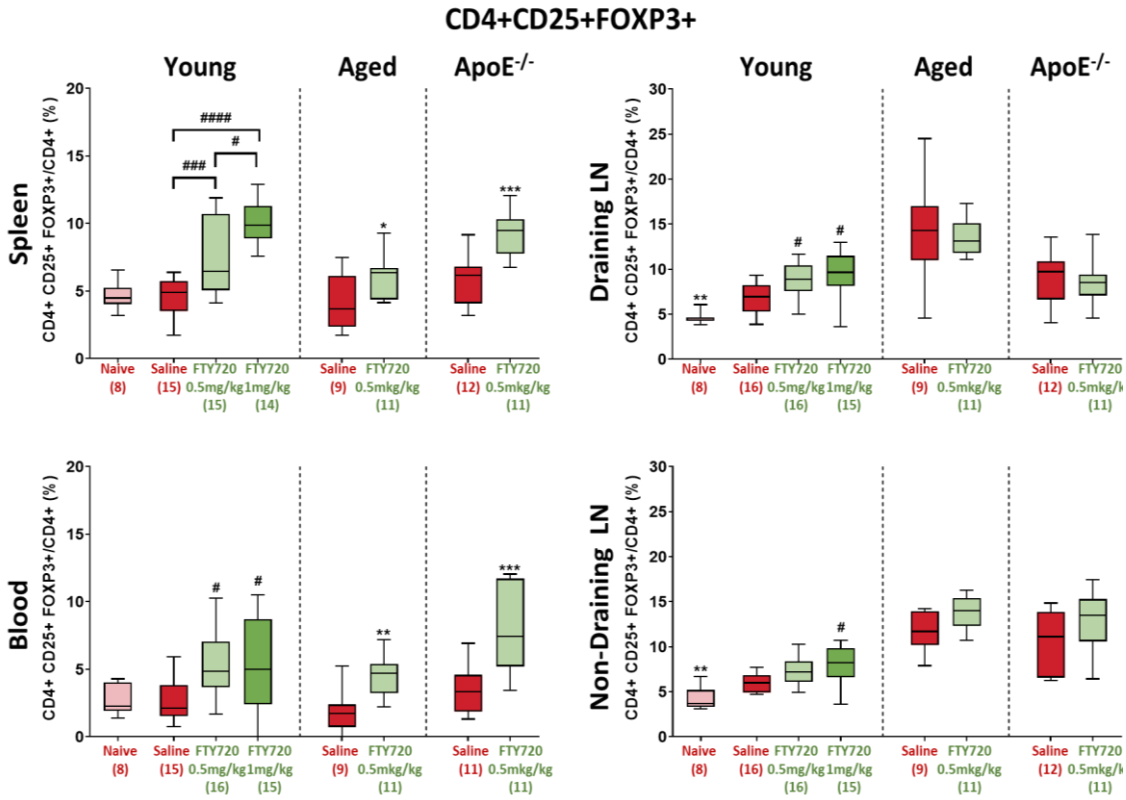


Figure 2.3: Frequency of CD4+ CD25+ FoxP3+ T cells in the blood and secondary lymphoid tissue across three individual mouse cohorts of brain ischaemia at 7 days as a result of fingolimod (FTY720) treatment on days 0, 1, 2. Two-sided, independent-samples T tests investigated differences between two groups (* = p<0.05, ** = p<0.01, *** = p<0.001 as compared to saline). One-way analysis of variance (ANOVA) tests with post hoc Tukey's multiple comparisons were performed to investigate differences between three or more groups (# = p<0.05, ## = p<0.01, ### = p<0.001 as compared to saline). Number of mice per group shown in parentheses on x-axis. Box-and-whisker plots exhibit 10-90 percentiles

response (p = 0.0150). Once more, however, this increase was only recorded in young mice. Overall, these results demonstrate that fingolimod treatment significantly increases the frequency of CD4+ CD25+ FoxP3+ Treg cells in the periphery (spleens and blood) of all three cohorts under study. Significant increases in Treg frequency in in lymph nodes were only observed in young mice.

2.3.2 Age has a major impact on peripheral Treg frequencies in lymph nodes at baseline and at 7 days post-pMCAO

In the last few years, the pivotal role draining lymph nodes in particular may play in brain immune surveillance and the development of neuroinflammatory disorders has

been proposed (292). Given the profound differences observed in Treg frequency in draining lymph nodes between young and aged mice post-pMCAO in **Fig. 2.3**, a follow-up study investigated whether age, ischaemia, or a combination of both factors was responsible. Peripheral Treg frequency was determined in young (n = 7 males, 6 females) and aged (n = 6 males, 8 females) mice cohorts at 7 days post-ischaemia. A corresponding group of young (n =7 males, 7 females) and aged (n = 7 males, 7 females) untreated naïve mice acted as non-ischaemic controls. A separate group of young mice (n = 9) underwent sham surgery as detailed above to confirm the validity of using non-ischaemic naïve mice as immunological control. When comparing sham mice to untreated young naïve mice, a significant difference in Treg frequency was only noted in draining lymph nodes ($p = 0.0362$). Treg frequencies in spleen and blood were not affected by the induction of ischaemia in either young or aged mice (**Fig. 2.4**). Similarly, no change was observed in cervical or inguinal lymph nodes post-pMCAO. This latter result conflicts with results seen in the first group of young mice (**Fig. 2.3**), where ischaemia increased Treg frequency in lymph nodes. A different supplier for young mice was used in these two studies (Envigo, UK (**Fig. 2.3**) vs. Charles River, UK (**Fig. 2.4**)). It has been recognised that slight changes in T cell phenotype can be observed between strains (293).

In blood, higher Treg frequencies were noted in aged mice ($p = 0.0039$). Likewise, in draining lymph nodes and non-draining lymph nodes, significantly higher Treg frequencies were observed in naïve aged mice compared to naïve young mice ($p < 0.0001$). This demonstrates that age was the major factor which determined differences in peripheral Treg frequencies between groups, whereas ischaemia tended to reduce Treg frequency only in draining lymph nodes ($p = 0.0271$) but not in other

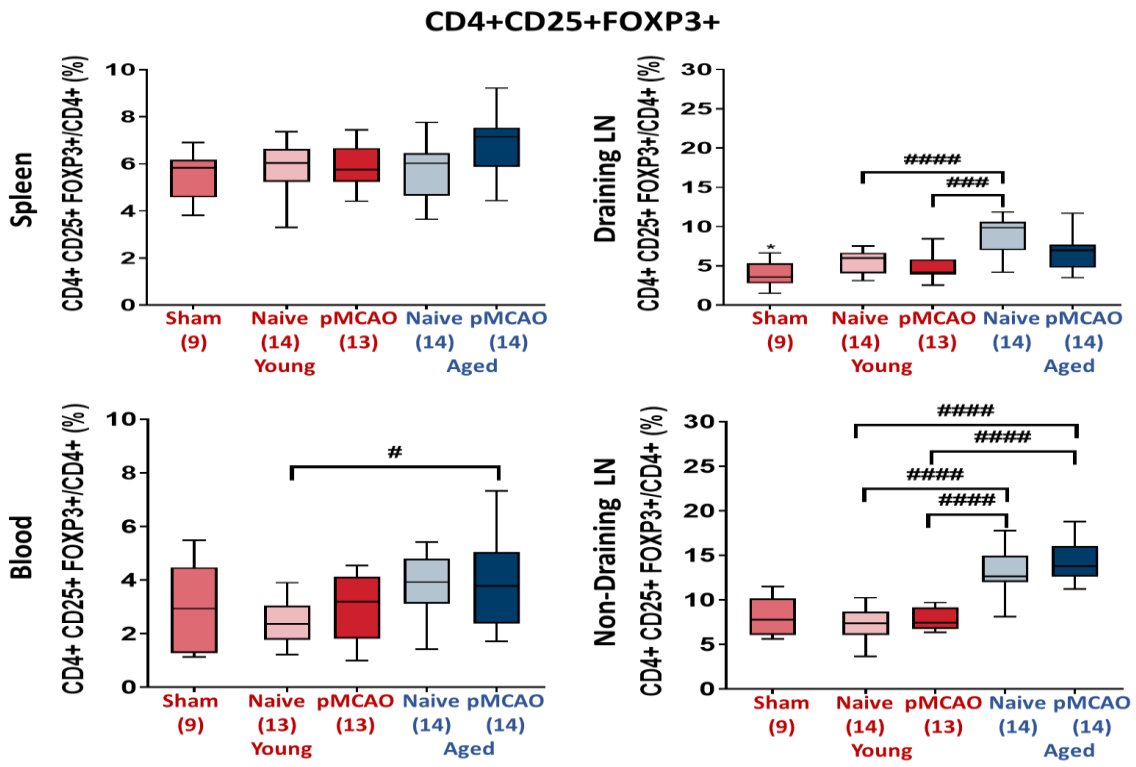


Figure 2.4: Effect of pMCAO on the frequency of CD4+ CD25+ FoxP3+ T cells in blood and secondary lymphoid tissue of young and aged mice (t = 7 days). Young mice are shown in red, aged mice are shown in blue. Sham mice only received initial incision and exposure of the skull. Naïve mice were age-matched mice who did not undergo any surgery. Two-sided, independent-samples T tests investigated differences between two groups (* = p<0.05, ** = p<0.01, *** = p<0.001. Two-way analysis of variance (ANOVA) tests with post hoc Tukey's multiple comparisons were performed to investigate differences between three or more groups (# = p<0.05, ## = p<0.01, ### = p<0.001). The number of mice per group shown in parentheses on x-axis. Box-and-whisker plots exhibit 10-90 percentiles.

sites. The sex of mice did not influence Treg frequency (Supplementary Material, **Fig. S2.3).** Separately, no immunological controls for ApoE-/- mice fed a high-fat diet were available, meaning the effect of ischaemia on peripheral Treg frequencies in this cohort remains unknown.

2.3.3 Extending fingolimod treatment duration from 5 days to 10 days post-pMCAO increased Treg frequencies in lymph nodes

To date, the effect of fingolimod treatment has not been reported beyond 7 days post-ischaemia in a pre-clinical study (265). However, evidence from multiple sclerosis

patients treated with fingolimod suggests the amplification of Tregs may increase with longer-term administration (294, 295). As a result, the effect of an extended treatment duration on peripheral Treg frequencies at 10 days post-pMCAO was also investigated (**Fig. 2.5**).

Extending drug treatment from 5 to 10 days did not further increase the frequency of Tregs in circulation (spleen and blood). However, in lymph nodes extended fingolimod treatment had a significant impact on the frequency of Tregs. In draining lymph nodes, 10-day fingolimod treatment significantly increased Treg frequency (p = 0.0028), whereas 5-day treatment only resulted in a trend towards increased Treg frequency. In non-draining lymph nodes, however, both short-term (p = 0.0016) and long-term (p =0.0062) fingolimod treatment significantly enhanced Treg frequency. Overall, longer term fingolimod treatment increased Treg frequency in all peripheral tissues analysed. Notably, short-term fingolimod treatment only failed to enhance Treg frequency in draining lymph nodes, suggesting many immunomodulatory effects of the drug remain for at least five days after withdrawal.

2.3.4 Fingolimod increases FoxP3+ cell infiltration into the brain post-pMCAO

The effect of fingolimod on Treg numbers in the brain post-ischaemia was investigated by immunohistochemical labelling of brain sections (n = 10 per group) with anti-CD3 and anti-FoxP3 antibodies. Positively stained cells were counted in both the ischaemic core (**Fig. 2.6A**) and peri-infarct (**Fig. 2.6B**) regions, in accordance with the results of previous studies (116, 296).

In young mice, both doses of fingolimod reduced the total number of CD3+ T cells infiltrating into the ischaemic core at 7 days post-pMCAO (p = 0.0048 and 0.0060,

respectively). Low dose fingolimod (0.5 mg/kg) also reduced CD3+ T cell counts in the peri-infarct region (p = 0.0153). Interestingly, the administration of fingolimod caused an increase in the number of FoxP3+ cells in the core, which was significant in the high dose group of young mice (p = 0.0016). No effect of fingolimod on Foxp3+ cell numbers was observed in the peri-infarct of young mice. In aged mice, low dose fingolimod did not significantly reduce total CD3+ T cell numbers in the ischaemic core at 7 days post-pMCAO (p = 0.0825), but a significant decrease in the peri-infarct region was observed (p = 0.0192). Significant increases in FoxP3+ cell counts were noted in both the core and peri-infarct regions of aged mice treated with fingolimod (p = 0.0035 and 0.0437 respectively). Fingolimod had a similar effect in ApoE$^{-/-}$ mice fed a high-fat diet. Specifically, low dose fingolimod failed to produce any significant change in CD3+ T cells in the ischaemic core (p = 0.3475) but reduced CD3+ numbers in the peri-infarct region (p = 0.0492). Likewise, significantly higher numbers of FoxP3+ cells were observed in both the core (p = 0.0073) and peri-infarct region (p = 0.0492).

In order to investigate the potential relationship between fingolimod treatment duration and FoxP3+ cell infiltration into the brain post-pMCAO, a final study with low dose fingolimod was conducted. Low dose fingolimod significantly decreased total T cell numbers in the core in both short-term (p = 0.0005) and long-term treatment groups (p <0.0001), whereas only long-term fingolimod dosing increased FoxP3 cells in the ischaemic core at 10 days post-pMCAO (p = 0.0019). Overall, these results highlight that fingolimod treatment results in significant enrichment of Foxp3+ cells in the infarct site, independently of age or co-morbidity. In young mice, fingolimod also significantly depletes CD3+ T cells at the infarct site.

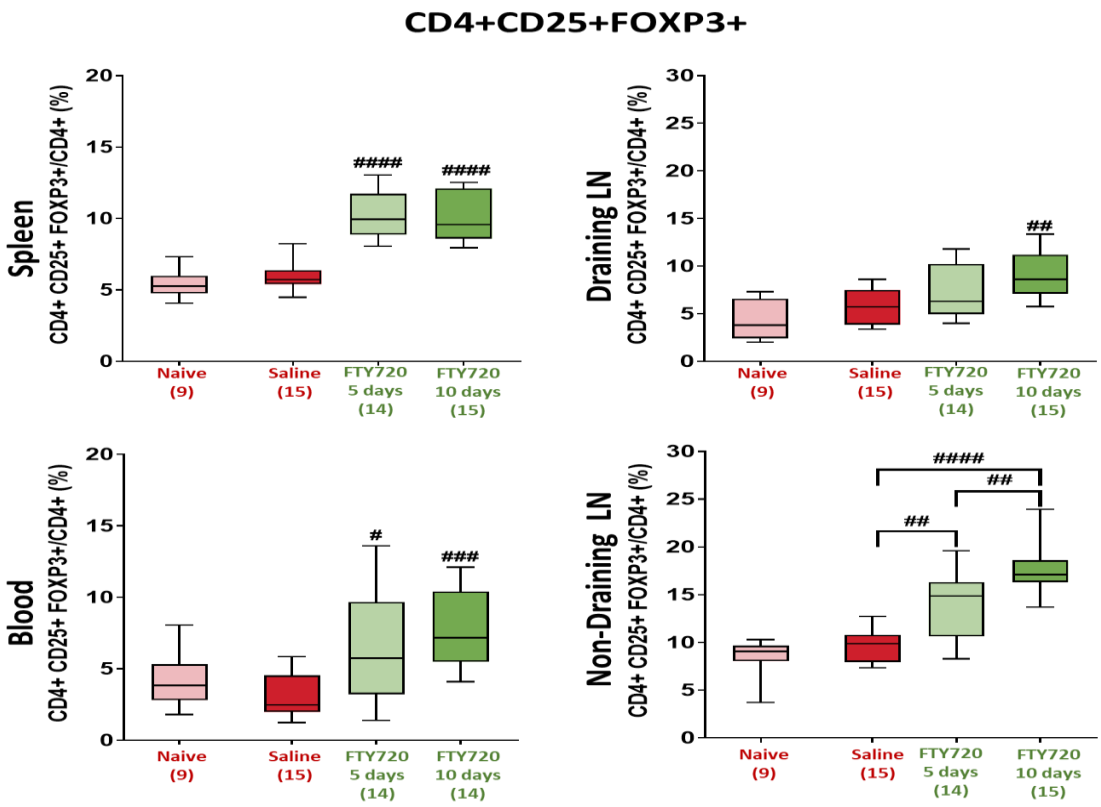


Figure 2.5: Frequency of CD4+ CD25+ FoxP3+ T cells in blood and secondary lymphoid tissue in response to short-term (once daily for 5 days, light green) and long-term (once daily for ten days, dark green) fingolimod (FTY720) treatment post-brain ischaemia in young mice (t = 10 days). Two-sided, independent-samples T tests investigated differences between two groups (* = p<0.05, ** = p<0.01, *** = p<0.001 as compared to saline). One-way analysis of variance (ANOVA) tests with post hoc Tukey's multiple comparisons were performed to investigate differences between three or more groups (# = p<0.05, ## = p<0.01, ### = p<0.001 as compared to saline). Number of mice per group shown in parentheses on x-axis. Box-and-whisker plots exhibit 10-90 percentiles

2.3.5 Fingolimod produces profound lymphopenia and causes a re-distribution of T cells in mice post-pMCAO

Fingolimod is known to influence the homing of CD3+ T cells. By inducing internalisation of the S1P receptor, the drug effectively sequesters lymphocytes within secondary lymphoid organs, denying them access to blood or peripheral sites of inflammation (275). Separately, brain ischaemia itself has been shown to induce marked immunodepression, marked by lymphopenia and splenic atrophy (43). Due to the known roles T cells play in stroke inflammation and host defence, the impact of

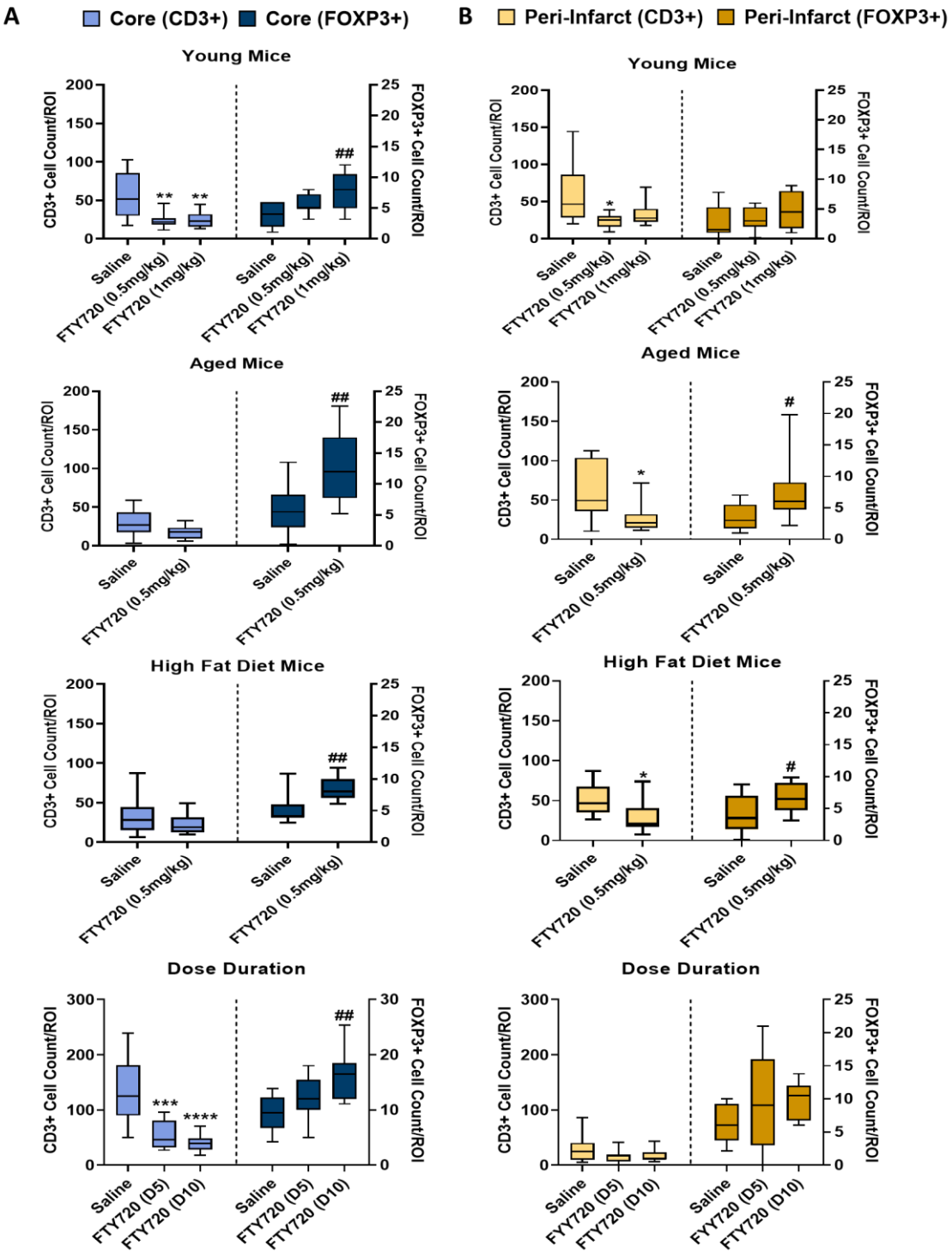


Figure 2.6: Total CD3+ and FoxP3+ cell counts in the infarct core (A) and peri-infarct zone (B) of mice post-pMCAO (t = 7-10 days) (n = 10 per group). DAB-based Immunohistochemistry was used to determine cell counts. Two-sided, independent-samples T tests investigated differences between two groups. One-way analysis of variance (ANOVA) tests with post hoc Tukey's multiple comparisons were performed to investigate differences between three or more groups. For comparisons between CD3+ groups, * = p<0.05, ** = p<0.01, *** = p<0.001 (vs. saline). For comparison between FoxP3+ groups, # = p<0.05, ## = p<0.01, ### = p<0.001 (vs. saline).

both stroke and fingolimod treatment on peripheral immunity was investigated as a final part of this study.

In young mice, the induction of stroke reduced CD3+ T cell frequency in non-draining lymph nodes (**Fig. 2.7**). In spleen, a statistically significant difference was recorded between groups ($p = 0.047$). Both doses of fingolimod reduced T cell frequency in blood ($p < 0.0001$) and draining lymph nodes ($p < 0.0001$). Conversely, in non-draining lymph nodes, only the higher dose of fingolimod reduced T cell frequency ($p = 0.005$).

In both aged and ApoE-/- cohorts, fingolimod did not affect CD3+ T cell frequency in spleen. As per young mice, however, low dose fingolimod depleted T cell frequency in blood (Aged: $p = 0.045$, ApoE-/-: $p = 0.043$). Fingolimod also reduced T cell frequency in draining lymph nodes in both models (Aged: $p < 0.0001$, ApoE-/-: $p = 0.001$).

In the treatment duration study, stroke increased CD3+ T cell frequency in blood ($p = 0.0041$) (**Fig. 2.8**). In spleen, 5-day fingolimod treatment alone reduced T cell frequency ($p = 0.0008$). Only 10-day fingolimod treatment reduced CD3+ T cell frequency in draining lymph nodes ($p = 0.033$), while in blood, both the 5-day ($p = 0.012$) and 10-day ($p < 0.0001$) fingolimod treatment regimens produced a drop in circulating T cell frequency.

The fingolimod-induced reduction in T cell frequency in spleen and blood combined with the depletion in lymph nodes led to an investigation of lymphocyte distribution in terms of absolute CD3+ T cell counts (**Fig. 2.9**). In young mice, ischaemia alone decreased T cell numbers in spleen ($p = 0.0435$ and non-draining lymph nodes ($p < 0.0001$). In all cohorts, fingolimod treatment profoundly reduced circulating T cell

numbers (p <0.001). No increase in CD3+ T cells was observed in either draining or non-draining lymph nodes in young, aged, or ApoE$^{-/-}$ mice. In the treatment duration study, ischaemia alone reduced circulating T cell counts (p = 0.0016). Both 5- and 10-day fingolimod treatment decreased CD3+ T cell numbers in spleen (p <0.001) and blood (p <0.001). As per previous cohorts, however, no increase in CD3+ T cells were noted in draining or non-draining lymph nodes.

I next assessed the effects of the drug on CD4+ and CD8+ T cell frequencies at 7 days post-pMCAO (**Fig. 2.7**). In young mice, the induction of brain ischaemia produced a significant drop in CD4+ T cell frequency in non-draining lymph nodes (p = 0.001). Low dose fingolimod decreased CD4+ T cell frequency in spleen (p = 0.001), blood (p = 0.002), and non-draining lymph nodes (p = 0.001). High dose fingolimod also decreased CD4+ T cell frequency in spleen (p = 0.046), blood (p <0.0001), draining lymph nodes (p = 0.009), and non-draining lymph nodes (p <0.0001).

In aged mice, low dose fingolimod reduced CD4+ T cell frequency in spleen (p = 0.041), draining lymph nodes (p = 0.001), and non-draining lymph nodes (p <0.0001). In ApoE-/- mice, a decreased CD4+ T cell frequency was only recorded in blood (p = 0.032) and non-draining lymph nodes (p = 0.003).

In the treatment duration study, stroke increased CD4+ T cell frequency in spleen (p = 0.0178) (**Fig 2.8**). Meanwhile, 5-day fingolimod treatment reduced the frequency of CD4+ T cells in spleen (p = 0.0001) and non-draining lymph nodes (p <0.0001). Extending treatment to 10 days decreased the frequency of CD4+ T cells in spleen (p = 0.0015), draining lymph nodes (p = 0.0034), non-draining lymph nodes (p <0.001), and blood (p = 0.0002).

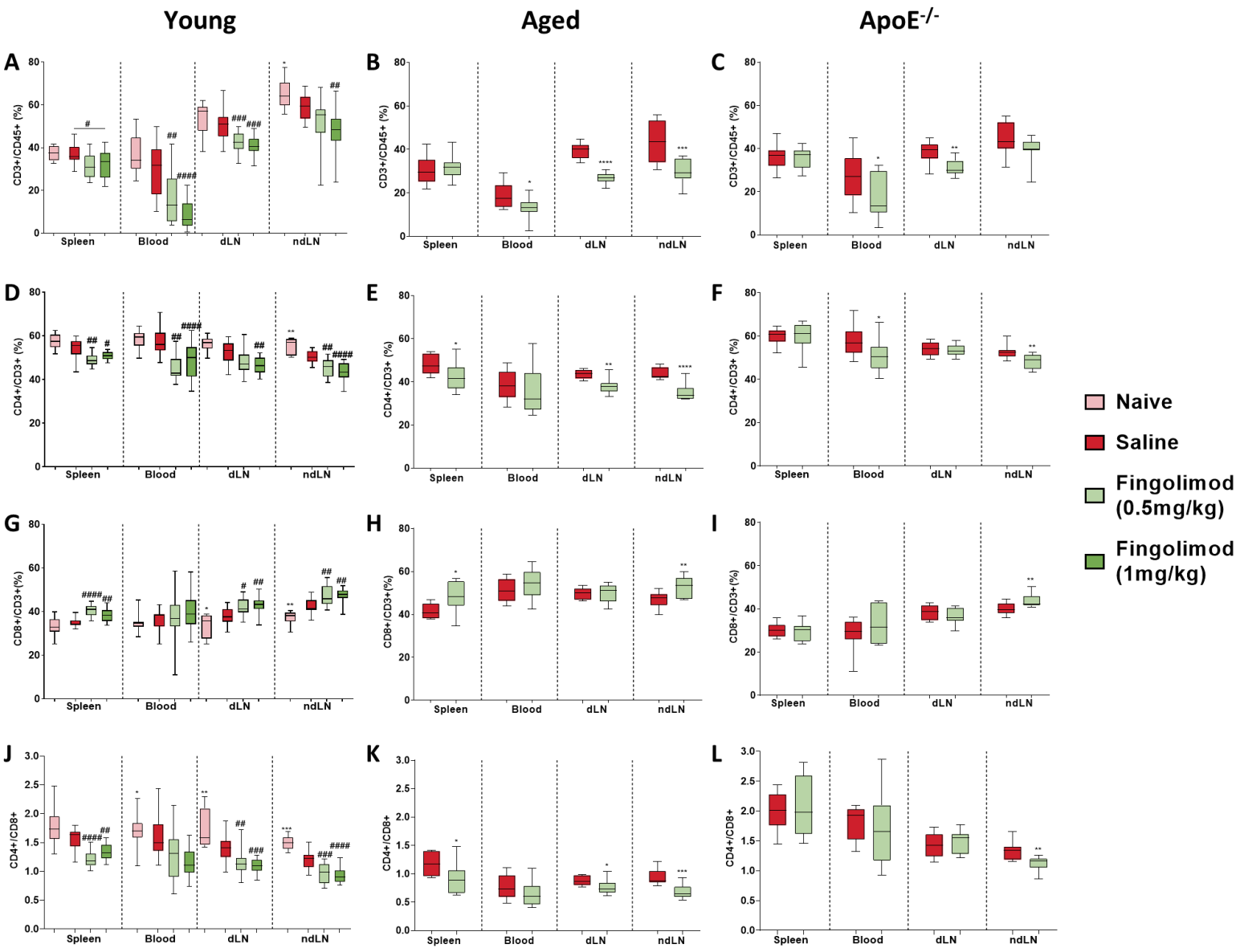

Young
Aged
ApoE-/-
A
B
C
D
E
F
G
H
I
J
K
L
CD3+/CD45+ (%)
CD4+/CD3+ (%)
CD8+/CD3+(%)
CD4+/CD8+
Spleen
Blood
dLN
ndLN
Naive
Saline
Fingolimod (0.5mg/kg)
Fingolimod (1mg/kg)

Figure 2.7: Frequency of CD3+ T cells in blood and secondary lymphoid tissue at 7 days post-pMCAO in A) young, B) aged, and C) $ApoE^{-/-}$ mice following saline/fingolimod treatment (fingolimod 0.5mg/kg or 1mg/kg administered once daily on days 0, 1, 2). Frequency of CD4+ T cells in blood and secondary lymphoid tissue at 7 days post-pMCAO in D) young, E) aged, and F) $ApoE^{-/-}$ mice following saline/fingolimod treatment. Frequency of CD8+ T cells in blood and secondary lymphoid tissue at 7 days post-pMCAO in G) young, H) aged, and I) $ApoE^{-/-}$ mice following saline/fingolimod treatment. Ratio of CD4+:CD8+ T cells in blood and secondary lymphoid tissue at 7 days post-pMCAO in J) young, K) aged, and L) $ApoE^{-/-}$ mice following saline/fingolimod treatment. Two-sided, independent-samples T tests investigated differences between two groups (* = $p<0.05$, ** = $p<0.01$, *** = $p<0.001$ as compared to saline). One-way analysis of variance (ANOVA) tests with post hoc Tukey's multiple comparisons were performed to investigate differences between three or more groups (# = $p<0.05$, ## = $p<0.01$, ### = $p<0.001$ as compared to saline). Relevant tissue depicted on x-axis. Box-and-whisker plots exhibit 10-90 percentiles

In young mice, the induction of brain ischaemia alone raised the frequency of CD8+ T cells in both draining ($p = 0.041$) and non-draining ($p = 0.002$) lymph nodes (**Fig 2.7**). Low dose fingolimod increased the CD8+ T cell frequency in draining lymph nodes ($p = 0.012$), non-draining lymph nodes ($p = 0.002$), and spleen ($p < 0.0001$).

High dose fingolimod caused a similar increase in the frequency of CD8+ T cells in the spleen ($p = 0.009$), draining lymph nodes ($p = 0.001$), and non-draining lymph nodes ($p = 0.003$).

In aged mice, fingolimod increased the frequency of CD8+ T cells in spleen ($p = 0.001$) and non-draining lymph nodes ($p = 0.009$). In ApoE-/- mice a raised CD8+ T cell frequency was only recorded in non-draining lymph nodes ($p = 0.006$).

In the treatment duration study, short-term fingolimod treatment increased the frequency of CD8+ T cells in non-draining lymph nodes alone ($p < 0.0001$) (**Fig 2.8**). A 10-day treatment regimen, conversely, increased CD8+ T cell frequency in spleen ($p = 0.0170$), draining lymph nodes ($p = 0.0003$), and non-draining lymph nodes ($p < 0.0001$). Extending treatment duration from 5 to 10 days also produced an increase in circulating CD8+ T cell frequency ($p = 0.0085$).

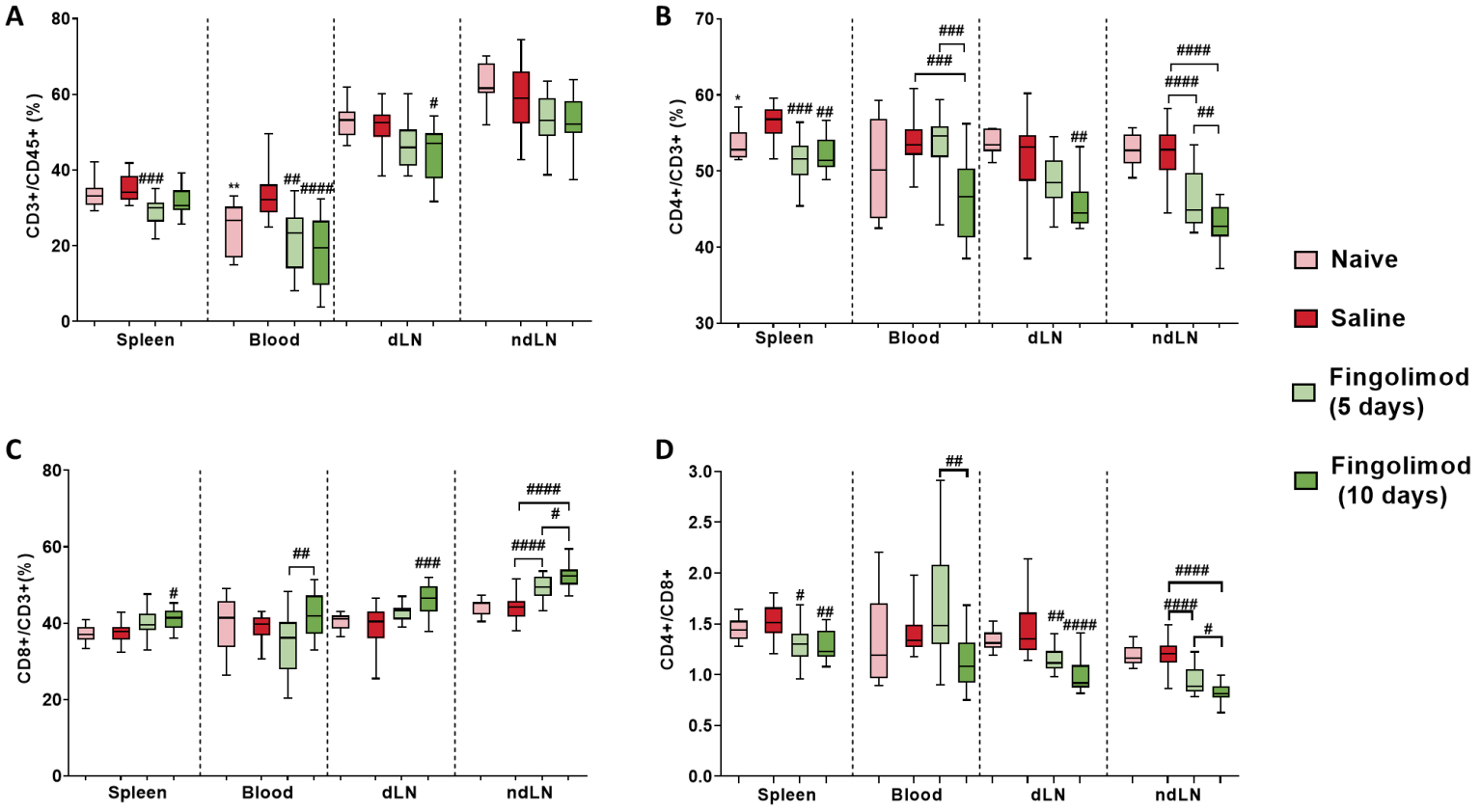


Figure 2.8: A) CD3+ T cell frequency, B) CD4+ T cell frequency, C) CD8+ T cell frequency, and D) CD4+/CD8+ T cell ratio in blood and secondary lymphoid tissue in response to short-term (5 days) and long-term (10 days) fingolimod (FTY720) treatment post-brain ischaemia in young mice (t = 10 days). Two-sided, independent-samples T tests investigated differences between two groups (* = p<0.05, ** = p<0.01, *** = p<0.001 as compared to saline). One-way analysis of variance (ANOVA) tests with post hoc Tukey's multiple comparisons were performed to investigate differences between three or more groups (# = p<0.05, ## = p<0.01, ### = p<0.001 as compared to saline). Box-and-whisker plots exhibit 10-90 percentiles.

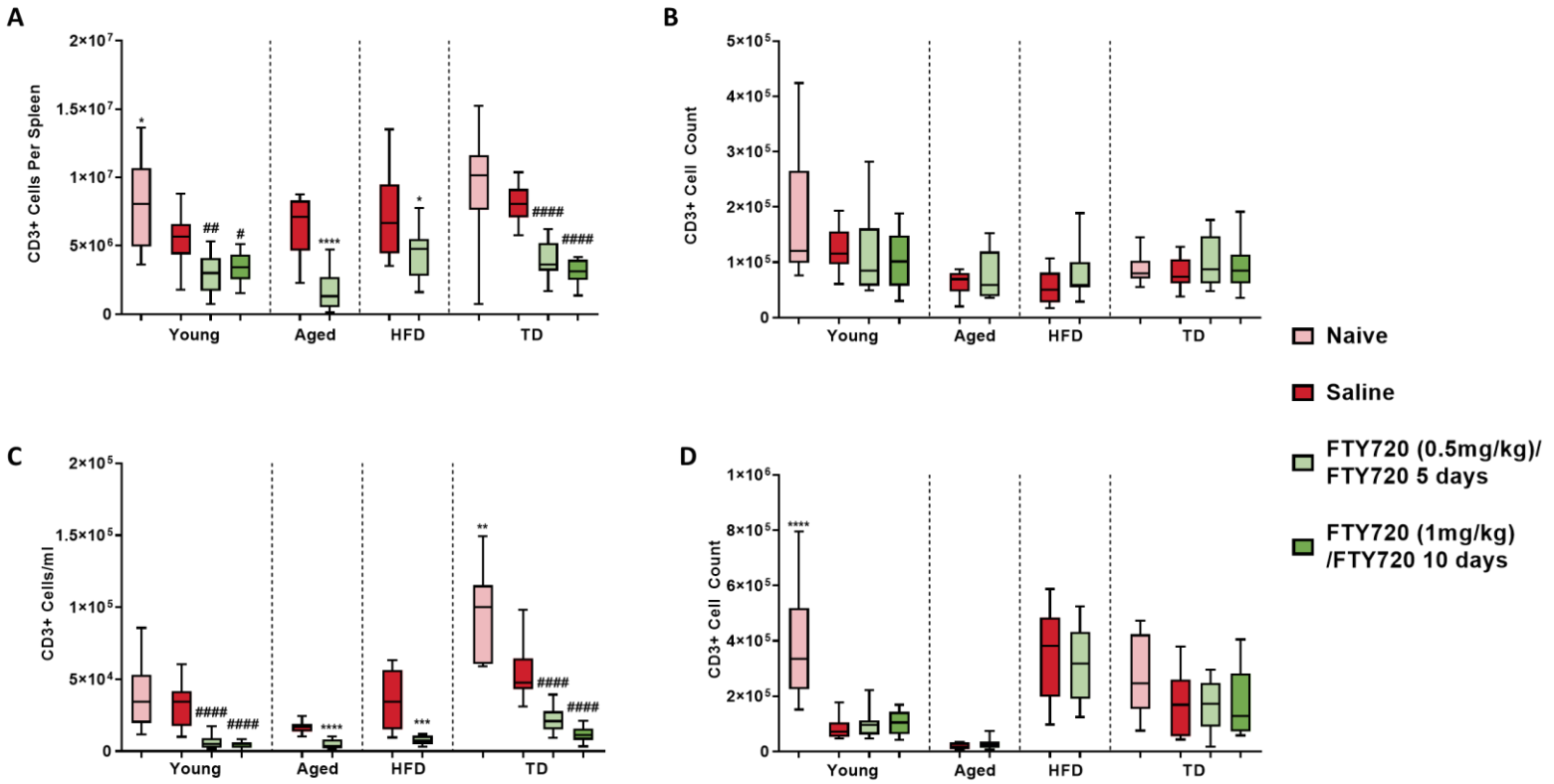


Figure 2.9: CD3+ T cell counts at 7 days post-pMCAO in A) spleen, B) cervical lymph nodes, C) blood, and D) inguinal lymph nodes in young, aged, and ApoE$^{-/-}$ mice following saline/fingolimod treatment, as well as in young mice receiving either short-term (5 days) or long-term (10 days) fingolimod treatment. Two-sided, independent-samples T tests investigated differences between two groups (* = p<0.05, ** = p<0.01, *** = p<0.001 as compared to saline). One-way analysis of variance (ANOVA) tests with post hoc Tukey's multiple comparisons were performed to investigate differences between three or more groups (# = p<0.05, ## = p<0.01, ### = p<0.001 as compared to saline). Box-and-whisker plots exhibit 10-90 percentiles.

2.3.6 Fingolimod decreases the ratio of CD4+ to CD8+ T cells in mice post-pMCAO

Both CD4+ and CD8+ T cells are known to play key roles in stroke pathophysiology (297). More importantly, however, the ratio between CD4+ and CD8+ T cells in peripheral tissue in the acute post-stroke period may also determine the risk of infection (298). Given the impact of fingolimod on both CD4+ and CD8+ T cell frequencies, the effect of the drug on the CD4+/CD8+ ratio was also determined.

In young mice, both doses of fingolimod decreased the ratio of CD4+ to CD8+ T cells in spleen (p = 0.0002), draining lymph nodes (p <0.0001), and non-draining lymph nodes (p <0.0001) (**Fig 2.7**). In blood, only high dose fingolimod produced this result (p = 0.0119).

In aged mice, fingolimod again decreased the CD4+/CD8+ ratio in spleen (p = 0.0184), draining lymph nodes (p = 0.0481), and non-draining lymph nodes (p = 0.0002). As per young mice, no effects were noted in blood at this dose. In $ApoE^{-/-}$ mice fingolimod treatment only induced a change in the CD4+/CD8+ ratio in non-draining lymph nodes (p = 0.0012).

In the treatment duration study, short-term fingolimod treatment reduced the CD4+/CD8+ ratio in spleen (p = 0.0116), draining lymph nodes (p = 0.0011), and non-draining lymph nodes (p <0.0001) (**Fig. 2.8**). A 10-day treatment regimen reduced the CD4+/CD8+ ratio in spleen (p = 0.0039), draining lymph nodes (p <0.0001), and non-draining lymph nodes (p <0.0001) versus saline control. The extension of fingolimod treatment from 5 to 10 days also reduced the CD4+/CD8+ ratio in blood (p = 0.0020).

2.3.7 Improvement in fingolimod-treated mice at 7 days post-pMCAO correlated with higher CD8+ T cell frequency, lower CD4+T cell frequency, and lower Treg frequency in the periphery.

As three studies (Dose Response, Aged, ApoE-/-) employed a three-day, once daily saline/fingolimod (0.5 mg/kg) treatment protocol, data were combined in order to investigate any potential relationship between lymphocyte subpopulations and experimental outcomes for both saline and fingolimod-treated mice. The results of this correlation analysis are displayed in (**Fig. 2.10**).

In saline-treated mice, CD4+ T cells in spleen ($p = 0.0245$), draining lymph nodes ($p = 0.0004$), non-draining lymph nodes ($p = 0.0240$), and blood ($p = 0.0017$) showed a significant negative correlation with behavioural scores as assessed by grid-walking test at day 3 post-brain ischaemia. Conversely, CD8+ T cells in spleen ($p = 0.0330$), draining lymph nodes ($p = 0.0042$), and blood ($p = 0.0061$) displayed a significant positive correlation with behavioural scores. The administration of fingolimod delayed this phenomenon until 7 days post-ischaemia, with CD4+ T cells in spleen ($p = 0.0462$) showing significant negative correlations, while CD8+ T cells in non-draining lymph nodes ($p = 0.0109$) and blood ($p = 0.0058$) displayed positive correlations. An analysis of the combined data from saline-treated and fingolimod-treated mice shows this treatment effect is still evident at 7 days, with CD4+ T cells in spleen ($p = 0.0430$) and draining lymph nodes ($p = 0.0372$) negatively correlated with recovery, whereas CD8+ T cells in spleen ($p = 0.0289$), non-draining lymph nodes ($p = 0.0271$), and blood ($p = 0.0061$) showed significant positive correlations.

In saline-treated mice, regulatory T cells (Tregs) showed a weak positive correlation with 7-day recovery as assessed by the grid-walking test (e.g., blood: $p = 0.1447$).

Post-fingolimod treatment however, Tregs in spleen (p = 0.0095) and blood (p = 0.0005) displayed a significant negative correlation with 7-day grid-walking test scores.

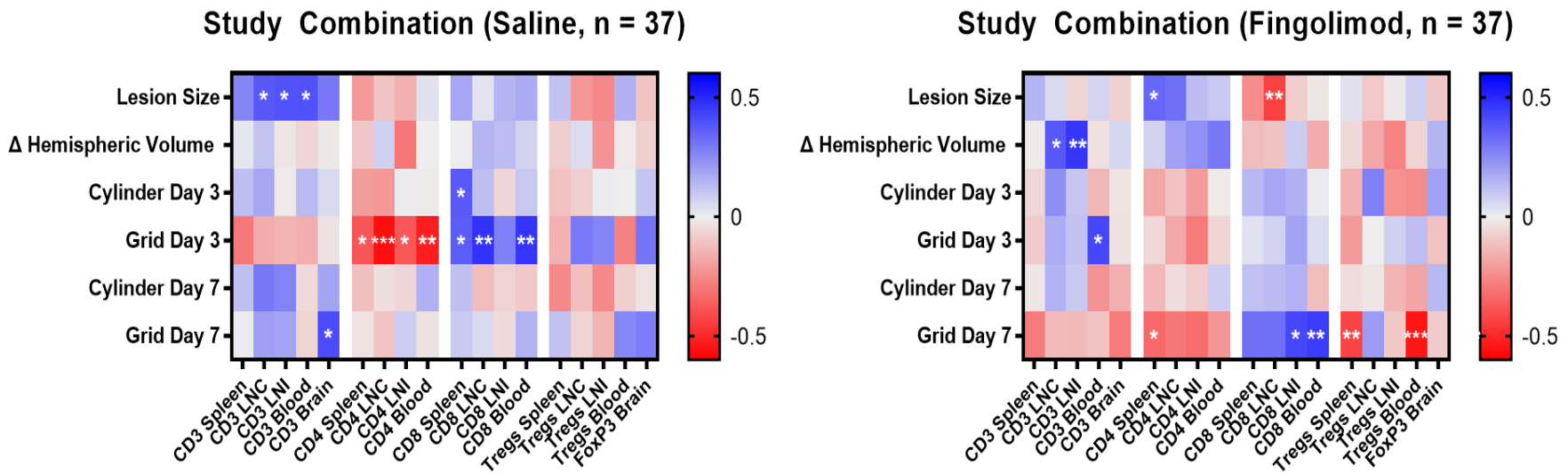


Figure 2.10: Correlation matrix between the proportion of T lymphocytes and experimental outcomes. Heat map depicting correlations between lymphocyte proportions and experimental outcomes (infarct volume, hemispheric volume, and cylinder/grid scores at days 3 and 7) for (a) all young, aged, and ApoE$^{-/-}$ saline-treated mice, and (b) all young, aged, and ApoE$^{-/-}$ fingolimod-treated mice. The colour bar represents Pearson r value on a scale from -0.75 to +0.75. For statistical significance, $p<0.05$ = *, $p<0.01$ = **, $p<0.001$ = ***.

2.4 Discussion

Fingolimod, approved for the treatment of MS, shows promise as a clinical candidate for stroke treatment (299). Despite supporting data from numerous pre-clinical studies, questions related to the mechanism(s) of action persist. This study explored the effect of fingolimod on the known neuroprotective lymphocyte subpopulation of regulatory T cells in a mouse model of brain ischaemia. Overall, our results demonstrate that fingolimod treatment significantly increased Treg frequency in the spleen and blood of young, aged, and ApoE$^{-/-}$ mice at 7 days post-brain ischaemia. Fingolimod significantly increased Treg frequency in both draining and non-draining lymph nodes of young but not aged or ApoE-/- mice post-ischaemia. Fingolimod enhanced the number of FoxP3+ cells in the infarcted brain, independently of age or co-morbidity. Peripherally, the drug induced a profound lymphopenia, coupled with a decreased CD4+/CD8+ T cell ratio. Interestingly, circulating Tregs were positively correlated with functional recovery at 7 days. Post-fingolimod treatment, however, a significant negative correlation between Tregs in spleen/blood and 7-day recovery was observed.

The relative strengths of our study include appropriate sample sizes determined by *a priori* power calculation, the administration of two different fingolimod doses, and the testing of numerous dosing schedules. The use of mice with common stroke-related co-morbidities also increases the clinical relevance of this work (300). Conversely, a limitation of our study is that the Treg profile was only examined at a single timepoint in each study. Previous research was consulted to choose a timepoint at which Treg entry to the brain was expected (301). Nevertheless, the precise relationship between onset of therapy and increased Tregs in our model was not examined. Furthermore, the impact of fingolimod treatment on the Treg suppressive function in the setting of

ischaemic stroke was not determined. Finally, only the electrocoagulation model of permanent middle cerebral artery occlusion was employed in this study. Notably, a previous published study demonstrated that fingolimod failed to improve experimental stroke outcome in young mice in this model (253). Conversely, the drug has proven effective in mice which underwent transient models of middle cerebral artery occlusion (tMCAO)(265). Some evidence suggests a cerebral ischemia–reperfusion model such as tMCAO should be preferentially used for testing anti-inflammatory drugs (36).This is particularly true in cases where the drug candidate may be used as an adjunct to thrombolysis (302).

Previous studies in MS, acute kidney injury, and colitis showed that fingolimod increased the proportion of Tregs in blood and secondary lymphoid tissues (278-281, 303). In stroke, other Treg-modulating therapies, including CD28 superagonist, IL-33, IL-2/IL-2-antibody complex, and adoptive Treg cell transfer, have been shown to increase peripheral Treg frequencies by two- to three-fold in young mice (120, 140, 160, 184). However, questions related to these modulators remain, including issues of cost, length of treatment window, potential toxicity of Treg stimulants, and the stability of the expanded Tregs (224). In contrast, an abundance of clinical data exists for the use of fingolimod in central nervous system (CNS) disorders (304). Therefore, fingolimod may provide a safe and robust alternative for effectively boosting Tregs in the periphery post-stroke. Its known neuro- and vaso-protective properties may also offer added bonuses over other small molecule Treg-modulators such as rapamycin (135).

The mechanism underlying the effect of fingolimod on Tregs could be related to its effects on CD4+ T cells that do not display a regulatory phenotype i.e., “non-Tregs”.

The observation that fingolimod reduced total CD4+ T cell numbers in spleen and blood while increasing Treg frequency suggests Tregs may be refractory to fingolimod treatment. Notably, non-Treg cells have been shown to depend more on the S1P gradient to recirculate from the lymph node to the blood in comparison to Tregs, as evidenced by higher levels of S1PR1 on these cells (305). Therefore, the modulation of S1PR1 by fingolimod treatment may preferentially sequester non-Tregs in lymph nodes. Alternatively, or additionally, interruption of S1PR1 signalling by fingolimod could enhance modulation of T cells towards a regulatory phenotype. Under normal circumstances, the S1P-mTOR axis antagonises TGF-β function (306, 307). In the presence of fingolimod, however, internalisation of the S1PR1 may promote expansion of the Treg pool through increased TGF-β-Smad3 signalling. Overall, a combination of reduced non-Treg trafficking and enhanced TGF-β-driven Treg evolution may underlie the observed increased Treg frequencies in young mice post-ischaemia.

In the current study, the effect of fingolimod on Tregs in mice with common stroke co-morbidities was also determined. The fingolimod-induced increase in Treg frequency in the spleen and blood of aged mice is of particular interest in light of recent work that highlights the frequency of circulating Tregs correlates with age in ischaemic stroke patients (158). The magnitude of Treg frequency change in spleen and blood was also notably higher in aged mice than in young mice, suggesting older cohorts may, in theory, derive greater benefit from fingolimod treatment. Separately, the ability of fingolimod to boost Tregs in spleen and blood of $ApoE^{-/-}$ mice fed a high-fat diet is promising, as there is substantial evidence to suggest Treg numbers and function are impaired during atherosclerosis development (308, 309). Atherosclerosis

drives Treg plasticity, resulting in the accumulation of an intermediate dysfunctional Th1-like IFN-γ+ phenotype which permits further arterial inflammation (310). Our results demonstrate that fingolimod may modulate CD4+ T cell populations away from these inflammatory phenotypes towards Tregs post-pMCAO; an effect that, if properly exploited, might improve long-term brain tissue repair (311).

Fingolimod treatment also increased Treg frequency in draining and non-draining lymph nodes in young mice. These results are similar to those observed in experimental autoimmune uveitis (312). Recently, the pivotal contribution of cervical lymph nodes in particular to post-stroke systemic inflammation and subsequent infarct growth has been described with respect to macrophage-mediated inflammation (313). The same study suggested T cells may also be involved. Combined with the known ability of lymph node Tregs to influence inflammatory outcomes in distal organs, these findings suggest that in the immediate aftermath of stroke, cervical lymph node Tregs might help coordinate the peripheral immune response through the release of anti-inflammatory cytokines such as IL-10 (314, 315). In the current study, fingolimod increased Treg frequency in CNS-draining lymph nodes, although the effect was only observed in young mice. Higher Treg frequencies were observed in the lymph nodes of naïve aged compared to naïve young mice (**Fig. 2.4**). This is in line with previous results which suggest Tregs accumulate in secondary lymphoid tissue in aged mice (285). It is possible an upper plateau exists in aged mice beyond which higher Treg frequencies cannot be induced. Therefore, if the primary mechanism of action by which fingolimod affords neuroprotection post-stroke is by increasing Tregs in draining lymph nodes, it would not provide any clinical benefit in older populations. In contrast, the phenotype of lymph node T cells in young mice appears more dynamic

and responsive to pharmacological modulation. Previous work examining the chronic accumulation of Tregs in both brain and non-draining lymph nodes post-ischaemia in young mice suggests such long-lasting immunological consequences could positively impact stroke recovery (52). In particular, the ability of cervical lymph node Tregs to prevent deleterious antigen-specific immune reactions developing post-stroke may play a crucial role (316).

Recent evidence suggests Tregs must traffic to the infarcted brain in order to provide maximum benefit, while effector T cells contribute most to post-stroke neurodegeneration after gaining access to the lesion site (121, 317). As a result, the crucial balance between regulatory and effector T cells in the post-ischaemic brain was examined by immunohistochemistry. In line with previous results, fingolimod reduced CD3+ T cell infiltration in the brains of young mice (246, 253). Recent research suggests this might be primarily due to interference with S1P receptor signalling which facilitates recruitment of splenic T cells to the infarcted hemisphere (127). FoxP3+ cells, meanwhile, represented approximately 10% of all infiltrating T cells in saline-treated young mice, in broad agreement with other studies (134). Uniquely, the FoxP3+ to CD3+ T cell ratio was higher in fingolimod-treated aged brains than fingolimod-treated young brains, correlating with results noted in spleen and blood. However, the observation that fingolimod increases FoxP3+ cell counts in the ischaemic brain conflicts with a recent finding wherein once daily dosing of fingolimod reduced brain Tregs (116). Importantly, however, this same study only initiated fingolimod treatment in the subacute period (6-13 days post-stroke), in direct contrast with the acute dosing regimen chosen here. Furthermore, the study employed a transient (60 minute) model of middle cerebral artery occlusion. There are profound

differences in the numbers of inflammatory cells which enter the brain when reperfusion is allowed to occur compared to the permanent model utilized here (148). The higher numbers of leukocytes which infiltrate in the first 24 hours after permanent ischaemia may present fingolimod with an increased number of T cells it can direct towards a regulatory phenotype.

Overall, the enhanced number of FoxP3+ cells observed in the infarcted brain as a result of fingolimod treatment may represent increased Treg recruitment or an *in-situ* expansion of the regulatory phenotype in response to the local inflammatory milieu. Chemokine receptors including CCR5, CCR6, and CCR8 have been proposed as mediators of Treg mobilization to the ischaemic brain (121). The ability of fingolimod to positively influence the capacity of Tregs to traffic to the brain by upregulating expression of these receptors remains unclear (318). Recent evidence does suggest a link between the drug and the local inflammatory milieu through upregulation of the anti-inflammatory "M2" microglia phenotype (264). It is possible fingolimod enhances modulation to a Treg phenotype via M2 microglia-mediated release of anti-inflammatory cytokines at the infarct site (319).

The most pronounced effects of fingolimod on brain FoxP3+ cell counts were observed when the drug was administered once daily for ten days. To date, clinical trials of fingolimod in ischaemic stroke have only administered the drug in the first 72 hours post-ischaemia (267-269). In terms of the future use of extended treatment regimens, careful consideration should be paid to the impact of fingolimod on wider host immunity (e.g. CD4+/CD8+ ratio), especially in the acute post-stroke period where widespread stroke-induced immunodepression occurs (320). Evidence suggests Tregs might attenuate SIID in the subacute phase after brain injury in mice (137).

Notably, fingolimod does not increase the risk of spontaneous bacterial infection post-cerebral ischaemia in young mice (321). Therefore, fingolimod may reduce the incidence of bacterial infection through fine-tuning the Treg response in the acute post-stroke period. Nevertheless, the potential for expanded Tregs to convert into pro-inflammatory effector T cells post-ischaemia needs to be balanced with the beneficial effect on neuroinflammation (322).

To increase the external validity of this study, and to investigate any potential links between Tregs and experimental stroke outcome, data obtained from young, aged, and atherosclerotic mice treated with either saline or fingolimod (0.5 mg/kg) was pooled for correlation analysis (Supplementary Material**, Fig. S2.7**). As an outcome marker, only the grid-walking test showed a significant treatment effect, suggesting this may be the most robust predictor of functional improvement in the model of pMCAO employed. Indeed, in saline-treated mice, a strong positive correlation was noted between peripheral CD8+ T cell frequencies and performance in the grid-walking test at 3 days. A strong negative correlation existed between peripheral CD4+ T cell frequencies and performance at the same timepoint. Due to effect of fingolimod on both cells noted above, changes in such correlations may have been expected. Despite weakening the association at day 3, however, fingolimod markedly strengthened the same correlations at day 7. Focusing in on Tregs, positive correlations were noted between peripheral Treg frequencies and grid-walking test performance at day 7 in saline-treated mice, particularly in young and $ApoE^{-/--}$ cohorts (Supplementary Material**, Fig. S2.8**). This is in line with the results of previous clinical studies, wherein patients with higher circulating Tregs post-cerebral ischaemia displayed better functional recovery (152-154). Interestingly, however, fingolimod treatment reversed

the correlation between these cells and functional outcome. This may suggest that, despite upregulating Treg frequency, fingolimod may have a deleterious effect on Treg function post-ischaemia or may potentiate pro-inflammatory functions among non-Treg lymphocytes. Whether this relationship between Tregs and neurobehavioural outcome in fingolimod-treated mice is dependent on dose and/or treatment window remains unknown.

2.5 Conclusion

Fingolimod has attracted attention in stroke research due to its proposed ability to sequester neurotoxic immune cells within lymph nodes while possibly also providing direct protection to the blood brain barrier (BBB) and brain cells. This study shows for the first time that fingolimod also increases peripheral Treg frequency post-ischaemia and enhances FoxP3+ cells in the infarcted brain. These effects were observed in young mice but also notably in aged and $ApoE^{-/-}$ mice, two common stroke co-morbidities with known alterations in T cell function (117, 310). While the 0.5 mg/kg dose of fingolimod was shown to increase peripheral and brain Tregs across all models, it is at the lower end of effective doses used in preclinical studies of fingolimod in stroke. A pooled analysis revealed Treg frequencies in drug-treated mice were also inversely correlated with functional recovery at seven days post-ischaemia. Therefore, a longer treatment window may be desirable to ensure improved stroke recovery in the clinic. In order to confirm Tregs play a role in the neuroprotective effect of fingolimod, the drug should be tested in mice in which Tregs are depleted (e.g., anti-CD25) or downregulated (e.g., diabetic stroke) (301, 323). Separately, an evaluation of the factors which determine Treg numbers and function in human stroke could help identify further patient populations who may benefit. Finally, the

possibility to combine immunomodulatory drugs such as fingolimod with intravenous or intra-arterial reperfusion therapy should be considered, whether as a means to extend the reperfusion window, ameliorate reperfusion injury, or enhance immunomodulatory activity at the infarct site (324). Overall, this study provides key information on the potential mechanism of action of fingolimod as a treatment for stroke needed for successful clinical translation.

Supplementary material related to chapter 2

Study	# of mice allocated to pMCAO/Sham	# of mice excluded for serious uncontrollable haemorrhage	# of mice culled for reaching humane endpoint (HEP)	# of surgical mice tissue collected from	# of samples excluded by ROUT method	# of samples included in final analysis
Dose response in young mice	51 (+ 8 naïve controls): 59 total	3	1	47 (except n = 44 spleen and n = 46 blood)	n = 0 cell frequency n = 2 cell counts	n = 55 unless otherwise indicated
Aged	32	3	2	20	n = 0 cell frequency n = 3 cell counts	n = 20 unless otherwise indicated
ApoE$^{-/-}$	38	7	0	23 (except n = 22 blood)	n = 0 cell frequency n = 1 cell counts	n = 23 unless otherwise indicated
Young vs. Aged mice (including naïve)	39 (+28 naïve controls): 67 total	2	1	55	n = 0 cell frequency n = 0 cell counts	n = 64 unless otherwise indicated
Treatment Duration	52 (+ 9 naïve controls): 61 total	2	2	45 (except n = 44 blood)	n = 0 cell frequency n = 0 cell counts	n = 57 unless otherwise indicated
Total:	257	17	6	190	n = 0 cell frequency n = 6 cell counts	N = 219

Table S2.1: Detailed breakdown of number of mice excluded pre-surgery, mid-surgery for serious uncontrollable haemorrhage, or post-surgery for reaching a humane endpoint. Details of naïve mice added, as well as samples missed or excluded post-analysis by ROUT method also outlined.

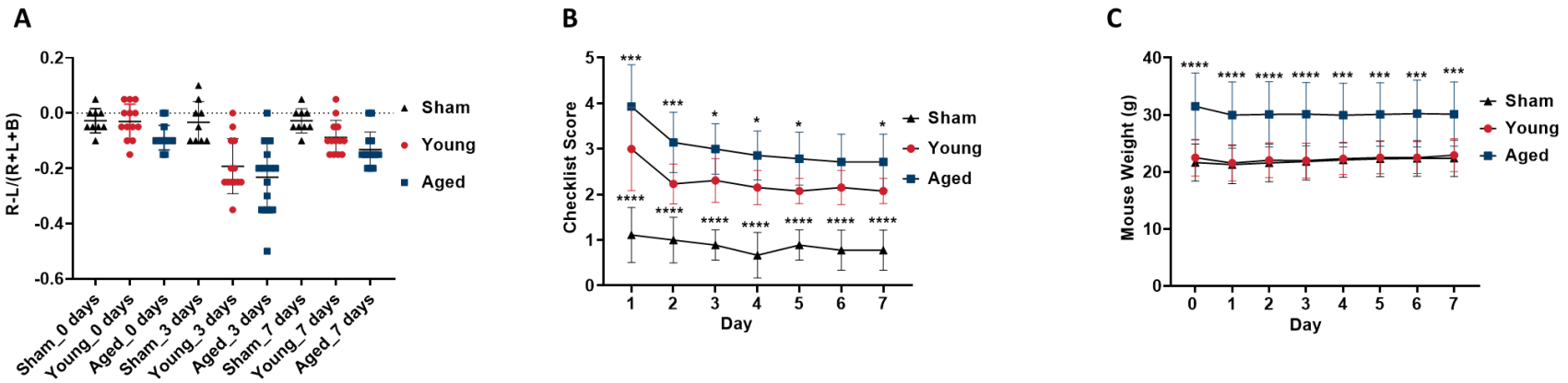


Figure S2.1: Comparison of A) neurological deficit score (as assessed by cylinder test (t = 3, 7 days), B) total checklist neuroscore, and C) mouse weight between sham, young and aged mice. Two-way repeated measures ANOVA followed by post-hoc Tukey's multiple comparisons were used to investigate differences between groups (* = p<0.05, ** = p<0.01, *** = p<0.001 as compared to young mice). Plots depict mean +/- standard deviation. Firstly, in sham mice, it was confirmed that no change in neuroscore was observed between any timepoints (p = 0.9931). In young and aged mice, a significant drop in neuroscore was observed between pre-behaviour and 3-days post-ischaemia (p <0.0001). This had significantly recovered in both cohorts by 7-days post-ischaemia (p = 0.0014). Older mice showed a worse neuroscore than young mice (p <0.0469). However, this did not achieve significance at any individual timepoint. For total checklist scores, we confirmed sham mice showed no significant difference between timepoints (p > 0.9999), and that the induction of ischaemia produced an increase in checklist score (p <0.0001). For both young and aged mice, checklist scores deteriorated post-ischaemia and remained significantly lower at all timepoints (p <0.0001). At all but one timepoint (D6), aged mice showed markedly higher checklist scores (p <0.0001). An investigation of mice weight showed no change pre- and post-surgery in sham mice (p = 0.5645). Conversely, for both young (p = 0.0001) and aged (p <0.0001) mice, a significant drop occurred between D0 and D1. For young mice, no significant difference from pre-surgery weight existed from D2 onwards, while aged mice remained significantly lower at all timepoints (p <0.0001 each). No difference was observed in weight between sham and young mice at any timepoint. Conversely, aged mice were significantly heavier than young mice (p = 0.0001). This difference narrowed but remained significant between D4-D7 post-ischaemia.

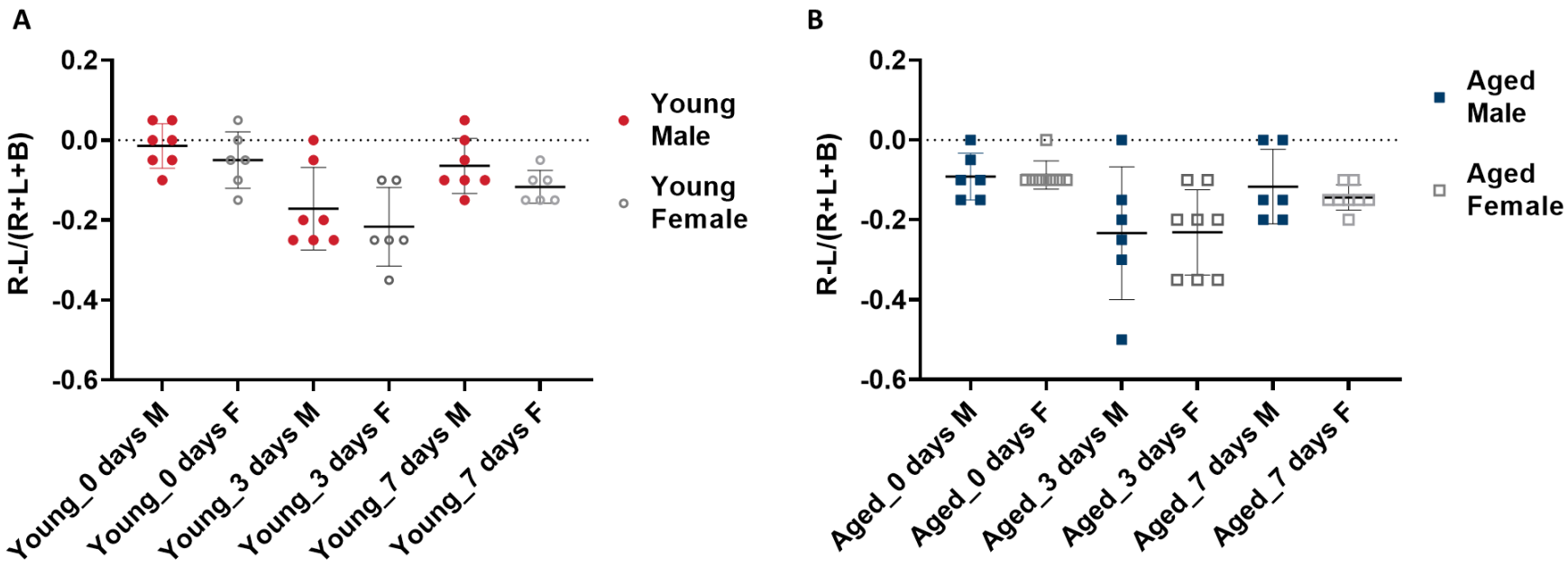


Figure S2.2: Comparison of neurological deficit score (as assessed by cylinder test (t = 3, 7 days) in A) young male and female mice, and B) aged male and female mice. Two-way repeated measures ANOVA followed by post-hoc Tukey's multiple comparisons were used to investigate differences between groups (* = $p<0.05$, ** = $p<0.01$, *** = $p<0.001$). Plots depict mean +/- standard deviation. In young mice, a significant drop in neuroscore was observed between pre-behaviour and 3-days post-ischaemia in both male (p = 0.0001) and female (p = 0.0002) mice. This had significantly recovered by 7-days post-ischaemia (p = 0.0066, 0.0201 respectively). No differences were observed between young male and female mice at any timepoint (p = 0.2111). In aged mice, similar deteriorations in neuroscore from pre-behaviour to 3-days post-ischaemia were noted in male (p = 0.0247) and female (p = 0.0075) mice. No significant improvement for either male (p = 0.0781) or female (p = 0.1529) was observed between 3 and 7 days. However, by 7-days post-ischaemia neuroscores in both male (p > 0.9999) and female (p = 0.5970) mice were indistinguishable from pre-behaviour. Once more, no effect of sex was observed at any timepoint (p = 0.8277).

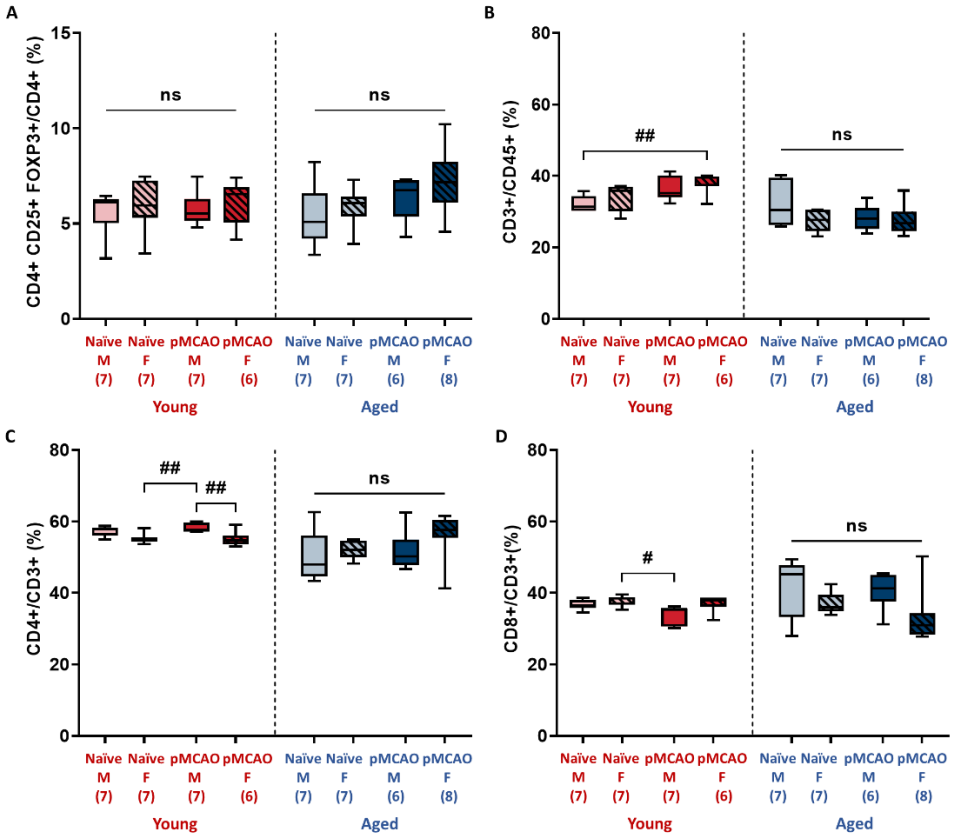


Figure S2.3: Effect of sex and pMCAO on the frequency of A) CD4+ CD25+ FoxP3+, B) CD3+, C) CD4+, and D) CD8+ T cells in spleen of young and aged mice (t = 7 days). Young mice are shown in red, aged mice are shown in blue. Male mice are shown in clear boxes, female mice are shown in hatched boxes. Naïve mice were age-matched mice who did not undergo any surgery. Two-way analysis of variance (ANOVA) tests with post hoc Tukey's multiple comparisons were performed to investigate differences between groups (# = $p<0.05$, ## = $p<0.01$, ### = $p<0.001$). The number of mice per group shown in parentheses on x-axis. Box-and-whisker plots exhibit 10-90 percentiles.

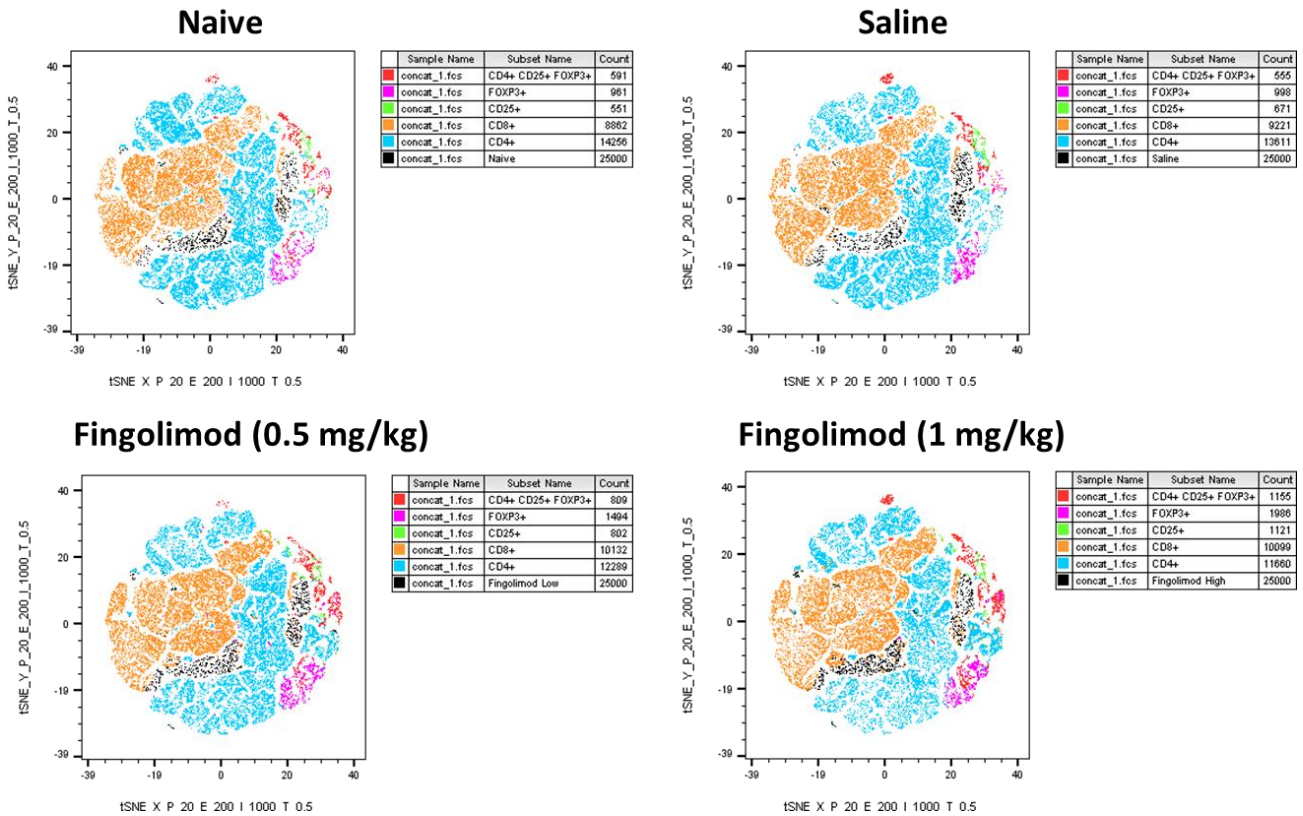


Figure S2.4: t-Distributed stochastic neighbour embedding (t-SNE) plot showing clusters and annotations of spleen cells obtained from young mice receiving either saline, low dose (0.5 mg/kg) fingolimod treatment or high dose (1 mg/kg) fingolimod treatment at 7 days post-pMCAO. An increased in Tregs (coloured in red) can be noted between saline-treated and fingolimod-treated mice.

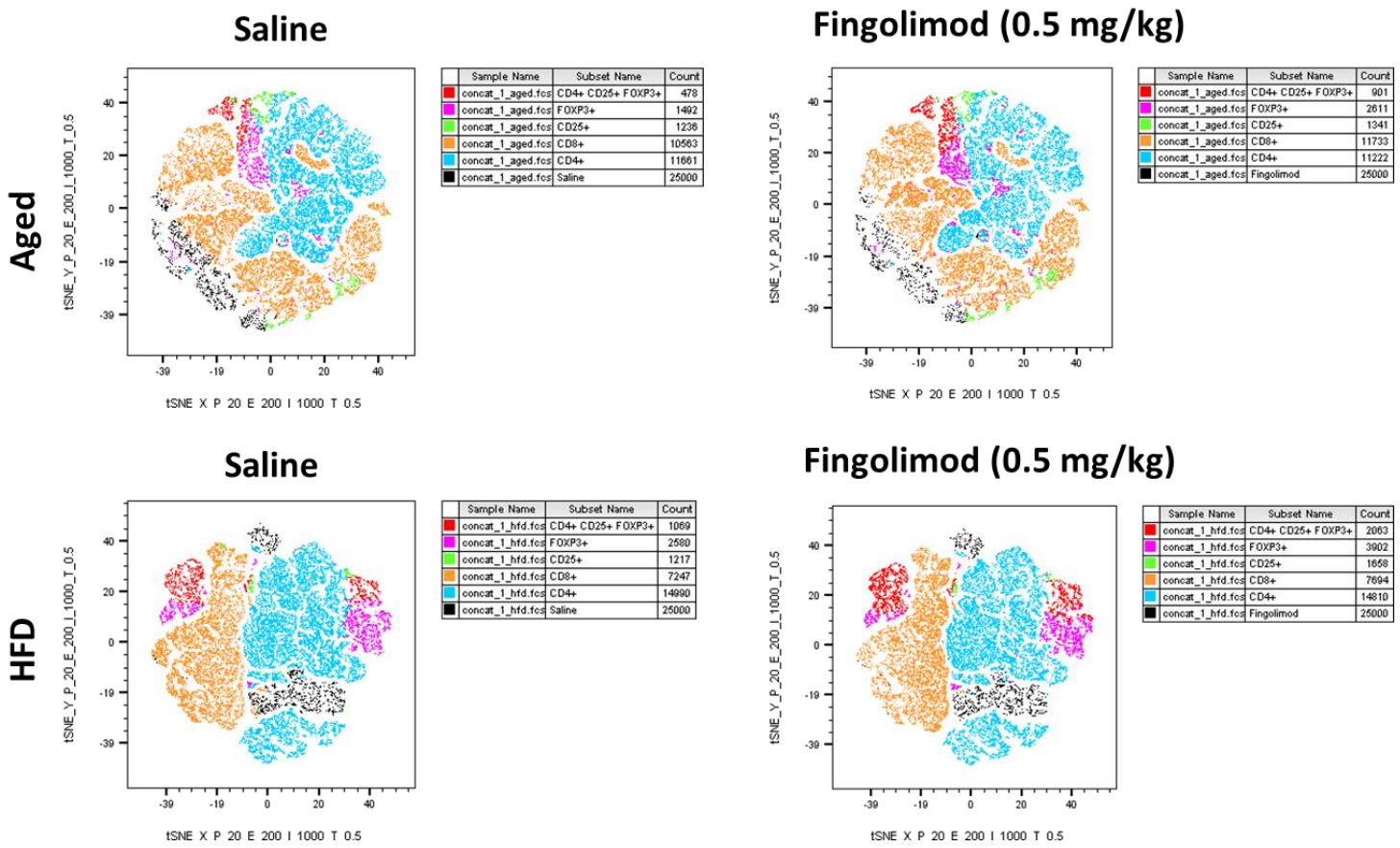


Figure S2.5: t-Distributed stochastic neighbour embedding (t-SNE) plot showing clusters and annotations of spleen cells obtained from aged mice and ApoE$^{-/-}$ mice fed a high-fat diet (HFD) receiving either saline or fingolimod treatment at 7 days post-pMCAO. An increased in Tregs (coloured in red) can be noted between saline-treated and fingolimod-treated mice.

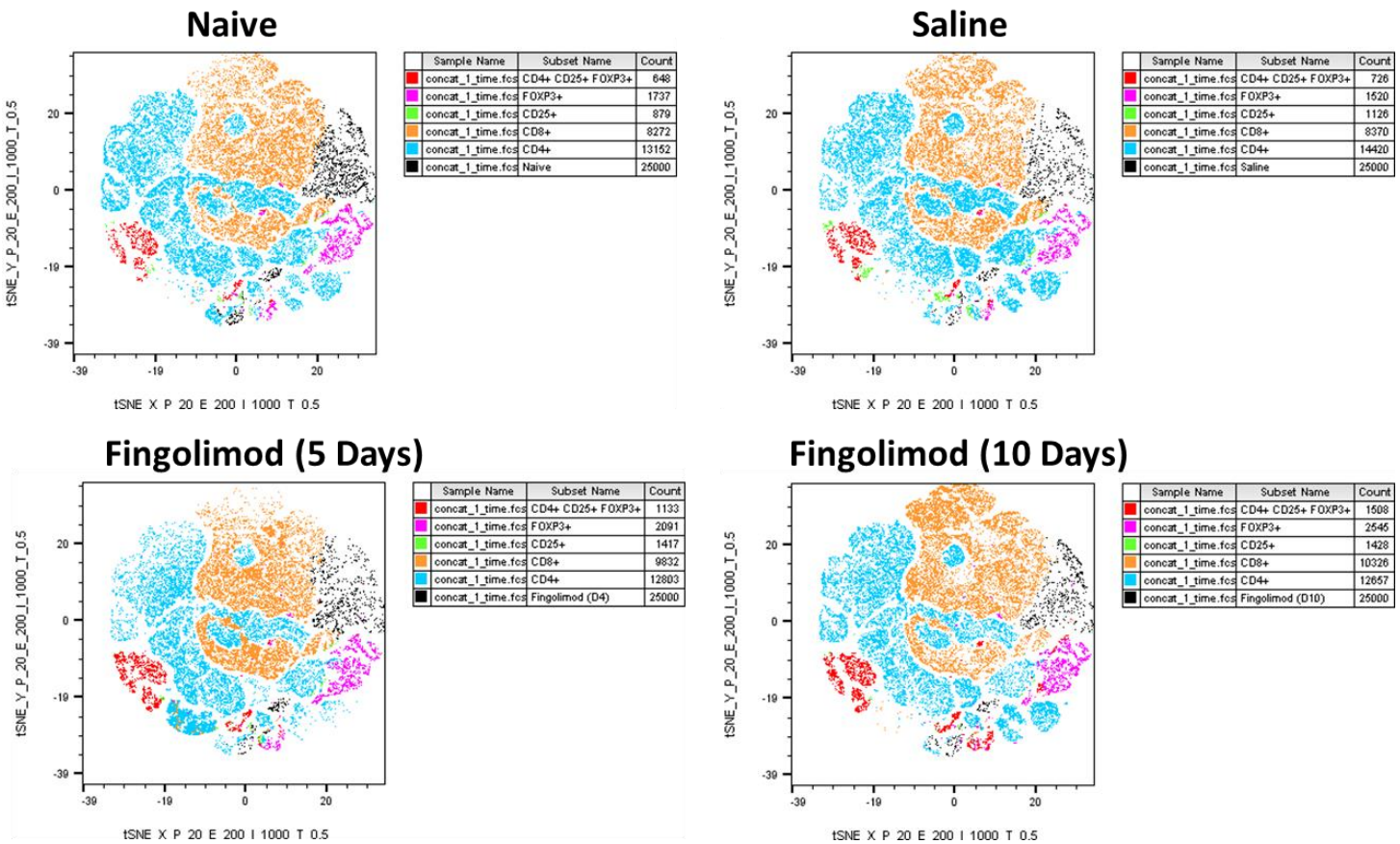


Figure S2.6: t-Distributed stochastic neighbour embedding (t-SNE) plot showing clusters and annotations of spleen cells obtained from young mice receiving either saline, short-term (5 days) fingolimod treatment, or long-term (10 days) fingolimod treatment at 10 days post-pMCAO. An increased in Tregs (coloured in red) can be noted between saline-treated and fingolimod-treated mice.

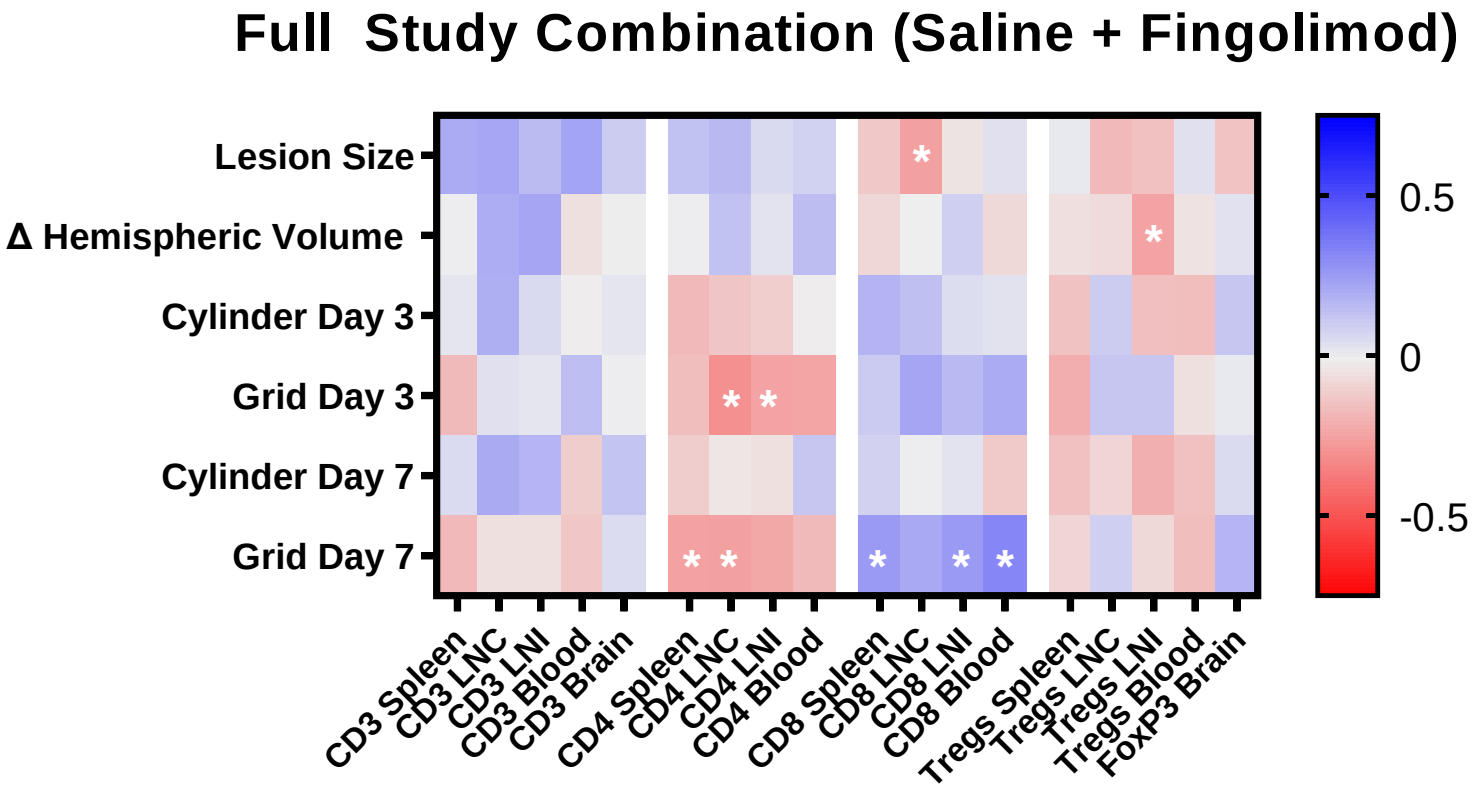


Figure S2.7: Correlation matrix between the proportion of T lymphocytes and experimental outcomes. Heat map depicting correlations between lymphocyte proportions and experimental outcomes (infarct volume, hemispheric volume, and cylinder/grid scores at days 3 and 7) for young, aged, and ApoE$^{-/-}$ mice. The colour bar represents Pearson r value on a scale from -0.75 to +0.75. For statistical significance, $p<0.05$ = *, $p<0.01$ = **, $p<0.001$ = ***. The same general associations are observed between CD4+/CD8+ T cells and grid day 7 results as for fingolimod-treated mice alone.

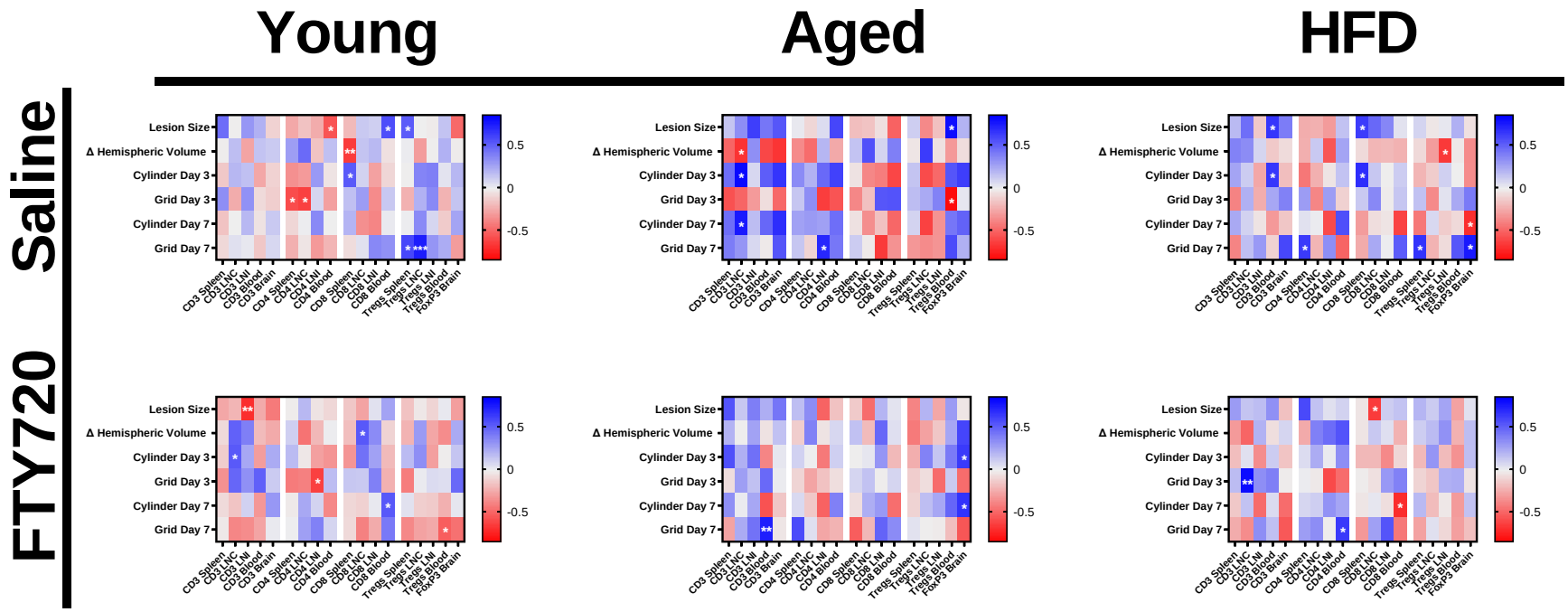


Figure S2.8: Correlation matrix between the proportion of T lymphocytes and experimental outcomes. Heat map depicting correlations between lymphocyte proportions and experimental outcomes (infarct volume, hemispheric volume, and cylinder/grid scores at days 3 and 7) for young, aged, and ApoE$^{-/-}$ mice receiving either saline or fingolimod (0.5 mg/kg) treatment. The colour bar represents Pearson r value on a scale from -0.75 to +0.75. For statistical significance, $p<0.05$ = *, $p<0.01$ = **, $p<0.001$ = ***. Notably, positive correlations observed between Treg cells in saline-treated young and ApoE$^{-/-}$ mice are reversed with fingolimod treatment.

Chapter 3

The Impact of Fingolimod on Treg Function in Brain Ischaemia

In Chapter 2, the effect of fingolimod on regulatory T cells in a mouse model of permanent brain ischaemia was characterised. Specifically, it was shown that fingolimod increases peripheral Treg frequency post-ischaemia and enhances FoxP3+ cells in the infarcted brain. However, correlation analysis did not reveal a strong link between Tregs and functional recovery in fingolimod-treated mice. In this chapter, I investigated why fingolimod failed to improve neurobehavioural outcome despite enhancing the frequency of neuroprotective Tregs. My hypothesis was that fingolimod would increase Treg suppressive function. However, I also aimed to investigate conventional T cell susceptibility to such suppression.

The text of this chapter is the submitted manuscript:

Malone K, Shearer JA, Waeber C, Moore AC. The Impact of Fingolimod on Treg Function in Brain Ischaemia. *Submitted to Journal of Neuroimmune Pharmacology (May 2022).*

Abstract

Background*:* Fingolimod can have a neuroprotective effect in mouse models of stroke. We previously showed fingolimod increases the frequency of regulatory T cells (Tregs) in permanent brain ischaemia. Here, we tested the hypothesis that as well as selectively enhancing peripheral Treg frequency and the number of Tregs in the post-ischaemic brain, fingolimod modulates T cells towards a regulatory phenotype with respect to cytokine production. Secondly, we investigated how fingolimod altered the Treg suppressive function and the sensitivity of effector T cells to regulation.

Methods: Mice that had underwent permanent electrocoagulation of the left middle cerebral artery received saline or fingolimod (0.5mg/kg) once daily for ten days post-ischaemia. The effect of brain ischaemia in the presence and absence of fingolimod on Treg phenotype, CD4+ and CD8+ T cell cytokine expression, and suppressive function was determined at day 10 post-ischaemia.

Results: Fingolimod improved neurobehavioural recovery compared to saline control. Fingolimod treatment increased Treg frequency in the periphery and brain. Tregs from fingolimod-treated animals also had higher expression of CCR8 but not CCR5 or CCR6 in these tissues. Fingolimod increased the frequencies of CD4+ IL-10+/CD4+ IFN-γ+ T cells in spleen and blood, as well as CD4+ IL-17+ T cells in the spleen but did not affect CD8+ T cell cytokine production. Brain ischaemia reduced Treg suppressive function compared to untreated animals. Fingolimod treatment rescued this function against saline-treated but not fingolimod-treated CD4+ effector T cells.

Conclusions: In summary T cells from fingolimod-treated mice showed enhanced secretion of Th1, Th17 and Treg cytokines. Fingolimod improved the suppressive

function of Treg post-stroke but also increased the resistance of CD4+ effector cells to this suppression. This capacity of fingolimod to increase both effector and regulatory functions likely contributes to the lack of consistent improvement in functional recovery in brain ischaemia.

3.1 Introduction

Fingolimod (FTY720) was introduced as an FDA-approved drug for the treatment of multiple sclerosis (MS) in 2010 under the brand name Gilenya (230, 231). The principal mechanism of action of fingolimod is thought to involve its action as a functional antagonist of the S1P1 receptor. This function prevents the movement of potentially neurotoxic T cells from the lymph nodes to the peripheral circulation and, by extension, the central nervous system (236). Due to the negative role T cells play in the evolution of acute brain ischaemia, and other commonalities between MS and stroke pathophysiology, fingolimod has also been extensively trialled in both pre-clinical and clinical ischaemic stroke (317, 325). It has been reported that the drug reduces infarct size and ameliorates neurological deficit in transient and permanent models of experimental cerebral ischemia in both mice and rats (244, 245, 249, 265). A meta-analysis concluded infarct volume was reduced by 30.4% and behavioural outcome improved by 34.2% (265). Pilot clinical studies in small numbers of ischaemic stroke patients have also demonstrated fingolimod to be safe and effective, alone or when combined with thrombolysis (267-269). Mechanistically, the lymphopenia associated with fingolimod treatment in MS may also play a major role in the neuroprotection observed in stroke (60). However, effects unrelated to recirculating lymphocytes are also likely to be involved. For example, fingolimod may also reduce leukocyte adhesion markers, improve endothelial cell function, enhance

blood-brain barrier integrity, skew microglia towards an anti-inflammatory M2 phenotype, or afford direct neuroprotection (249, 264, 283, 326-329). Receptor-independent mechanisms involving increased histone acetylation or neurotrophic factor generation might also contribute (240).

We previously demonstrated that fingolimod increased a subpopulation of T cells termed regulatory T cells (or "Tregs"; defined as being CD4+CD25+Foxp3+ T cells) in blood and secondary lymphoid organs at seven days post-permanent middle cerebral artery occlusion (pMCAO), and enhanced the number of brain infiltrating FoxP3+ cells in young, aged and hyperlipidaemic mice (330). We also determined that the frequency of Treg positively correlated with behavioural recovery to ischemic stroke in saline-treated mice, suggesting a potential neuroprotective effect of this T cell population (289). Indeed, previous research has shown Tregs improve disease outcome in stroke, with the only detrimental effects thought to be a role in secondary microthrombosis (134).

By combining our observation that fingolimod increases Treg frequency post-ischaemia with the known beneficial effect of this drug in pre-clinical models of stroke, we hypothesised that fingolimod shifts T cells towards a regulatory phenotype, and also enhances suppressive function. The primary aim of this study was to address these hypotheses. We determined the impact of fingolimod on Treg suppressive capacity, and the sensitivity of conventional T cells to such suppression. Secondly, we focussed on determining fingolimod's *in vivo* effects on CD4+ and CD8+ T cell cytokine production and chemokine receptor expression, at 10 days post-pMCAO in young mice. Recent reports suggest Tregs which accumulate in brain tissue in the weeks following ischaemic stroke highly express CCR6 and CCR8 (121). Given that

the infusion of wild-type Tregs but not $CCR5^{-/-}$ Tregs attenuated brain injury in a model of transient brain ischaemia, this receptor may, as well as CCR6 or CCR8, be involved in the fingolimod-mediated recruitment of Tregs to the infarct site. A 10-day regimen of fingolimod (0.5 mg/kg) was chosen as our previous research demonstrated this would significantly enhance the Treg phenotype in spleen, as well as maximize the number of Tregs that we could retrieve from infarcted brain tissue (330). A secondary aim of this study was to confirm whether the 10-day course of fingolimod would improve neurobehavioural recovery post-ischaemia.

3.2 Methods

3.2.1 Materials

Fingolimod hydrochloride was obtained from Novartis Institutes for Biomedical Research, Basel. Complete medium consisted of RPMI-1640 (with 2mM L-glutamine and 1mM sodium pyruvate) (Sigma-Aldrich, #R7658), 10% FCS (Sigma-Aldrich, #F2442), 10 mM HEPES (Sigma-Aldrich, #H0887), 0.01 mM mercaptoethanol (Sigma-Aldrich, #M3148), 100U/ml Penicillin/Streptomycin (#P4458). All flow cytometry antibodies were obtained from eBioscience or Miltenyi Biotec. All other reagents and materials were obtained from Sigma-Aldrich or Miltenyi Biotec as detailed below.

3.2.2 Mice

Animal experiments were carried out in accordance with the European Directive 2010/63/EU, following approval by the Animal Ethics Committee of University College Cork and under an authorization issued by the Health Products Regulatory Authority Ireland (license number AE19130/P075). The study was conducted and its

results reported according to the ARRIVE guidelines (288). All mice were sourced from Envigo unless otherwise stated. For cytokine and chemokine work, n = 21 male C57BL/6JOlaHsd (7-week-old) mice were used. For suppression assay work, n = 25 male C57BL/6 (7-week-old) mice were used. All mice were acclimatized for at least one week before any procedure took place. Mice were group housed in individually ventilated cages in a specific-pathogen-free facility. Mice were exposed to a 12-hour light/12 hour-dark cycle and kept at a temperature of 20-24°C and a relative humidity of 45-65%. Mice were provided with environmental enrichment and *ad libitum* access to both food and water. A total of n = 46 were included as part of this study.

3.2.3 Ischaemia Model

A permanent distal middle cerebral artery occlusion model (pMCAO) was employed, as previously described (38, 330). Briefly, mice were anesthetized by vaporiser with isoflurane (3-4% for induction; 1-2% for maintenance) in O_2/N_2 (30%/70%). The skin between the left ear and eye was incised, and the temporal muscle retracted to expose the temporal and parietal bones. In sham animals, only the skin incision and exposure of the skull was performed. A small craniotomy was performed, and the meninges perforated to expose the MCA. The distal portion, including the branches and the main artery below the bifurcation, were occluded using a small vessel bipolar electrocoagulation forceps (Bovie Bantam Pro electrosurgical generator (#A952) /McPherson 3 1/2" straight forceps (#A842) (Symmetry Surgical Inc, USA)). The MCA was cut to confirm successful occlusion, after which the incision was sutured, and anaesthesia discontinued. Mice were allowed to recover in a heated chamber (32°C) for 30 minutes before being returned to their home cage. Experimental mice were monitored daily using a scoresheet which graded weight loss (from 0-3),

appearance changes (from 0-3), behaviour (from 0-3), and neurological score (0: no observable deficit, 1: forelimb flexion, 2: decreased resistance to lateral push and forelimb flexion without circling, 3: same as 2, with circling) (331).

3.2.4 Fingolimod Treatment

Once daily for 10 days post-ischaemia, mice received either normal saline or 0.5 mg/kg fingolimod via interperitoneal (i.p.) injection. A researcher not associated with the surgery prepared treatment solutions (pH 7.0) for volumes no greater than 250µl per injection.

3.2.5 Neurological Deficit Evaluation

Mice underwent neurological evaluation at 3- and 10-days post-stroke. Each mouse was placed in a clear Perspex cylinder (12.5 cm Diameter x 23.5 cm Height) for 5 minutes. The sessions were videoed (Canon Legria HFR706). The number of times the mouse used a paw for weight support against the wall of the cylinder was counted over a five-minute period (a minimum of 20 contacts were recorded). Specifically, the independent use of the left (L) or right (R) forepaw, or simultaneous use of both (B) forepaws was noted. The 3 numbers were then expressed as a percentage of all paw contacts with the wall to obtain a neurological deficit score (R-L)/(R+L+B).

3.2.6 Tissue Collection and Processing

At 10 days post-ischaemia, mice were culled by anaesthetic overdose (200 mg/ml i.p.; Euthatal; Merial, France). Blood was collected from the descending aorta and transferred into EDTA (approximately 500 µl). Mice were then perfused transcardially with 20ml cold phosphate buffered saline (PBS) (Sigma-Aldrich, #P4417). The brain, spleen, Peyer's patches, and cervical/inguinal lymph nodes were harvested. Spleen

and lymphoid tissue was processed as previously reported (330). Where relevant, red blood cells were lysed using lysis buffer (eBioscience, #430054). After washing, samples were re-suspended in PBS and counted using trypan blue (Sigma-Aldrich, #T8154) to determine total cell number and viability. Brains were divided into ipsilateral and contralateral hemispheres. After mechanical dissociation, leukocytes were isolated using discontinuous 30/70% Percoll (Sigma-Aldrich, #P1644) gradients, as previously described (332). Post-centrifugation, the cell fraction was collected, washed and then counted.

3.2.7 Flow Cytometric Analysis

For the analysis of intracellular cytokines, 2 x 10^6 cells per well of a 96 well V-bottom plate were resuspended in 200µl complete medium and stimulated for 4 hours at 37°C in a CO2 incubator with PMA plus ionomycin, in the presence of brefeldin A and monesin (Cell Stimulation Cocktail eBioscience, #00497593). Post-incubation, Fc receptors were blocked by incubation for 5 minutes with 50µl of anti-mouse CD16/CD32 (Clone 93, 1:100) (eBioscience, #14016182). Cells were then stained for 30 minutes at 2-8°C in the dark with anti-mouse CD45 (PerCP-CY5.5, eBioscience, # 45045182) (30-F11, 1:100), CD3 (PE-Cy7, eBioscience, #14003182) (145-2C11, 1:100), CD4 (FITC, eBioscience, #11004282) (RM4-5, 1:800), CD8 (Pacific Blue, eBioscience, #MCD0828) (5H10, 1:100), CD195 (PerCP eFluor710, eBioscience, #46195182) (HM-CCR5 (7A4), 1:100), CD196 (PE-Vio615, Miltenyi Biotec, #130108396) (REA277, 1:20), CD198 (PE-Vio615, Miltenyi Biotec, #130119922) (REA921, 1:50), and CD25 (APC, eBioscience, #17025182) (PC61.5, 1:100). A live/dead stain (1:10,000 solution) was also added to each sample (Fixable Viability Dye eFluor 780, #65086514) (eBioscience). Samples were then washed, fixed,

permeabilised, and stained intracellularly for 30 minutes at room temperature with either anti-mouse FoxP3 (PE, #12577382) (FJK-16s, 1:100), in accordance with the instructions provided with the Mouse Regulatory T Cell Staining Kit #1 (eBioscience, #88811140), or a cocktail of anti-IFN-γ (eFluor610, eBioscience, #61731182) (XMG1.2, 1:100), anti-IL-10 (PerCP-Cy5.5, eBioscience, #45710182) (JES5-16E3, 1:50), and anti-IL-17 (PE, BD, #559502) (TC11-18H10, 1:100). Samples were washed with permeabilization buffer, then re suspended in PBS. Flow cytometric analysis was performed with a LSRII flow cytometer (Becton Dickinson). Compensation control was set using BD CompBead Anti-Rat/Anti-Hamster Particles Set (BD, #552845). Data was analysed using FlowJo (v10) according to the following initial gating strategy: live cells (as determined by live/dead stain), lymphocytes (as determined by FSC/SSC), T lymphocytes (defined as CD3+), CD4+ and CD8+, and regulatory T cells (CD4+ T cells which co-express high levels of CD25 and FoxP3). Gates were set according to unstained samples, and fluorescent-minus-one controls (**Fig. 3.1**). Absolute cell counts for all tissues were calculated according to instructions provided with the CountBright Absolute Counting Beads (Molecular Probes, # C36950). All results were reported according to the Minimum Information About a Flow Cytometry Experiment (MIFlowCyt).

3.2.8 Isolation of Tregs from Post-Ischaemic Spleen

Treg cells were isolated using a mouse CD4+CD25+ Regulatory T Cell Isolation Kit, (Miltenyi Biotec, #130091041). Briefly, spleens were harvested from culled naïve (N), saline-treated (S), and fingolimod-treated (F) mice. For ischaemic mice, n = 3 spleens were pooled. For naïve controls, n = 2 spleens were pooled. CD4+ T cells were first

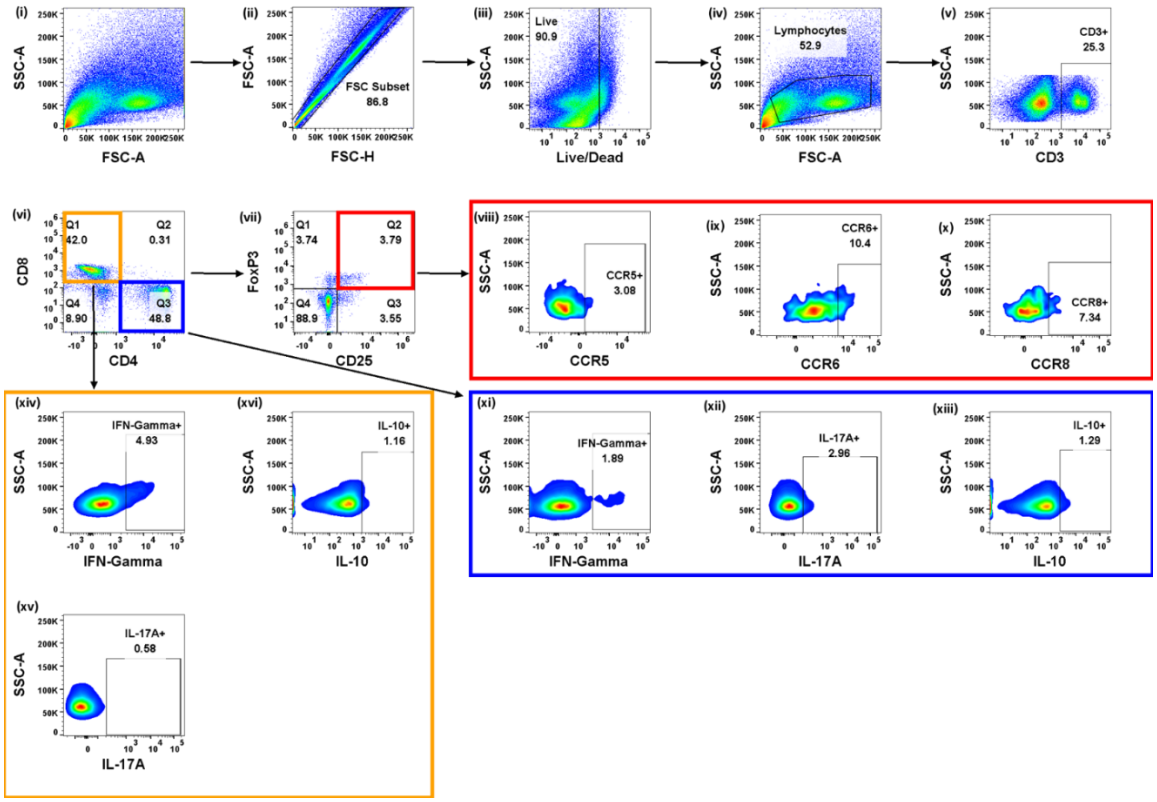


Figure 3.1: Gating strategy for determination of chemokine expression among Tregs (red), cytokine expression among CD4+ T cells (blue), and cytokine expression among CD8+ T cells (yellow) in representative mouse splenocytes post-brain ischaemia (t = 10 days). (i) = Initial population, (ii) = singlets, (iii) = Live cells, (iv) = lymphocytes, (v) = CD3+ T cells (T cells), (vi) = CD4+ vs. CD8+ T cells, (vii) = CD4+ CD25+ FoxP3+ T cells (quadrant in red) designated Tregs, (viii) = CCR5+ Tregs, (ix) = CCR6+ Tregs, (x) = CCR8+ Tregs, (xi) = CD4+ IFN-γ+ T cells, (xii) CD4+ IL-17A+ cells, (xiii) CD4+ IL-10+ T cells, (xiv) CD8+ IFN-γ+ T cells, (xv) CD8+ IL-17+ T cells, (xvi) CD8+ IL-10+ T cells. All gates were determined by both negative cells and fluorescence minus one controls.

negatively selected by magnetically labelling non-CD4+ T cells (CD8+, CD11b+, CD45R+, CD49b+, Ter-119+ cells). CD25+ (termed Treg) and CD25- (termed Tconv) T cells were then separated by magnetically labelling CD25+ T cells. To achieve higher purity, the CD4+ CD25+ fraction was re-applied to a second MS column and processed as before. Flow cytometry was used to determine the purity of the isolated Treg and Tconv populations for each condition (**Fig. 3.2**). The mean percentages of CD25- cells were 96.77+/-2.1, 96.80+/-1.67, and 93.97+/-3.36 for naïve, saline, and fingolimod conditions respectively (n = 3 replicates). The mean percentages of Treg (CD4+ CD25+) among CD4+ T cells were 98.3+/-0.4, 97.9+/-0.7, and 96.3+/-1.5 for

cells from naïve, saline, and fingolimod treated mice, respectively for the same samples.

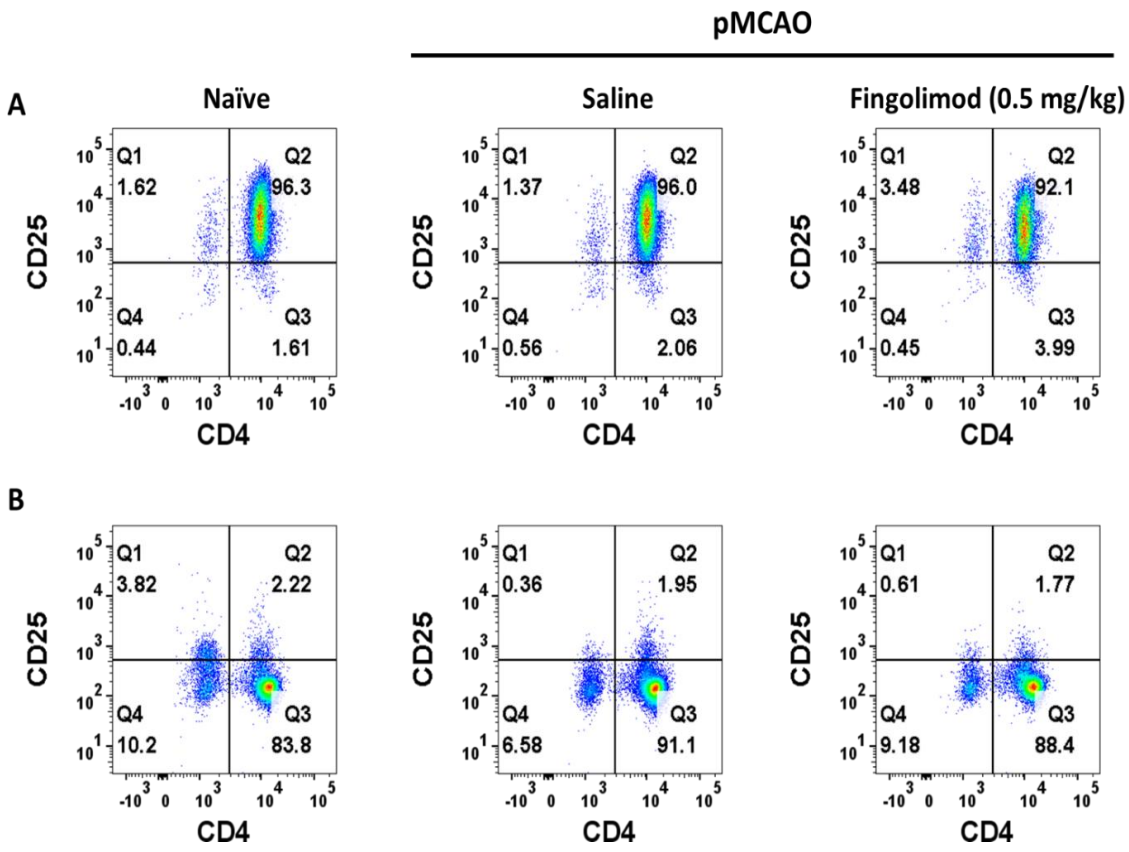


Figure 3.2: Treg and Tconv cells were isolated from spleens of naïve, saline-treated, and fingolimod-treated mice. Pseudocolour plots depict representative image from 1 replicate (n = 3 replicates total). A) Frequency of CD4 and CD25 +/- cells among enriched CD4+ CD25+ "Treg" cells. B) Frequency of CD4 and CD25 +/- cells among remaining cells in the CD25- fraction, termed "Tconv" cells.

3.2.9 Treg Suppression Assay

Wells of a 96-well U-bottomed plate were coated with anti-mouse CD3 (145-2C11) (eBioscience, #14003182) (50µl of a 1µg/ml solution) for 2 hours at 37°C, and then washed twice with PBS. Anti-mouse CD28 (eBioscience, #14028182) was added at a final concentration of 1µg/ml. Edge wells of the plates were filled with 200µl PBS. Isolated Tconv were first re-suspended at 1 x 10^6 cells/ml and Tregs at 2 x 10^6 cells/ml. For each condition, 5 x 10^4 Tconv were incubated with Tregs, the latter in decreasing

number to create Treg:Tconv ratios of 1:1, 1:2, 1:4, 1:8, 1:16, and 1:0. Each condition was plated in triplicate and incubated for 37°C/5% CO2 for 72 hours. At hour 68, thiazolyl blue tetrazolium bromide (MTT) (Sigma-Aldrich, #M5655) labelling reagent was added to each well at a final concentration of 0.5 mg/ml. After 4 hours, plates were centrifuged at 1500rpm for 5 minutes. The supernatant was carefully removed. The cell pellet was then dissolved in 200µl DMSO (Sigma-Aldrich, #D8418)/Ammonium hydroxide (800mM) (Sigma-Aldrich, #221228) and absorbance 570nm was read (333). For each condition, Treg suppression was calculated as a proportion of Tconv cell proliferation in the absence of Treg.

3.2.10 Statistical Analysis

The Kolmogorov–Smirnov test was used to ascertain that all data were normally distributed. Flow cytometric data are displayed as 10-90 percentile box-and-whisker plots. The ROUT method (Q = 1%) was used to identify possible outliers, which were then screened for exclusion. Two-sided, independent-samples T tests were employed to investigate differences between two groups. One-way analysis of variance (ANOVA) followed by post-hoc Tukey's multiple comparisons was used to investigate differences between three or more groups. One-way repeated measures ANOVA with post-hoc Tukey's multiple comparisons was used to investigate neurobehavioural results. Two-way repeated measures ANOVA followed by post-hoc Tukey's multiple comparisons was used to investigate differences between groups when the effect of two independent variables were studied. A p-value <0.05 was considered statistically significant. Statistical analysis was performed using GraphPad Prism 8.0. All investigators remained blinded to treatment groups throughout mouse husbandry, data acquisition and analysis.

3.3 Results

3.3.1 Fingolimod attenuates neurobehavioural deficits post-pMCAO

The impact of fingolimod (0.5 mg/kg) treatment on functional recovery, at 3- and 10-days post-stroke, was assessed by quantifying the effect of the drug on ischaemia-induced changes in cylinder test performance as compared to saline control. Before stroke induction ("pre-behaviour" baseline), no significant difference was observed between saline and fingolimod-treated mice ($p = 0.8857$). An increased deficit score, reflecting poorer performance, in saline-treated mice was confirmed at days 3 ($p = 0.0003$) and 10 ($p = 0.0017$) post-brain ischaemia compared to pre-stroke baseline (**Fig. 3.3**). In contrast, fingolimod-treated mice did not show different deficits at baseline, day 3 and day 10 ($p > 0.9999$). No significant differences were noted between saline and fingolimod-treated mice in terms of mouse weight ($p = 0.9872$) or checklist neuroscore ($p = 0.7483$). As expected, the time since ischaemia positively impacted on recovery for both metrics (checklist score: $p < 0.0001$, mouse weight $p < 0.0001$). In contrast fingolimod did not affect lesion size ($p = 0.6647$), ipsilateral/contralateral ratio ($p = 0.6433$), or tissue loss ($p = 0.5321$) vs. saline control (**Fig. 3.4**).

3.3.2 Fingolimod increases the frequency of CCR8+ Tregs in spleen, blood, lymph nodes, and brain post-pMCAO

To determine if modulation of chemokine receptor expression on Tregs may be associated with fingolimod's effect on previously observed increased Treg numbers in the brain (330), here we determined the surface expression of CCR5, CCR6 and CCR8 in both the brain and periphery of mice treated or untreated with fingolimod post-stroke, compared to mice who did not have stroke (naïve). As fingolimod differentially affects the sequestration of Treg and effector T cells (334), we examined

the frequency of Treg in multiple tissues. Peyer's patches were included as intestinal T cells have also been shown to migrate to the meninges post-ischaemia (63).

We first confirmed the fingolimod-mediated increase in Treg proportion of CD4+ T cells, observed in previous studies (**Fig. 3.5**) (330). This was observed in the periphery, except for the Peyer's patches, and in the post-ischaemic brain (spleen: $p = 0.0258$, draining lymph nodes: $p = 0.033$, inguinal lymph nodes: $p = 0.0013$, blood: $p = 0.0044$, brain: $p = 0.0408$, compared to saline treated animals).

The frequency of Tregs that expressed CCR5 or CCR6 was not significantly altered by brain ischaemia or by fingolimod treatment at 10 days post-ischaemia in any organ (**Fig. 3.6**). CCR8 expression on Tregs was significantly affected by stroke and by fingolimod treatment in most tissues. Brain ischaemia significantly reduced the frequency of CCR8+Tregs in spleen ($p = 0.0156$) and non-draining lymph nodes ($p = 0.0235$) (as well as to a lesser degree, draining lymph nodes ($p = 0.0489$)), but caused a significant increase in CCR8+ Tregs in blood. Fingolimod significantly increased CCR8+ Treg frequency in spleen ($p = 0.0007$), draining lymph nodes ($p = 0.0015$), non-draining lymph nodes ($p = 0.0067$), blood ($p = 0.0105$), and brain ($p = 0.0248$) compared to saline-treated animals, with levels restored to (spleen, draining lymph nodes, non-draining lymph nodes) or exceeding (blood) those observed in naïve, non-pMCAO controls. No ischaemia or fingolimod-induced changes were observed in CCR8+ Tregs in Peyer's patches. Overall, these findings demonstrate that fingolimod can restore or increase CCR8 expression on Treg in ischemic mice. Given the proposed role of CCR8 in Treg trafficking to the post- ischaemic brain (116), this trafficking may contribute to the enhanced frequency of Tregs observed in brains of

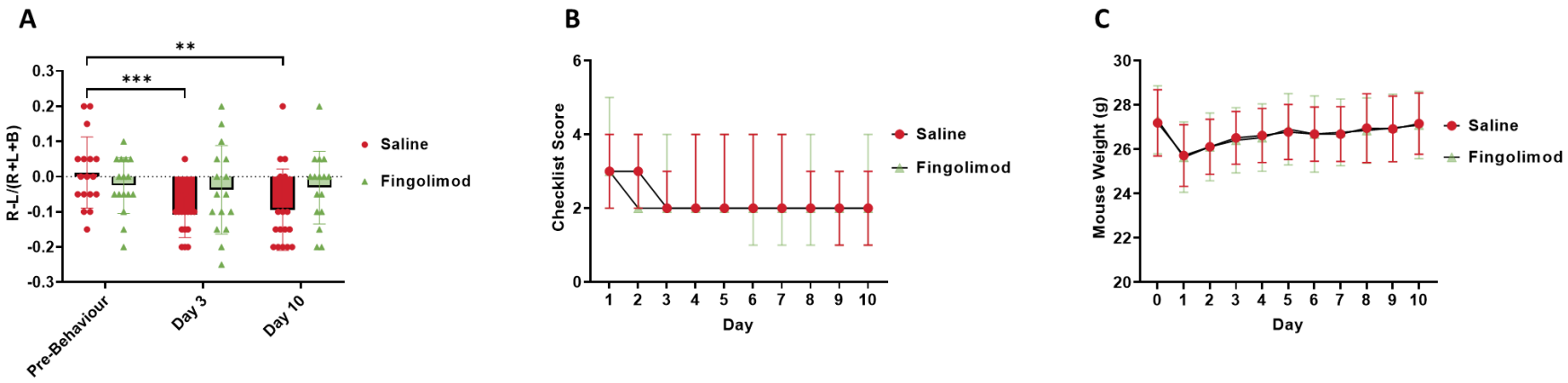


Figure 3.3: Neurobehavioural and clinical outcome of mice post-stroke with or without fingolimod treatment. A) Neurological deficit score (as assessed by cylinder test (t = 3, 10 days) B) Total checklist neuroscore C) Body weight in saline and fingolimod-treated mice. Two-way repeated measures ANOVA followed by post-hoc Tukey's multiple comparisons was used to investigate differences between groups (* = $p<0.05$, ** = $p<0.01$, *** = $p<0.001$ as compared to saline). Plots A, C depict mean ± standard deviation. Plot B depicts median (with range). N = 16-17 per group.

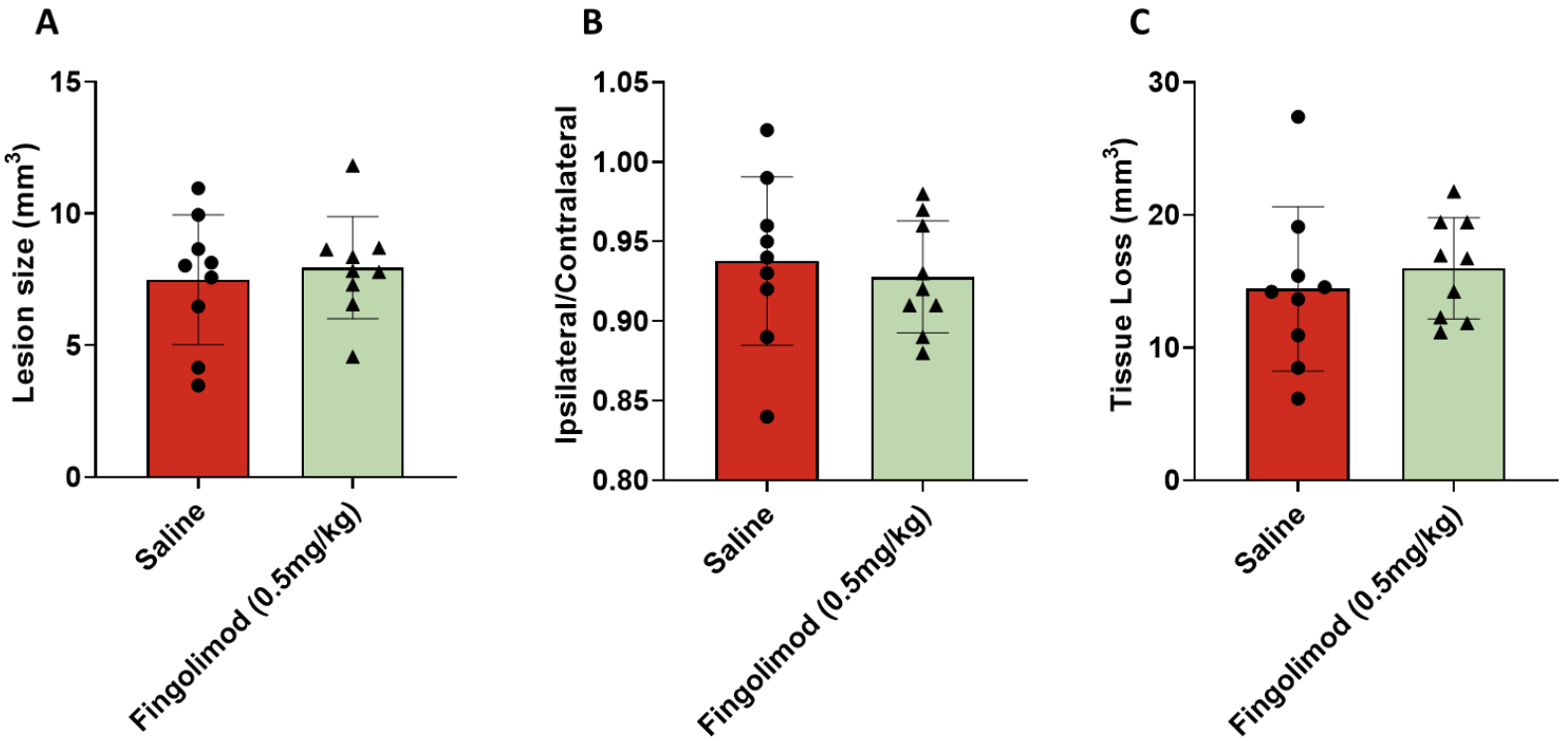


Figure 3.4: Comparison of A) lesion size (mm^3), B) ipsilateral/contralateral hemispheric volume ratio, and C) tissue loss (mm^3) between saline (n = 9) and fingolimod-treated (n = 9) mice as quantified by H & E staining (t = 10 days). Two-sided, independent-samples t-tests was used to investigate differences between groups. Scatter plots depict mean ± standard deviation.

fingolimod treated mice.

3.3.3 Fingolimod enhances secretion of IFN-γ, IL-17, and IL-10 by CD4+ T cells post-pMCAO

Next, we investigated how fingolimod modulates cytokine expression by all T cells from mice post-stroke. The expressions of IFN-γ, IL-17, and IL-10, subsequent to *in vitro* polyclonal stimulation, were used as markers of Th1, Th17, and Treg cells respectively for CD4+ T cells. We also examined the effect of fingolimod on CD8+ T cell cytokine expression.

Brain ischaemia alone did not influence IL-10, IFN-γ, or IL-17 from CD4+ T cells in any tissue (**Fig. 3.7)**. Fingolimod significantly increased the frequency of IL-10 and IFN-γ expressing CD4+ T cells in the spleen (p = 0.0254, 0.0006 for IL10 and IFN- γ respectively) and blood (p = 0.0027, 0.0232 respectively) compared to saline-treated animals (**Fig. 3.7)**. Elevated frequencies of CD4+ IL-17+ T cells were noted in fingolimod-treated spleen (p = 0.0168). Expression of IL-10, IFN-γ, or IL-17 by CD4+ T cells from lymph nodes, including Peyer's Patches, were not significantly different in fingolimod-treated mice compared to saline-treated mice. Few significant changes were detected in CD8+ T cells (**Fig. 3.8**). Brain ischaemia alone increased the frequency of CD8+IFN-γ+ T cells (p = 0.0487 compared to naive) in blood; this was not further affected by fingolimod treatment. Fingolimod increased the frequency of CD8+ IL-10+ T cells in non-draining lymph nodes (p = 0.0035).

We next investigated the effect of brain ischaemia and/or fingolimod on the polyfunctionality of CD4+ and CD8+ T cells in blood to determine if fingolimod modulated the plasticity of CD4+ T cells or if the drug caused selective expansion of

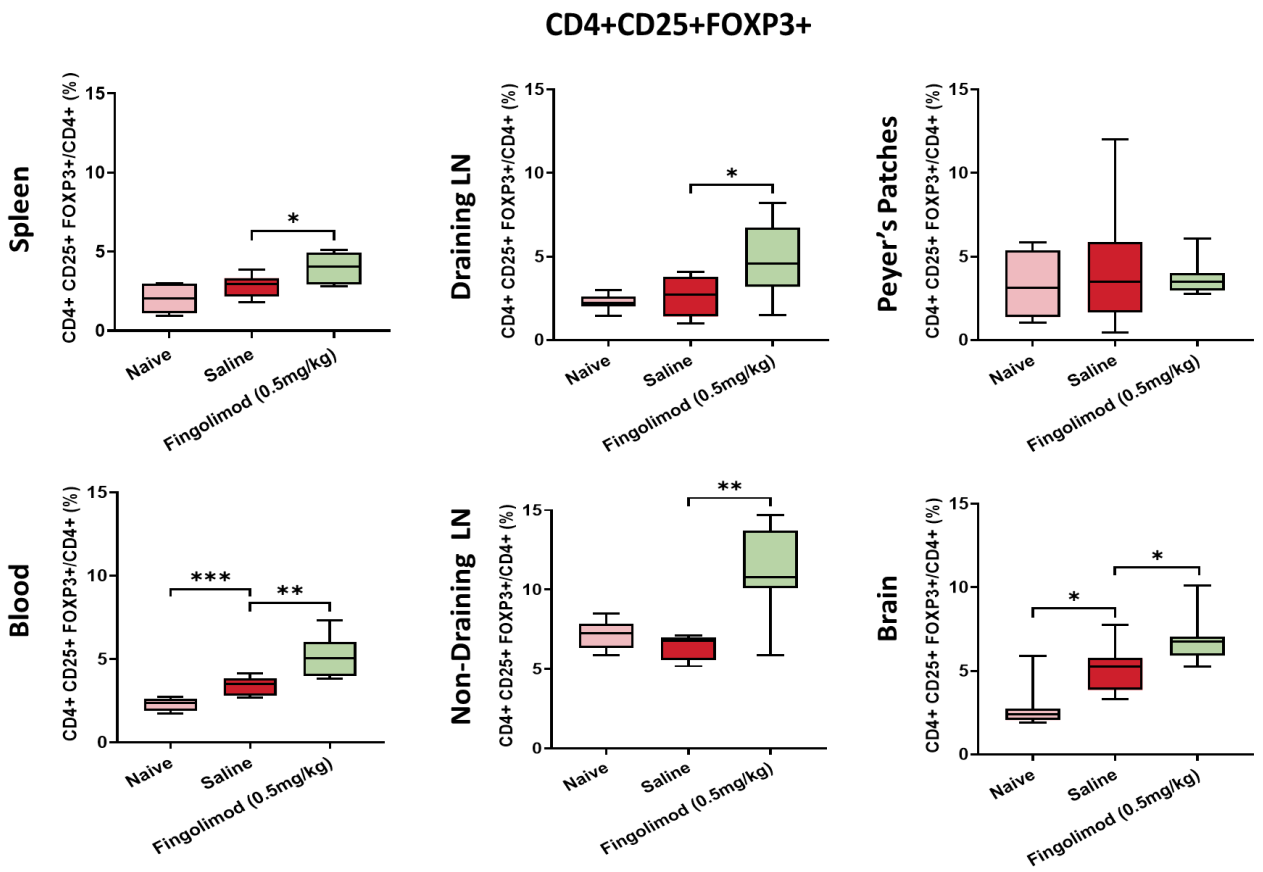


Figure 3.5: Frequency of CD4+ CD25+ FoxP3+ T cells in blood, brain, and secondary lymphoid tissue in response to saline or fingolimod (0.5 mg/kg)) treatment post-brain ischaemia in young mice (t = 10 days). Two-sided, independent-samples T tests investigated differences between two groups (* = $p<0.05$, ** = $p<0.01$, *** = $p<0.001$). Box-and-whisker plots exhibit 10-90 percentiles. Notably, once daily fingolimod 0.5 mg/kg treatment caused an increased Treg frequency in spleen, draining lymph nodes, non-draining lymph nodes, blood, and brain.

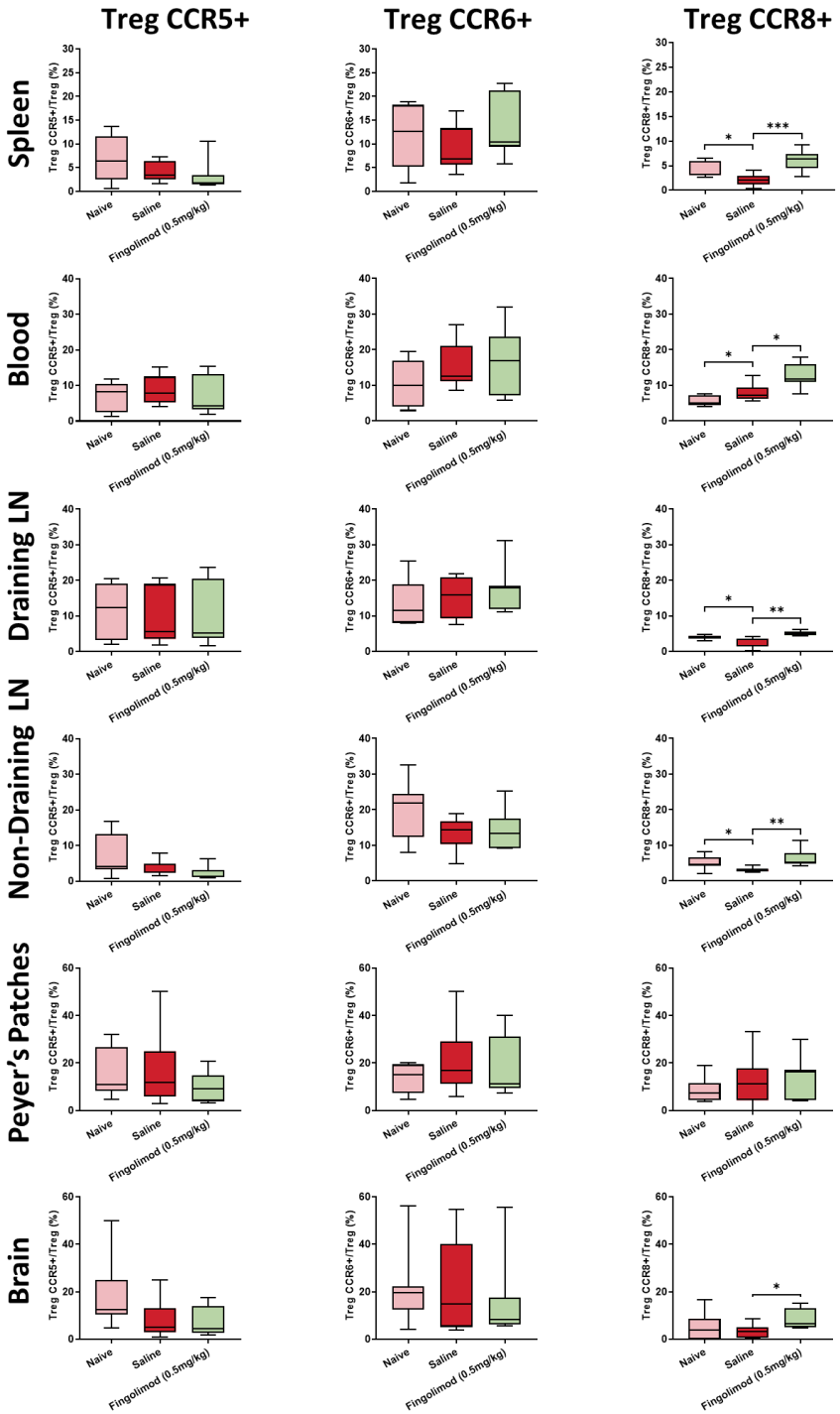


Figure 3.6: Frequency of CCR5+, CCR6+, and CCR8+ CD4+CD25hiFoxp3+ Treg cells in blood, brain, and secondary lymphoid tissue in response to saline or fingolimod (0.5 mg/kg)) treatment post-brain ischaemia in young mice (t = 10 days) (n = 7 per group). Two-sided, independent-samples T tests investigated differences between two groups (* = p<0.05, ** = p<0.01, *** = p<0.001 as compared to saline). Box and whisker plots display the 90/10 percentile at the whiskers, the 75/25 percentiles at the boxes, and the median in the centre line

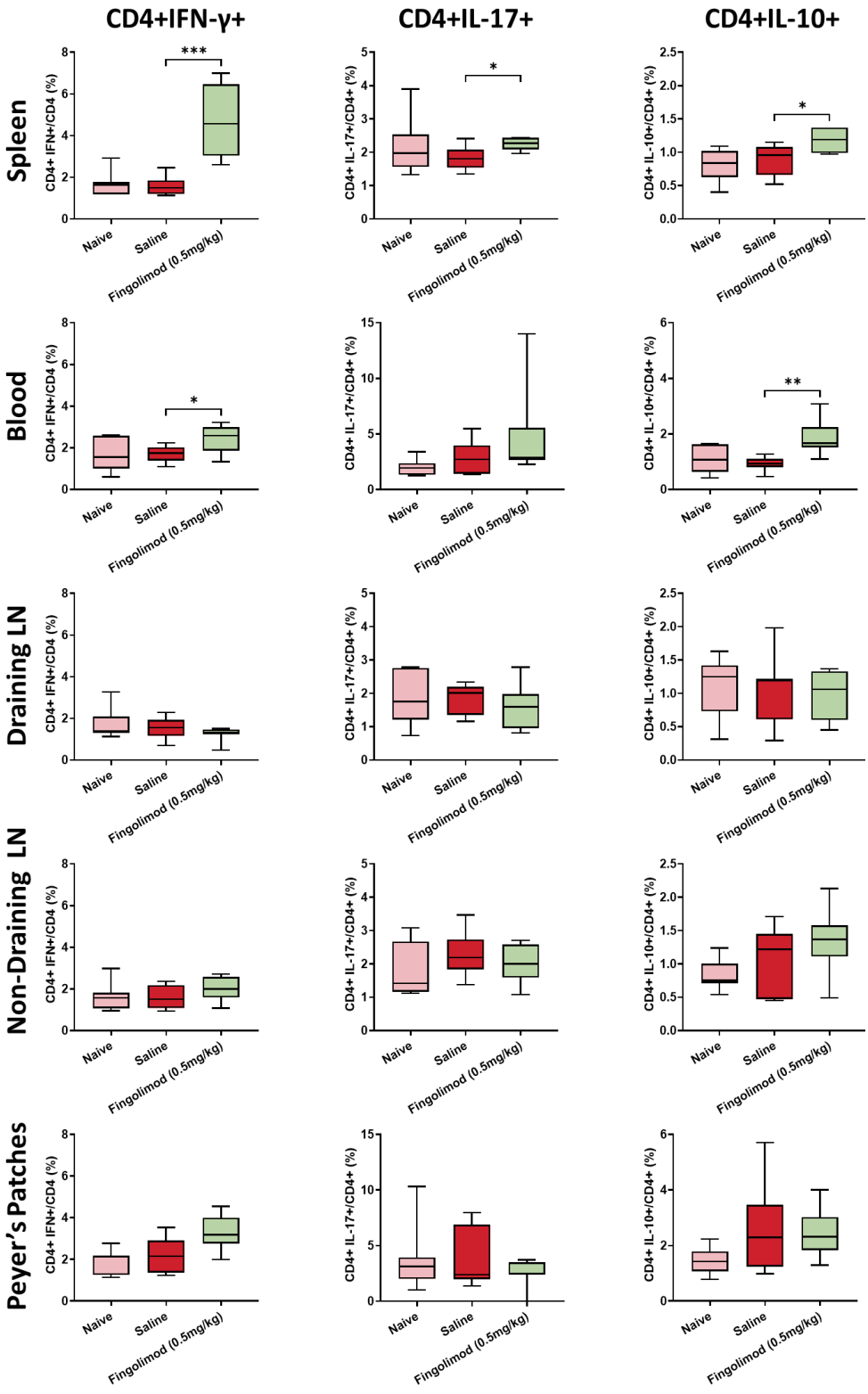


Figure 3.7: Frequency of CD4+ IFN-γ+, CD4+ IL-17+, and CD4+ IL-10+ T cells in blood and secondary lymphoid tissue in mice treated with saline or fingolimod (0.5 mg/kg)) post-brain ischaemia in young mice (t = 10 days) or in untreated, naïve, mice (n = 7 mice per group). Two-sided, independent-samples t-tests investigated differences between two groups (* = $p<0.05$, ** = $p<0.01$, *** = $p<0.001$ as compared to saline). Box and whisker plots display the 90/10 percentile at the whiskers, the 75/25 percentiles at the boxes, and the median in the centre line.

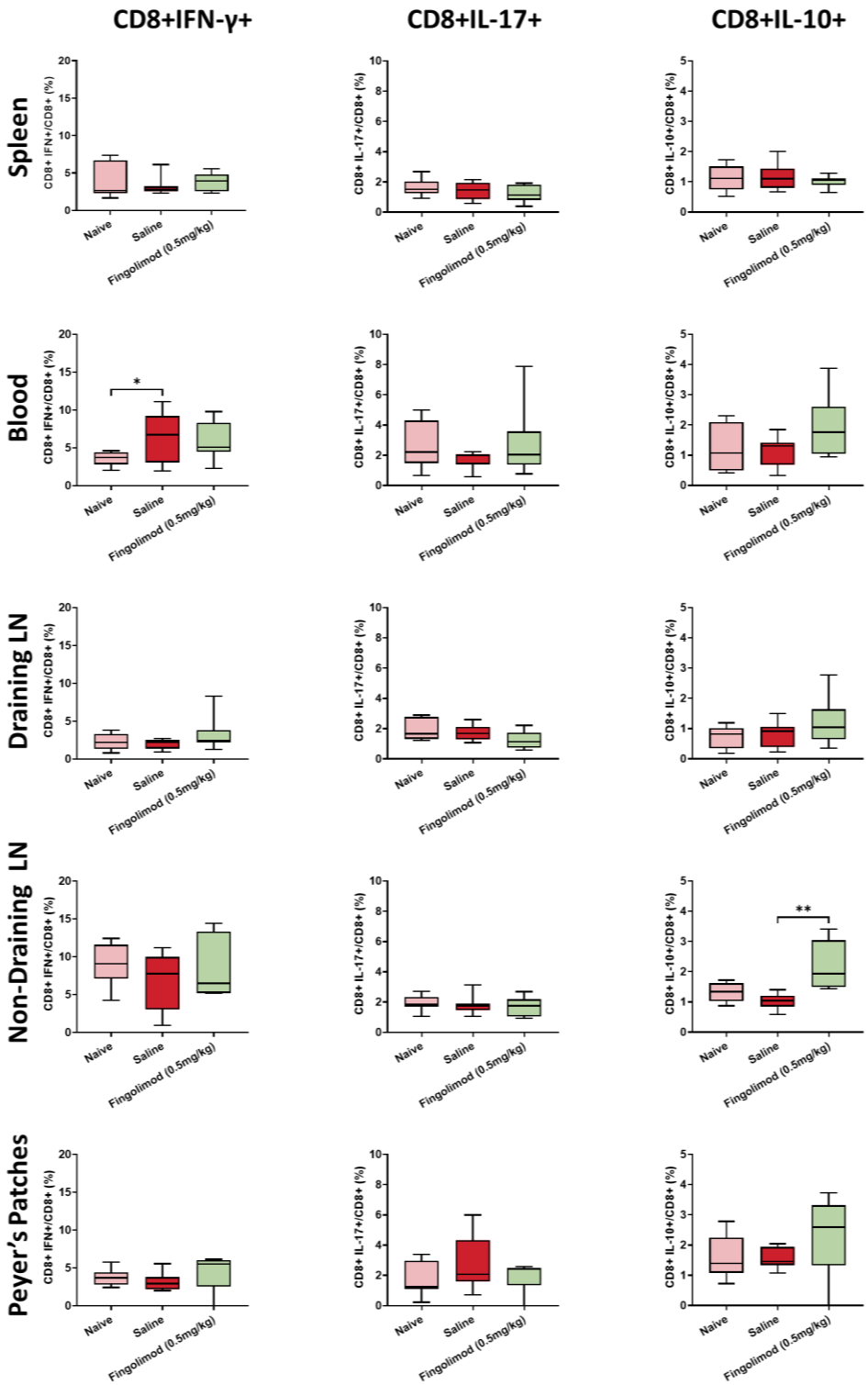


Figure 3.8: Frequency of CD8+ IFN-γ+, CD8+ IL-17+, and CD8+ IL-10+ T cells in blood and secondary lymphoid tissue in mice treated with saline or fingolimod (0.5 mg/kg)) post-brain ischaemia in young mice (t = 10 days) or in untreated, naïve, mice (n = 7 mice per group). Two-sided, independent-samples T tests investigated differences between two groups (* = $p<0.05$, ** = $p<0.01$, *** = $p<0.001$ as compared to saline). Box and whisker plots display the 90/10 percentile at the whiskers, the 75/25 percentiles at the boxes, and the median in the centre line

polarised Th1, Th117 or Treg cells (**Fig. 3.9**). Fingolimod treatment resulted in significantly increased frequencies of single-positive IFN-γ+ ($p = 0.0378$) and IL-10+ ($p = 0.0035$) CD4+ T cells. Fingolimod also significantly enhanced the frequency of double-positive CD4+ IFN-γ+ IL-10+ T cells ($p = 0.0428$). No effects of either brain ischaemia or fingolimod treatment on CD8+ T cells were observed. These results demonstrate fingolimod likely promotes secretion of one cytokine among unpolarised cells or causes expansion of CD4+ T cells that are already polarised to secrete one cytokine (namely IFN-γ secreting CD4+ Th1 cells or IL-10 secreting regulatory T cells). In contrast, brain ischemia significantly increased the proportion of single-positive CD4+ IL-17+ Th17 cells; fingolimod reduced this population to frequencies observed in untreated animals. Fingolimod does not cause CD4+ T cells to become polyfunctional and secrete all three cytokines.

3.3.4 Fingolimod treatment rescues Treg suppressive function against saline-treated but not fingolimod-treated Tconv cells.

Based on the effect on CD4+ cytokine production, we hypothesised that fingolimod might not consistently impact clinical outcome because of a dual effect on both regulatory and effector functions. To test this hypothesis, splenic Tregs (CD4+ CD25+) were isolated and pooled (n = 3 per pool) from post-ischaemic mice treated for ten days with either saline (S-Treg) or fingolimod (0.5mg/kg) (F-Treg) or from naïve controls (N-Treg) (n = 2 per pool)). The ability of these Tregs to suppress proliferation of conventional CD4+ T cells from each treatment group (N-Tconv, S-Tconv and F-conv) was assessed. When Tconv and Treg were both derived from naïve mice (i.e., in mice in which no stroke occurred) a linear increase in Treg suppression was observed as the number of Treg increased in the culture (**Fig. 3.10A**, black line).

Tregs isolated from saline-treated post-ischaemic mice (S-Treg) were significantly less suppressive than N-Treg against N-Tconv at a 1:1 ratio ($p = 0.0062$) (**Fig. 3.10A**, red line) but had equivalent suppressive capacities at lower Treg:Tconv ratios. S-Treg (red line) were also significantly less suppressive compared to N-Treg when either subset was co-cultured with S-Tconv ($p = 0.0039$ at 1:1 ratio) (**Fig. 3.10B**). No difference in efficacy was noted when N-Tregs and S-Tregs were co-cultured with F -Tconv (**Fig. 3.10C**). There was a trend for higher suppression of N-Tconv by Tregs from fingolimod-treated mice (F-Treg), compared to S-Treg at low ratios. At a 1:1 ratio, F-Treg were more suppressive compared to S-Treg ($p = 0.0364$). F-Tregs were also significantly more suppressive compared to S-Treg in suppressing S-Tconv ($p = 0.0378$ at 1:1 ratio), demonstrating that the drug enhances Treg suppressive capacity subsequent to brain ischemia. However, no difference was seen between the suppressive capacity of Tregs from saline (S-Treg) and fingolimod (F-Treg) treated mice when F-Tconv were the targets of suppression ($p = 0.1681$ at 1:1 ratio) (**Fig. 3.10C**). Furthermore, F-Treg were significantly more capable of inhibiting N-Tconv ($p = 0.0364$ at 1:1 ratio) and S-Tconv ($p = 0.0034$ at 1:1 ratio) proliferation than F-Tconv. These results support our hypothesis that fingolimod is having a dual effect on suppressive function and on resistance to suppression, i.e., on both enhancing Treg activity but also resistance to suppression by effector T cells.

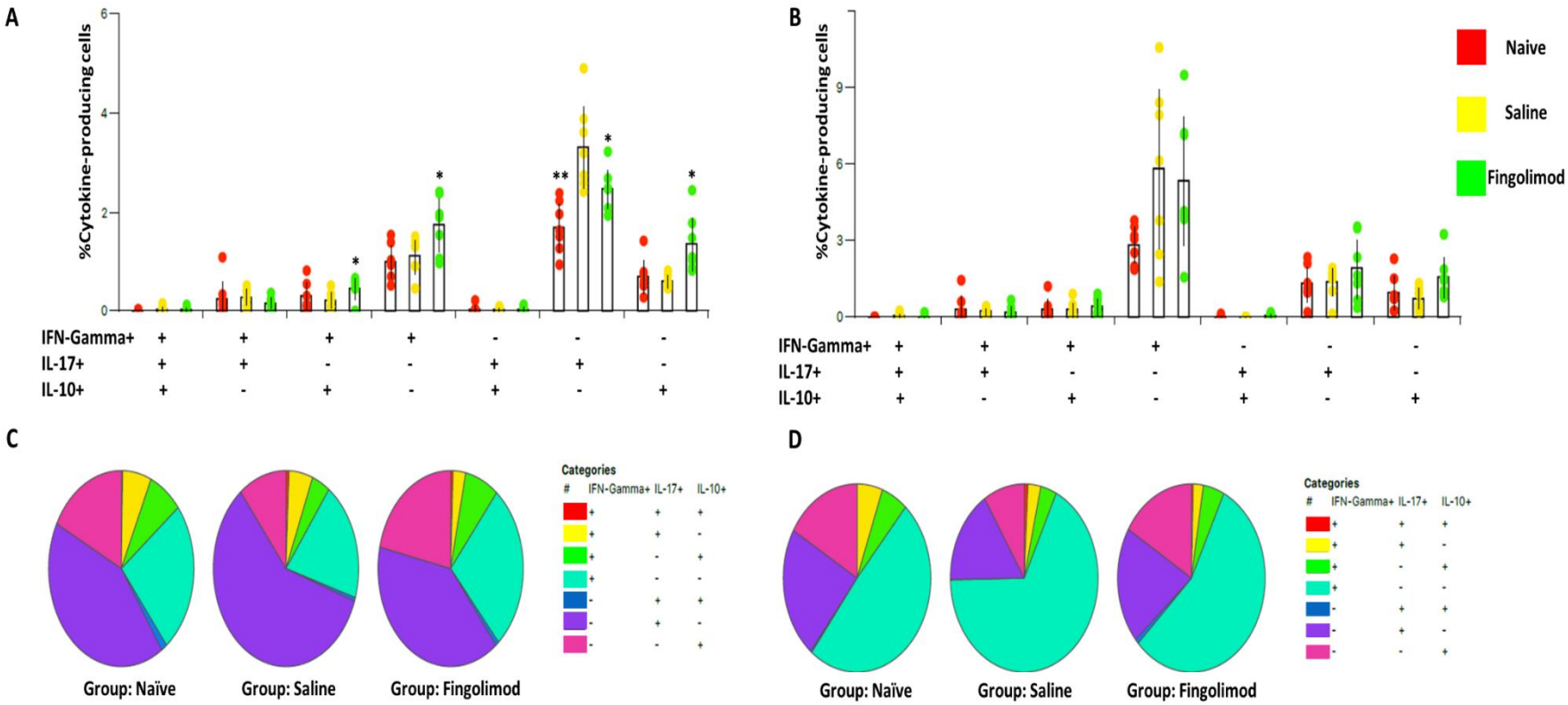


Figure 3.9: The percentage of cytokine-producing cells in blood of naïve, saline treated, and fingolimod treated CD4+ and CD8+ T cells stained intracellularly for IFN-γ, IL-17, and IL-10. Bar graphs display the percentage of single, double, and triple cytokine positive CD4+ (A) and CD8+ (B) cells in naïve (red), saline treated (yellow), or fingolimod treated (green) mice (n = 7). Each dot represents one mouse. Pie charts (C/D) display relative percentages of CD4+ CD8+ T cells that are single, double, or triple cytokine producers. Graphs were generated after performing a Boolean analysis in FlowJo and data analysis in SPICE software. Two-sided, independent-samples T tests investigated differences between two groups (* $p<0.05$, ** $p<0.01$, ***$p<0.001$ compared with saline-treated mice).

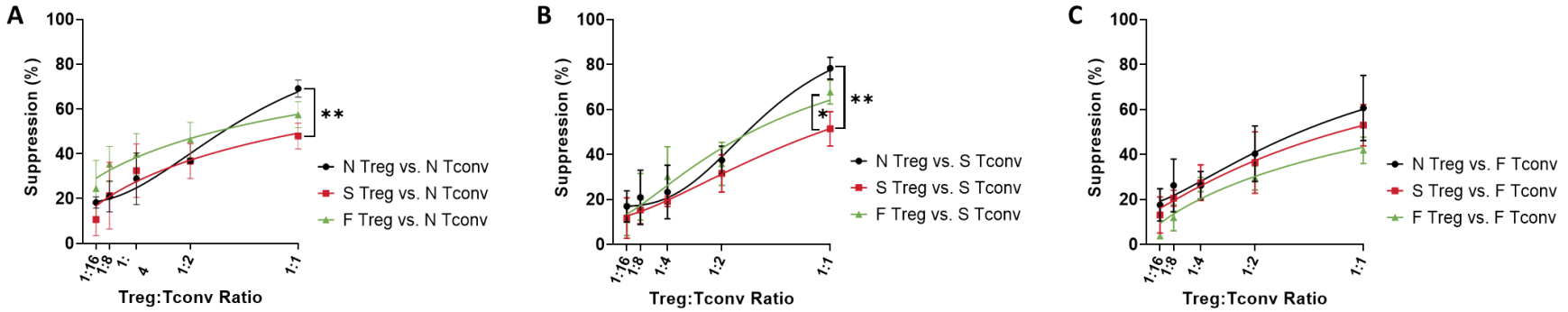


Figure 3.10: Suppressive capacity of Tregs and susceptibility of Tconv, isolated from naïve, saline-treated and fingolimod-treated mice. A) naïve (black), saline-treated (red), and fingolimod-treated (green) Treg suppressive capacity vs. naïve CD4+ T cells at various ratios. B) naïve (pink), saline-treated (red), and fingolimod-treated (green) Treg suppressive capacity vs. saline-treated pMCAO CD4+ T cells at various ratios. C) naïve (pink), saline-treated (red), and fingolimod-treated (green) Treg suppressive capacity vs. fingolimod treated pMCAO CD4+ T cells at various ratios. One-way analysis of variance (ANOVA) tests with post hoc Tukey's multiple comparisons were performed to investigate differences between groups (* = $p<0.05$, ** = $p<0.01$, *** = $p<0.001$ as compared to saline). Curves depict mean ± standard deviation for n = 3 replicates. Each replicate is a poll of samples from n = 2 (naïve) or 3 (saline/fingolimod) mice.

3.4 Discussion

In our previous study, we demonstrated that fingolimod increased peripheral Treg frequency and enhanced the number of brain infiltrating FoxP3+ cells in mice that had undergone pMCAO (330). However, the impact of fingolimod on actual Treg suppressive function remained unknown. This study primarily investigated the effect of fingolimod on modulating T cell function in order to better understand the "disparity" between the drug's effect on T cells and the variable effect on "clinical outcome" in the post-ischaemic mouse. Overall, fingolimod-treated mice displayed no neurological deficit at days 3 and 10 post-pMCAO. Fingolimod modulated both Treg and effector T cell functions. Fingolimod increased the frequency of CCR8+ (but not CCR5+ or CCR6+) Tregs. Fingolimod also increased single-positive CD4+ T cells expressing IL-10 or IFN-γ and dual-positive CD4+ IL-10+ IFN-γ+ in blood. Finally, brain ischaemia reduced Treg suppressive function. Fingolimod treatment rescued this suppressive function, however the drug also increased the resistance of effector T cells to suppression. These findings indicate that fingolimod broadly enhances the function of both regulatory and effector CD4+, but not CD8+ T cells. This dual effect likely underlies the lack of consistent efficacy of fingolimod in pMCAO.

Our finding that fingolimod treatment improved neurobehavioural recovery post-ischaemia is in line with a recent pre-clinical meta-analysis showing fingolimod ameliorates functional deficits after acute ischaemic stroke (265). However, most studies included in the analysis that recorded a positive treatment effect used a transient model of middle cerebral artery occlusion (tMCAO) as opposed to the pMCAO employed here (251, 265). Of the three studies wherein fingolimod failed to improve experimental stroke outcome in young mice, one employed the same surgical

model described above (253). We also previously observed in the pMCAO model that a 10-day course of once daily fingolimod treatment had no effect on functional outcome in young mice (335). In fact, fingolimod only improved functional recovery in aged mice, despite a rise in Treg frequency in all of the young, aged, and $ApoE^{-/-}$ cohorts employed (289). In fact, pooling data from all fingolimod-treated mice under study, we observed Treg frequency negatively correlated with 7-day improvement. It is possible a fine balance exists in the pro-inflammatory and anti-inflammatory effects of fingolimod described in this and other studies, and that this same balance determines the beneficial and deleterious effects of fingolimod in stroke. Factors included but not limited to surgeon, animal husbandry, the gut microbiome, and the neurobehavioural test employed may also have an effect on this delicate balance. Overall, there remains an inconsistent effect of fingolimod on pre-clinical stroke outcomes, especially in the pMCAO model of the disease.

To date, both pre-clinical and clinical stroke studies have focused on temporal shifts in circulating levels of chemokines such CCL5, CCL20, and CCL1 in AIS (123-125). Recent stroke research suggests corresponding chemokine receptors (CCR5, CCR6, and CCR8) play a role in the neuroprotective activity of Tregs (151). CCR5 signalling positively influences the immunosuppressive function of adoptively transferred Tregs via molecules such as PD-1, CTLA-4, and CD39 (122). However, it is possible chemokine receptor expression on Tregs may also negatively influence neuroprotection, as highlighted by a recent clinical trial wherein Tregs were positively correlated with better functional outcome at 3 months, while CCR5+ Tregs remained negatively associated (153). In the current study, brain ischaemia had no effect on the frequency of Tregs expressing CCR5 or CCR6 at day 10 (nor did fingolimod

administration). Previous research employing transient MCAO suggested the expression of CCR5 was upregulated on peripheral Tregs post-ischaemia, especially in the subacute (14 days) stages, and its ligand, CCL5, was upregulated on endothelial cells at the ischemic site at this time (122). Given infarct volume has been shown to directly influence the extent of post-stroke immune changes (e.g., lymphopenia, monocyte dysfunction), it is possible a larger lesion, coupled with the inflammatory changes seen during reperfusion, are required to stimulate acute changes in chemokine receptor expression (64). Nevertheless, ischaemia-induced changes in CCR8+ Tregs in spleen, blood, draining lymph nodes, and non-draining lymph nodes were observed in this study, suggesting focal injuries of the cortex can still produce peripheral immunomodulation in the absence of reperfusion. Notably, however, the absence of changes within the Peyer's patches implies ischaemia-induced changes in gut-derived T cells may not be as pronounced in mild stroke compared to larger infarct models (336). The time since ischaemia onset itself may also affect the expression of CCR markers on Treg cells (337), but in order to confirm this, a comprehensive time course of the expression levels of CCR5/6/8+ cells on brain-invading leukocytes post-ischaemia is required. In the current study, we also observed that fingolimod upregulated CCR8+ Tregs and enhanced functional recovery. Intraventricular CCL1 injection was previously shown to produce both an increase in CCR8+ Tregs in the injured brain and an improvement in neurological function (116). Overall, it is likely that chemokine receptors such as CCR8 play a role in Treg-afforded neuroprotection, and this mechanism may underlie the improved recovery observed in fingolimod-treated mice in this study. Recent research in lung carcinomas shows levels of the S1PR1 positively correlate with CCR8 expression on Tregs, and it is possible the transient agonism of the S1PR1 by fingolimod leads to an increase in the frequency of

CCR8+ Tregs post-ischaemia (338). A greater understanding of the changes in the CCL-1-CCR8 axis post-ischaemia may allow researchers to pinpoint the optimum time at which to intervene with fingolimod to exploit this mechanism.

The role of T cells in AIS has been robustly studied (317). Overall, the balance between cytotoxic Th1 and Th17 cells with neuroprotective (Treg) T cell phenotypes helps dictate the local inflammatory milieu at the infarct site and influences long-term stroke recovery (339). Previous work suggests brain ischaemia increases IFN-γ secretion among brain-infiltrating T cells while also reducing plasma levels of IL-10 (57, 157). Here, the induction of pMCAO induced a significant increase in single-positive IL-17-producing CD4+ T cells, 10 days post-stroke. These cells likely exacerbate post-stroke neuroinflammation (340). There was no observable effect on CD4+ or CD8+ single-positive IFN-γ+ or IL-10+ T cells. The demonstration of these cells at this time point is novel, as this time of analysis is later than other studies, which usually analyse cytokine changes at the early acute (<5 days) post-stroke period (167, 341).

In disease states such as MS, myasthenia gravis and colitis, fingolimod administration was associated with reduced levels of IFN-γ and IL-17 coupled with enhanced production of IL-10 (278, 342, 343). Here, alongside an expected increase in CD4+ IL-10+ T cells, fingolimod also enhanced CD4+ IFN-γ+ in spleen and blood, and CD4+ IL-17+ T cells in blood respectively. Meanwhile, in line with published literature no major impact of acute fingolimod treatment on cytokine producing CD8+ T cells was observed (344, 345). This is consistent with findings that chronic fingolimod treatment is required to reduce pro-inflammatory CD8+ function (346). Analysis of polyfunctionality of CD4+ T cells revealed fingolimod expanded single

positive IFN-γ-producing Th1 and IL-10-producing Treg cells but decreased the frequency of Th17 cells in blood. Furthermore, fingolimod did not promote the emergence of polyfunctional CD4+ T cell phenotypes. In a previous study in multiple sclerosis patients, fingolimod reduced mRNA levels of IL-17 (as well as CD4+ IL-17+ T cells) but not IFN-γ in isolated CD4+ effector cells (303). In sorted Tregs, fingolimod significantly reduced mRNA levels of IL-17 and IFN-γ, suggesting the impact of fingolimod on IFN-γ may be specific to certain T cell phenotypes. Separate research suggests the time since treatment initiation may also influence this pattern, as a 6-month course of fingolimod to treat MS in humans did not affect either serum IL-17 or frequency/number of CD4+ IL-17+ T cells but upregulated both CD4+ IFN-γ+ and CD4+ IL-10+ T cells over the same period (347). An enhancing effect of fingolimod on IL-17/IFN-γ has been shown to be transient, emerging in the first few weeks or months of treatment and fading away thereafter (281, 344). Mechanistically, this increase in IL-17/IFN-γ+ T cells may be explained by a relative expansion of effector memory T cells (which contain Th1/Th17 cells) upon acute fingolimod treatment (347). Indeed, after 12 months of treatment, rigorous studies in MS patients show fingolimod significantly decreases the percentage of IFN-γ+/IL17+CD4+ and CD8+ T cell subsets while also upregulating CD4+ IL-10+ T cells (346, 348). Overall, acute fingolimod treatment in our study promoted both pro and anti-inflammatory cytokine secretion among CD4+ T cells in the post-ischaemic mouse. This dual effect of fingolimod on Treg/Tconv has important consequences for clinical trials or treatment regimens which will only employ short-term fingolimod treatment.

Understanding the balance of T cell cytokines may also aid in understanding the impact fingolimod had on Treg suppressive function in this study. Similar to other

papers, we demonstrated that the induction of brain ischaemia reduced Treg suppressive function (162, 165). The administration of fingolimod improved Treg suppressive function compared to effector cells from the saline-treated post-pMCAO condition. Given isolated Tregs were lower in percentage than in saline condition (92 vs. 96% (**Fig. 3.2)**), the observed improvement in Treg suppression may even be an underestimation of the true result. The general observation that fingolimod enhances Treg suppressive capacity is also in line with published results in MS (272, 277, 349). However, in this study, fingolimod-treated Tregs did not display enhanced suppressive function when co-cultured with effector cells from fingolimod-treated mice. Furthermore, fingolimod-treated Tregs were significantly less capable of inhibiting the proliferation of fingolimod-treated CD4+ T cells as compared to naïve/saline-treated effectors. Combined, these observations suggest a joint effect of fingolimod on both Treg and on CD4+ effector T cells. Previous MS and simian immunodeficiency viruses (SIV) infection studies in macaques demonstrate fingolimod is capable of rapidly increasing the frequency of proliferating CD4+ T cells (as quantified by Ki67+ expression) (343, 350). The enhanced secretion of pro-inflammatory cytokines by mitogen stimulated isolated CD4+ T cells (noted above) may also destabilize co-cultured Tregs and produce more plastic phenotypes with reduced suppressive capacity (351). It is possible an alternative suppression assay employing dendritic cells (DCs) may have more accurately captured an *in vivo* situation, as prior work suggests it is through DCs that fingolimod modulates effector T cell proliferation (as opposed to any direct effect of the drug on T cells themselves) (295). However, the assay we used demonstrates that fingolimod did impact on the capacity of a Treg to directly suppress T effectors Separately, the use of *in vitro* systems wherein only the Treg portion was pre-incubated with fingolimod may also have historically overestimated

the effect of the drug on suppressive capacity (277). Overall, our study reveals that while fingolimod does enhance the suppressive capacity of Tregs, it also promotes resistance among CD4+ effector T cells to regulation. This may limit the usefulness of fingolimod as a Treg-expanding therapy in disease states (such as AIS) where acute increases in Treg function alone are desirable.

Finally, it is possible that drug dose and treatment duration may need to be altered to optimise the balance between Treg and effector T cell functions. A previous study noting an enhanced regulatory capacity in fingolimod-treated mice administered a higher dose (1 mg/kg) of the drug, albeit at a reduced (thrice weekly) frequency (352). In a clinical study involving Tregs isolated from fingolimod-treated MS patients, Treg suppressive capacity was reduced in MS patients compared to control, in line with results noted here (272). After 3 months of fingolimod treatment, however, this effect was reversed, with a reduction in effector T cell proliferation also observed. Given this enhanced suppression remained at 6 months, it is possible chronic treatment may be required to produce the same phenomena in the post-ischaemic patient.

A limitation of this study is that the effect of fingolimod on cellular function was assessed at a single timepoint. Previous research was consulted to choose appropriate timepoints for all metrics (301, 330, 353). Nevertheless, additional and perhaps opposing effects of the drug on Treg trafficking, cytokine release, or suppressive function in either the immediate aftermath or chronic recovery stage of ischaemic stroke cannot be discounted. The strengths of this study include the selection of chemokine receptors based on an extensive literature search, the quantification of Tregs across brain and several peripheral tissues, and the determination of Treg suppressive capacity against CD4+ T cells isolated from both saline and fingolimod-

treated post-ischaemic mice, as well as naïve controls. As a result, our findings provide comprehensive and evidence-based information on how fingolimod works in acute ischaemic stroke.

3.5 Conclusion

Despite recent conflicting results surrounding the efficacy of fingolimod in pre-clinical models of brain ischaemia, the drug continues to be assessed as a potential stroke immunotherapy. Alongside known mechanisms of action such as drug-induced lymphopenia, vasoprotection and neuroprotection, an increase in regulatory T cells may also underlie its neuroprotective activity. This study shows for the first time fingolimod also mediates an increase in CCR8+ expression on Tregs trafficking to the infarcted brain. It was confirmed that fingolimod administration upregulates Treg suppressive function. An increased production of IL-10 may be responsible, but other mechanisms involving CD39, CTLA-4, or other surface markers cannot be discounted (274, 278, 354). The fact that this enhanced suppressive function was not noted specifically when fingolimod-treated Tregs were co-cultured with their fingolimod-treated effector T cell counterparts demonstrates the drug also promotes resistance to Treg suppression. This phenomenon may explain why fingolimod failed to improve functional outcome in recent studies employing permanent models of cerebral ischaemia. Further studies would ascertain whether the administration of fingolimod over a longer time window may maximize its Treg-mediated effects. However, the testing of drugs which can specifically enhance Treg suppressive function without upregulating inflammatory subsets should be prioritized.

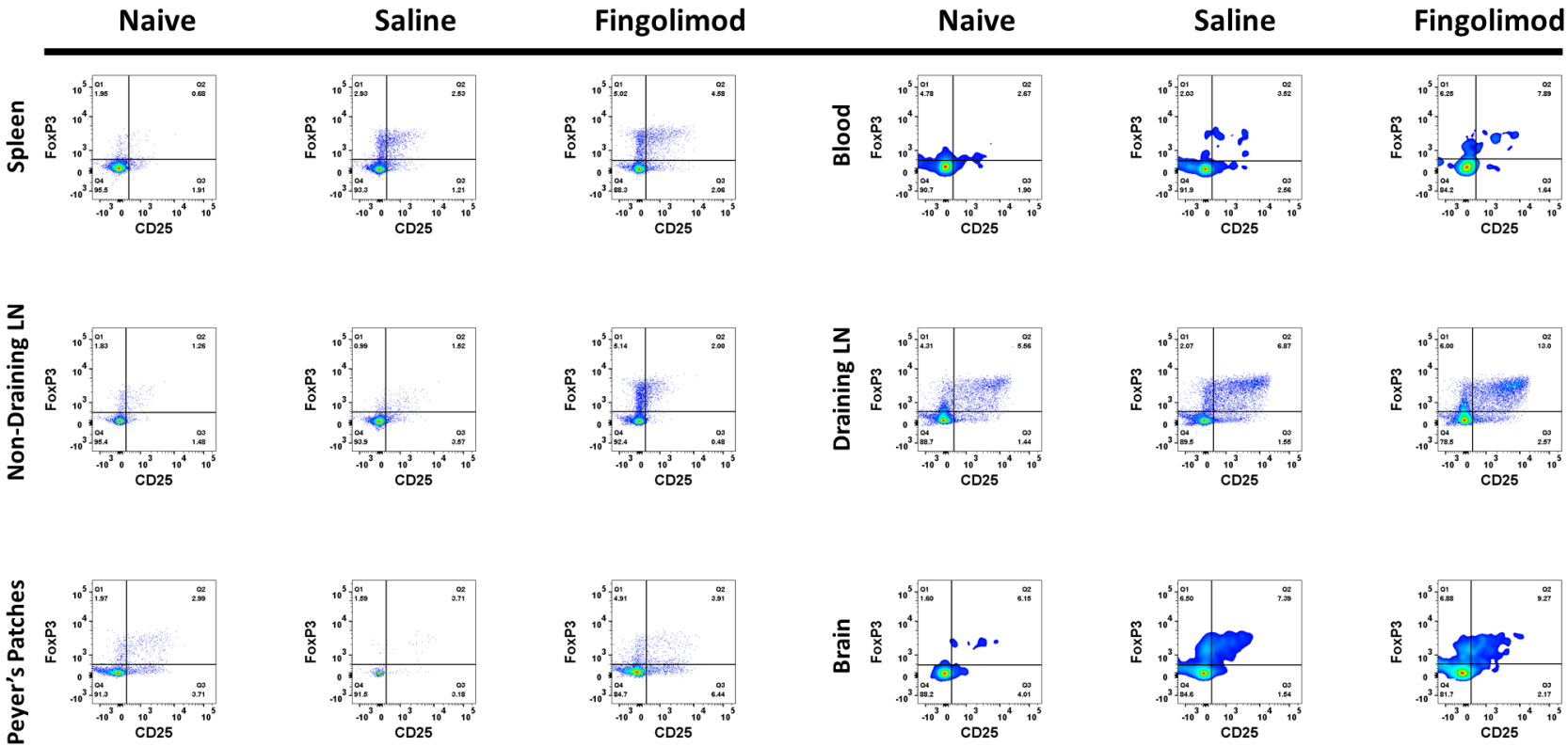


Figure S3.1: Representative FACS pseudocolour plots depicting CD4+ CD25+ FoxP3+ T cells in spleen, blood, non-draining lymph nodes, draining lymph nodes, Peyer's patches, and brain in naïve as well as saline and fingolimod-treated post-pMCAO mice.

Chapter 4

Recombinant pregnancy-specific glycoprotein-1-Fc reduces functional deficit in a mouse model of permanent brain ischaemia

Despite increasing secretion of IL-10 among CD4+ T cells and enhancing overall Treg suppressive function, my results in Chapter 3 demonstrated that fingolimod may also promote resistance to suppression among conventional T cells. This may explain why fingolimod shows inconsistency in terms of improving functional outcome in recent studies employing permanent models of cerebral ischaemia. In this chapter, I trialled a second immunomodulatory drug, recombinant pregnancy-specific glycoprotein-1, for the treatment of experimental stroke. My hypothesis was that by shifting T cells towards an anti-inflammatory phenotype (e.g., increased IL-10), instead of enhancing Treg frequency alone, rPSG1-Fc may show superior efficacy to fingolimod in improving functional stroke outcome.

The text of this chapter is the submitted manuscript:

Malone K, Shearer JA, Moore AC, Moore T, Waeber C. Recombinant pregnancy-specific glycoprotein-1 reduces functional deficit in a mouse model of permanent brain ischaemia. *Submitted to Brain, Behaviour, and Immunity (May 2022).*

Abstract

Background: The well-characterised role of the immune system in acute ischaemic stroke has prompted the search for immunomodulatory therapies. Pregnancy-specific glycoproteins (PSGs) are a group of proteins synthesised by placental trophoblasts which show immunomodulatory properties. The aim of this study was to determine whether a proposed PSG1-based therapeutic enhanced recovery in a mouse model of brain ischaemia and to explore possible immunomodulatory effects.

Methods*:* Male and female C57BL/6JOlaHsd mice underwent permanent electrocoagulation of the left middle cerebral artery (pMCAO). They received saline (n = 20) or recombinant pregnancy-specific glycoprotein-1-alpha fused to the Fc domain of IgG1 (rPSG1-Fc) (100 µg) (n = 22) at 1-hour post-ischaemia. At 3- and 5-days post-ischaemia, neurobehavioural recovery was assessed by the grid-walking test. At 5 days post-ischaemia, lesion size was determined by NeuN staining. Peripheral T cell populations were quantified via flow cytometry. Immunohistochemistry was used to quantify ICAM-1 expression and FoxP3+ cell infiltration in the ischaemic brain. Immunofluorescence was employed to determine microglial activation status via Iba-1 staining.

Results: rPSG1-Fc significantly enhanced performance in the grid-walking test at 3- and 5-days post-ischaemia. No effect on infarct size was observed. A significant increase in circulating CD4+ FoxP3+ cells and brain-infiltrating FoxP3+ cells was noted in rPSG1-Fc-treated mice. Among CD4+ T cells, rPSG1-Fc enhanced the expression of IL-10 in spleen, blood, draining lymph nodes, and non-draining lymph node, while downregulating IFN-γ and IL-17 in spleen and blood. A similar cytokine

expression pattern was observed in CD8+ T cells. rPSG1-Fc reduced activated microglia in the infarct core.

Conclusion: The administration of rPSG1-Fc improved functional recovery in post-ischaemic mice without impacting infarct size. Improved outcome was associated with a modulation of the cytokine-secreting phenotype of CD4+ and CD8+ T cells towards a more regulatory phenotype, as well as reduced activation of microglia. This establishes proof-of-concept of rPSG1-Fc as a potential stroke immunotherapy.

4.1 Introduction

Acute ischaemic stroke is a leading cause of death and long-term disability worldwide (355). Despite the devastating impact of the disease, currently there is only one approved drug (intravenous recombinant tissue plasminogen activator) for treatment (2). Thrombectomy is another option, but while it has prolonged the time window in which patients can benefit from reperfusion therapy (24 hours in select cases), this approach is not without risk and an overall low number of patients (~10%) remain eligible (356). It is clear that novel treatments are urgently needed. The immune response plays an important roles in the pathogenesis of ischaemic stroke, with innate and adaptive immune cells implicated in both stroke risk and brain injury post-ischaemia (25). Immunomodulatory therapeutic strategies are therefore a compelling target for the management of stroke (50).

Pregnancy-specific glycoproteins (PSG) are a family of proteins expressed predominantly by placental trophoblasts (357, 358). Detectable in maternal blood in all trimesters, the serum levels of PSGs reach >100 μg/ml by the end of gestation, making them the major group of secreted placenta proteins (359). Altered PSG levels

may be associated with various pregnancy disorders, and these proteins have garnered interest for their diverse immunomodulatory and anti-platelet properties (360, 361). PSGs impair T cell proliferation, enhance secretion of anti-inflammatory cytokines (e.g., IL-10) by macrophages, reduce pro-inflammatory factor production, and shift T cell differentiation towards a Th2-type immunity (362-366). PSGs may also be strong promoters of a subpopulation of CD4+CD25+ Foxp3+ T cells termed regulatory T cells (or "Tregs"), a cell type well-characterised as contributing to post-stroke repair (367). This is most likely due to the activation of latent TGF-β (368). Increased FoxP3 expression was observed in cells incubated with PSG1 (369). Likewise, mice administered PSG1 showed increased numbers of Tregs in the colonic lamina propria, a response which proved protective in a model of colitis (370). Enhanced numbers of Tregs and improved recovery was also noted in a mouse model of acute graft-versus-host disease (371). Finally, vector-based expression of PSG1 in a model of rheumatoid arthritis ameliorated clinical symptoms while increasing splenic Treg cells (359).

Taken together, these data suggest PSG1 strongly promotes the Treg phenotype and provides marked improvement in disease states characterised by excess inflammation. The primary aim of this study was to test the hypothesis that rPSG1-Fc treatment (a) enhances neurobehavioural recovery and/or (b) decreases lesion size in the post-ischaemic mouse. The secondary objective of this study was to test the hypothesis that a beneficial role of rPSG1-Fc in experimental stroke is mediated by skewing the immune response to a suppressive phenotype, as assessed by increased FoxP3+ cell counts and IL-10/TGF-β production/reduced microglial and endothelial activation.

4.2 Methods

4.2.1 Ethics Statement

Animal experiments were carried out in accordance with the European Directive 2010/63/EU, following approval by the Animal Experimentation Ethics Committee at University College Cork and the Health Products Regulatory Authority Ireland (license number AE19130/P128). The study was conducted and is reported according to the ARRIVE guidelines (288).

4.2.2 PSG Protein Production

The pTT3-PSG1-Fc expression vector was used to produce rPSG1-Fc protein. Briefly, the expression vector was transiently transfected into Freestyle HEK293-F cells (Thermofisher Scientific, #R79007) using Freestyle MAX reagent (Thermofisher Scientific, #16447100). The plasmid DNA was diluted in OptiPRO Serum Free Medium (Thermofisher Scientific, #12309019) at a ratio of 1µg DNA in 20µl OptiPRO per ml of cells. Freestyle MAX reagent was also diluted in OptiPRO at the same ratio (1µl Freestyle MAX reagent in 20µl OptiPRO per ml of cells). Diluted DNA and Freestyle MAX reagent were combined, mixed gently, and incubated at room temperature (RT) for 20 minutes. The mixture was added to the cell suspension, cultured for 72 hours and then centrifuged at 1000 rpm for 5 minutes at RT to separate the protein-containing medium. rPSG1-Fc protein was purified from cell culture medium using a Cytiva 5ml HiTrap Protein G column and AKTA explorer FPLC in 20mM sodium phosphate, pH 7.0 binding buffer, and eluted with 0.1 M glycine-HCl, pH 2.7 in 3-5ml elution volumes. Fractions were pooled and concentrated to a volume of 1ml using a Millipore Amicon Ultra Ultracel 10K centrifugal filter (Millipore, #UFC901096). The concentrate was then gel filtrated using a HiLoad® 16/60 Superdex® 75pg (Sigma-Aldrich, #GE28-9893-33) column and AKTA explorer FPLC, in phosphate buffered saline (PBS) at 4°C. The resultant peak was fractionated,

and the purified rPSG1-Fc protein was concentrated to a volume of 1ml and sterile filtered (0.2µm filter). Protein was quantified by Bradford Assay or UV Spectroscopy, checked by polyacrylamide gel electrophoresis, tested for LPS contamination (Limulus Amebocyte Lysate QCL-1000; Cambrex BioScience, Germany), aliquoted and frozen at -80°C.

4.2.3 Mice

A total of 45 6–7-week-old C57BL/6J mice (Envigo, UK) were used in this study (21 males and 24 females). Mice were acclimatised for seven days before the start of the study. Mice were group-housed in individually ventilated cages in a specific-pathogen-free facility. Mice were exposed to a 12-hour light/12-hour dark cycle and maintained at a temperature of 20-24°C and relative humidity of 45-65%. Mice were provided with environmental enrichment and *ad libitum* access to food and water. Group sizes were determined by an *a priori* sample size calculation which calculated the number of mice required to detect a 40% improvement in grid walking test score based on the variability typically observed in this test (alpha=0.05; power = 80%) (289). While these studies were powered to detect an improvement in behavioural outcome, data from previous studies showed n > 3 per group would be sufficient to detect the expected effect of rPSG1-Fc on Treg frequency in spleen, while n > 6 per group would be sufficient to detect the expected change of CD3+ T cells in brain. Pre-determined exclusion criteria included mice reaching a humane endpoint, with uncontrollable haemorrhage, or thermal damage to the cortex during surgery (n = 3).

4.2.4 Ischaemia Model

A permanent distal middle cerebral artery occlusion model (pMCAO) was employed, as previously described (38). Briefly, mice were anesthetized with isoflurane (3-4%

for induction; 1-2% for maintenance) in O_2/N_2 (30%/70%). The skin between the left ear and eye was infiltrated with 0.5% bupivacaine (0.1ml) before being incised. The temporal muscle was retracted to expose the temporal and parietal bones. A small craniotomy was performed to expose the MCA and the distal portion, including the branches and main artery below the bifurcation. The MCA was occluded by bipolar electrocoagulation (Bovie Bantam Pro electrosurgical generator (#A952) /McPherson 88.9mm straight forceps with a 0.5mm tip (#A842) (Symmetry Surgical Inc, USA)). The MCA was partially cut to confirm successful occlusion and the incision was sutured. Mice were allowed to recover in a heated chamber (32°C) for 30 minutes before being returned to their home cage. At 1-hour post-ischaemia, mice received either saline (n=20) or 100µg rPSG1-Fc (n=22) via subcutaneous injection. A researcher not associated with the surgery prepared treatment solutions for volumes no greater than 250µl per injection. Experimental mice were monitored daily using a scoresheet (checklist score) which graded weight loss (from 0-3), appearance changes (from 0-3), behaviour (from 0-3), and neurological score (0: no observable deficit, 1: forelimb flexion, 2: decreased resistance to lateral push and forelimb flexion without circling, 3: same as 2, with circling) (331).

4.2.5 Neurological Deficit Evaluation

Mice underwent behavioural evaluation at 3- and 5-days post-stroke. To do so, they were placed on a wire grid (25cm x 35cm) with $1cm^2$ openings and encouraged from one end to the other where a cardboard cylinder was situated. Videos were recorded (angled from below, Canon Legria HFR706) as mice crossed the grid to allow visualisation of steps and paw placement. The first 100 steps were assessed and the number of missed contralateral and ipsilateral steps were counted by an investigator

blinded to the treatment groups. The deficit score was then calculated as the ratio of ipsilateral/contralateral steps missed.

4.2.6 Tissue Collection and Processing

At 5 days post-ischaemia, mice were culled by anaesthetic overdose (Euthatal, 200mg/ml i.p.; Merial). Approximately 500µl of blood was collected from the descending aorta and transferred into EDTA-coated tubes (Cruinn Diagnostics, #262197). Mice were then perfused transcardially with 20ml cold PBS. The brain was removed and frozen in isopentane (-42°C). Brain sections (10µm) were cut on a cryostat at 500µm intervals and stored at -20°C. Cervical and inguinal lymph nodes, and spleen tissue were harvested and stored in PBS, before being mechanically dissociated using the back of a plunger from a 3ml syringe (Fisher Scientific, #14955451) in approximately 3ml PBS in a sterile 6-well plate. The resulting cell suspensions were passed through a 70µm cell strainer (Cruinn Diagnostics, #2272906G) and collected in a 50ml conical tube. Wells and strainers were washed twice with 1X Dulbecco's PBS (Sigma-Aldrich, #D8537). Spleen and blood samples were resuspended in 5ml of 1X Red Blood Cell Lysis Buffer (eBioscience, #430054) and incubated for 5 minutes at RT. The lysis reaction was stopped by adding 2ml of PBS. All samples were then washed twice with PBS and counted using trypan blue (Sigma-Aldrich, #T8154) to determine total cell concentration and viability.

4.2.7 Infarct Size Measurement

Brain sections from each mouse (n = 20-22) were analysed by NeuN immunohistochemistry to quantify infarct and oedema volume. Slides were stained according to our previously published protocol (289). Stained sections were then scanned at 3,200 dpi on an Epson Perfection V550 scanner. Lesion size and

hemispheric atrophy were measured on scanned images using ImageJ (291) (**Fig. S4.1**). The areas (mm^2) of interest were measured and multiplied by the distance between sections (500 µm) to calculate volume (mm^3).

4.2.8 Flow Cytometric Analysis

To analyse intracellular cytokines, cells (2 x 10^6 per well) were resuspended in culture medium (RPMI (Sigma-Aldrich, #R7658) + 10% FCS (Sigma-Aldrich, #F2442)) and stimulated with Cell Stimulation Cocktail (1X) (eBioscience, #00497593) at 37°C in a CO_2 incubator. After 4 hours, stimulated and non-stimulated samples were resuspended for 5 minutes with 50µl of anti-mouse CD16/CD32 (Clone 93, 1:100) (eBioscience). The respective cell suspensions were then stained for anti-mouse CD45 (PerCP-CY5.5) (30-F11, 1:100), CD3 (PE-Cy7) (145-2C11, 1:100), CD4 (FITC) (RM4-5, 1:800), CD8 (Pacific Blue) (5H10, 1:100), and CD25 (APC) (PC61.5, 1:100) (all sourced from eBioscience). A live/dead stain (1:10,000 solution) was also added to each sample (Fixable Viability Dye eFluor 780) (eBioscience, #65086514). Samples were then incubated for 30 minutes at 2-8°C in the dark. Post-incubation, the samples were washed, fixed, permeabilised, and stained intracellularly for 30 minutes at RT with either anti-mouse FoxP3 (PE) (FJK-16s, 1:100) (in accordance with the manufacturer's instructions in the Mouse Regulatory T Cell Staining Kit #1 (eBioscience, #88811140)), or a cocktail of anti-IFN-γ (eFluor610, eBioscience, #61731182) (XMG1.2, 1:100), anti-IL-10 (PerCP-Cy5.5, eBioscience, #45710182) (JES5-16E3, 1:50), and anti-IL-17 (PE, BD, #559502) (TC11-18H10, 1:100). Samples were then re-suspended in an appropriate volume of PBS. Flow cytometric analysis was performed with a LSRII flow cytometer (BD). Compensation control was set using BD CompBead Anti-Rat/Anti-Hamster Particles Set (BD, #552845). Data was

analysed using FlowJo (v10) according to the following initial gating strategy: live cells (as determined by live/dead stain), lymphocytes (as determined by FSC/SSC), T lymphocytes (as determined by CD3+, CD4+ and CD8+), and regulatory T cells (CD4+ T cells which co-express CD25 and FoxP3). Gates were set according to unstained samples and fluorescent minus one controls. The gating strategy for final determination of intracellular cytokine staining is outlined in **Fig. 4.1**. Absolute cell counts for all tissues were calculated in accordance with instructions provided with the CountBright Absolute Counting Beads (Molecular Probes, #C36950). All results were reported according to the Minimum Information About a Flow Cytometry Experiment (MIFlowCyt) (290).

4.2.9 Immunohistochemistry (CD3, FoxP3, ICAM)

Endothelial activation (ICAM-1 staining) and lymphocyte infiltration (CD3, FoxP3) were examined in 10 randomly selected mice per group. Sections were fixed with ice cold acetone (-20°C) for 10 minutes, dried and washed with PBS. Slides were incubated in blocking solution (5% Rabbit Serum/PBS for CD3/FoxP3, 10% Rabbit Serum/PBS for ICAM-1) for 30 minutes. For CD3 staining, endogenous biotin was blocked according to the instructions provided with the Avidin/Biotin Blocking Kit (Vector Laboratories, #SP-2001). Sections were incubated with primary antibodies against CD3 (145-2C11, 1:500), FoxP3 (FJK-16s, 1:300), or ICAM-1 (1A29, 1:200) (eBioscience, #MA5407) at RT for 1 hour (all sourced from eBioscience). Slides were washed twice with PBS then incubated with 3% H_2O_2 for 30 minutes. Subsequently, slides were incubated with either a biotinylated goat anti-hamster (1:500, eBioscience, #PA132045) or a donkey anti-rat secondary antibody (1:500, eBioscience, #A18739)

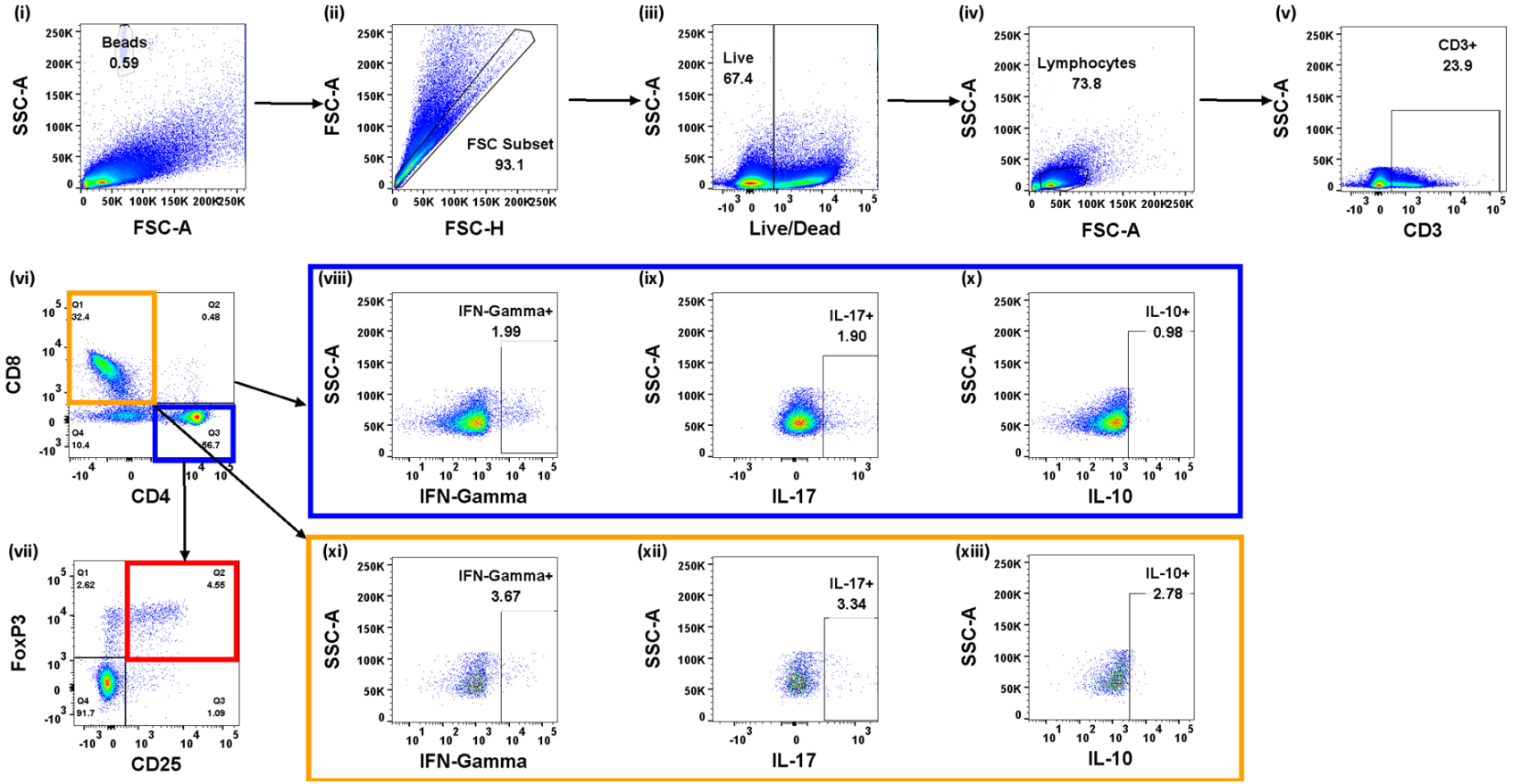


Figure 4.1: Gating strategy for determination of Tregs (red frame), cytokine expression among CD4+ T cells (blue frame), and cytokine expression among CD8+ T cells (yellow frame) in representative mouse splenocytes 5 days post-brain ischaemia. (i) = Initial population, (ii) = singlets, (iii) = Live cells, (iv) = lymphocytes, (v) = CD3+ T cells (T cells), (vi) = CD4+ vs. CD8+ T cells, (vii) = CD4+ CD25+ FoxP3+ T cells (quadrant in red) designated Tregs, (viii) = CD4+ IFN-γ+ T cells, (ix) = CD4+ IL-17A+ cells, (x) = CD4+ IL-10+ T cells, (xi) = CD8+ IFN-γ+ T cells, (xii) = CD8+ IL-17A+ cells, (xiii) = CD8+ IL-10+ T cells. All gates were determined by both negative cells and fluorescence minus one controls.

for 1 hour at RT. Slides were washed twice with PBS. Immunoreactivity was visualized by the avidin-biotin complex method (Vectastain Avidin-Biotin Complex Kit, Vector Laboratories, #PK-4000) and developed for 10 minutes with diaminobenzidine (DAB). Slides were counterstained with eosin, dehydrated sequentially in graded ethanol (70%, 95% and 100%), immersed in HistoChoice and coverslippped with Permount. A single random representative image of the ischaemic core, undamaged ipsilateral tissue, and contralateral tissue was taken using the 20X objective lens (Olympus BX51 microscope). Three random images were taken in the peri-infarct zone (**Fig. S4.2**). All images were quantified using ImageJ in a blinded manner (291). CD3+ and FoxP3+ cells were counted manually. Total ICAM-1 vessel length (μm) was quantified and then expressed per mm^2.

4.2.10 Immunofluorescence (Iba-1)

Immunofluorescent analysis of microglia was performed on 10 mice per group. Sections were fixed with 2% paraformaldehyde (Sigma-Aldrich, #HT501128) for 1 hour, dried, and washed with 0.5% Triton (Sigma-Aldrich, #X100)/PBS. Slides were incubated in blocking solution (5% BSA/20% Goat Serum (Vector Laboratories, #S-1000) in 0.5% Triton/ PBS)) for 30 minutes. Sections were stained with primary antibodies against Iba-1 (1:500) (Wako, #019-19741) for 2 hours. Slides were washed and incubated with goat anti-rabbit Alexa Fluor 488 (1:500) (eBioscience, #A11008) secondary antibody for 1 hour, washed and cover-slipped with Vectashield (Vector Laboratories, #H-1200). A single representative image of the ischaemic core, undamaged ipsilateral tissue, and contralateral tissue were taken using the 20X objective lens (Olympus BX51 microscope). Three representative images of the peri-infarct zone were also taken (**Fig. S4.3**). Positively stained cells were counted using

ImageJ (291). Microglia were differentiated into “activated” and “quiescent” states based on morphology (amoeboid or ramified).

4.2.11 Determination of TGF-β1 in Spleen by ELISA

Samples of spleen tissue (approximately 20mg) were frozen in isopentane (-42°C) and stored at -80°C. Spleen (10-40mg) was processed by homogenisation in cold RIPA buffer containing HALT protease inhibitor cocktail (Thermofisher Scientific, #78429) at 30µl per 1mg tissue using a Potter-Elvehjem tissue grinder (PTFE pestle). Lysates were centrifuged at 12,000rpm for 20 minutes at 4°C, supernatants were collected and stored at -80°C. The quantification of TGF-β1 was conducted according to the instructions provided with the TGF-β1 Mouse ELISA Kit (Invitrogen, #BMS608-4) with samples and standards run in duplicate. Prior to analysis, samples were diluted in assay buffer, activated with 1M HCl for 1 hour and further diluted in assay buffer (final dilution 1:30). Samples were incubated with Biotin Conjugation Solution (100µl) for 1 hour. For visualisation, samples were incubated with TMB substrate (100µl) for 30 minutes in the dark. The reaction was halted with Stop Solution and the plate was read on a Wallac Victor2 Multilabel plate reader (Perkin Elmer) at 450nm followed by correction at 620nm. Total protein concentration (mg/ml) was quantified using a Pierce BCA protein assay kit (Thermofisher Scientific, #23227) according to manufacturer’s instructions. Samples were diluted 1:5 in distilled water, and BSA standards were prepared in 20% RIPA buffer. Samples and standards were run in technical duplicate. TGF-β1 concentration (ng/ml) was calculated from the standard curve (**Fig. S4.4)** and expressed as ng/mg total protein.

4.2.12 Statistical Analysis

The Kolmogorov–Smirnov test was used to ascertain that the distribution of all data was normal. Flow cytometric and immunohistochemical data are displayed as 10-90 percentile box-and-whisker plots. Two-sided, independent-samples T tests were employed to investigate differences between two groups. Two-way repeated measures ANOVA followed by post-hoc Tukey's test for multiple comparisons was used to investigate differences between groups when the effect of two independent variables (e.g., time, treatment) were studied. A p-value <0.05 was considered significant. Statistical analysis was performed using GraphPad Prism 8.0. All investigators were blinded to treatment groups throughout data acquisition and analysis.

4.3 Results

4.3.1 rPSG1-Fc significantly improves neurobehavioural recovery post-pMCAO without impacting infarct size

The effect of rPSG1-Fc on functional recovery was assessed by determining whether the treatment improved grid-walking test performance post-ischaemia as compared to saline control. All mice underwent testing pre-surgery to establish baseline scores. The grid-walking test was then repeated at days 3 and 5 post-pMCAO.

In both saline and rPSG1-Fc-treated mice, a reduction in the ipsilateral/contralateral foot fault ratio was observed at both days 3 (saline: p <0.0001, rPSG1-Fc: p <0.0001) and 5 (saline: p = 0.0007, rPSG1-Fc: p = 0.0031) post-pMCAO, compared to before stroke (**Fig. 4.2**). When comparing treatment groups, no significant difference was noted between saline and rPSG1-Fc-treated mice at baseline (p >0.9999). However, rPSG1-Fc treatment resulted in highly significant improvements in the

ipsilateral/contralateral foot fault ratio at both days 3 (p <0.0001) and 5 (p = 0.0015) post-ischaemia compared to saline-treated animals. No significant change was observed between saline and rPSG1-Fc-treated mice at any timepoint in checklist score (p = 0.9845) or mouse weight (p = 0.7916) (Fig. 2). A beneficial effect of time since ischaemia onset on recovery was confirmed for both measurements (checklist score: p <0.0001, mouse weight p <0.0001).

The effect of rPSG1-Fc on histological stroke outcome was measured at day 5 post-ischaemia (**Fig. 4.3**). In contrast to the impact of treatment on functional recovery, there was no significant difference in lesion size compared to saline-treated mice (p = 0.7344). Likewise, no effect on either tissue loss (p = 0.7459) or the ratio of ipsilateral/contralateral hemisphere volume (p = 0.6571) was observed.

4.3.2 rPSG1-Fc increases circulating CD4+ CD25+ and CD4+ FoxP3+ T cell frequencies but does not increase CD4+CD25+Foxp3+ Treg frequency in the periphery post-pMCAO

Based on previous research suggesting that rPSG1-Fc treatment may increase Treg frequency, coupled with the known neuroprotective effects of this lymphocyte subpopulation post-pMCAO, the effect of rPSG1-Fc on peripheral Tregs was investigated in blood, spleen, draining (cervical) and non-draining lymph nodes (inguinal), and Peyer's patches harvested from mice at 5 days post-ischaemia (118, 369). rPSG1-Fc did not increase the frequency of Tregs in any tissues (**Fig. 4.4**). rPSG1-Fc significantly increased the frequency of CD4+ CD25+ T cells in spleen (p = 0.0140), blood (p = 0.0060), and non-draining lymph nodes (p = 0.0122). PSG1-Fc likewise increased CD4+ FoxP3+ frequency in blood (p = 0.0002). Examples of flow cytometric gating of key results are displayed in **Fig. S4.5**.

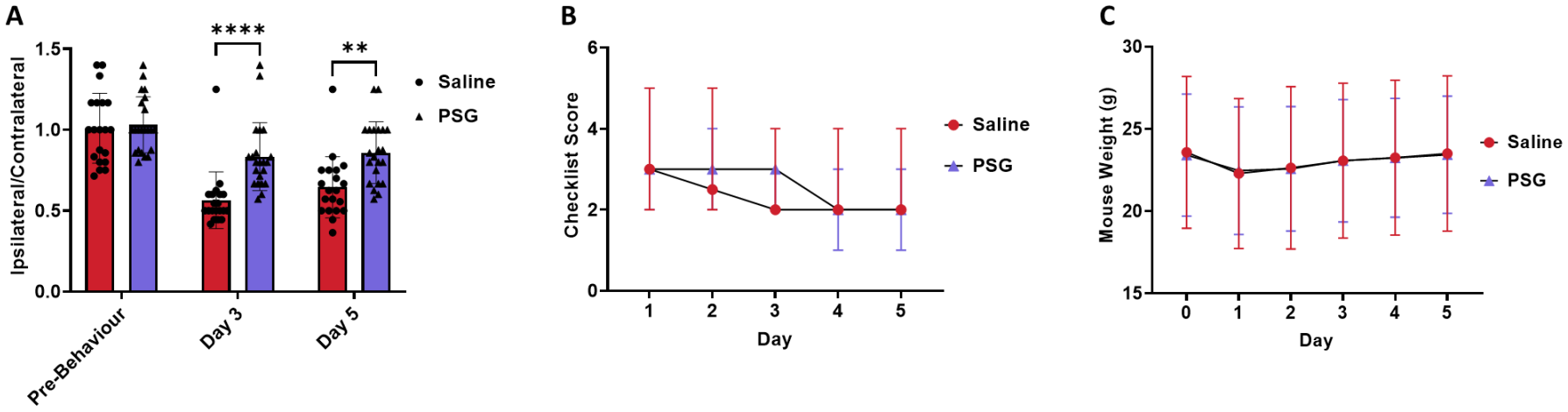


Figure 4.2: Comparison of A) ipsilateral/contralateral foot fault ratio as assessed by grid-walking test (t = 3, 5 days), B) total checklist score, and C) mouse weight between saline (n = 20) and rPSG1-Fc-treated (n = 22) mice. Two-way repeated measures ANOVA followed by post-hoc Tukey's multiple comparisons was used to investigate differences between groups (* = $p<0.05$, ** = $p<0.01$, *** = $p<0.001$ as compared to saline). Scatter plots depict mean ± standard deviation.

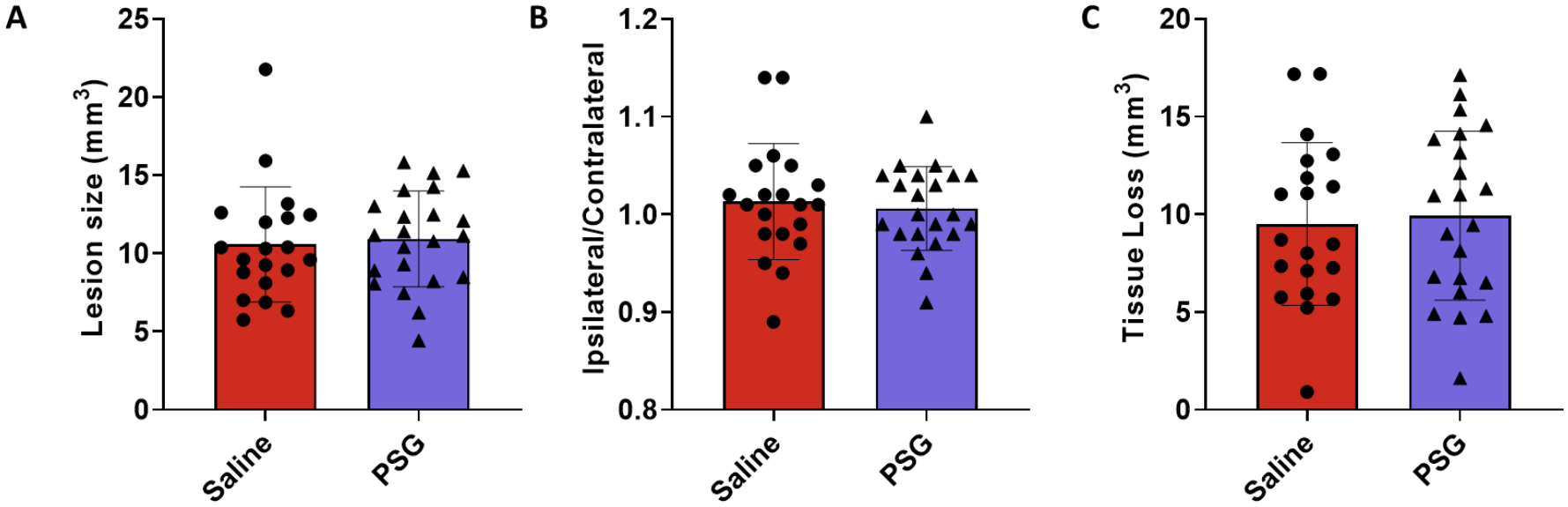


Figure 4.3: Comparison of A) lesion size (mm^3), B) ipsilateral/contralateral hemispheric volume ratio, and C) tissue loss (mm^3) between saline (n = 20) and rPSG1-Fc-treated (n = 22) mice as quantified by NeuN staining (t = 5 days). Two-sided, independent-samples t-tests was used to investigate differences between groups. Scatter plots depict mean ± standard deviation.

4.3.3 rPSG1-Fc increases FoxP3+ cell infiltration into the brain post-pMCAO

The results above suggest although a 100µg dose of rPSG1-Fc was not sufficient to increase peripheral Treg frequency post-ischaemia, rPSG1-Fc may promote Treg-like phenotypes in specific tissues and/or enhance anti-inflammatory cytokine secretion. In order to test both hypotheses, we next assessed the effects of PSG1-Fc on brain-infiltrating Tregs, and on T cell cytokine production (next section). CD3+ and FoxP3+ cells were counted in the ischaemic core (**Fig. 4.5A**) and peri-infarct (**Fig. 4.5B**) regions. While no change in CD3+ T cell counts were observed in either region ($p = 0.4278$, $p = 0.5347$ respectively), rPSG1-Fc treatment significantly increased FoxP3+ cells in both regions (core: $p = 0.0263$, peri-infarct: $p = 0.0324$). This mirrored an increased number of FoxP3+ cells in blood ($p = 0.0015$) (**Fig. S4.6**).

4.3.4 rPSG1-Fc increases the secretion of IL-10 and downregulates the production of IFN-γ and IL-17

As rPSG1-Fc increased FoxP3 expression in blood and brain, and as FoxP3 acts as the master switch of regulatory activity, we postulated that rPSG1-Fc may improve recovery post-pMCAO by skewing the T cell phenotype from pro-inflammatory subsets such as Th1 and Th17 towards an anti-inflammatory subset such as Treg. In order to investigate this hypothesis, the expression of interferon gamma (Th1), IL-17 (Th17), and IL-10 (Treg) was quantified in blood and secondary lymphoid tissue via flow cytometric analysis.

PSG1-Fc significantly decreased the production of interferon gamma (IFN-γ) among CD4+ T cells in spleen ($p = 0.0356$) and blood ($p = 0.0021$) (**Fig. 4.6**). Similarly, a reduction in CD4+ IL17+ cells was observed in rPSG1-Fc-treated mice in spleen ($p =$

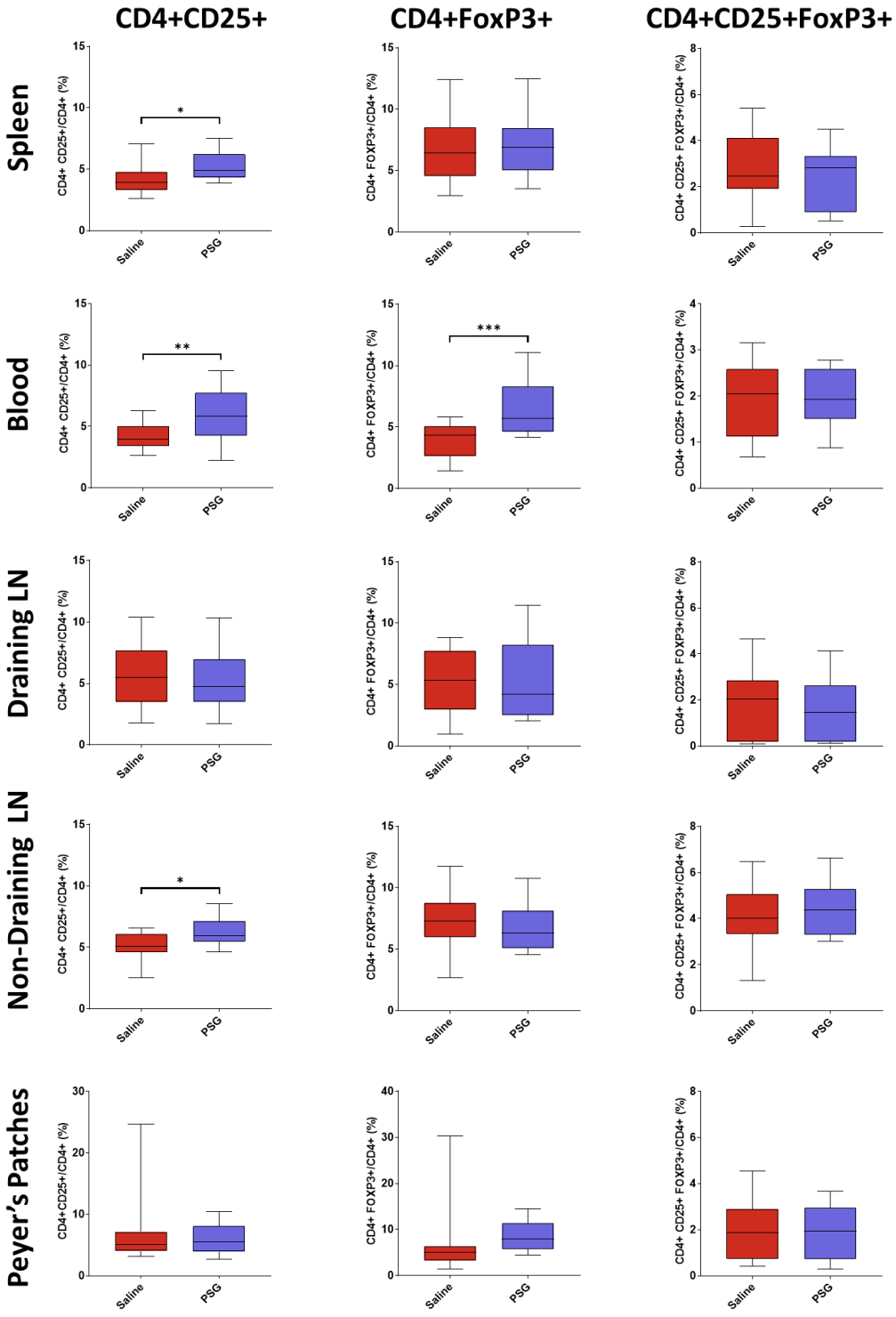


Figure 4.4: Frequency of CD4+ CD25+, CD4+ FoxP3+, and CD4+ CD25+ FoxP3+ T cells in blood and secondary lymphoid tissue in response to either saline (n = 20) or rPSG1-Fc (n = 22) treatment post-pMCAO (t =5 days). Two-sided, independent-samples T-tests used to investigate differences between groups (* = $p<0.05$, ** = $p<0.01$, *** = $p<0.001$ as compared to saline). Box-and-whisker plots exhibit 10-90 percentiles.

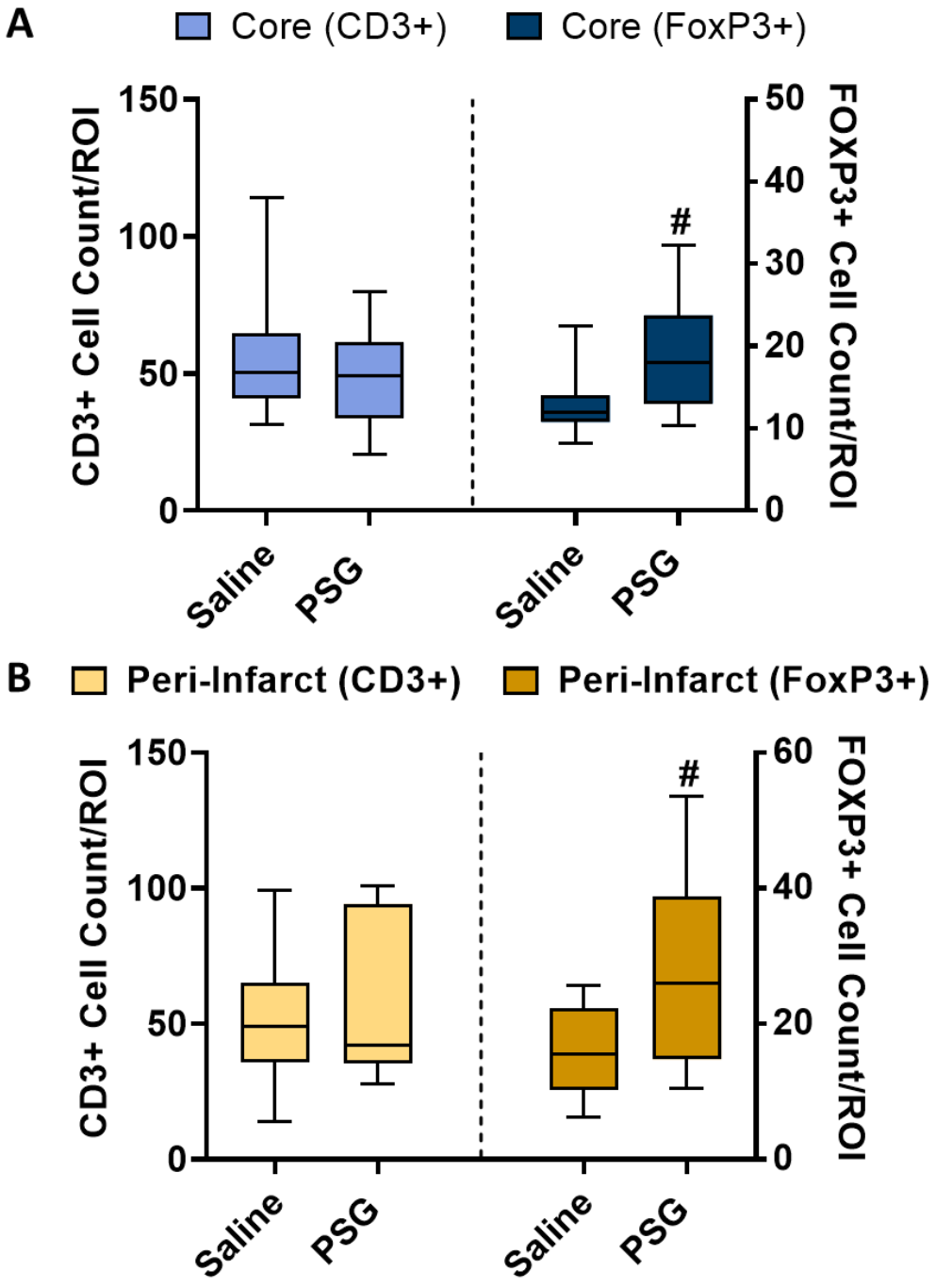


Figure 4.5: Total CD3+ and FoxP3+ cell counts in the infarct core (A) and peri-infarct zone (B) of saline-treated and rPSG1-Fc -treated mice post-pMCAO (t = 5 days) (n = 10 per group). DAB-based immunohistochemistry was used to determine cell counts. Two-sided, independent-samples T-tests or Mann-Whitney tests were used to investigate differences between groups. For comparisons between CD3+ groups (* = $p<0.05$, ** = $p<0.01$, *** = $p<0.001$ as compared to saline). For comparison between FoxP3+ groups (# = $p<0.05$, ## = $p<0.01$, ### = $p<0.001$ as compared to saline). Box and whisker plots display the 90/10 percentile at the whiskers, the 75/25 percentiles at the boxes, and the median in the centre line.

0.0444), blood (p = 0.0317), and non-draining lymph nodes (p = 0.0090). PSG1-Fc caused an increase in IL-10 production in CD4+ T cells in spleen (p = 0.0011), blood (p <0.0001), draining lymph nodes (p = 0.0078), and non-draining lymph nodes (p <0.0001).

Among CD8+ T cells (**Fig. 4.7**), rPSG1-Fc significantly reduced IFN-γ and IL-17 production in spleen (p = 0.0068, p = 0.0416 respectively) and increased IL-10 in spleen (p = 0.0274), blood (p = 0.0094), and non-draining lymph nodes (p = 0.0067).

Overall, the administration of rPSG1-Fc modulated T cell cytokine production in blood and spleen away from IFN-γ/IL-17 and towards IL-10. This effect was not observed in draining lymph nodes in the case of CD8+ cells.

4.3.5 rPSG1-Fc reduces activated microglia in the infarct core of post-ischaemic mice

Infiltrating Tregs may restrain post-stroke neuroinflammation via a microglia-dependent mechanism (135, 178, 323, 372). Thus, the effect of rPSG1-Fc on microglial activation was investigated using Iba-1 staining to analyse microglia morphology (**Fig. 4.8**).

rPSG1-Fc significantly reduced activated microglia (Iba-1 positive cells with an "ameboid" morphology) in the infarct core (p = 0.0007), with a trend towards reduced numbers of quiescent microglia in the core region (p = 0.0583). rPSG1-Fc had no effect on activated microglial cell numbers in the peri-infarct zone (p = 0.6767), healthy ipsilateral tissue (p = 0.8413), or contralateral tissue (p = 0.8875) compared to saline-treated mice. No impact on quiescent microglia (displaying a "ramified"

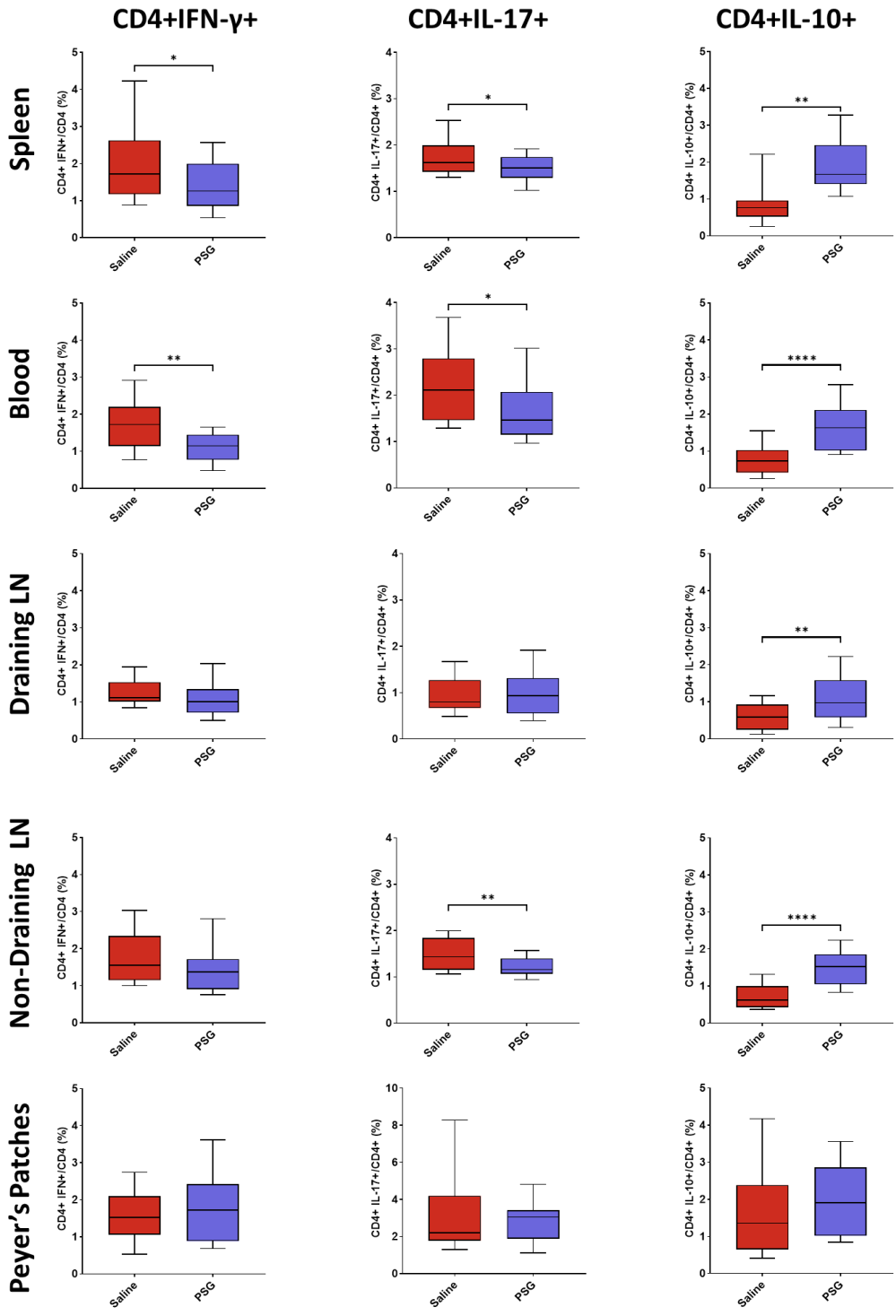


Figure 4.6: Frequency of CD4+ IFNγ+, CD4+ IL-17+, and CD4+ IL-10+ T cells in blood and secondary lymphoid tissue in response to either saline (n = 20) or rPSG1-Fc (n = 22) treatment post-pMCAO (t =5 days). Two-sided, independent-samples T-tests were used to investigate differences between groups (* = p<0.05, ** = p<0.01, *** = p<0.001 as compared to saline). Box and whisker plots display the 90/10 percentile at the whiskers, the 75/25 percentiles at the boxes, and the median in the centre line.

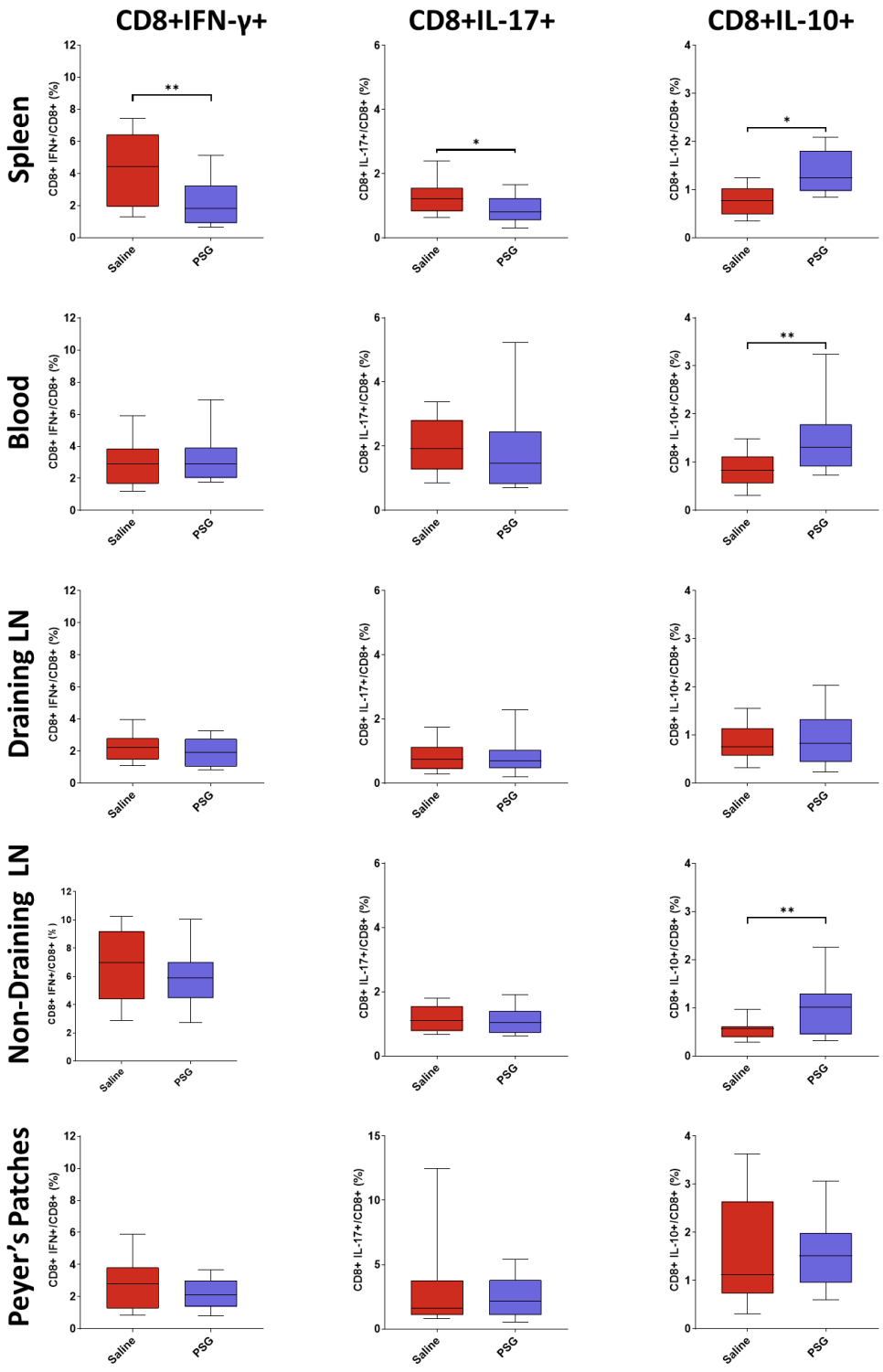


Figure 4.7: Frequency of CD8+ IFNγ+, CD8+ IL-17+, and CD8+ IL-10+ T cells in blood and secondary lymphoid tissue in response to either saline (n = 20) or rPSG1-Fc (n = 22) treatment post-pMCAO (t =5 days). Two-sided, independent-samples T-tests were used to investigate differences between groups (* = $p<0.05$, ** = $p<0.01$, *** = $p<0.001$ as compared to saline). Box and whisker plots display the 90/10 percentile at the whiskers, the 75/25 percentiles at the boxes, and the median in the centre line.

morphology) was noted in these regions (p >0.9999, p = 0.1504, p = 0.9371 respectively).

4.3.6 rPSG1-Fc does not influence ICAM-1 expression in post-pMCAO brain tissue

Based on previous work which identified CD9 (a key regulator of cell adhesion) as a receptor for some mouse PSGs, we postulated that rPSG1-Fc may decrease leukocyte infiltration into the ischaemic brain and thus promote stroke recovery via reduced adhesion molecule expression (366). As per **Fig. 4.9**, however, no significant change in ICAM-1 expression was observed in either core (p = 0.6376) or peri-infarct (p = 0.8003) tissue.

4.3.7 rPSG1-Fc treatment does not increase TGF-β1 expression in spleen post-ischaemia

Previous research suggests PSG1 activates latent TGF-β1 (368, 373). Indeed, the effect of PSGs on this cytokine is believed to be responsible for their ability to upregulate Treg cells and drive improvement in inflammatory disease states (370, 374). Therefore, although no increase in peripheral Tregs was observed in this study, the levels of splenic TGF-β1 were determined by ELISA at 5 days post-ischaemia to determine whether an increase in expression of this cytokine may underlie any of the immunomodulatory responses observed in this study. However, no changes in the amount of TGF-β1 (p = 0.4054) in post-ischaemic mouse spleens were observed (p = 0.1566) **(Fig. 4.10**).

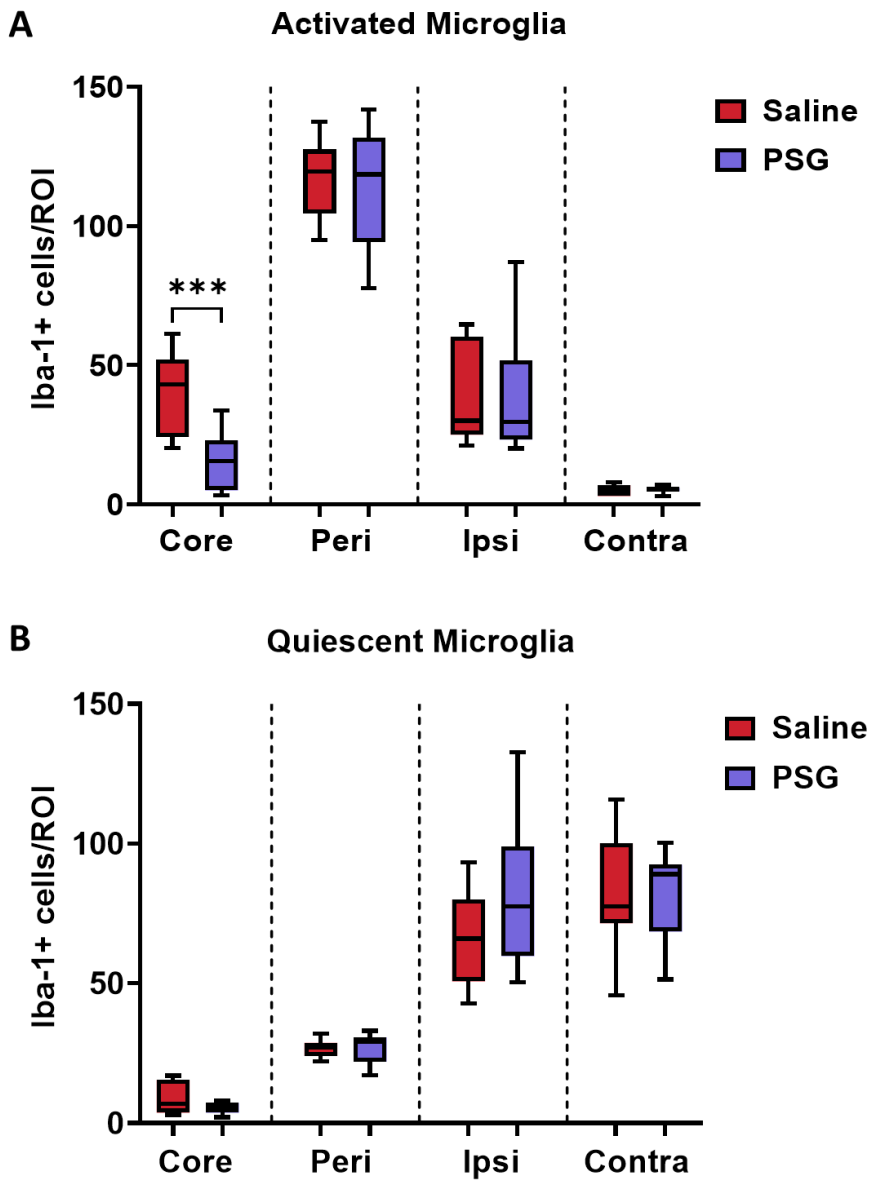


Figure 4.8: Total numbers of A) activated microglia and B) quiescent microglia in the core, peri-infarct zone, healthy ipsilateral tissue, and contralateral tissue of saline-treated and rPSG1-Fc -treated mice post-pMCAO (t = 5 days) (n = 10 per group). Microglia morphology was determined as "activated" (amoeboid) or "quiescent" (ramified) via Iba-1 immunofluorescent staining. Two-sided, independent-samples T-tests were used to investigate differences between groups (* = $p<0.05$, ** = $p<0.01$, *** = $p<0.001$ compared to saline). Box and whisker plots display the 90/10 percentile at the whiskers, the 75/25 percentiles at the boxes, and the median in the centre line.

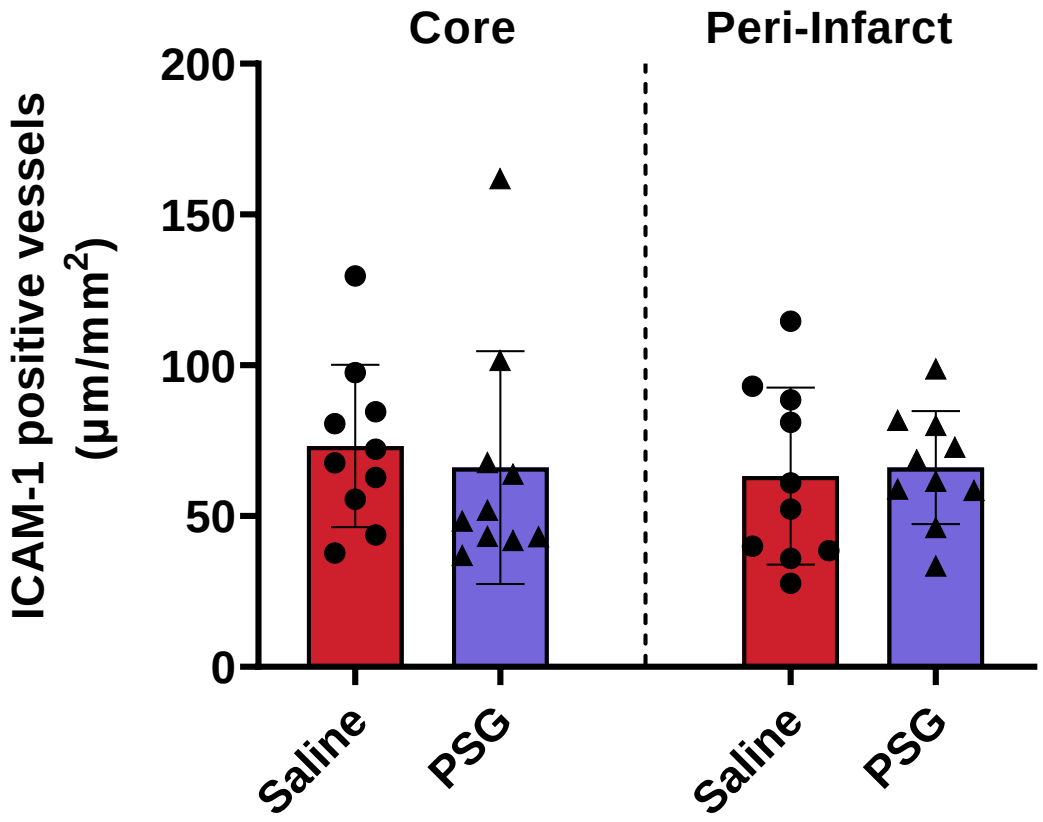


Figure 4.9: Total ICAM-1 positive vessel length (µm) in the infarct core and peri-infarct zone of saline-treated and rPSG1-Fc -treated mice post-pMCAO (t = 5 days) (n = 10 per group). DAB-based immunohistochemistry was used to determine cell counts. Two-sided, independent-samples T-tests were used to investigate differences between groups (* = $p<0.05$, ** = $p<0.01$, *** = $p<0.001$ compared to saline). Bar plots display the mean +/- SD. Dots represent individual mouse values.

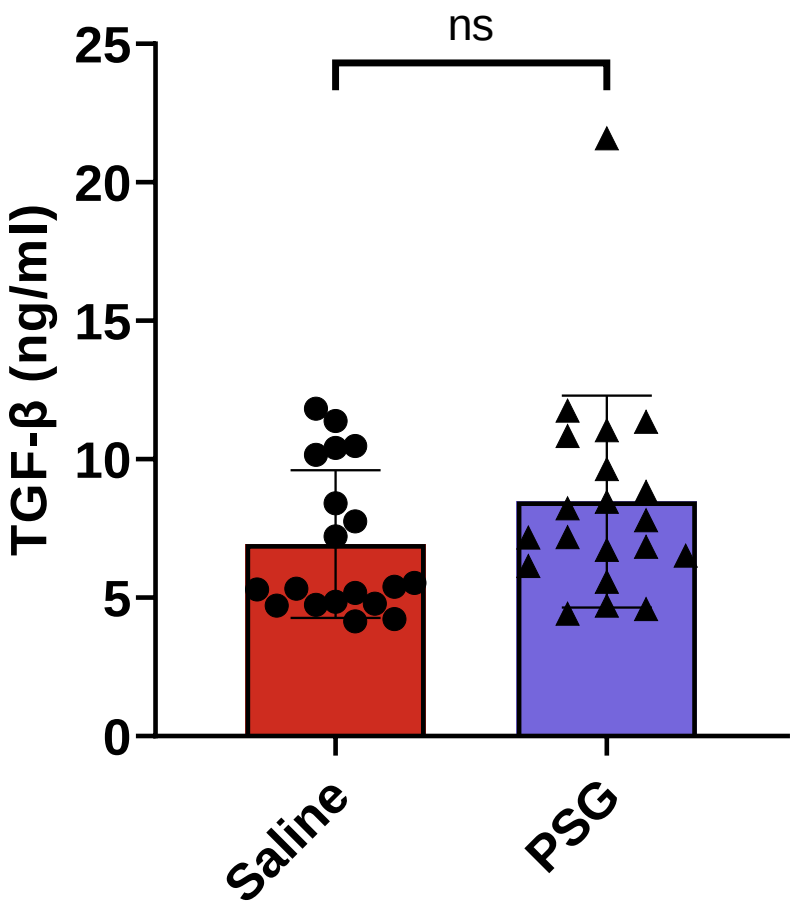


Figure 4.10: Total TGF-β1 in the spleens of saline and rPSG1-Fc-treated mice expressed as picograms/milligram tissue (normalised for protein content) (t = 5 days) (n = 19-20 per group). Two sided, independent-samples T tests were used to investigate differences between groups (* = $p<0.05$, ** = $p<0.01$, *** = $p<0.001$ compared to saline).

4.4 Discussion

Pregnancy-specific glycoproteins exhibit a variety of immunomodulatory properties and have been shown to improve recovery in disease models including acute graft-versus-host disease, colitis and arthritis (357, 359, 369-371, 374, 375). Specifically, PSG1 increases Tregs, a lymphocyte subpopulation associated with improved ischaemic stroke recovery (359, 370, 371, 376). Here, we determined the effect of an IgG1-Fc tagged recombinant pregnancy-specific glycoprotein-1 (rPSG1-Fc) on ischaemic stroke recovery in mice, using a permanent model of brain ischaemia. Our results demonstrate that rPSG1-Fc treatment significantly improved neurobehavioural recovery at days 3 and 5 post-ischaemia compared to saline-treated controls. However, no impact on histological outcome was observed. In CD4+ T cells, rPSG1-Fc enhanced secretion of IL-10 in spleen, blood, and draining and non-draining lymph nodes, while downregulating the production of IFN-γ and IL-17 in spleen and blood but not in draining lymph nodes. rPSG1-Fc also reduced CD8+ IFN-γ and CD8+ IL-17+ T cells in spleen, while upregulating CD8+ IL-10+ T cells in spleen, blood, and non-draining lymph nodes. rPSG1-Fc increased both circulating CD4+ FoxP3+ cells and brain-infiltrating FoxP3+ cells, but failed to increase Treg frequencies in any tissue. rPSG1-Fc also reduced activated microglia in the infarct core. Overall, rPSG1-Fc appears a promising candidate stroke immunotherapy, possibly due to a strong enhancing effect on IL-10 secretion.

The lack of effect of rPSG1-Fc on checklist scores or mouse weights may be due to the lack of sensitivity of these measures, as they are only minimally impacted by small cortical lesions obtained in our model. The lack of correlation between the effects of rPSG1-Fc on functional and histological outcomes may seem unexpected. In stroke

patients, however, a treatment-induced improvement in behaviour does not necessarily reflect a concomitant reduction in lesion size (377). The early reliance on infarct size as the main experimental readout has been suggested to account, at least in part, for the lack of translation to clinical efficacy (37, 378), leading to the suggestion that neurobehavioural tests used to detect experimental stroke-induced changes in cognition, mood, and sensorimotor function would be better predictors for clinical efficacy (379). Future studies of rPSG1-Fc as a potential stroke therapy should therefore prioritise behavioural testing, as recommended by STAIR guidelines, with a focus on long-term prognosis (266).

The finding that rPSG1-Fc improved post-stroke recovery matches results seen with PSG1 in models of colitis, arthritis, and acute graft-versus-host disease (359, 370, 371). While these disorders all involve immune and/or inflammatory factors, the exact mechanisms of action of PSG1 in each model may differ. We initially postulated rPSG1-Fc would provide neuroprotection via a Treg-dependent mechanism, based on studies showing that *in vivo* expression of PSG1 enriched CD4+ CD25+ FoxP3+ T cells in spleen (359, 380). Similar effects were reported after intraperitoneal administration of 100µg PSG1 every 2 days (371). In this study, rPSG-1-Fc did not modulate CD4+CD25+Foxp3+ Tregs in any analysed tissue. Increased CD4+ FoxP3+ T cells however are in line with the increased CD4+ FoxP3+ LAP+ T cells observed in PSG1-treated mice, the heightened levels of FoxP3 mRNA noted among CD4+ T cells, and the results obtained with isolated mouse and human CD4+ T cells (369-371). Our observations are in agreement with effects of other PSG family members such as PSG9 (374). Given that CD4+ CD25+ FoxP3+ T cells tripled after ten doses of PSG1, it is possible that an extended treatment regimen is required to fully expand

the Treg compartment i.e., convert CD4+ FoxP3+ CD25- precursors into fully delineated Tregs (371). However, while a pathway for such development has been proposed for thymic Tregs (381), no evidence yet confirms the same development can occur in the case of peripheral Tregs (382). The single dose of rPSG1-Fc employed in this study may have increased Tregs only transiently post-ischaemia. Since elevated Tregs were observed two weeks after PSG1 withdrawal in the ten-dose study, however, it appears more likely a multiple dose regimen is required to produce the known effects of PSG1 on these cells (371).

Our observation that rPSG1-Fc treatment reduced levels of both secreted IFN-γ and IL-17, as measured by intracellular cytokine staining, is consistent with several previous studies (359, 362, 365, 370). Similarly, increased IL-10 production in several tissues observed here (principally among CD4+ T cells) matches a wealth of evidence wherein PSG-1 is expressed *in vivo* (359, 362, 371), administered as a recombinant protein (370, 380), and when examined *in vitro* (364). In acute ischaemic stroke, low levels of IL-10 predict worse outcomes, while exogenous administration of the cytokine improves recovery in experimental stroke (167). Previous work with other Treg-targeted immunotherapies shows IL-10 plays a central role in Treg-mediated neuroprotection (128, 140). Taken together with the observed effects on FoxP3, the boosted secretion of IL-10 noted in rPSG1-Fc-treated mice may suggest a mechanism wherein PSG enhances regulatory cells which, following infiltration into the infarcted brain, provide neuroprotection via IL-10. Elements of the immune system beyond Tregs are likely involved. rPSG1-Fc reduced microglial activation in this study. Based on the fact that PSGs enhanced IL-10 production among myeloid cells, coupled with the known links between Tregs and microglia in post-stroke repair, a more complex

mechanism involving modulation of microglia phenotype by rPSG1-Fc is also possible (135, 323, 362, 364). However, further data on the impact of PSG on M1 and M2 phenotypes is required.

The differential effect of rPSG1-Fc on the secretion of IL-10 among CD8+ T cells in spleen, blood, and non-draining lymph nodes (where increases were noted) versus the draining cervical lymph nodes (where no change was observed) requires further study. Similarly, rPSG1-Fc reduced CD4+ IL-17+ and CD4+ IFN-γ T cells in spleen and blood but not draining lymph nodes. One possible explanation may involve the intimate connection between these draining lymph nodes and the brain. Even under non-stroke conditions, the meningeal lymphatic system facilitates the drainage of cerebrospinal fluid macromolecules to the cervical lymph nodes (383). Post-stroke, such "brain-cervical lymph nodes crosstalk" systems are crucially involved in the clearance of neurotoxic material from the infarcted brain (384). Recently, Esposito *et al.*, identified that this same lymphatic fluid can activate macrophages (and likely other immune cells) in the draining lymph nodes as early as 24 hours post-ischaemia (313). Therefore, it is possible that in the spleen and blood, rPSG1-Fc has the capacity to shift the immune response away from IFN-γ/IL-17 and towards IL-10 as normal. But in the draining lymph node, the tolerizing signal of rPSG1-Fc is cancelled out by the acute pro-inflammatory signalling described above.

Analysis of spleen TGF-β1 levels revealed no significant differences between rPSG1-Fc and saline-treated mice. Previous evidence shows PSGs increase free levels of this cytokine in autoimmune disease models (7) and in the steady state (12, 16, 18, 31, 32). However, most studies associating PSGs with increased TGF-β1 were conducted with cell lines, protein systems, or in vivo expression models, as opposed to subcutaneous

injection employed here (7, 12, 16, 31, 32, 40). In the two studies where PSG1 was administered directly via intraperitoneal injection, TGF-β1 levels were not directly determined (18, 19). Indeed, only the downstream hallmarks of increased TGF-β1-signalling (elevated FoxP3, increased Tregs, upregulated IL 10 signalling, and higher SMAD2/3 phosphorylation) were demonstrated. In the current study, TGF-β1 levels were quantified only in the spleen at 5 days post-ischaemia. It is possible that TGF-β1 may have been sequestrated in insoluble extracellular matrix, and that the use of serum, lymph nodes or brain may have yielded different results (47). Given the ELISA assay employed in this study measured total TGF-β1 levels, and not the active or latent form independently, it is also possible the activating effect of rPSG1-Fc on latent TGF-β1 previously described was not accurately captured (16).

The relative strengths of this study include appropriate sample sizes determined by *a priori* power calculation, use of both male and female mice, and behavioural outcome in a permanent model of brain ischaemia which more accurately mirrors the clinically observed low reperfusion rates (385, 386). We demonstrate the *in vivo* effect of rPSG1-Fc in ischaemic stroke with a clear impact on the cytokine-secreting phenotypes of CD4+ and CD8+ T cells. While this study provides preliminary evidence for several potential mechanisms of action for rPSG1-Fc in stroke, it should be emphasized that this is only evidence of association and not causation. Greater understanding of the exact pharmacokinetic/pharmacodynamic properties of this proposed rPSG1-Fc therapy is required. The fusion of PSG1 to an Fc tag likely extends half-life up to several days (387). However, the relationship between the pharmacokinetic profile and mechanism of action in particular needs investigating. Another limitation of this study is that the impact of PSG1-Fc in post-stroke mice was

only examined at one timepoint. However, the selected treatment regimen was based on experience with rPSG1-Fc in other disease models and, more generally, with other putative Treg-targeted stroke immunotherapies (140, 184, 370). Further prospective studies are required to fully determine which aspects of the immune system play a definitive causative role.

4.5 Conclusion

Pregnancy-specific glycoproteins (PSGs) have garnered recent interest for the treatment of a number of inflammatory conditions, principally due to their observed effects on regulatory immune cells such as Tregs and anti-inflammatory cytokines (e.g. TGF-β, IL-10) (375). This well-powered study provides strong evidence that a recombinant form of PSG1 improves functional recovery in a permanent model of brain ischaemia, without impacting infarct size. We identify a possible mechanism through enhanced secretion of IL-10 among circulating CD4+ T cells, and decreased expression of IFN-γ and IL-17, suggesting an overall modulation towards a suppressive phenotype. Reduced microglial activation supports this hypothesis. The apparent lack of an effect on TGF-β levels in this study requires further investigation (372). In order to confirm whether IL-10 and/or Tregs play a role in the neuroprotective effect of rPSG1-Fc, it should now be tested in mice in which IL-10 or Tregs are blocked or depleted (388, 389). Confirmation of dose and treatment duration required to confer maximal benefit is also required. Potential adverse effects of rPSG1-Fc treatment in stroke also must be assessed. rPSG1-Fc may lack the toxicity and immunogenicity observed with other stroke immunotherapies (as suggested by high levels of the protein found during human pregnancy and its expression in gastrointestinal tract epithelium) (390). But while the absence of drug-induced

lymphopenia would reduce the risk of treatment-associated infection, it should be recognised that pregnancy itself is associated with increased risks for certain types of infections, and that the immunological changes behind this trend (e.g., increased Treg-derived IL-10) could be conferred by rPSG1-Fc treatment (390-393). Finally, the possibility to combine rPSG1-Fc with currently available methods of recanalization (i.e., tPA, thrombectomy) should be investigated, especially given the expanding indications for such interventions (394). Overall, this study provides the first insight into the effect of rPSG1-Fc in acute ischaemic stroke, alongside potential mechanisms of action.

Supplementary material related to chapter 4

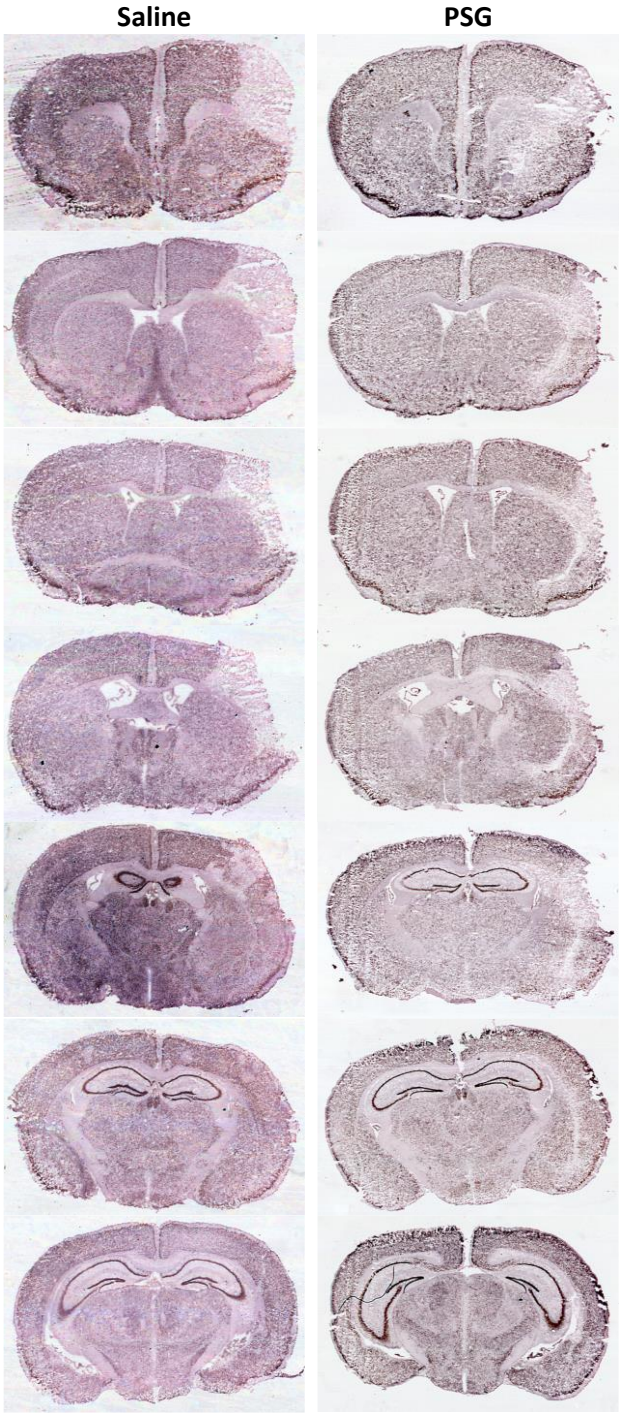


Figure S4.1: Representative images of NeuN stained coronal brain sections from saline and rPSG1-Fc treated mice at 5 days post pMCAO.

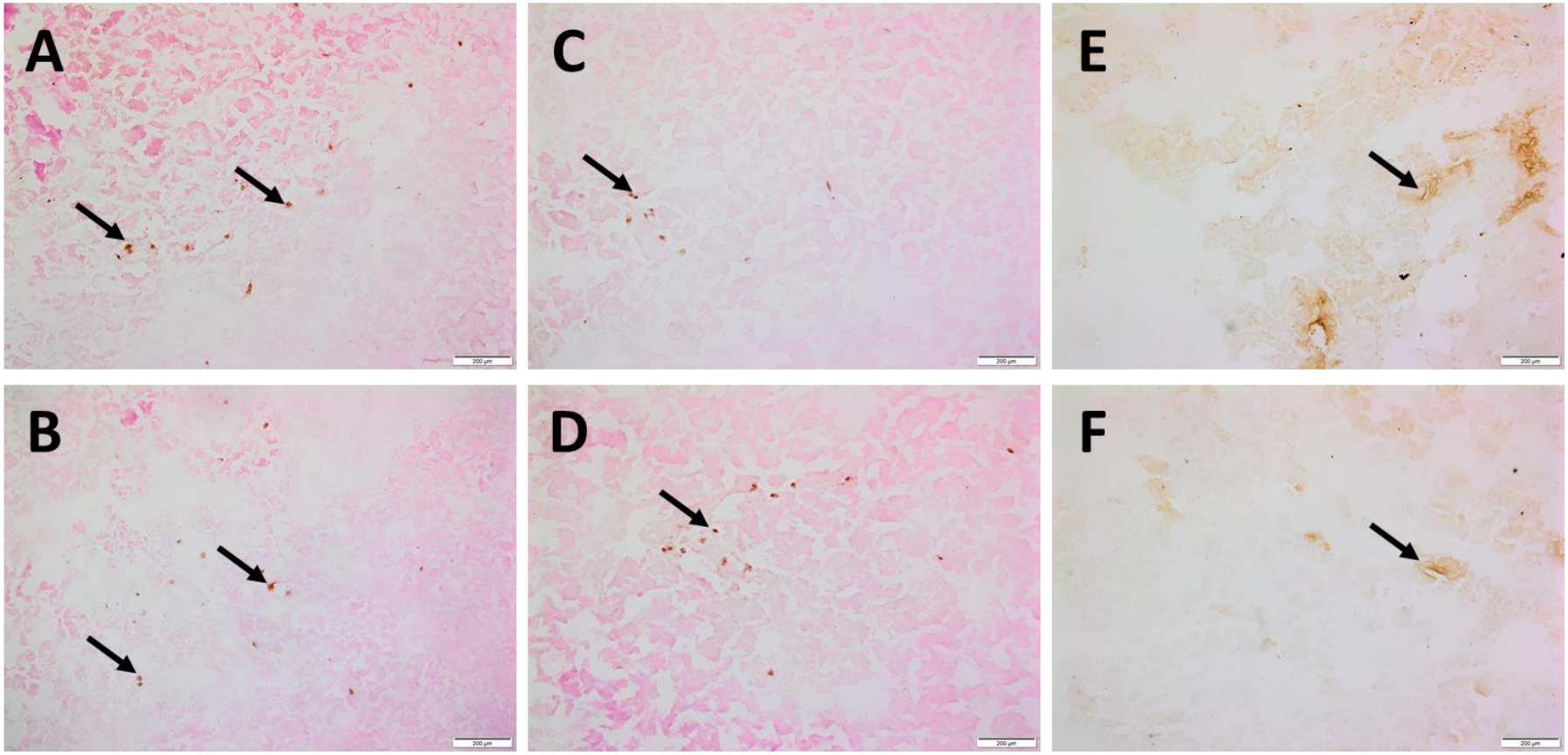


Figure S4.2: Representative immunohistochemistry images of CD3+ (A, B), FoxP3+ (C, D), and ICAM-1 (E, F) staining in the peri-infarct zones of mice post-pMCAO (t = 5 days). CD3+/ICAM-1 images acquired with the 20X objective lens of an Olympus BX51 microscope. FoxP3+ images acquired with the 40X objective lens. Positive cells counted using ImageJ. A = CD3 (saline), B = CD3 (rPSG1-Fc), C = FoxP3 (Saline), D = FoxP3 (rPSG1-Fc), E = ICAM-1 (saline), F = ICAM-1 (rPSG1-Fc). Sample positive staining indicated via black arrows.

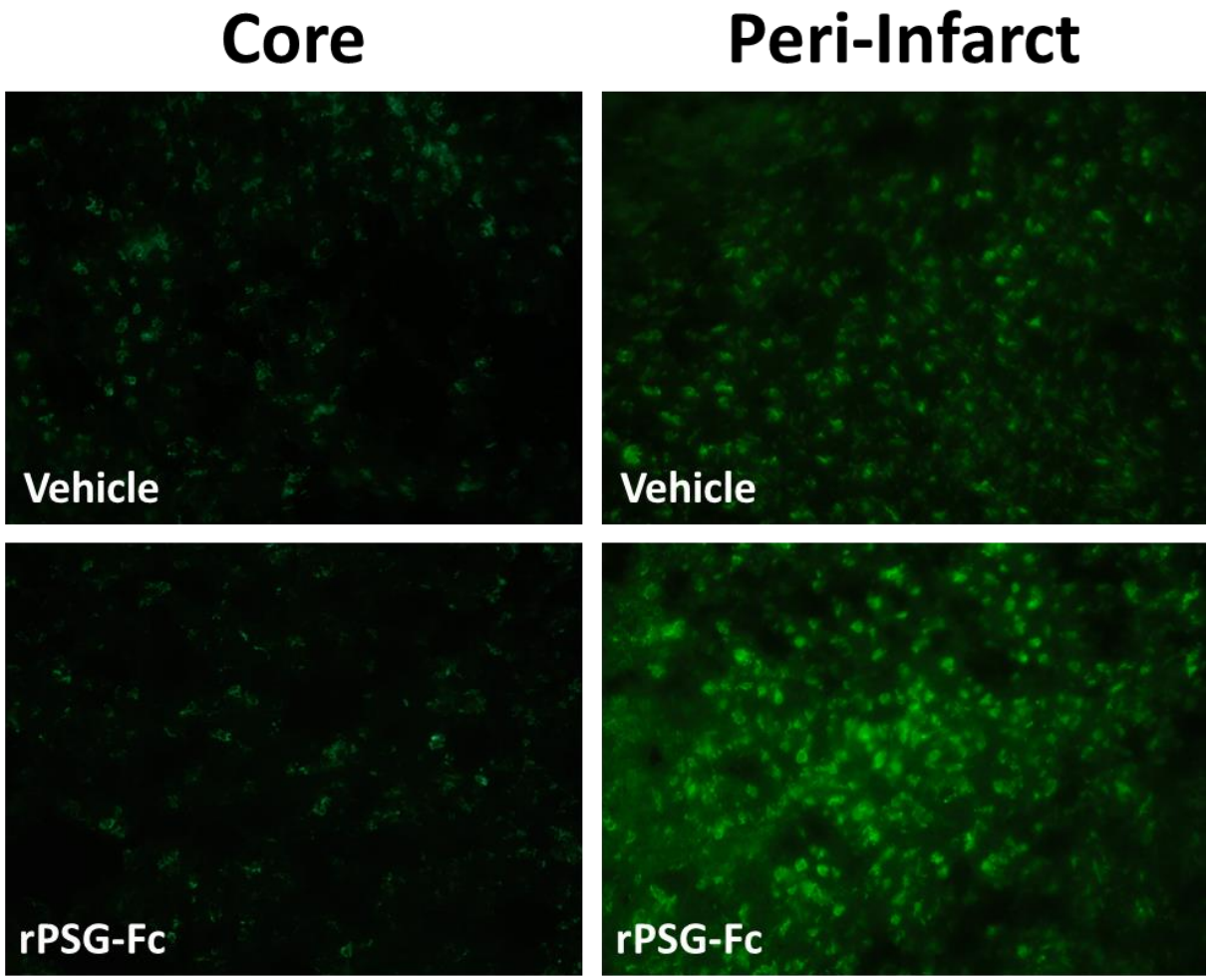


Figure S4.3: Representative immunofluorescence images of Iba-1 staining in the core and peri-infarct zones of mice post-pMCAO (t = 5 days). Images acquired with the 20X objective lens of an Olympus BX51 microscope. Positive cells counted using ImageJ.

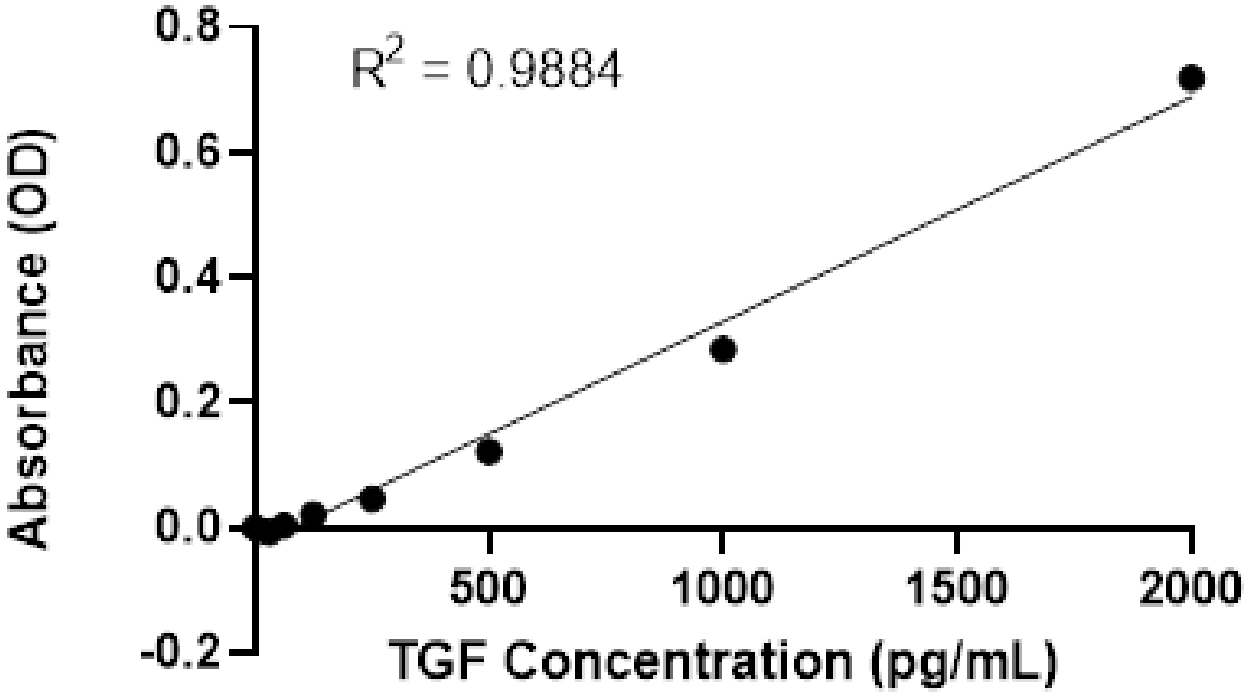


Figure S4.4: Representative standard curve employed for the determination of TGF-β in spleen of saline-treated or rPSG1-Fc-treated mice (n = 19-20 per group) post-pMCAO (t =5 days).

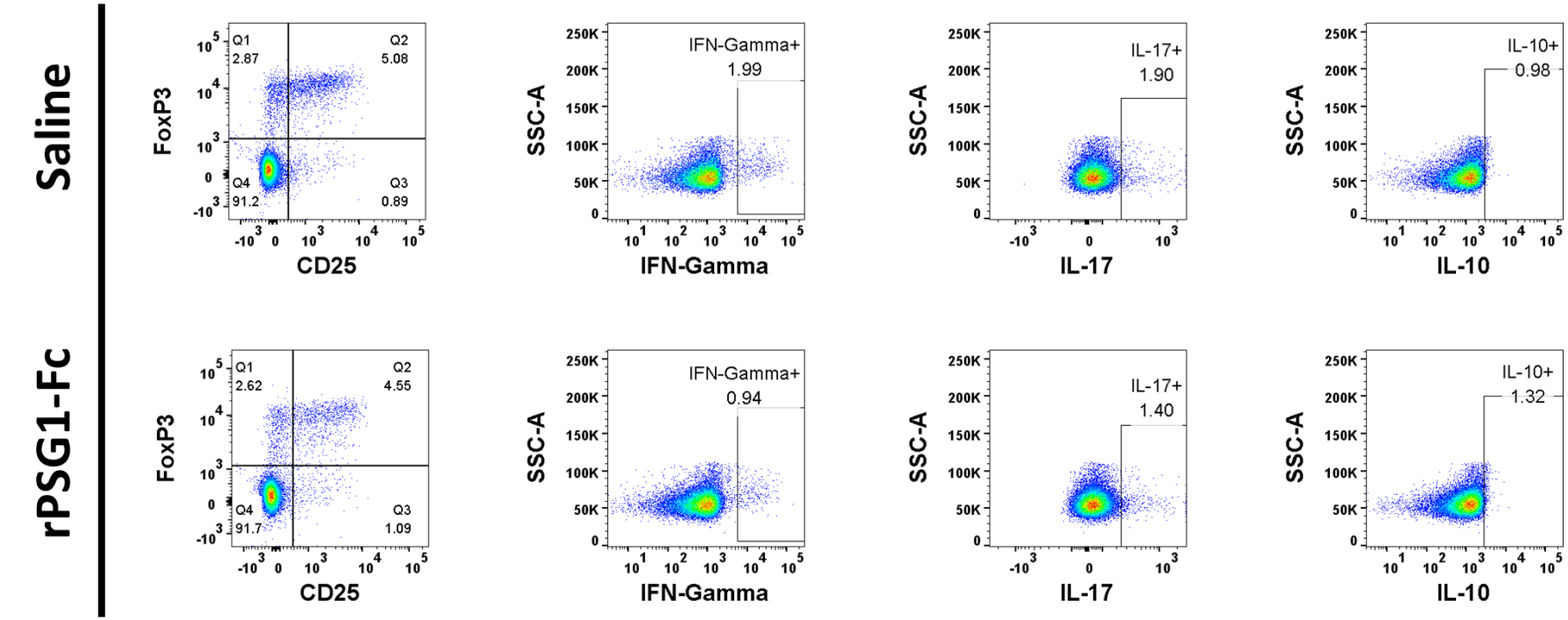


Figure S4.5: Representative FACS pseudocolour plots depicting CD4+ CD25+ FoxP3+ T cells, CD4+ IFN-γ+ T cells, CD4+ IL-17+ T cells, and CD4+ IL-10+ T cells in saline and rPSG1-Fc treated mice

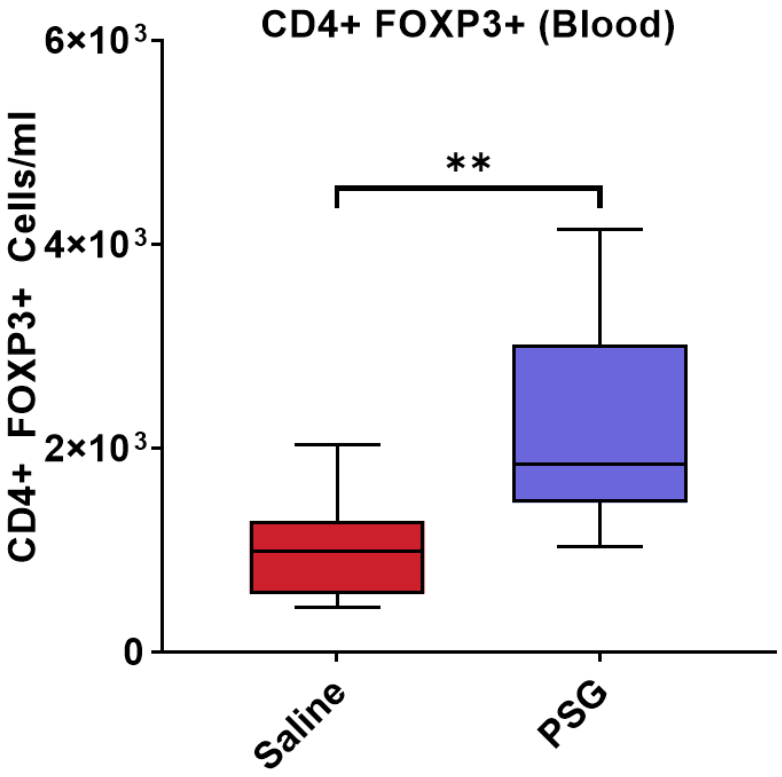


Figure S4.6: Total CD4+ FoxP3+ T cells in blood in response to either saline (n = 20) or rPSG1-Fc (n = 22) treatment post-pMCAO (t =5 days). Two-sided, independent-samples T-tests used to investigate differences between groups (* = $p<0.05$, ** = $p<0.01$, *** = $p<0.001$ as compared to saline). Box-and-whisker plots exhibit 10-90 percentiles.

Chapter 5

Regulatory T Cell Frequency is Acutely Increased in Mild Ischaemic Stroke Patients

In the previous chapters, I characterised the impact of fingolimod and rPSG1-Fc in acute ischaemic stroke and demonstrated both improved functional outcome in a permanent model of middle cerebral artery occlusion while modulating Tregs. However, while fingolimod and rPSG1-Fc show promise as possible Treg-targeted immunotherapies in stroke, to date, our understanding of Tregs in human stroke remains limited. Without understanding how the onset of brain ischaemia modifies peripheral levels of Treg, it is difficult to select the best timepoint to intervene with Treg-targeted therapies. To this end, I comprehensively characterised both Treg frequency and function in the blood of stroke patients at two timepoints. Levels of T cell-secreted cytokines were also measured. My hypothesis was that through these analyses, I would be able to identify whether there was any relationship between Tregs and functional recovery in stroke and, if so, when might be the most opportune moment to intervene with Treg-targeted immunotherapies.

The text of this chapter is the draft publication:

Malone K, Shearer JA, Kelly A, Moore AC, Merwick A, Waeber C. Regulatory T Cell Frequency is Acutely Increased in Mild Ischaemic Stroke.

Abstract

Background*:* Stroke is a major cause of morbidity and mortality worldwide. While many parts of the immune system contribute to stroke damage, a lymphocyte subset termed regulatory T cells (or "Tregs") has been shown to provide neuroprotection. To date, however, the impact of mild brain ischaemia on leukocytes, and in particular, peripheral Tregs in stroke patients remains understudied. The aim of this study was to comprehensively quantify Treg frequency and function in both the acute and subacute post-ischaemic period.

Methods: Blood was collected from mild transient ischaemic attack (TIA) or mild-moderate acute ischaemic stroke (modified Rankin score </= 2) patients (n = 12) at 24 hours (T1) and one week (T2) post-brain ischaemia, and age-matched controls (n = 9). Frequencies of major immune subsets, namely T cells (as well as naïve and memory phenotypes), B cells, monocytes, and natural killer cells were quantified. Levels of plasma cytokines were also determined. I next quantified the frequency of circulating Tregs, as well as the frequency of naïve, memory, and proliferating subsets. The expression of functional markers of suppression (CD39, CTLA-4, PD-1) by these subsets was also quantified.

Results: Stroke reduced CD3+ T cell, regulatory NK cell, and intermediate monocyte frequency while increasing CD19+ B cell, $CD56^{dim}$ NK cell, and classical monocyte frequency in the blood of stroke patients compared to age-matched controls. Stroke also increased the frequency of Tregs. Subset analysis revealed proliferating, Ki67+, proliferating Tregs were elevated at 24 hours post-ischaemia. Enhanced expression of both PD-1 and CTLA-4 by Ki67+ Tregs was also observed. A reduction in circulating CTLA4+ and PD-1+ proliferating Treg frequency occurred by 7 days post-ischaemia.

Increased plasma levels of IL-4 and IL-5 were noted at 7 days post-ischaemia compared to 24 hours.

Conclusions: Mild acute ischaemic stroke reduces CD3+ T cell frequency without affecting CD4+ or CD8+ T cell subsets. However, an increased frequency of circulating Treg is observed in the acute post-stroke period, with a specific rise in Ki67+ Tregs. Enhanced expression of functional markers of suppression (CTLA-4, PD-1) among Ki67+ Tregs also occurs. However, by 7 days post-ischaemia, a decrease in PD-1/CTLA-4+ Ki67+ Tregs is noted. Future post-stroke Treg-targeted immunotherapies may therefore need to target this subacute period (7 days+) to maximize Treg-afforded neuroprotection.

5.1 Introduction

Acute ischaemic stroke (AIS) is a leading cause of death and disability worldwide (11). However, despite the intensive search for neuroprotective therapies over the last few decades, recombinant tissue plasminogen activator (rtPA) remains the only FDA-approved pharmacotherapy, and this can only be administered within 4-6 hours of stroke onset. Although recent advances in mechanical thrombectomy have improved disease outlook for a subset of AIS patients, new treatments are still required (22). It is well established that the immune system plays a major role in all stages of AIS, from the pathogenesis of risk factors to the initial expansion of the infarcted core (25). However, while numerous aspects of the immune response have been shown to contribute to neurotoxicity, a lymphocyte subset termed regulatory T cells (or "Tregs") have garnered interest due to recent research highlighting a potential beneficial effect of these cells on both functional and histological stroke outcome, with the only negative effects thought to be a contribution to secondary microthrombosis (151).

Tregs, characterised by constitutive expression of both the surface receptor CD25 and the transcription factor forkhead box P3 (FoxP3), represent approximately 5-10% of the total CD4+ compartment, and play an important role in maintaining immune homeostasis, preventing autoimmunity and inflammation (105). Mechanisms of Treg-mediated neuroprotection specifically in AIS may include secretion of IL-10, production of TGF-β and IL-35, priming of M2 macrophages, and reduced inflammatory cytokine secretion (118). In pre-clinical stroke models, depletion of Tregs has been shown to increase infarct volume, while administration of exogenous Tregs provides neuroprotection (134, 137). However, while several therapeutic strategies aiming to promote Treg number and/or function in AIS have been proposed (140, 158, 184), to date, relatively few clinical studies have explored in detail these cells in AIS patients. Early studies suggested a reduction in circulating Treg number in the first few days after stroke (155, 165). An imbalance between Tregs and Th17 cells has also been shown to occur (157). However, more recent studies indicate a more nuanced relationship between AIS and Tregs, with early increases in peripheral Treg levels followed by a decrease during subacute (day 7+) stages (154). Therefore, it is clear that a temporal profile of Tregs post-ischaemia encompassing both acute and sub-acute periods is required. Data on the impact of AIS on markers of Treg suppressive function (e.g., CD39, CTLA-4) is also lacking. Similarly, while several studies have investigated leukocyte levels and secreted cytokines post-brain ischaemia in isolation, a more comprehensive image of the simultaneous changes in both is needed in order to investigate potential associations (124, 395-397). In particular, leukocyte levels in mild stroke, which can result in considerable morbidity, needs further evaluation (398). In this respect, the relationship between immune components and patient outcome such as modified Rankin Score remains under-studied. The

principal aim of this study was to determine, via flow cytometric analysis, the Treg frequency and function in the peripheral blood of mild stroke patients, at the time of recruitment and at 7 days post-ischaemia, as well as in age-matched controls. As a secondary objective, we aimed to quantify the T cell cytokine profile in the peripheral blood at time of recruitment as well as at 7 days post-stroke. Finally, we aimed to determine whether there was a relationship between Treg frequency and/or the frequency of other immune cells post-stroke and functional recovery, specifically by investigating whether immune cell frequencies or plasma cytokine levels correlated with modified Rankin score in stroke patients.

5.2 Methods

5.2.1 Ethics Statement

All patients were recruited, and blood sampled according to protocols approved by the Clinical Research Ethics Committee (ECM 4 (r) 14/01/2020 and ECM 3 (eee) 08/09/2020). All donors provided written informed consent.

5.2.2 Patients and Controls

Between September 2020 and August 2021, this study enrolled 12 patients during the acute phase of either transient ischaemic attack (TIA) or mild-moderate acute ischaemic stroke (modified Rankin score </= 2) from the Acute Stroke Unit of Cork University Hospital, Ireland. Patients were included if they had a recent stroke/TIA (< 1 week) and were aged ≥18 years. Exclusion criteria included pregnancy, an unstable medical condition, active malignancy, and the presence of dementia or a cognitive/learning disability that impacted on participants' ability to provide informed consent.

All patients were examined by a consultant neurologist on admission to the stroke unit and treated according to accepted stroke guidelines. Using a structured questionnaire, data including age, sex, presence of co-morbidities (atrial fibrillation, hypertension, hypercholesteremia, diabetes, prior history of TIA/stroke), prescribed medication, and time from symptom onset to brain imaging and sampling was collected. Phlebotomy was performed at the time of recruitment and 7 days later. A 40ml blood sample was taken, collected in heparinised tubes (BD Vacutainer Plastic K2EDTA), then transferred to the Neuropharmacology lab of the School of Pharmacy, University College Cork for immediate processing. A brief clinical follow-up at 7-, 30-, and 90-days post-TIA/stroke was conducted with each patient. Healthy, age-matched controls (n = 9) were also recruited as part of the study.

5.2.3 PBMC Isolation and Cryopreservation

Blood (4 x 10ml portions) was layered over 15ml lymphoprep (Stemcell Technologies, #7811) using Greiner 50ml Leucosep tubes (Cruinn Diagnostics, # 2272906G). Tubes were centrifuged at 2000 rpm with low accelerator and without brake for 20min. After centrifugation, plasma was collected and stored at -80^{0}C. PBMCs were collected and washed three times with PBS (Sigma-Aldrich, #D8537). Cells were counted and then re-suspended in a cryopreservation solution containing 90% fetal calf serum (FSC) (Sigma-Aldrich, #F2442) and 10% DMSO (Sigma-Aldrich, #D2650) at a concentration of 1 x 10^7 cells/ml. Cells were cooled at 1^{0}C per minute using a Corning CoolCell LX Container (Sigma-Aldrich, #CLS4322002) and stored in a-80^{0}C freezer overnight. Cells were stored long-term in liquid nitrogen. Cells were thawed to the last ice crystal in a water bath pre-warmed to 37°C. Cells were then diluted in 10X volume cell culture media (RPMI-1640 (Sigma-Aldrich, #R7658) with 10% Fetal calf serum

(FCS) (Sigma-Aldrich, #F2442 containing 1% Penicillin-Streptomycin (Sigma-Aldrich, #P4458). Cells were washed with medium 3-4 times and then counted. For each sample, approximately 2 x 10^6 cells were then added to wells of a 96-well plate.

5.2.4 Quantification of Treg Frequency and Function by Flow Cytometry

Cell suspensions were stained with cell surface antibodies (all eBioscience) for either Tregs (Staining Panel 1, **Table 5.1**) or general PBMCs (Staining Panel 2, **Table 5.2**). For both panels, a live/dead stain (1:10,000) was added to each sample (Fixable Viability Dye eFluor 780) (eBioscience, #65086514). For surface staining, samples were incubated for 30 minutes at 2-8°C in the dark. For Tregs, the samples were washed, fixed, permeabilised, and stained intracellularly for anti-human FoxP3 (eFluor 450, #A42925) (PCH101, 1:25), Ki67 (AF700, #56569882) (SolA15, 1:25) and CTLA-4 (PE-eFluor 610, #61152942) (14D3, 1:25) in accordance with the instructions provided with the Essential Human Treg Phenotyping Kit (eBioscience). All samples were then re-suspended in an appropriate volume of PBS.

Table 5.1: Antibodies used in Treg panel.

Antigen	Clone	Fluorophore	Dilution	Product Number
CD4	RPA-T4	FITC	1:50	#A42925
CD8	RPA-T8	PE-Cyn5.5	1:50	#35008842
CD3	OKT3	PE-Cy7	1:50	#25003742
CD45RA	HI100	APC	1:50	#17045842
CD25	CD25	PerCP-eFluor 710	1:50	#A42925
CD127	eBioRDR5	PE	1:25	#A42925

PD-1	J105	PE-Cyn5	1:25	#15279942
CD39	EBIOA1	SB600	1:25	#63039942

Table 5.2: Antibodies used in PBMC panel.

Antigen	Clone	Fluorophore	Dilution	Product Number
CD4	RPA-T4	FITC	1:50	#A42925
CD8	RPA-T8	PE-Cyn5.5	1:50	#35008842
CD3	OKT3	PE-Cy7	1:50	#25003742
CD45RA	30-F11	PerCP-Cyn5.5	1:50	#45045182
CD197	3D12	PerCP-eFluor 710	1:50	#46197942
CD19	HIB19	AF700	1:50	#56019942
CD16	CB16	APC	1:50	#17016842
CD56	CMSSB	PE-Cy5	1:50	#15056742
HLA-DR	LN3	APC-eFluor 780	1:50	#47995642
CD11c	3.9	PE-eFluor 610	1:50	#61011642
CD123	6H6	SB600	1:50	#63123942

5.2.5 Flow Cytometry Data Analysis

Flow cytometric analysis was performed with a LSRII flow cytometer (Becton Dickinson). Compensation control was set using BD CompBead Anti-Mouse Particles Set (BD, #552843). All data was analysed using FlowJo (v10). Tregs were determined according to the following gating strategy (**Fig. 5.1)**: live cells (as determined by

live/dead stain), lymphocytes (as determined by FSC/SSC), T lymphocytes (as determined by CD3+), CD4+ and CD8+, Tregs (CD4+ CD127- cells which co-express CD25 and FoxP3), proliferating Tregs (Ki67+ Tregs), naïve Tregs (CD45RA+ Tregs), memory Tregs (CD45RA- Tregs), as well as CD39+, CTLA-4+ and PD-1+ derivatives of same. Representative flow cytometry plots of the key results are displayed in **Fig. 5.2.**

Major PBMC immune subsets were determined with the following gating strategy (**Fig. 5.3)**: live cells (as determined by live/dead stain), lymphocytes (as determined by FSC/SSC), T lymphocyte subsets (as determined by CD3+, CD4+, CD8+, CD45RA+, CD197+), B cells as determined by CD19+, monocyte subsets as determined by CD14+ and CD16+, natural killer cell subsets as determined by CD16+ and CD56+, and dendritic cell subsets as determined by HLA-DR+, CD11c+ and CD123+. Representative flow cytometry plots of the key results are displayed in **Fig. 5.3.** Full details of markers used to define immune lineages are outlined in **Table 5.3**. All gates were set according to unstained samples and fluorescent minus one controls. All results were reported according to the Minimum Information About a Flow Cytometry Experiment (MIFlowCyt) guideline (51). High-dimensional cytometry data was also visualised in two dimensions based on the t-distributed Stochastic Neighbour Embedding (t-SNE) algorithm (Iterations = 1000, perplexity = 20) (**Fig. S5.1, S5.2**).

5.2.6 Quantification of Plasma Cytokines by Multiplex Assay

Twelve plasma cytokines (TNF-α, IFN-γ, IL-2, IL-4, IL-5, IL-6, IL-9, IL-10, IL-13, IL-17A/F, IL-21, and IL-22) were quantified using chemiluminescence-based assays from Meso Scale Discovery (MSD Inc, Rockville MD, USA), according to the

manufacturer's instructions. A subset of the U-PLEX Biomarker Group 1 (human) Assays was employed (#K15067L-1). The detection ranges (expressed in picograms/ml) were TNF-α: 0.54-3700, IFN-γ: 1.7-17000, IL-2: 0.7-1900, IL-4: 0.08-2100, IL-5: 0.24-4000, IL-6: 0.33-2000, IL-9: 0.14-1500, IL-10: 0.14-3700, IL-13 : 3.1-1900, IL-17A/F: 1.84-18400, IL-21: 1.2-12600, and IL-22: 0.13-3400. Analyses were completed using a QuickPlex SQ 120 instrument (MSD) and DISCOVERY WORKBENCH® 4.0 software. All samples were run undiluted in duplicate at the same time. Cytokine concentrations were calculated based on the four-parameter logistic fitting model generated from standards. Data below the lower limit of quantification were computed as (Limit of Detection/square root of 2).

5.2.7 Statistical Analysis

The Kolmogorov–Smirnov test was used to test normality of flow cytometric data, which are displayed as scatter plots with bar (mean +/- standard deviation). The ROUT method (Q = 1%) was used to identify possible outliers, which were then screened for exclusion. Two-sided T tests or Mann-Whitney tests were employed to investigate differences between control and stroke (T1) samples. Paired T tests or Wilcoxon signed-rank tests were employed to investigate differences between 24 hours post-stroke (T1) and 7 days post-stroke (T2) samples. A p-value <0.05 was considered statistically significant. Correlations between experimental outcomes and lymphocyte subpopulation frequencies were investigated using Spearman's correlation analysis. Statistical analysis was performed using GraphPad Prism 9.1.2. All investigators remained blinded to treatment groups throughout analysis.

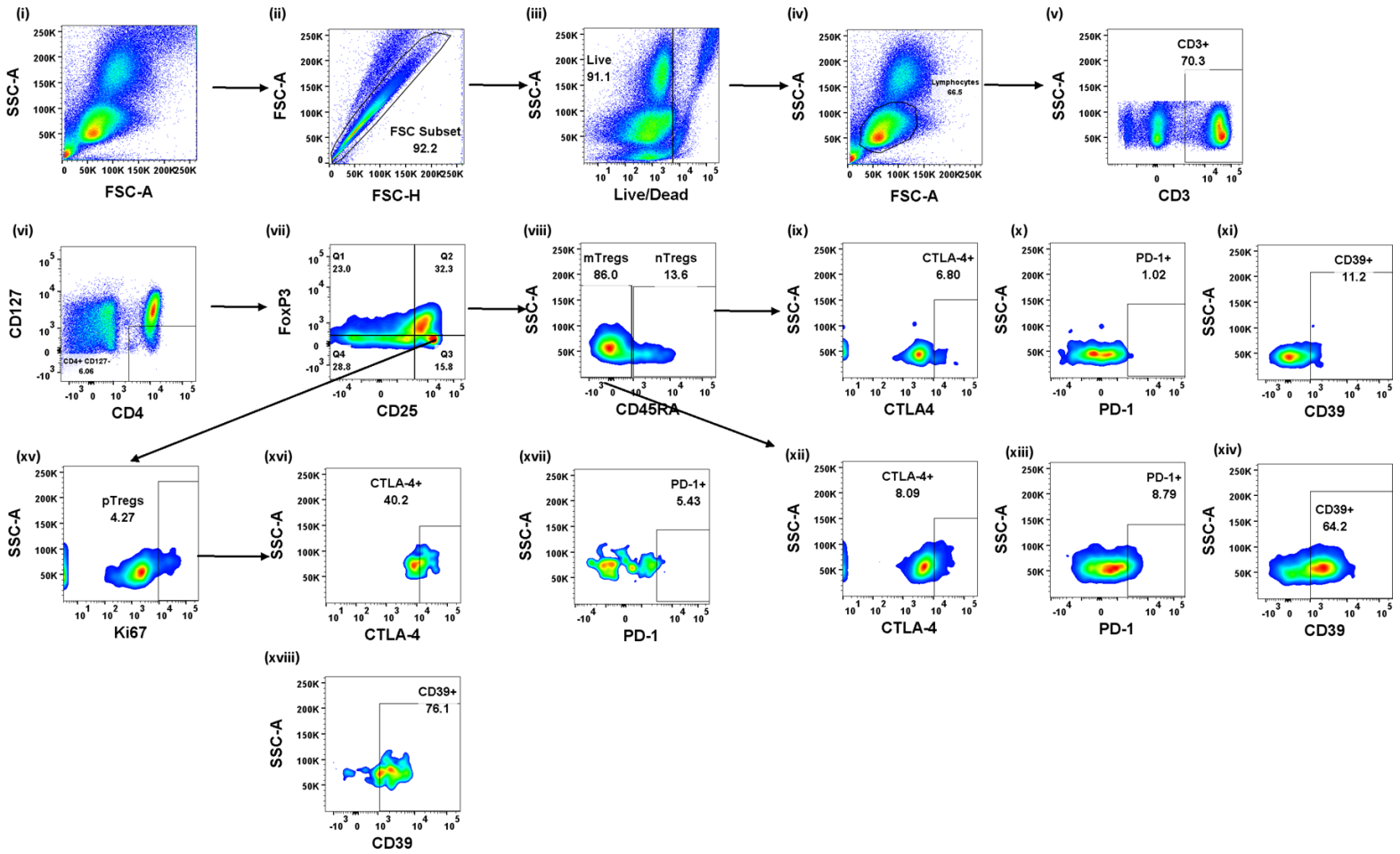


Figure 5.1: Gating strategy for determination of Tregs, as well as expression of CTLA-4, PD-1, and CD39 among naïve, memory and proliferating Tregs in blood. (i) Initial population, (ii) singlets, (iii) Live cells (live/dead stain negative), (iv) lymphocytes, (v) CD3+ T cells (T cells), (vi) CD4 versus CD127 CD3+ T cells, (vii) CD4+ CD25+ FoxP3+ T cells (upper right quadrant) designated Tregs, (viii) CD45RA+ (naïve Tregs) vs CD45RA- (memory Tregs) cells, (xv) Ki67+ Tregs (proliferating Tregs). All gates were determined by both negative cells and fluorescence minus one controls.

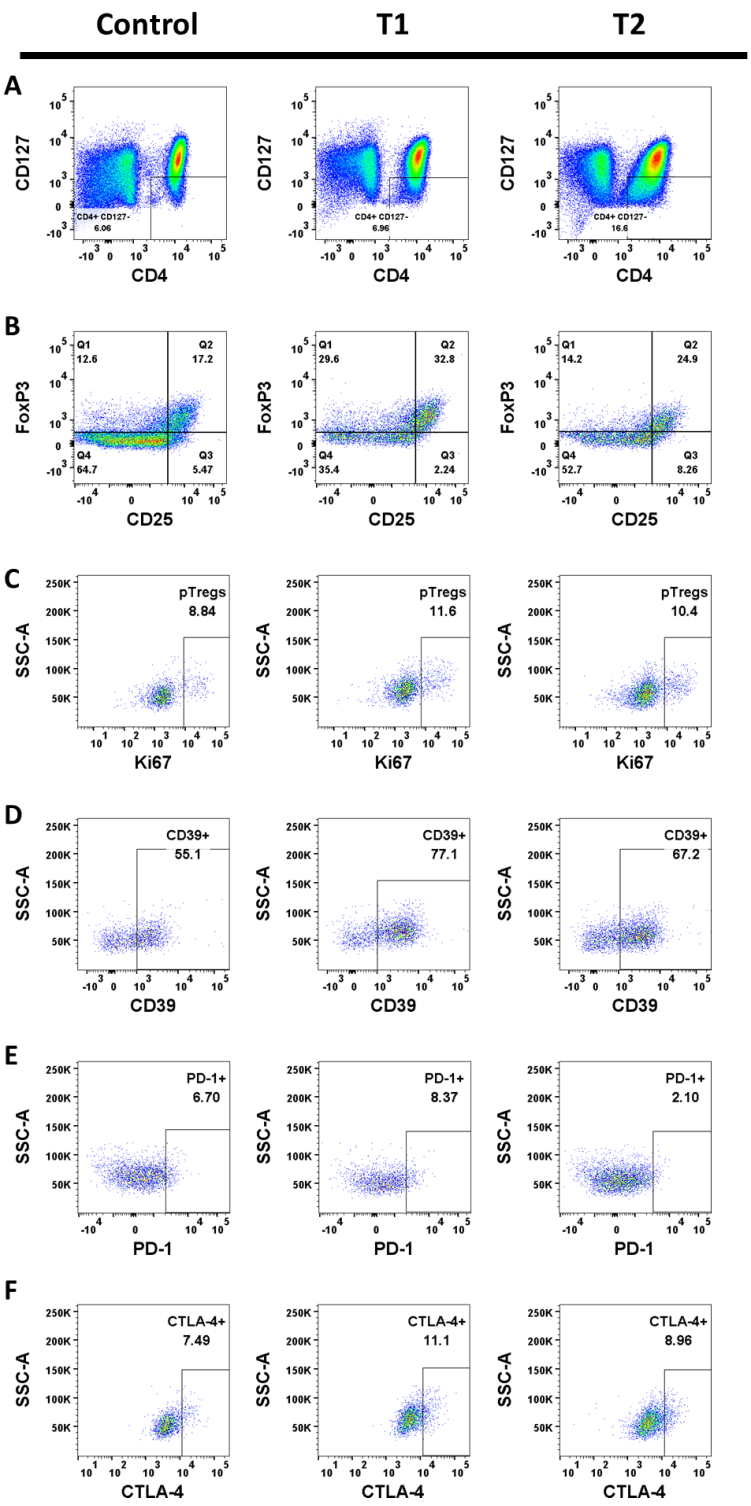


Figure 5.2: Representative FACS pseudocolour plots depicting key results from Treg panel in in stroke patients (n = 12) (at 24 hours (T1) and one week (T2) post-brain ischaemia) and age-matched controls (n = 9). A) CD4+CD127- cells, B) CD4+CD127-CD25+FoxP3+ T cells (Tregs), C) Ki67+ Tregs, D) CD39+ Tregs, E) PD-1+ Tregs, F) CTLA-4+ Tregs.

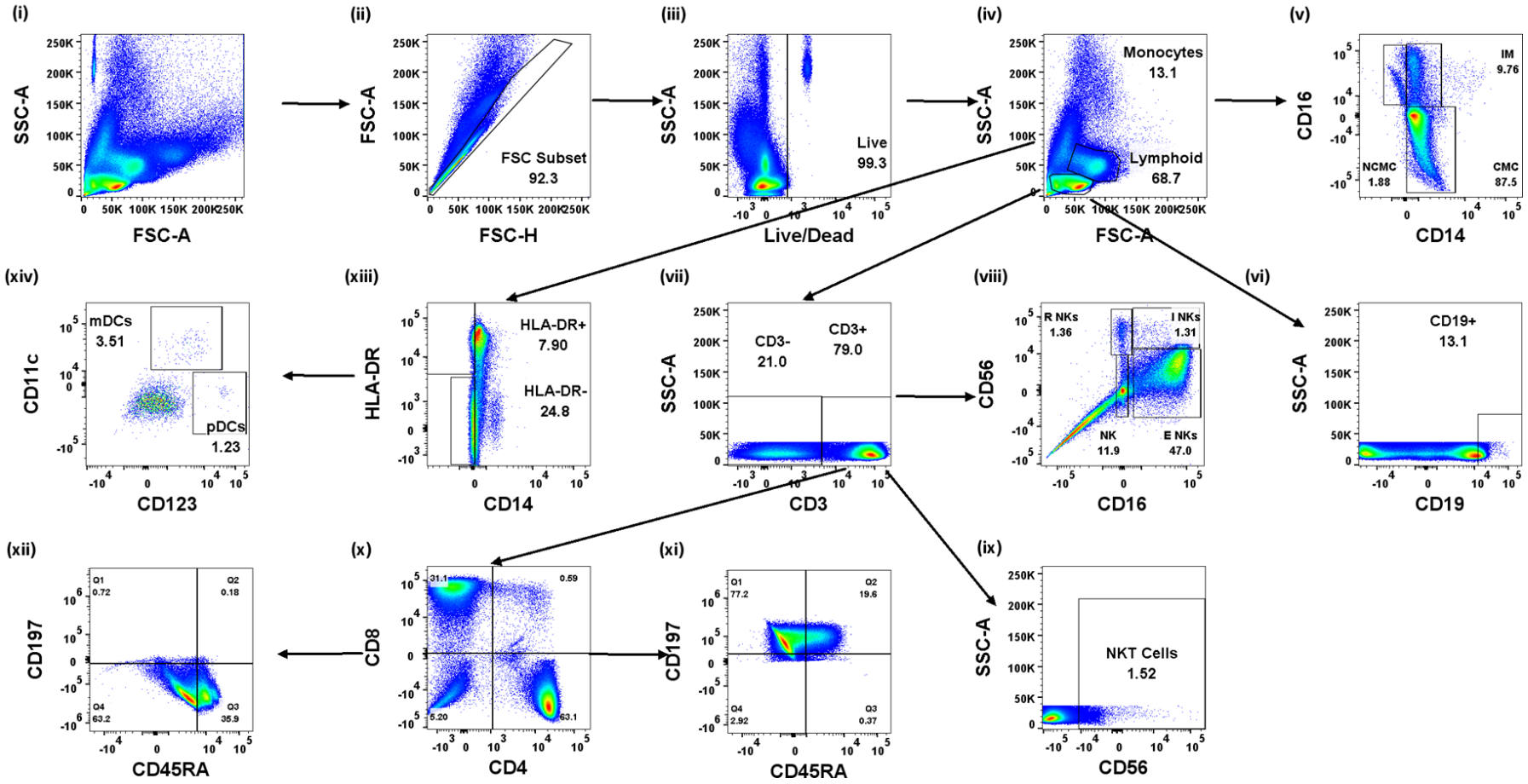


Figure 5.3: Gating strategy for determination of immune cell subsets in blood. (i) Initial population, (ii) singlets, (iii) Live cells, (iv) Leukocyte subsets, (v) = monocytes (Classical (CM), Non-Classical (NCMC), and Intermediate (IM), (vi) = CD19+ B cells, (vii) CD3+ T cells (T cells) vs CD3- cells, (viii) = NK Cells (Effector NKs, Intermediate NKs, NK Cells, and Regulatory NKs), (ix) = NKT cells, (x) = CD4+ vs CD8+ T cells, (xi) = CD4 cell subsets, (xii) = CD8 cell subtypes, (xiii) = Lineage negative cells (+/- HLA-DR), (xiv) = Dendritic cells (myeloid DCs, plasmacytoid DCs). For CD4+ and CD8+ T cells, Q1 = Central Memory, Q2 = Naïve, Q3 = Effector, Q4 = Effector Memory respectively. All gates were determined by both negative cells and fluorescence minus one controls.

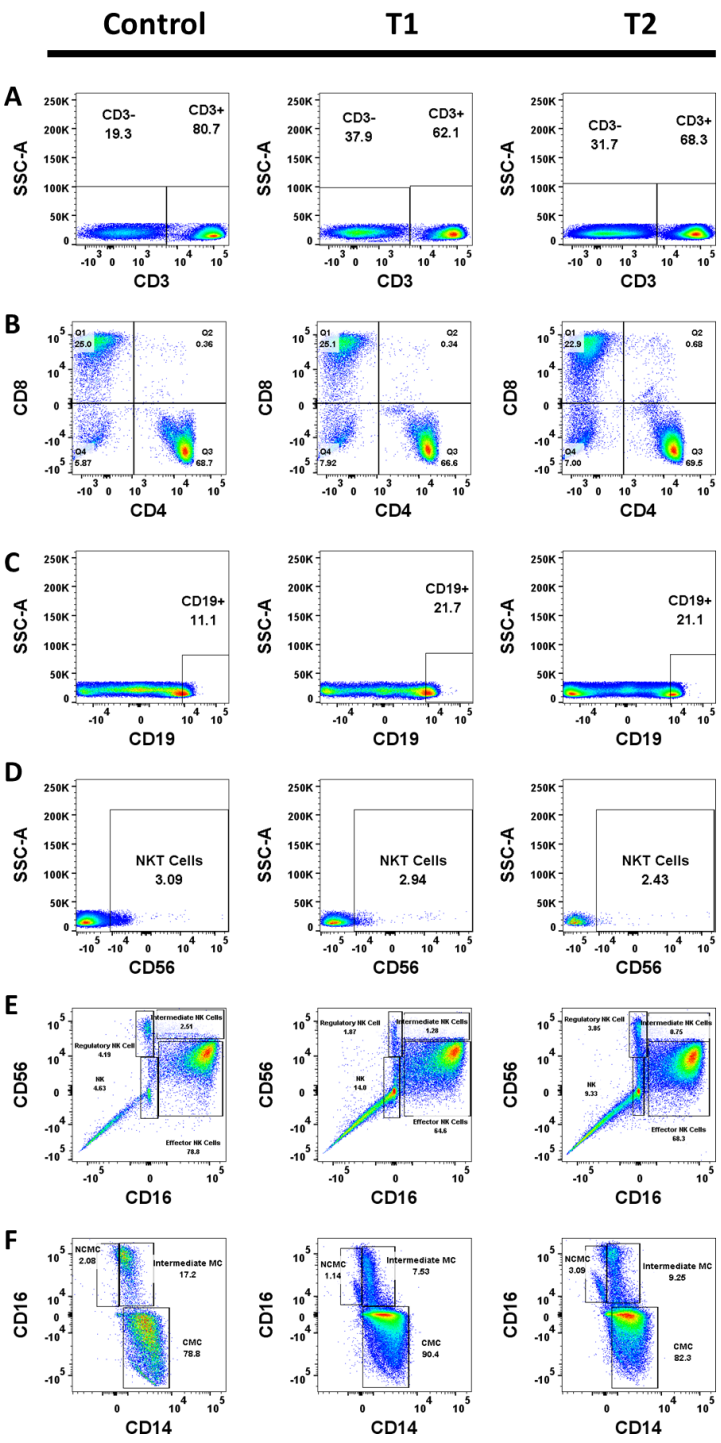


Figure 5.4: Representative FACS pseudocolour plots depicting key results from PBMC panel in in stroke patients (n = 12) (at 24 hours (T1) and one week (T2) post-brain ischaemia) and age-matched controls (n = 9). A) CD3+ (T cells) vs. CD3- cells, B) CD4+ vs. CD8+ T cells, C) CD19+ (B cells), D) CD3+CD56+ cells (NKT cells), E) CD3-CD56^{hi}CD16- cells (regulatory NK), CD3-CD56^{hi}CD16+ cells (Intermediate NK), CD3=CD56^{lo}CD16- cells (NK) and CD3-CD56+CD16+ (Effector NK) cells, F) CD14+CD16^{hi} (Non-classical monocytes), CD14^{hi}CD16+ (Intermediate monocytes), and CD14+CD16+ (Classical monocytes).

Table 5.3: Cell populations evaluated by flow cytometry panels. Lin = lineage markers (CD3/CD19/CD14). Singlet, live, and lymphoid/myeloid populations not listed.

Population Name	Corresponding Markers	Panel
Tregs	CD3+CD4+CD127-CD25+FoxP3+	Treg
CD4+ CD25+ T Cells	CD3+CD4+CD127-CD25+	Treg
CD4+ FoxP3+ T Cells	CD3+CD4+CD127-FoxP3+	Treg
Naïve Tregs (nTregs)	CD3+CD4+CD127-CD25+FoxP3+CD45RA+	Treg
Memory Tregs (mTregs)	CD3+CD4+CD127-CD25+FoxP3+CD45RA-	Treg
Proliferating Tregs (Ki67+ Tregs)	CD3+CD4+CD127-CD25+FoxP3+Ki67+	Treg
T Cells	CD3+	PBMC
CD4+ T Cells	CD3+CD4+	PBMC
CD8+ T Cells	CD3+CD8+	PBMC
Naïve CD4+ or CD8+ T Cells	CD3+CD4+ or CD8+CD197+CD45RA+	PBMC
Central Memory CD4+ or CD8+ T Cells	CD3+CD4+ or CD8+CD197+CD45RA-	PBMC
Effector CD4+ or CD8+ T Cells	CD3+CD4+ or CD8+CD197-CD45RA+	PBMC

Effector Memory (TEMRA) CD4+ or CD8+ T Cells	CD3+CD4+ or CD8+CD197-CD45RA-	PBMC
NKT Cells	CD3+CD56+	PBMC
B Cells	CD3-CD19+	PBMC
Non-Classical Monocytes	CD14+CD16^{hi}	PBMC
Intermediate Monocytes	CD14^{hi}CD16+	PBMC
Classical Monocytes	CD14+CD16-	PBMC
Regulatory NK Cells	CD3-CD56^{hi}CD16-	PBMC
Intermediate NK Cells	CD3-CD56^{hi}CD16+	PBMC
NK Cells CD56^{dim}	CD3-CD56^{lo}CD16-	PBMC
Effector NK Cells	CD3-CD56+CD16+	PBMC
Dendritic Cells (DCs)	Lin-HLA-DR+	PBMC
Plasmacytoid DCs (pDCs)	Lin-HLA-DR+CD123^{hi}CD11c^{lo}	PBMC
Myeloid DCs (mDCs)	Lin-HLA-DR+CD123^{lo}CD11c^{hi}	PBMC

5.3 Results

5.3.1 Study Cohort

In total, twelve patients were recruited who were stratified for stroke severity according to the NIHSS. We also recruited 9 age-matched control participants. Our cohort of stroke patients was 58.3% male with a median age of 60 [interquartile range (IQR) = 46.26–62.75] years. Our cohort of control participants was 66.6% male with a median age of 60 [interquartile range (IQR) = 40.5–67.5] years. No difference in mean age was evident between groups (p = 0.9585). Characteristics of both stroke (stratified by Day 0 Rankin Score) and control participants are summarized in **Table 5.4**.

Table 5.4: Participant demographics and clinical information. Stroke patients (n = 12) are stratified according to Day 0 Rankin Score. Age and biochemical results are depicted as mean +/- standard deviation (shown in parenthesis). Sex and smoker data is depicted as raw number (%). N/A = data not available.

Variable	Control (n = 9)	Rankin Score 0 (n = 3)	Rankin Score 1 (n = 5)	Rankin Score 2 (n = 4)
Age (years)	55.67 (12.52)	55.33 (16.52)	62.00 (7.55)	51.40 (15.19)
Male sex	6 (66.6)	2 (66.6)	2 (40)	3 (75)
Smoker	N/A	2 (66.6)	1 (20)	0 (0)
Lymphocytes (10^3 cells/μl)	N/A	2.58 (1.38)	1.99 (0.60)	2.10 (1.06)
WBC (10^3 cells/μl)	N/A	10.43 (4.09)	8.56 (2.16)	8.05 (1.71)

CRP (μg/ml)	N/A	1.47 (1.59)	4.80 (5.12)	6.83 (12.99)
Blood glucose (mmol/L)	N/A	5.53 (0.85)	7.45 (3.53)	7.35 (0.21)
Total Cholesterol	N/A	5.03 (1.12)	5.18 (1.47)	4.35 (0.69)
HDL	N/A	1.49 (0.63)	1.12 (0.14)	1.09 (0.31)
LDL	N/A	2.80 (1.15)	3.55 (1.63)	2.58 (0.33)
Triglycerides	N/A	1.56 (1.14)	1.55 (1.91)	1.49 (0.69)

5.3.2 Stroke reduces CD3+ T cell frequency without affecting the relative proportion of CD4+ or CD8+ subsets

Due to the diverse roles T cells may play in both exacerbating and ameliorating post-stroke neuroinflammation, we investigated whether ischaemic stroke influenced T cell populations (391). At the onset of ischaemic stroke (T1) significant reductions in CD3+ T cell frequency were observed compared to control samples (p =0.0441) (**Fig. 5.5**). However, no changes in either CD4+ or CD8+ T cell frequencies or in the CD4+/CD8+ ratio were observed. Similarly, an investigation of naïve, central memory, effector, or effector memory subsets among CD4+ or CD8+ T cells revealed no differences between stroke patients and control (**Fig. 5.6**). Likewise, no differences were noted in T cell populations between T1 and T2.

5.3.3 Stroke increases B cell frequency at 24 hours post-ischaemia

Other non-T cell lymphoid subsets might also influence post-stroke recovery. B cells may have a deleterious role post-stroke, with B-cell derived immunoglobulins

suggested to be involved in late-phase chronic inflammatory responses (48). Examination of B cells showed a significant increase in CD19+ B cell frequency at T1 compared to control (p = 0.0186) (**Fig. 5.7**). This can be noted in t-SNE plots (**Fig. S5.**1) by increased red (CD19) colours between no stroke and stroke 24-hour samples. However, no differences were noted in B cells between T1 and T2. As one of the earliest cells to infiltrate into the brain post-stroke (<3 hours), NK cells have been implicated in exacerbating neuroinflammation via IFN-γ and perforin/granzyme (399). NKT and NK cells have also been shown to play a vital role in host defence post-stroke (62, 64).

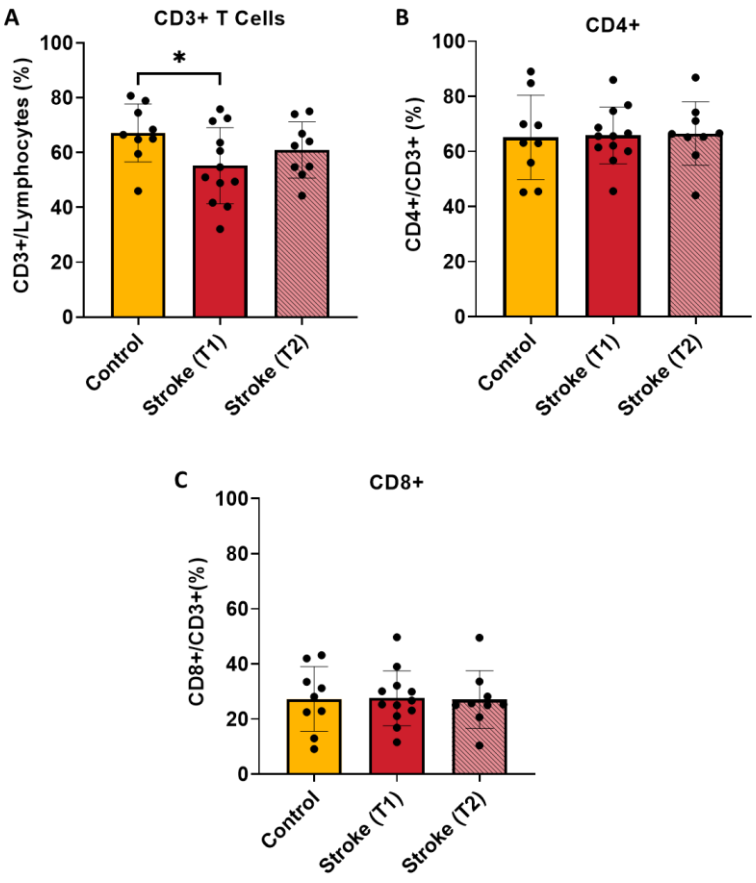


Figure 5.5: Frequencies of circulating **A:** CD3+ T, **B:** CD4+ T, and **C:** CD8+ T cells in stroke patients (n = 12) (at 24 hours (T1) and one week (T2) post-brain ischaemia) and age-matched controls (n = 9). Two-sided, independent, or paired sample T tests (or non-parametric equivalents) investigated differences between two groups (* = p<0.05, ** = p<0.01, *** = p<0.001).

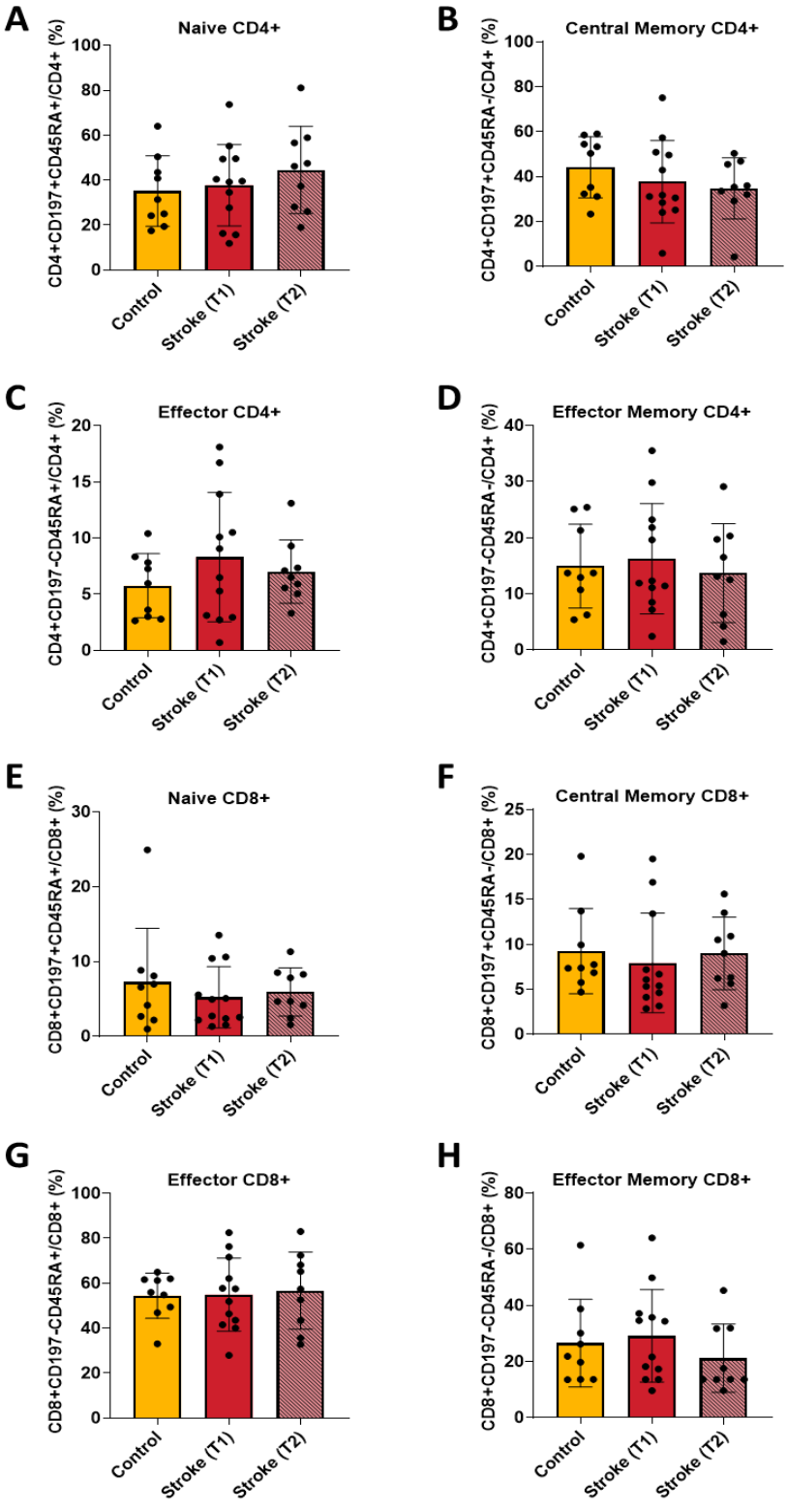


Figure 5.6: Frequencies of circulating CD4+ T cell (**A**-D) and CD8+ (**E**-H) subsets in in stroke patients (n = 12) (at 24 hours (T1) and one week (T2) post-brain ischaemia) and age-matched controls (n = 9). Two-sided, independent-samples T tests (or non-parametric equivalents) investigated differences between two groups (* = $p<0.05$, ** = $p<0.01$, *** = $p<0.001$).

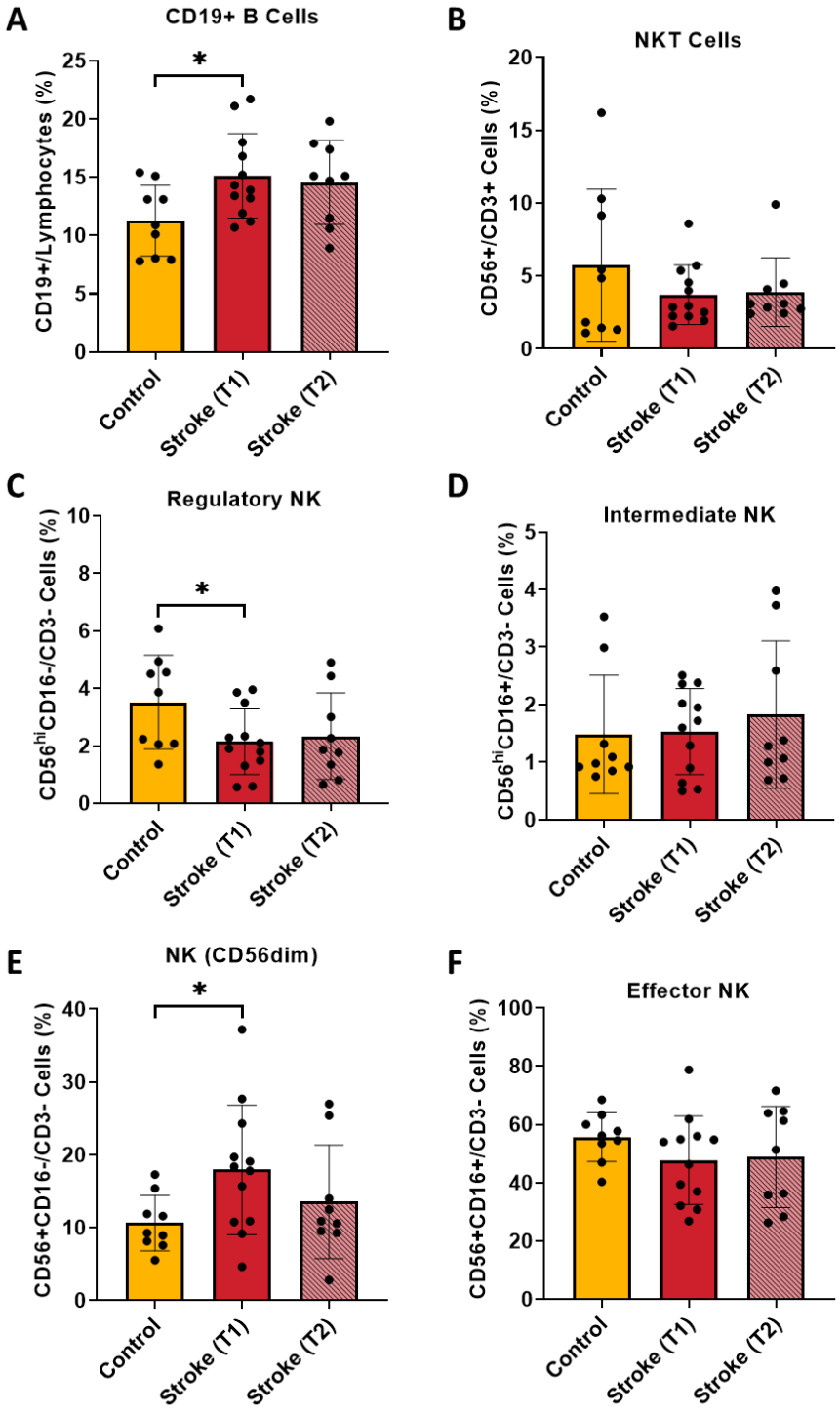


Figure 5.7: Frequencies of non-T cell lymphoid subsets in the total lymphocyte population in stroke patients (n = 12) (at 24 hours (T1) and one week (T2) post-brain ischaemia) and age-matched controls (n = 9). **A:** CD19+ B cells, **B:** NKT cells, **C:** Regulatory NK cells, **D:** Intermediate NK cells, **E:** NK ($CD56^{dim}$) cells, **F:** Effector NK cells, in in stroke patients (at 24 hours (T1) and one week (T2) post-brain ischaemia) and age-matched controls at 24 hours post-ischaemia. Two-sided, independent or paired sample T tests (or non-parametric equivalents) investigated differences between two groups (* = $p<0.05$, ** = $p<0.01$, *** = $p<0.001$).

No significant differences were noted in circulating CD3+ CD56+ NKT cell frequency between ischaemic stroke patients and controls. Notably, however, a reduced frequency of regulatory NK cells was observed at T1 compared to control ($p = 0.0343$). A significant increase in CD56dim NK cells was noted ($p = 0.0327$). No significant differences in intermediate or effector NK populations were noted between groups (**Fig. 5.7**).

5.3.4 Stroke acutely decreases intermediate monocyte frequency while increasing classical monocyte frequency

Monocytes infiltrate into the brain 1–2 days post-stroke. Pro-inflammatory M1 monocytes exacerbate neuroinflammation via cytokine such as IL-1β, TNF-α, and IL-6 (400). However, M2 monocytes can promote recovery via IL-10. Analysis of myeloid subsets revealed a significant reduction in intermediate monocytes between control and T1 ($p = 0.0157$) (**Fig. 5.8**). A significant increase in classical monocytes was observed in stroke patients compared to controls ($p = 0.0015$). However, this latter increase was transient, with a significant reduction in classical monocytes noted between T1 and T2 ($p = 0.0391$). No differences were observed in non-classical monocytes between groups.

Recently, dendritic cells (DCs) have been highlighted as potential key players in antigen presentation post-brain ischaemia (401). Both myeloid (mDCs) and plasmacytoid (pDCs) dendritic cells have also been shown to be involved in neuroprotection. In particular, pDCs have been highlighted as ameliorating brain injury in experimental stroke in mice via priming Tregs (402). Here, however, dendritic cell subsets remained unchanged between stroke and control patients.

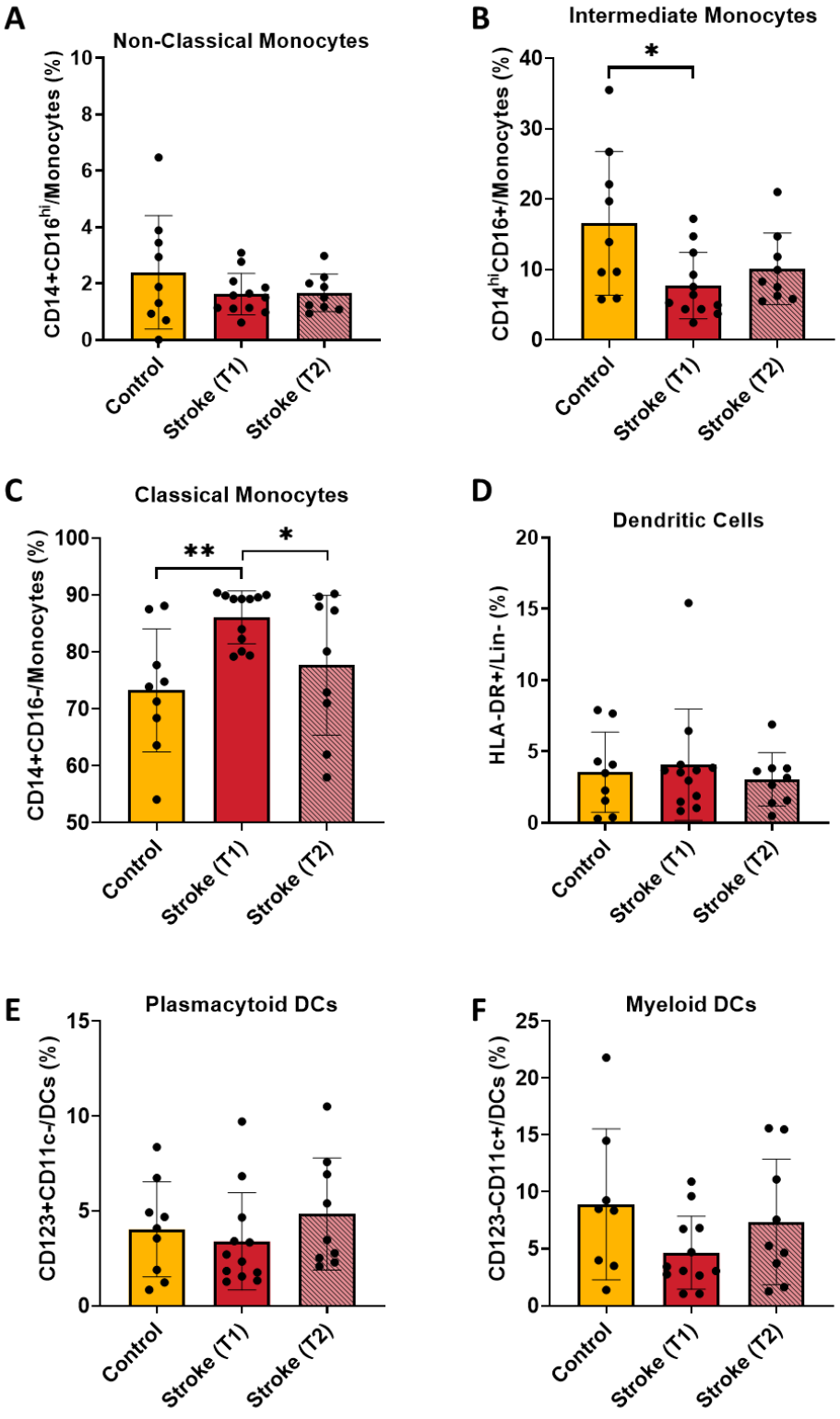


Figure 5.8: Frequencies of monocyte (**A-C**) and dendritic cells (**D-F**) in stroke patients (n = 12) (at 24 hours (T1) and one week (T2) post-brain ischaemia) and age-matched controls (n = 9). Two-sided, independent or paired sample T tests (or non-parametric equivalents) investigated differences between two groups (* = p<0.05, ** = p<0.01, *** = p<0.001).

5.3.5 Stroke increases circulating Treg frequency

Tregs were defined as CD4+CD25+FoxP3+CD127- cells in line with guidelines provided by the CIMT immunoguiding program (91). Quantification of circulating Tregs in the acute post-stroke period (24 hours post-ischaemia; T1) showed significantly higher frequencies among stroke patients compared to age-matched controls ($p = 0.0167$) (**Fig. 5.9**). No significant differences were observed between T1 and the second timepoint of seven days post-ischaemia (T2) ($p = 0.2379$). Examination of the CD25+ and FoxP3+ portions of the Treg phenotype revealed increased FoxP3 cells were evident at T1 compared to control ($p = 0.0425$). No change was noted in CD4+127-FoxP3+ T cells between T1 and T2 ($p = 0.6406$). No correlations were noted between CD4+CD25+FoxP3+CD127- cells at 24 hours post-ischaemia and admission modified Rankin Score ($p = 0.2727$).

5.3.6 Stroke transiently enhances markers of Treg suppressive activity

Treg surface markers including CD39, CTLA-4, and PD-1 have been shown or suggested to play a role in Treg-afforded neuroprotection post-brain ischaemia (138, 151, 165). However, to date, the impact of stroke on these markers in stroke patients has not been well characterised. Here, we observed stroke did not cause any change in CD39+ Tregs compared to control ($p = 0.6373$). Stroke increased the frequency of PD-1+ ($p = 0.0068$) and CTLA-4+ Tregs ($p = 0.0076$) at 24 hours post-stroke (T1) compared to control (**Fig. 5.9**). This can be noted in t-SNE plots (**Fig. S5.**2) by increased yellow (PD-1) and orange (CTLA-4) colours between no stroke and stroke 24-hour samples. However, this change was transient, with a decrease in PD-1/CTLA-4+ Tregs noted between T1 and T2 ($p = 0.0250, 0.0019$ respectively).

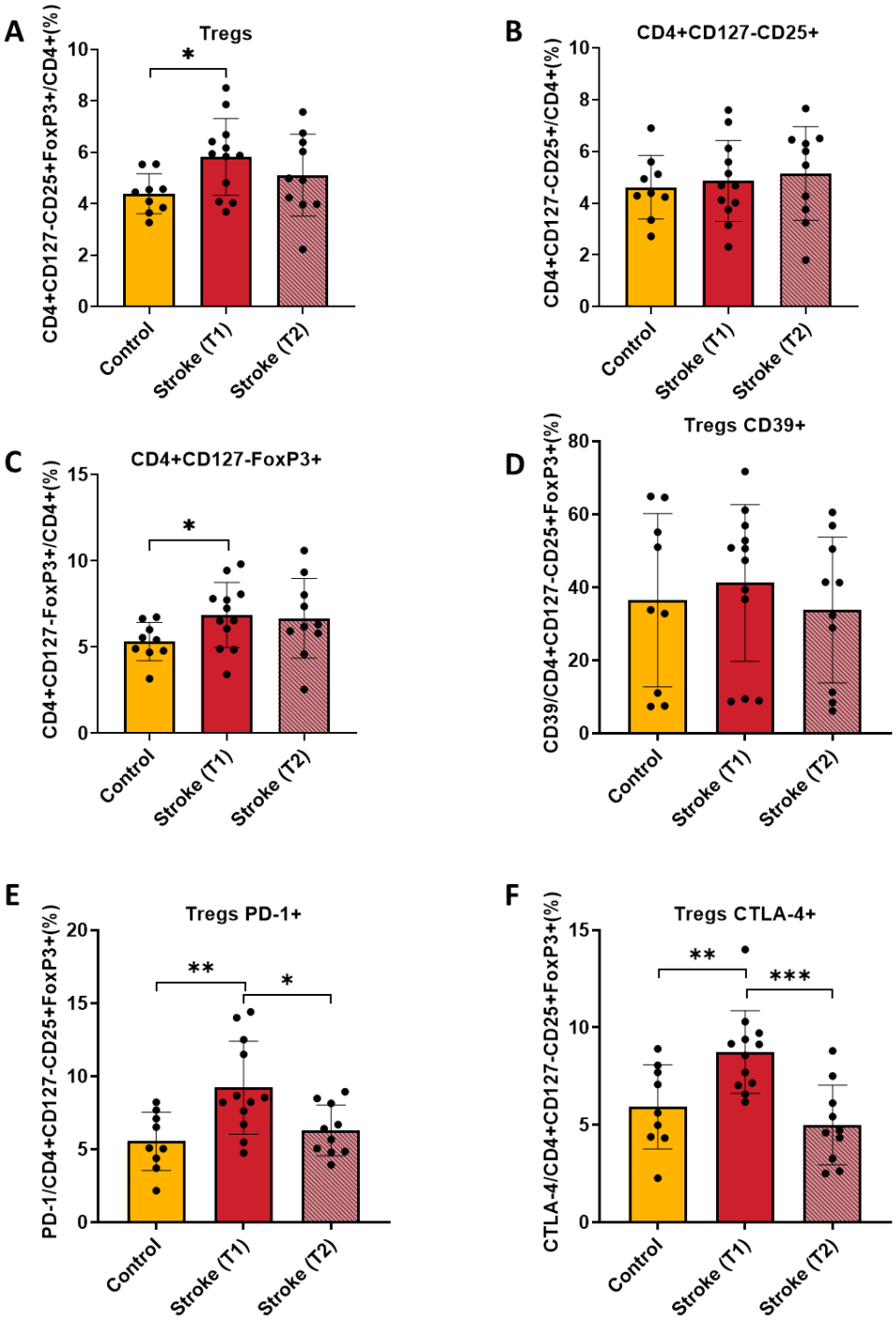


Figure 5.9: Frequencies of circulating Treg populations in stroke patients (n = 12), at 24 hours (T1) and one week (T2) post-brain ischaemia and age-matched controls (n = 9). **A:** The frequency of circulating Tregs (CD4+CD127-CD25+FoxP3+ T cells) compared to control. **B**: Subset analysis of the CD25 and FoxP3 portions of the Treg phenotype (**C, D**). **D:** The frequency of CD39+ Tregs compared to control. **E:** The frequency of PD-1+ Tregs compared to control. **F:** The frequency of CTLA-4+ Tregs compared to control. Two-sided, independent, or paired sample T tests (or non-parametric equivalents) investigated differences between two groups (* = p<0.05, ** = p<0.01, *** = p<0.001).

5.3.7 Stroke increases proliferating Tregs (Ki67+ Tregs) and the frequency of PD-1/CTLA-4+ Ki67+ Tregs at 24 hours post-ischaemia

To date, research investigating changes in Tregs post-stroke has only considered Tregs as a homogenous population. However, previous studies suggest stroke-induced alterations in T cell frequencies likely depends on whether naïve or previously activated (or "memory") T cells are considered (210, 403). Therefore, I next examined whether the impact of stroke on Tregs was specific to different Treg phenotypes, specifically naïve Tregs (nTregs; Treg that are CD45RA+), memory Tregs (mTregs; Treg that are CD45RA-), and proliferating Tregs (Treg that are Ki67+). Furthermore, I explored whether stroke influenced expression of functional markers of Treg suppressive activity (namely CD39, CTLA-4, and PD-1) among each of these Treg subpopulations. No changes in nTregs or mTregs were observed between stroke patients and controls, or between the T1 and T2 timepoints (**Fig. 5.10**). Likewise, neither stroke nor the time since ischaemia onset influenced CD39, CTLA-4 or PD-1 expression among these subpopulations. In contrast, Ki67, a global marker of proliferation, was significantly elevated among Tregs at T1 compared to control (p = 0.0363) **(Fig. 5.10**). This can be noted in t-SNE plots **Fig. S5.**2 by increased red (Ki67) between no stroke and stroke 24-hour samples. These proliferating Treg (Ki67+ Treg) displayed significantly increased levels of PD-1 (p = 0.0088) and CTLA-4 (p = 0.0021) but not CD39 on their surface at T1 compared to Ki67+Tregs from healthy controls. Significant drops in the frequencies of both PD-1+ and CTLA-4+ Ki67+ Tregs were observed between T1 and T2 (p = 0.0371, 0.0139 respectively). This indicates that while stroke may upregulate surface markers on Ki67+ Tregs associated with suppressive function, this effect is transient.

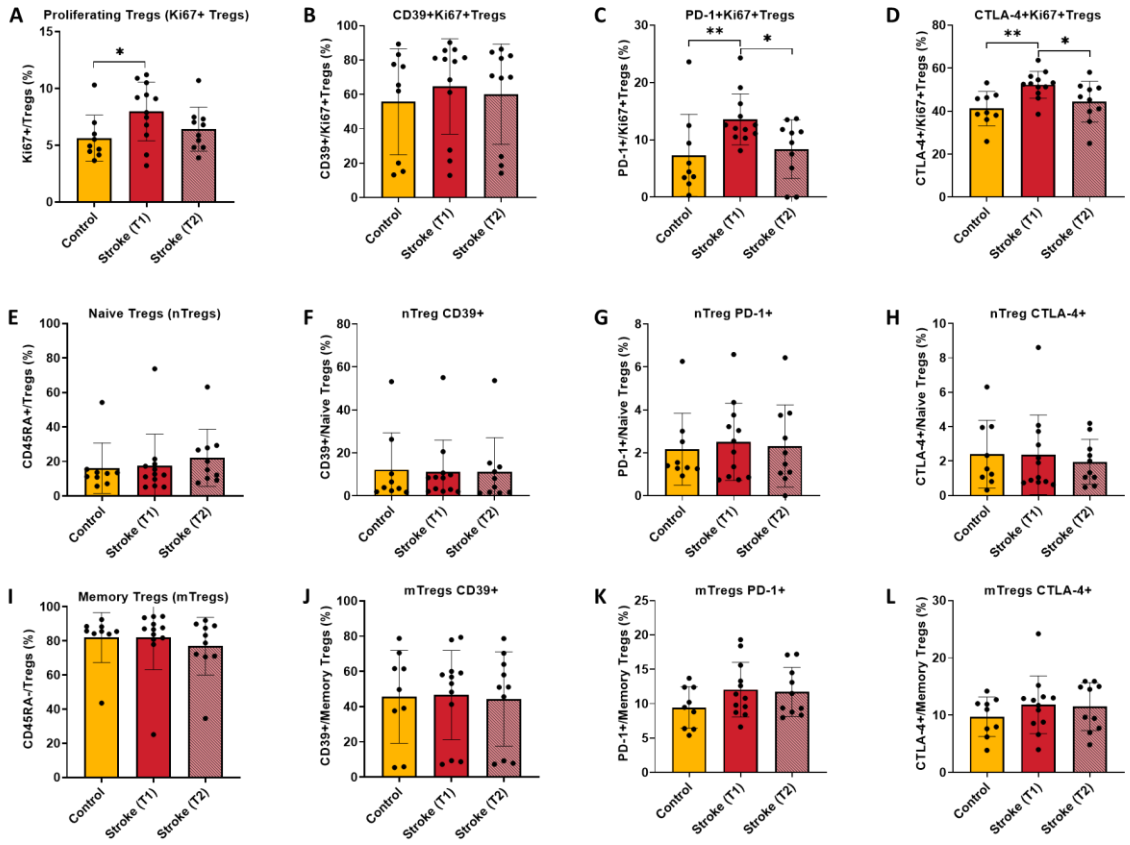


Figure 5.10: Frequencies of proliferating Tregs (Ki67+ Tregs), naive Tregs (nTregs) and memory Tregs (mTregs) within Treg population (CD4+CD127-CD25+FOXP3+) in stroke patients (n = 12) (at 24 hours (T1) and one week (T2) post-brain ischaemia) and age-matched controls (n = 9). Panel **A-D** depicts the frequency of Ki67+ Tregs alongside CD39+, PD-1+, and CTLA-4+ subsets. Panel **E-H** depicts the frequency of nTregs alongside CD39+, PD-1+, and CTLA-4+ subsets. Panel **I-L** depicts the frequency of mTregs alongside CD39+, PD-1+, and CTLA-4+ subsets. Two-sided, independent or paired sample T tests (or non-parametric equivalents) investigated differences between two groups (* = p<0.05, ** = p<0.01, *** = p<0.001)

No correlation was noted between Ki67+ Tregs at 24 hours and admission Rankin score (p = 0.3307).

5.3.8 IL-4 and IL-5 are significantly increased at 7 days post-ischaemia

Pivotal to the contribution of many immune cells to either promoting or ameliorating neuroinflammation post-stroke are secreted cytokines. TNF-α, IFN-γ, IL6, and IL-17 have been largely demonstrated to worsen ischaemic injury, while levels of IL-10, for example, are associated with better outcomes in patients (404).

Twelve cytokines were evaluated in the plasma of stroke and control patients (**Fig. 5.11**). Of these cytokines, IL-2 was below the detection limit for a majority of samples (64.5%). As a result, it was not considered for further statistical analysis. No significant differences in any cytokine were observed between control and T1. A significant increase in IL-4 (p = 0.0137) and IL-5 was noted between T1 and T2 (p = 0.0059). Interestingly, when the results of stroke patients were stratified by Rankin score (as per Supplementary Material**, Fig. S5.3)** a positive correlation was noted between circulating T1 IL-17A/F-α (p = 0.0440) and IL-9 (p = 0.0078) levels and presenting Rankin score (**Fig. S5.4)**. This correlation did not remain at the T2 timepoint, although a correlation between IL-22 (p = 0.0086) and Rankin score was observed.

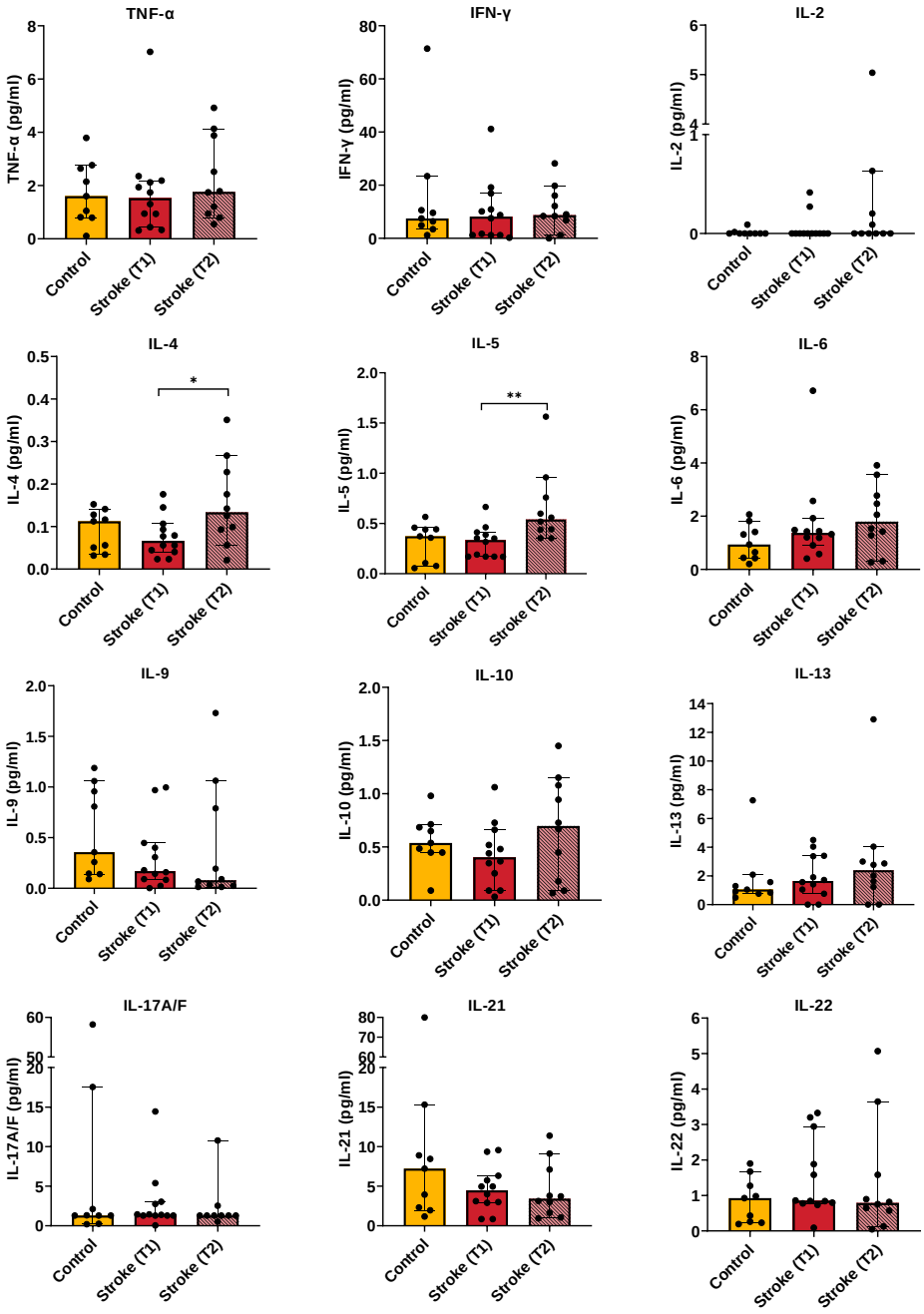


Figure 5.11: Plasma concentrations of 12 cytokines in stroke patients (n = 12) (at 24 hours (T1) and one week (T2) post-brain ischaemia) and age-matched controls (n = 9). Two-sided, independent or paired sample T tests (or non-parametric equivalents) investigated differences between two groups (* = p<0.05, ** = p<0.01, *** = p<0.001).

5.4 Discussion

Stroke yields profound changes in the immune system (320). To date, however, the effect of mild cerebral ischaemia in particular on immune cells remained understudied. Specifically, changes in the frequency of regulatory T cells, which have been shown to participate in acute ischaemic stroke recovery, remain to be fully elucidated (405). This study explored changes in major immune subsets and regulatory T cells in the acute window of mild ischaemic stroke. My results demonstrate that stroke reduces CD3+ T cell, regulatory NK cell, and intermediate monocyte frequency while increasing CD19+ B cell, $CD56^{dim}$ NK cell, and classical monocyte frequency in the blood of stroke patients at 24 hours post-ischaemia compared to age-matched controls. Elevated levels of IL-4 and IL-5 were noted at 7 days post-stroke compared to 24 hours. Levels of IL-9/IL-17 at 24 hours post-ischaemia also correlate with presenting Rankin score. Stroke also increases circulating Treg frequency. Specifically, stroke enhances Ki67+ Tregs, as well as the expression of the functional markers PD-1 and CTLA-4 by these cells. By 7 days post-stroke however, a reduction in circulating CTLA-4+/PD-1+ Ki67+ Tregs occurred. Separately, stroke produced no change in the circulating levels of cytokines associated with T cell function.

I first examined the effect of stroke on general immune cell subsets including T cells, B cells, monocytes, NK cells, and dendritic cells. In line with prior research documenting profound stroke-induced lymphopenia, here stroke acutely decreased circulating T cell frequency, although no further changes in the CD4+ or CD8+ compartments were observed (164, 395, 406, 407). Perhaps as a result of the contraction of the T cell compartment post-stroke, a previously described transient increase in B cell frequency was also noted (155). The lack of any change in NKT

cells, meanwhile, likely demonstrates that the sympathetic, parasympathetic, and hypothalamic pathways involved in post-stroke immunodepression are not overtly activated in mild stroke (408). Consistent with this theory, effector NK cells, another immune cell which play a major role in post-stroke host immune response, were also not downregulated (399). This is in general agreement with several previous studies examining NK cells post-brain ischaemia often reported non-significant decreases (155, 163, 409). A separate study also reported that while percentages of NK cells remained constant, intracellular interferon-γ (IFN-γ) and perforin expression (neither of which were examined here) could be reduced (62). Therefore, even with the lack of changes in host immunity captured in this study, an ability for milder stroke to predispose patients to infectious complications cannot be discounted. Likewise, as NK cells in particular can contribute to neurotoxicity via cytotoxic and cytolytic pathways, the potential for the combination of increased NK (CD56dim) cells alongside reduced regulatory NK cells noted in this study to contribute to poor outcome in mild stroke should be addressed (399). In terms of monocytes, early research by Urra *et al.* suggested no change in the proportion of the most abundant 'classical' CD14+CD16- monocytes after stroke (410, 411). Our result of a substantial increase in this phenotype versus control is therefore in more in line with Keito *et al.* (412) who notably recruited only ischaemic stroke patients, as opposed to the 75-25% ischaemic-haemorrhagic split sampled by Urra *et al.* The rapid expansion of classical monocytes post-stroke likely has major consequences even in mild stroke, as this cell type has been correlated with poor outcome, increased mortality and early clinical worsening (410). Nevertheless, the potential to exploit this population for neuroprotective purposes should not be dismissed, with a recent report in mice suggesting these classical monocytes could promote M2 macrophage polarisation at the infarct site

(413). Separately, our result that intermediate monocytes (CD14++CD16+) are reduced in stroke is in contrast to previous studies (410, 412). However, our study only recruited patients with mild stroke, whereas increased intermediate monocytes appear to characterise patients presenting with larger injuries, where levels acts as a as a marker of disease severity (414). Similarly, the strong reduction in non-classical monocytes noted by other researchers but not evident here is also likely a feature of large infarct stroke, where it correlates with stroke-associated infection. From a therapeutic point of view, our study suggests targeting classical monocytes may provide the greatest benefit in the mild stroke cohort.

Our finding that the onset of AIS increased circulating Tregs does not concur with the results of some early studies involving these cells (67, 155-160), but does align with a number of recent papers (153, 154, 161-164). The difference between these results may be explained by several stroke as well as study factors including disease severity, time of Treg quantification, and the definition of Treg employed. Previous research noted a negative correlation between stroke severity, namely infarct volume, and circulating Tregs, at 48 to 72 hours (154). This finding was echoed in a separate study in which an increased Treg frequency was observed at days 1 and 3 post-stroke in patients with smaller infarcts (such as those sampled here), versus a reduced Treg frequency in patients with larger infarcts (161). Notably, other studies have shown patients with severe stroke had higher circulating Treg frequencies, possibly due to enhanced signalling in pathways associated with stroke-induced immunodepression (SIID) (153, 164). However, if SIID was responsible for increased Treg frequency, then it would not explain why patients who developed stroke-associated infection showed significantly lower circulating Tregs than their non-infected counterparts

(165). Our research (Supplementary Material**, Fig. S5.5**) and others showed no relationship between infarct volume, gender, stroke location or post-stroke infection and Treg frequency. This indicates these are not the primary factors influencing circulating Tregs and could be in fact secondary to disease progression (158, 161). Indeed, whether increases or decreases in Treg frequency were observed in the acute stage of ischaemia (days 1-7), most studies agree that by the subacute (days 7-14) stage of AIS, Tregs have either returned to baseline, or show a slight increase on pre-ischaemic levels (67, 152, 154, 161-165). As Tregs are only expected to infiltrate into the infarcted brain at this point, the subacute stage may in fact present a crucial moment for intervention with Treg-targeted stroke immunotherapies (118).

Future attempts at manipulating Tregs post-brain ischaemia will perhaps rely not only on a pre-determined dosing schedule but also on a specific definition of the Treg phenotype itself. Here, we defined human Tregs as CD4+ CD25+ FoxP3+ CD127- cells, in line with current best practice (91, 415, 416). Interestingly, the only other article which employed this definition also showed an increased circulating Treg frequency post-stroke (162). Of the four studies which used a CD4+ CD127- CD25+ definition, three showed an increase in Treg frequency, with the last showing a slight decrease only at patient admission but not 7 days (152-154, 161). Of the six studies which employed the classic Treg definition used in mice (CD4+ CD25+ FoxP3+ T cells), five showed an acute decrease in Treg frequency (155-159, 164). Likewise, studies which relied only on FoxP3 as an identifier of Tregs among CD4+ T cells also showed acute decreases (67, 165). Potentially, the differences observed in peripheral Tregs post-brain ischaemia may be explained by these differences in Treg definition. Overall, our finding that mild stroke increases CD4+ CD127- CD25+ FoxP3+ T cells

at 24 hours post-stroke broadly agrees with recent studies in the field. Unlike other research, however, here higher Treg frequency did not correlate with better stroke outcome, highlighting either the lesser role these cells play in recovery in mild stroke or the pitfalls of recruiting a patient cohort with a limited range of Rankin scores (152-154).

To date, few clinical studies have examined the effect of ischaemic stroke on Treg function (162, 165). Results of Treg suppression assays show brain ischaemia acutely ameliorates Treg suppressive capacity (162, 165). The frequency of CD39+ Tregs is also strongly reduced (165). We found stroke increased the expression of CTLA-4 and PD-1 on Tregs, and specifically among proliferating (Ki67+) Tregs. Despite the dissimilarity between the reduction in CD39+ Tregs observed by Ruhnau *et al*. and the increase in CTLA-4+ and PD-1+ Tregs observed here, both we and Ruhnau *et al.* have shown that it is the function of activated or proliferating Tregs which is most susceptible to fluctuate post-stroke, as opposed to naïve or memory phenotypes (165). Given the important role PD-1 and CTLA-4 are expected to play in the function of brain-infiltrating Tregs, further work characterising the temporal expression of these markers in the post-stroke patient (encompassing both mild and severe cases) is evidently required (182, 405)

One aspect of Treg functionality which has received greater attention are the levels of anti-inflammatory cytokines. Treg-derived cytokines such as IL-10 and TGF-β have been shown to contribute to Treg-afforded neuroprotection (209, 417). Previous reports have shown ischaemic stroke can strongly decrease levels of these cytokines, while simultaneously increasing IL-17 (67, 157). Here, we showed no impact of brain ischaemia on IL-10 or IL-17 at 24 hours or 7 days. Likewise, no effect of stroke on

other cytokines routinely implicated in stoke damage (e.g., TNF-α, IFN-γ, IL-6) was observed (418-420). This may suggest a less prominent role of T cell-derived cytokines in mild stroke, or that peripheral levels may not accurately reflect the inflammatory milieu at the infarct site. However, two cytokines in which notable increases were noted between 24 hours and 7 days post-ischaemia were IL-4 and IL-5. Increased levels of IL-4 have previously been reported in AIS (421). Interestingly, while a recent genetic deletion study suggests a non-essential role of IL-4 (as well as other Th2-derived cytokines) in the progression of stroke neuropathology (422), separate reports argue IL-4 may mediate a vital neuroprotective function via promoting M2 microglia (423-425). IL-5 may also ameliorate stroke-induced neuroinflammation through reduced microglial iNOS activity (426). However, the argument that Th2-derived cytokines may be protective in mild stroke is complicated by the fact that in this study, increased plasma IL-9 levels at 24 hours correlated with worse functional outcome. The finding that IL-9 predicts worse stroke outcome is itself not novel (124), and may reflect a recently elucidated mechanism in which the cytokine promotes blood-brain permeability via astrocytes (427). However, it does suggest that much like other T cell subsets, Th2 cells may act as potentiators of stroke damage in acute stages through certain cytokines, while still contributing to long-term recovery at later stages (428).

A limitation of this study is that only a small number of patients were recruited. Likewise, both the cell and cytokine profiles could only be examined at two timepoints. Separately, as only patients with mild TIA/stroke were considered eligible, the results of this study may not be generalisable to patients who present with more debilitating symptoms. Interestingly, however, the same selection criteria make this

the first study to comprehensively quantify the Treg response in mild TIA/stroke. A further advantage of this study is that the impact of stroke on Treg functional markers and cytokines associated with Treg was characterised, as opposed to examining changes in Treg frequency alone. Finally, relationships between immune parameters and stroke outcome were assessed, revealing cytokines which potentially may act as early prognostic markers for outcome in mild TIA/ischaemic stroke. However, further studies are required in order to confirm these associations.

5.5 Conclusion

Regulatory T cells have garnered interest as potential therapeutic targets in AIS (151). This study shows that proliferating Tregs increase in the first 24 hours after mild stroke. Functional markers of suppression (CTLA-4, PD-1) on proliferating Tregs are also upregulated. However, despite an acute increase in frequency, no correlation was observed between proliferating Treg frequency and admission Rankin score. This may reflect the lack of changes in anti-inflammatory cytokines such as IL-10, which have been suggested as one of the pivotal mechanisms by which Treg promote neuroprotection (151). The fact that the frequency of CTLA-4+ or PD-1+ Ki67+ Tregs in blood had diminished by 7 days, when Tregs are believed to only begin infiltrating into the infarct site, may also play a role. Future post-stroke Treg-targeted immunotherapies may therefore need to exploit this subacute period. However, further work characterising components of Treg suppressive function in a broader range of stroke subtypes will also likely be required in order to successfully translate candidate drugs from bench to bedside.

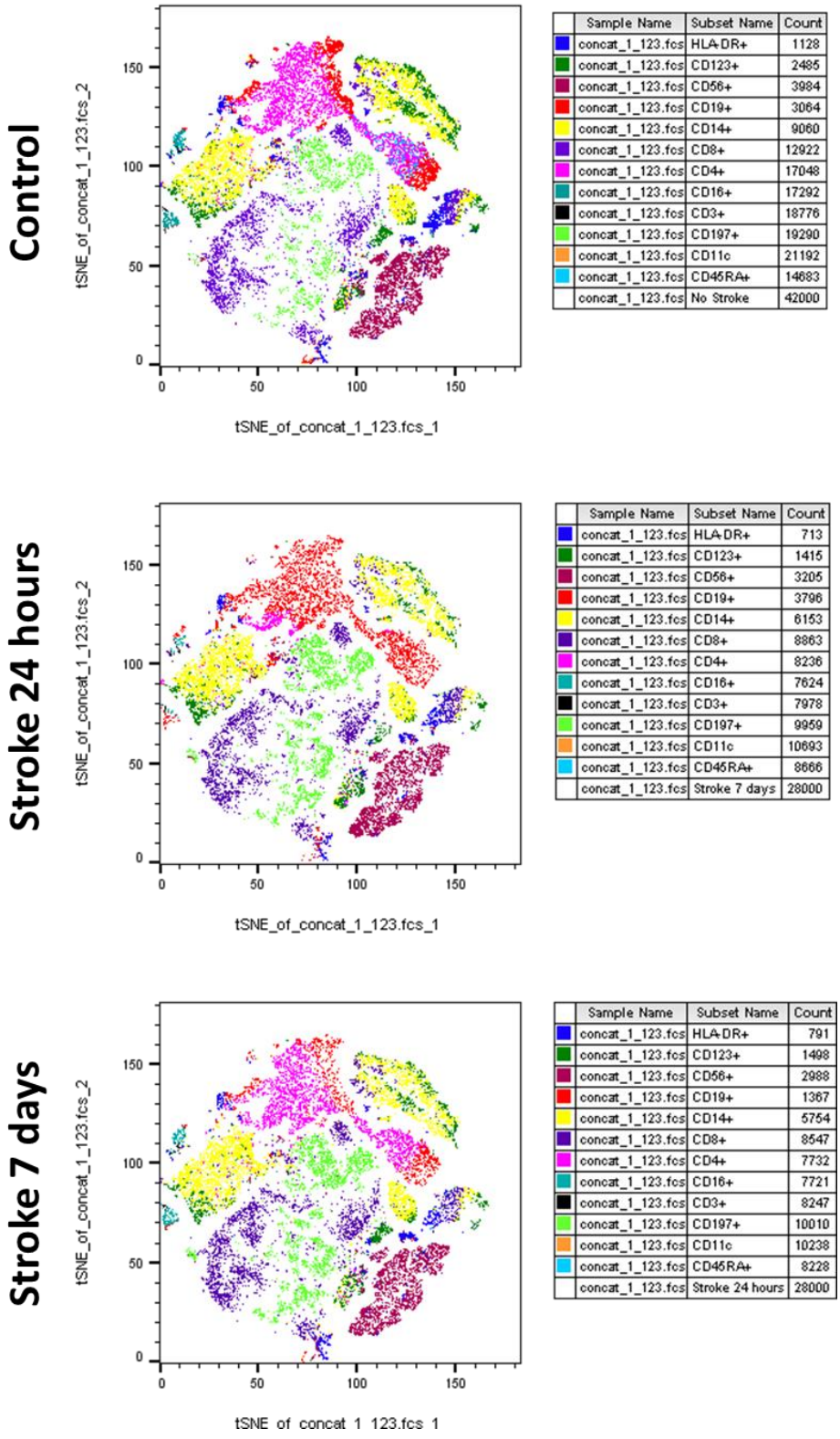


Figure S5.1: t-Distributed stochastic neighbour embedding (t-SNE) plot showing clusters and annotations of PBMCs cells obtained from humans (no stroke, stroke at 24 hours, stroke 7 days). An increase in B cells (red) at the expense of T cells is evident.

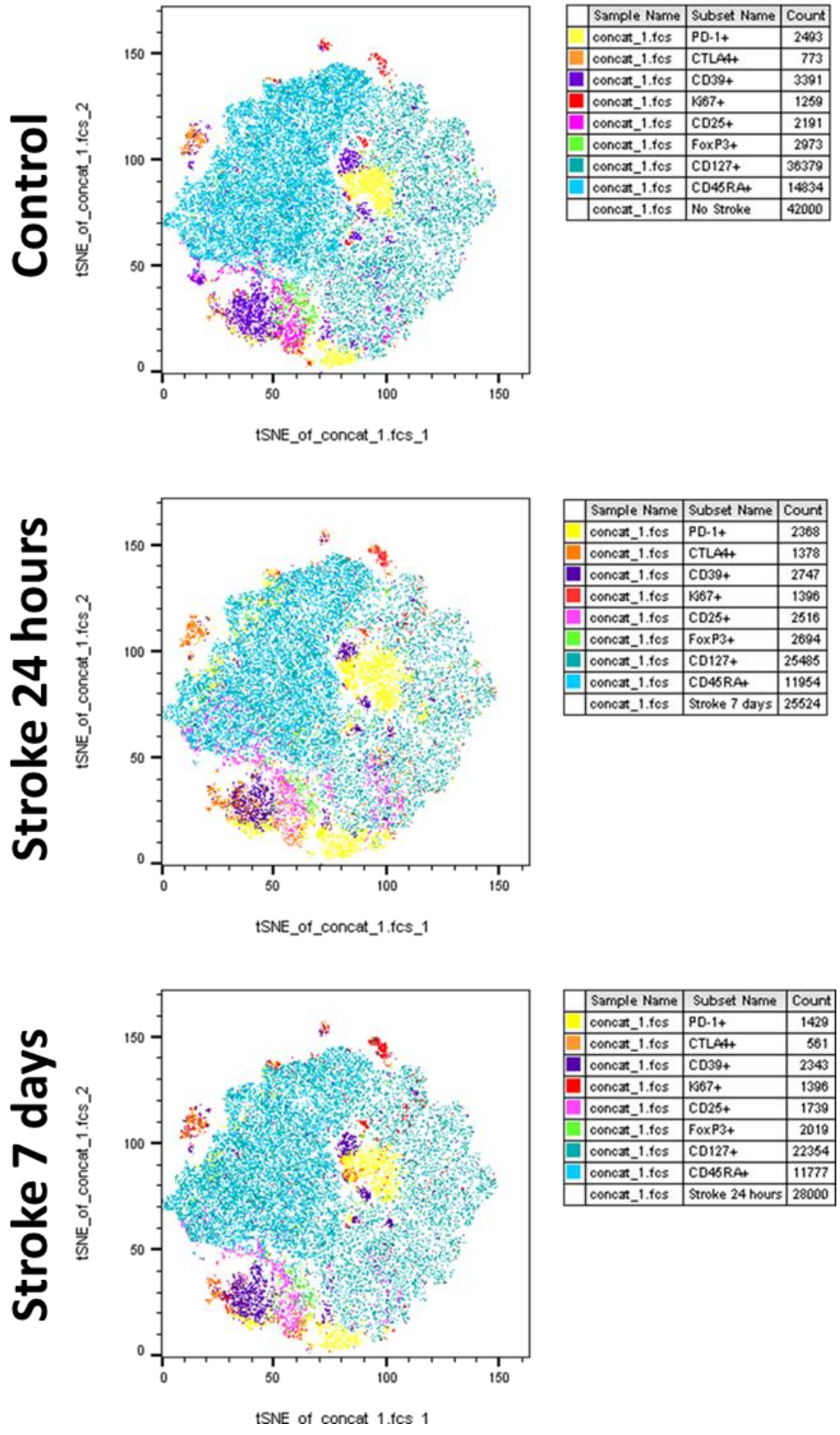


Figure S5.2: t-Distributed stochastic neighbour embedding (t-SNE) plot showing clusters and annotations of PBMCs cells obtained from humans (no stroke, stroke at 24 hours, stroke 7 days).

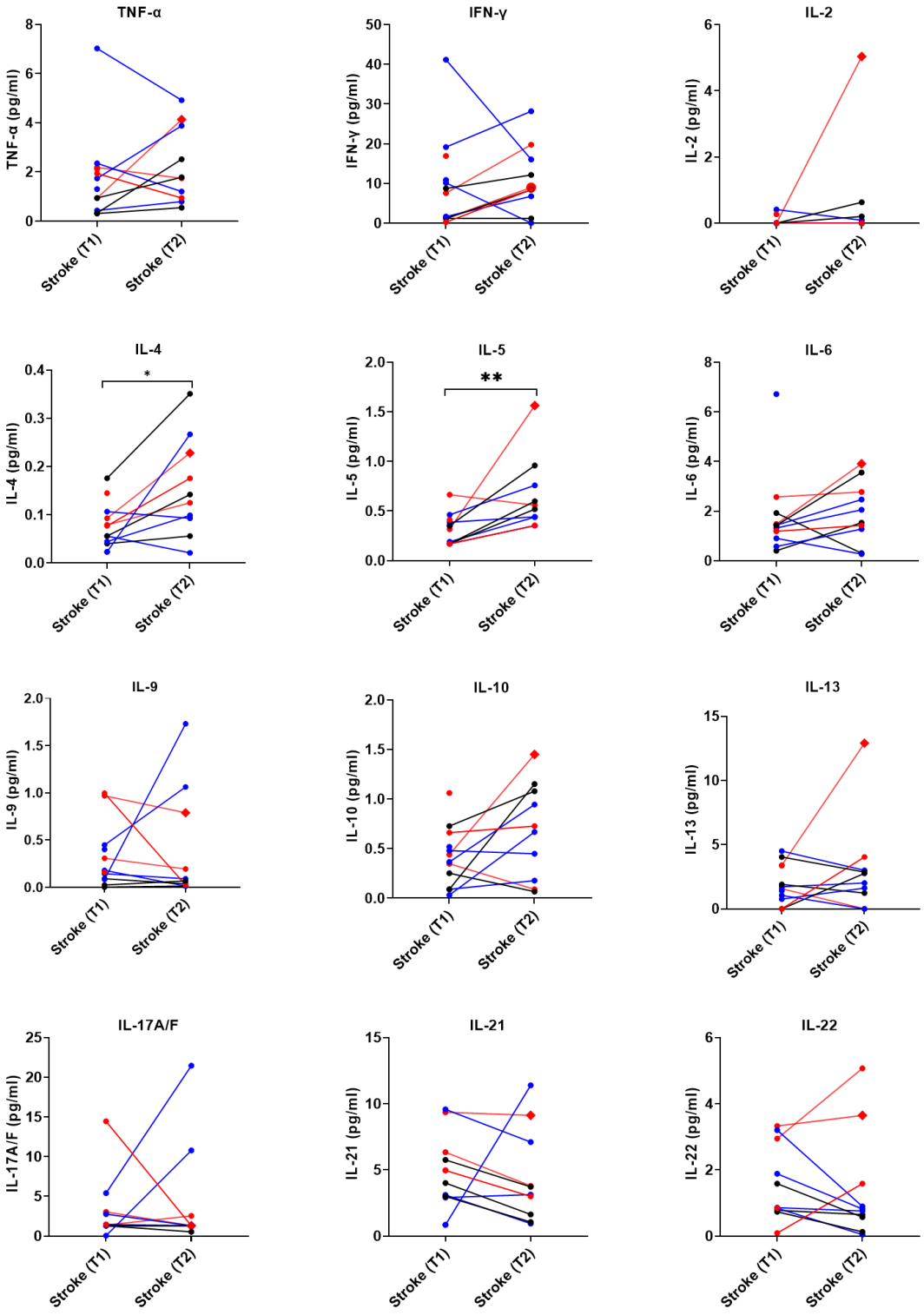


Figure S5.3: Plasma concentrations of 12 cytokines in stroke patients (n = 12) (at 24 hours (T1) and one week (T2) post-brain ischaemia) colour coded by Day 0 Rankin Score (Black = 0, Blue = 1, Red = 2). An increase in circulating IL-5 levels were noted between T1 and T2. Two-sided, independent-samples T tests (or non-parametric equivalents) investigated differences between two groups (* = p<0.05, ** = p<0.01, *** = p<0.001).

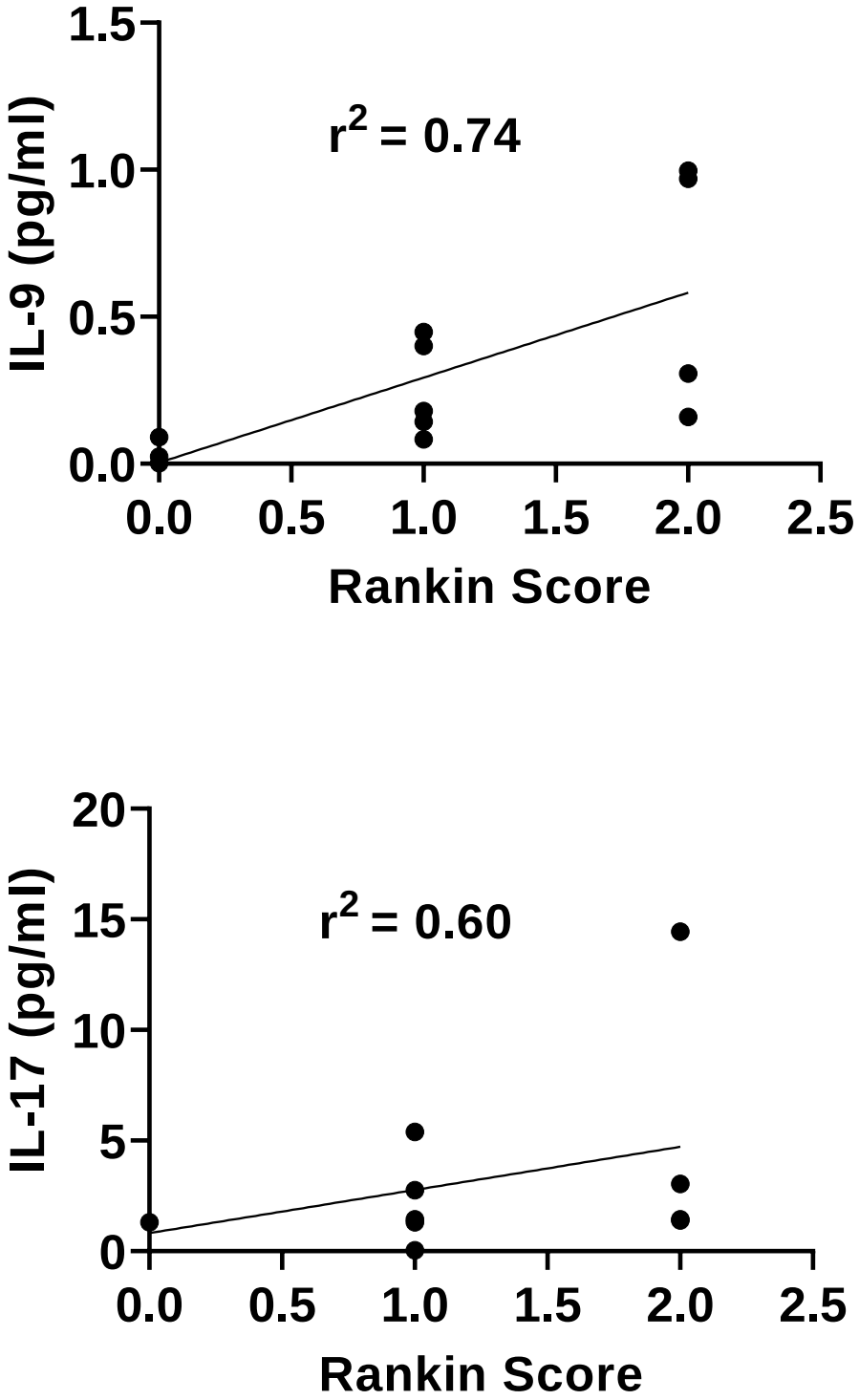


Figure S5.4: Correlation between plasma concentrations of IL-9 and IL-17 in stroke patients at 24 hours post-brain ischaemia with admission modified Rankin Score.

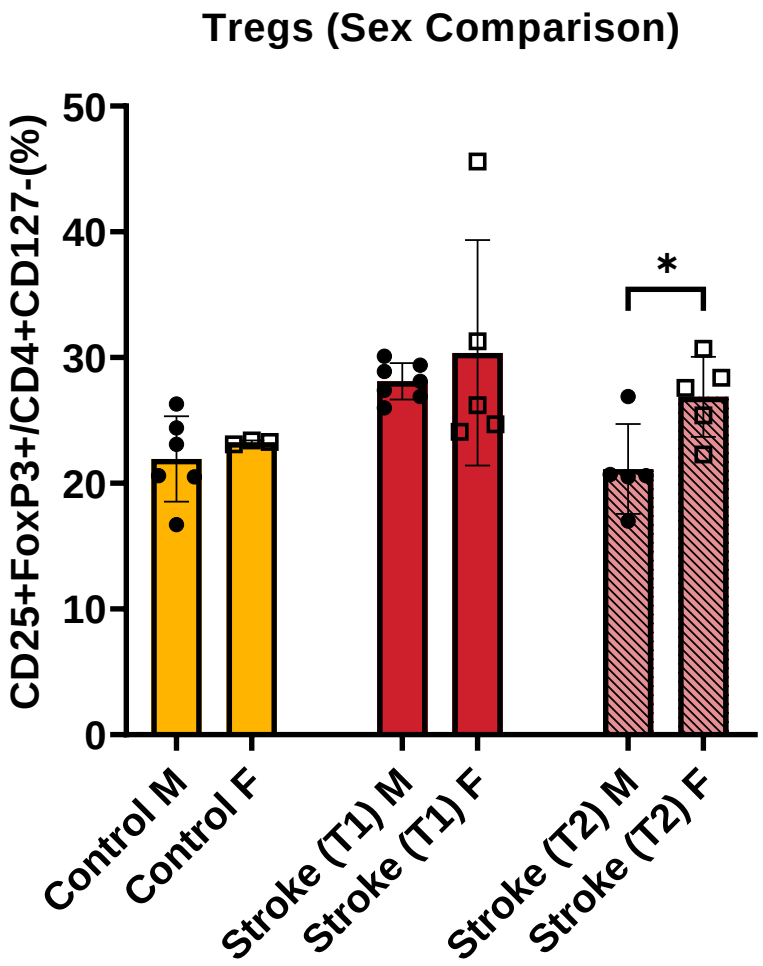


Figure S5.5: Frequencies of Tregs in male (n = 6) vs. female (n = 3) stroke patients at 24 hours (T1) and one week (T2) post-brain ischaemia) and age-matched controls. No differences in Tregs were observed between sexes in control or at 24 hours post-ischaemia. However, slightly greater Treg frequencies were noted in female vs. male patients at 7-days post-ischaemia. Two-sided, independent-samples T tests investigated differences between two groups (* = $p<0.05$, ** = $p<0.01$, *** = $p<0.001$).

Chapter 6

General Discussion

6.1 Overview and summary of key findings

Chapter 1 reviewed the current state of the art. Stroke, the majority of which are ischaemic in nature, is a major source of morbidity and mortality. Despite the global burden of the disease, however, the search for new therapeutic strategies has been confounded by poor clinical translation, and there remains only one FDA-approved medication for treatment. Decades of stroke research, however, has also revealed that the immune system plays a major role in ischaemic stroke pathophysiology (429). In particular, T cells have garnered major interest as therapeutic targets (391). However, while T cells generally contribute to neuroinflammation and ischaemic stroke progression, a subset of CD4+ T cells termed regulatory T cells (or "Tregs") have been hypothesized to provide neuroprotection (118, 151, 367). Initial research in human stroke suggests brain ischaemia may reduce both the number and function of these Tregs in peripheral blood post-stroke (165). Meanwhile, various Treg-targeted immunotherapies enhance functional recovery in pre-clinical stroke models (reviewed in (151)). By combining these two findings, I arrived at the hypothesis that Tregs do in fact play a pivotal neuroprotective role in ischaemic stroke, and that by administering immunomodulatory drugs which enhance Treg frequency and/or function, recovery can be improved. The principal aims of this thesis were therefore to explore the overall role of regulatory T cells in ischaemic stroke recovery, while also quantifying the neuroprotective and immunomodulatory effects of potential Treg-targeted stroke immunotherapies.

In **Chapter 2,** (**Objective 1**) I examined whether the promising candidate stroke immunotherapy fingolimod, which has previously displayed Treg-expanding properties in disease states such as MS and colitis, affected regulatory T cells in a mouse model of pMCAO (330). As well as increasing Treg frequency in the blood and

spleens of young, aged, and ApoE$^{-/-}$ mice post-pMCAO, fingolimod also significantly enhanced the number of FoxP3+ cells in the infarct core. By extending the treatment duration to ten days of once daily dosing, the number of brain-infiltrating FoxP3+ cells was further increased. Despite these pro-Treg effects, however, pooled analysis from young, aged, and ApoE-/- mice showed a negative correlation between circulating Tregs and functional recovery in fingolimod-treated mice (289).

This last finding was further developed in **Chapter 3,** where I investigated whether fingolimod-mediated increases in Tregs explain neuroprotective activity and what impact, if any, fingolimod had on Treg suppressive function (**Objectives 2**). Here, alongside increasing Treg frequency, we observed fingolimod did improve neurobehavioural recovery compared to saline control. As Treg cells from fingolimod-treated animals had higher expression of CCR8, it is conceivable this may be the principal chemokine receptor influencing Treg trafficking to the infarct site. The fact that brain ischaemia reduced Treg suppressive function, and fingolimod treatment rescued this function against saline-treated CD4+ effector T cells also supports the involvement of Tregs. However, fingolimod also enhanced IFN-γ and IL-17. Furthermore, fingolimod-treated Tregs did not show enhanced suppression against fingolimod-treated CD4+ effector T cells.

Following on from this, in **Chapter 4,** I investigated whether a biologic immunomodulator (rPSG1-Fc) with demonstrated Treg effects enhanced functional recovery (**Objective 3**). Interestingly, rPSG1-Fc significantly enhanced performance in the grid-walking test at 3- and 5-days post-ischaemia, although no effect on infarct size was observed. Among CD4+ T cells, rPSG1-Fc enhanced the expression of IL-10 in several tissues, while also downregulating IFN-γ and IL-17. A significant

increase in circulating CD4+ FoxP3+ T cells and brain-infiltrating FoxP3+ cells was also noted in rPSG1-Fc-treated mice. However, no changes in peripheral Tregs were observed post-rPSG1-Fc treatment.

Finally, in line with **Objective 4**, in **Chapter 5** I quantified the impact of mild ischaemic stroke on Treg frequency and function in patients. Here, stroke increased circulating Treg frequency compared to control. In particular, Ki67+ proliferating Tregs were elevated at 24 hours post-ischaemia. Enhanced expression of both PD-1 and CTLA-4 among Ki67+ Tregs was also observed. However, by 7 days post-ischaemia, the frequency of Ki67+ Treg CTLA4+/PD-1+ had once more reduced to back in line with pre-stroke baselines.

6.2 Interpretation of key findings

6.2.1 Mild stroke acutely increases Treg frequency and function, but these cells do not play a major role in the early stages of recovery

In addressing my first aim (to explore the overall role of regulatory T cells in ischaemic stroke recovery), I hypothesised that a) stroke acutely increases Treg frequency and/or function and b) these Tregs then play a central role in post-stroke recovery.

Evidence from this thesis suggests that the first hypothesis is partially true: mild stroke does increase Treg frequency and suppressive function. This change, however, is transient, and frequency/function falls back to (or below) baseline by the subacute stages (day 7+) (as per published literature (67, 152, 154, 161-165)). In support of this finding, I saw in **Chapter 5** that mild stroke increased Treg frequency, and markers of Treg suppression (CTLA-4, PD-1) among Ki67+ proliferating Tregs at 24 hours post-ischaemia in stroke patients. The frequency of CTLA4+/PD-1+ Ki67+ Tregs, however, returned to baseline by 7 days. At this timepoint, no rise in Treg-derived

cytokines such as IL-10 was noted. In post-pMCAO mice, ischaemia alone did not produce major changes in peripheral Tregs (blood, spleen, lymph nodes) at 7 days in either young or aged cohorts. No evidence of increased CD4+ IL-10+ T cells was likewise observed (**Chapters 3, 4**). In fact, I demonstrated Treg suppressive capacity is reduced in saline-treated post-ischaemic mice compared to naïve controls at 10 days post-ischaemia (**Chapter 3**). This finding aligns with prior research demonstrating a loss of functionally active (e.g., CD39+) Tregs post-stroke (165). Therefore, stroke might increase Treg frequency and suppressive capacity in humans at 24 hours post-ischaemia, but in both humans and mice, no enhanced Treg function was noted at 7 days. A major implication of this finding is that the subacute period (7 days), rather than the acute phase, may in fact be the best moment to intervene with Treg-targeted immunotherapies.

The repercussions of Treg frequency and/or function only transiently increasing post-stroke likely explains why our second hypothesis (that Tregs play a central role in post-stroke recovery) is false, at least at it relates to the early stages (<7 days). Treg frequency at 7-days post-ischaemia showed no strong correlations with 3-day recovery in either saline or fingolimod-treated mice (**Chapter 2**) or with functional recovery (lower modified Rankin score) in stroke patients (**Chapter 5**). We observed rPSG1-Fc significantly improved stroke outcome without strongly influencing Treg frequency. All of this evidence suggests that the frequency of Tregs do not play a large role in ischaemic stroke recovery. Notably, research highlighting a predictive relationship between Tregs and outcomes in acute ischaemic stroke usually involves patients with more disabling stroke as well as mild cases (152). It is possible Tregs are more centrally involved in recovery in large infarct strokes, while contributing minimally to the resolution of inflammation and improved outcome in milder cases.

However, in **Chapter 2,** Tregs did positively correlate with 7-day recovery in saline-treated mice. It is also possible that while not contributing majorly to either infarct growth or neuroprotection in the acute stages of ischaemia (<7 days), Tregs may infiltrate into the brain after 7 days and thereafter play a more pronounced role in chronic recovery. Indeed, the extremely low number of Tregs in the infarcted brain in the acute stages (days 1-7), coupled with the time required for antigen-specific activation and proliferation of Tregs to occur, suggests any benefit conferred by Tregs in the first few days after stroke likely represent bystander effects, such as paracrine effects of IL-10 (430). In the subacute (day 7-14) and chronic phases (day 14+), on the other hand, greater attention may now be due to mechanisms including Treg-microglia crosstalk (178) or Treg-mediated reductions in astrogliosis (116). Overall, researchers involved in developing Treg-targeted immunotherapies may need to consider where in the post-stroke window treatment should be administered. The use of a neurological impairment threshold above which a Treg-targeted immunotherapy may offer benefit may also need to be considered.

6.2.2 Fingolimod and rPSG1-Fc impact Tregs and this mechanism may contribute to improvements in functional recovery

In addressing my second aim (i.e., characterising the neuroprotective and immunomodulatory effects of potential Treg-targeted stroke immunotherapies), I hypothesised that both fingolimod and rPSG1-Fc would increase Treg frequency and/or function post-brain ischaemia. Several strands of evidence show this hypothesis was true.

In **Chapters 2** and **3**, fingolimod increased peripheral Treg frequency, the brain-infiltration of FoxP3+ cells, and the frequency of CCR8+ Tregs. Fingolimod also

enhanced the frequency of CD4+ IL-10+ T cells and the suppressive capacity of Tregs. In **Chapter 4**, rPSG1-Fc increased CD4+ FoxP3+ T cell counts in blood, enhanced the infiltration of FoxP3+ cells into brain, upregulated the secretion of IL-10 by CD4+ T cells, and reduced the secretion of IFN-γ and IL-17 among CD4+ T cells. Interestingly, in **Chapters 3** and **4,** improvements in functional recovery were also observed in both fingolimod and rPSG1-Fc-treated mice respectively. Admittedly, the studies in this thesis did not directly test the involvement of Tregs in either fingolimod or rPSG1-Fc-afforded neuroprotection, for example through Treg depletion studies. While the above evidence suggests there may be some relationship between the beneficial effects observed with these stroke immunotherapies and Treg, one finding against this theory is that rPSG1-Fc did not significantly affect peripheral Treg frequencies. In fact, the most consistent effects of rPSG1-Fc were on the secretion of IL-10 by peripheral CD4+ T cells. As fingolimod also enhanced IL-10 secretion among CD4+ T cells in spleen and blood, an IL-10-based mechanism is more likely to represent the true means by which fingolimod and rPSG1-Fc improve stroke recovery. Notably, however, rPSG1-Fc increased IL-10 secretion among CD4+ T cells in both systemic and lymph node compartments, while fingolimod only increased CD4+ IL-10+ T cells in blood and spleen. Given the cervical lymph nodes in particular have been proposed as a route for immune cell infiltration via meningeal vessels (53, 431), the fact rPSG1-Fc produces a tolerizing signal at the site may explain why more pronounced improvements in functional recovery appear to be noted in rPSG1-Fc-treated mice. It also identifies immune cells of the draining lymph nodes as important targets for future stroke immunotherapies.

Overall, therefore, the stroke immunotherapies fingolimod and rPSG1-Fc do impact Tregs in terms of both frequency and function. However, it is not clear if this mechanism definitively contributes to functional recovery in experimental stroke.

6.2.3 The inconsistent neuroprotection observed with fingolimod in experimental stroke may stem from a promotion of both pro and anti-inflammatory T cell phenotypes

The observation that both fingolimod and rSPG1-Fc increased Treg frequency and/or function combined with the known beneficial effects of this population in brain ischaemia suggest both would improve post-stroke functional recovery. However, while rPSG1-Fc strongly ameliorated neurological dysfunction in mice post-pMCAO, the evidence surrounding fingolimod is conflicting (289).

To date, the immunomodulator fingolimod has proven effective in various rodent models of stroke, including both transient and permanent focal ischaemia. A meta-analysis of fingolimod in experimental ischaemic stroke revealed the drug reduces infarct volume and neurobehavioural outcomes (265). Yet in our pMCAO model, we noted no marked improvements in functional or histological outcome in young, aged, or ApoE$^{-/--}$ mice (**Chapter 2** (289)). Indeed, only when we administered 0.5mg/kg fingolimod once daily for ten days did a modest improvement in performance in the cylinder test occur. As noted in **Chapter** 3, it is possible a fine balance exists in the pro-inflammatory and anti-inflammatory effects of fingolimod, and that this same balance explains the internal contradiction observed between results in **Chapters 2** and **3**. Returning to potential mechanisms, however, I noted that post-fingolimod treatment, Treg frequency was actually negatively correlated with 7-day recovery. This led to the hypothesis that while fingolimod does increase Treg frequency, it must also promote pro-inflammatory T cell phenotypes. I demonstrated this in **Chapter 3;**

fingolimod enhanced the secretion of IFN-γ and IL-17 as well as IL-10 from CD4+ T cells. Likewise, while Tregs isolated from fingolimod-treated mice showed greater suppressive capacity than Tregs isolated from saline-treated controls, fingolimod also increased the resistance of CD4+ effector cells to this suppression.

Overall, the capacity of fingolimod to increase both effector/conventional and regulatory functions may explain the inconsistent neuroprotection observed with fingolimod in recent pMCAO studies (including those described in **Chapter 2, 3**). This has crucial implications for researchers aiming to use fingolimod as an immunotherapy in clinical stroke (267-269). The fact fingolimod transiently enhances IL-17/IFN-γ (281, 344) would likely nullify any favourable effect of the drug on stroke outcome in large trials. However, were the immunological profiles of fingolimod-treated stroke subjects to follow a similar trend as that seen in MS (decreased IFN-γ+/IL17+CD4+, upregulated CD4+ IL-10+ T cells (346, 348), a beneficial effect on chronic recovery could theoretically emerge. Therefore, the use of extended treatment regimens which maximize pro-Treg effects while minimizing pro-effector effects is worth further consideration.

6.3 Strengths and Limitations

There are limitations to this research. In **Chapters 2-4**, for example, which involved evaluation of candidate stroke immunotherapies in mice, only a single model of brain ischaemia (pMCAO) was employed. As noted in the introduction chapter, this model likely best mimics the pathology of human stroke and is recommended as the core model for pre-clinical testing (432). However, it also means that this research has only quantified Treg frequency and/or function in one post-stroke immune landscape. The results are therefore not generalisable to transient models of the disease, where

substantially lower numbers of lymphocytes infiltrate into the brain in early stages of the disease (119, 433). As our model of pMCAO involved a distal vessel occlusion, results may likewise not be strictly comparable to proximal pMCAO studies in which infarct sizes are larger (434).

Similarly, research in **Chapters 2-4** predominantly examined Tregs in blood/brain/peripheral lymphoid tissue at only a single timepoint. Pilot studies and the wider literature informed the choice of timepoint, with the subacute period (7 or 10 days) frequently selected due to the expectation Tregs would have infiltrated into the infarct site in detectable numbers by this point (118). Nevertheless, it should be recognised that the impact of brain ischaemia or indeed stroke immunotherapies on Tregs may look quite different in the acute or chronic post-stroke periods.

Furthermore, the use of a different dose or treatment duration of either fingolimod or rPSG1-Fc may have also produced varying effects on resulting Treg levels (or indeed functional recovery). Again, the doses and treatment windows selected for this research were derived from pre-existing literature. In the case of fingolimod, a wealth of published pre-clinical stroke studies supported the use of 0.5 or 1 mg/kg (265). On the other hand, as ours is the first study to determine the effect of rPSG1-Fc on stroke recovery, the 100µg dose was derived from previous work with PSG1 in colitis and acute graft-versus-host disease (371).

As noted in **Chapter 1**, this thesis also investigated Tregs largely under the premise that these cells are CD4+ CD25+ FoxP3+ (especially in mice). However, while this definition allows us to compare our findings to other researchers in the stroke immunology field, this definition may include activated T cells (CD4+ CD25+) (435).

It is possible results in **Chapters 2-4** may have differed had a stricter definition of Treg (e.g., CD4+ $CD25^{hi}$ FoxP3+ CD127-) been employed.

Finally, it should be noted that the majority of the research in **Chapters 2-4** employed male mice only. While this does make these studies comparable to the wider literature (where male mice predominate) (436), it means results such as a beneficial effect of rPSG1-Fc on ischaemic stroke recovery must be interpreted with caution. Minocycline, one of the most compelling candidate stroke immunotherapies ever tested, has been shown to be ineffective at reducing ischemic damage in females, with a beneficial effect in male mice alone (437). Despite this, sex as a variable remains critically underassessed in stroke studies (438). Given female mice display differences in the immune response to stroke (439), particularly among T cells (440), it is clear future research involving stroke immunotherapies should be designed and powered to detect potential differences in efficacy between sexes (441).

This thesis has several strengths. First was my commitment to the principles set out in the STAIR guidelines (266). All studies detailed in **Chapters 2-4** employed a) rigorous sample size calculations, b) detailed pre-defined inclusion and exclusion criteria, c) randomisation, d) blinding, e) allocation concealment, and f) reported details of animals excluded from further analysis. **Chapter 2** in particular also considered the role of different doses/treatment durations as related to fingolimod.

Until now, research focused on Tregs post-stroke often examined these cells in either animal models of the disease or in the clinic. This thesis represents one of the first attempts to synthesise data from both a mouse model of brain ischaemia and stroke patients to comprehensively determine the role of Tregs in stroke recovery. The fact

that the mild stroke patients recruited as part of the clinical study mimicked the mild cortical injury employed in the animal studies further helped this purpose.

Finally, this thesis, and in particular **Chapter 2**, also involved the use of animals with stroke-related co-morbidities such as age and hypercholesteremia. The use of such animals has been low (~12% of total animals employed in pre-clinical studies) (442). However, given that a relative reduction in treatment efficacy of 20% is observed compared with non-comorbid models (442), the use of young, healthy mice may actually explain the gap between pre-clinical testing and clinical translation (443). Factors such as age are also known to profoundly alter the immune response to stroke, further endorsing our decision to include such mice in our study (444, 445).

6.4 Implications for Future Research

This thesis provides novel insights on the role of regulatory T cells in acute ischaemic stroke recovery. However, while adding to our understanding of fingolimod, pregnancy-specific glycoprotein, and the immunological impacts of both post-brain ischaemia, it raises research questions that are worthy of further consideration.

- Despite the low number of patients recruited, the study detailed in **Chapter 5** still represents of one the most comprehensive attempts to characterise both the frequency and function of circulating Tregs post-stroke. However, larger clinical studies with longer follow-up (6 months+) are required. Such studies should stratify patients by stroke severity, infection status, demographic factors, and co-morbidities. Such studies should also employ rigorous definitions of Treg. If large, multi-centre studies can be performed, data generated from immunophenotyping (e.g., flow cytometry, mass cytometry), transcriptomic (microarray, RNA-Seq), and plasma cytokine (ELISA,

multiplex) experiments should be integrated. Finally, the purification of Tregs from patient PBMCs for cell culture should be performed to generate sufficient numbers of cells for detailed suppression assays.

- To date, Treg-targeted stroke immunotherapies, e.g., adoptive cell transfer, CD28SA, IL-2/IL-2 antibody complex, have largely focused on finding means by which to rapidly expand the pool of circulating Tregs post-brain ischaemia (151). However, evidence from this thesis suggests that a drug-mediated increase in Tregs may not always translate to functional improvement (fingolimod, **Chapter 2**), while a beneficial effect may be observed even in the absence of a direct impact on Treg frequency (rPSG1-Fc, **Chapter 4**). Evidence from this thesis suggests it is when stroke immunotherapies influence CD4+ production of IL-10 that consistent improvements in recovery are observed (**Chapter 3, 4**). This suggests that Treg-targeted treatments which promote the "quality" as opposed to the "quantity" of Tregs may provide greater clinical utility. Greater attention should therefore be paid to known Treg-targeted stroke immunotherapies which upregulate Treg function.
- While this thesis does provide data on the effect of stroke on Tregs in both male and female subjects (**Chapter 2/5**), as well as in subjects with stroke co-morbidities (**Chapter 2**), it follows the trend of published stroke literature by largely focusing on young, male subjects (446). It is imperative that future basic research works toward improving our understanding of how stroke impacts Tregs in female (447) and co-morbid subjects (e.g., diabetes (323). Future work with Treg-targeted stroke immunotherapies should also include both male and female subjects, consider possible sex differences in analysis, and report these differences (448).

- The use of fingolimod in both pre-clinical and clinical stroke has to date mostly involved once daily dosing during days 1-7 after the onset of brain ischaemia (265). In fact, our use of a ten-day once daily course of fingolimod 0.5mg/kg in **Chapters 3, 4** may represent one of the more prolonged treatment durations examined to date. However, data from this thesis suggests it is this extended treatment duration which results in greater infiltration of FoxP3+ cells into the infarct site. Based on the pharmacology of fingolimod (325), research in MS patients (281), and the dynamics of T cells in stroke (391), it is expected the pro-inflammatory effects of fingolimod noted in **Chapter 4** may also subside with chronic treatment. Therefore, future studies should consider delaying the start of fingolimod therapy in stroke patients until the subacute stages of stroke (after day 7). Alternatively, the use of a chronic regimen to maximize the beneficial Treg-mediated effects of the drug could be considered.
- Work in **Chapter 4** revealed rPSG1-Fc to be a promising stroke immunotherapy. However, to date, only a single dose and treatment duration of rPSG1-Fc in stroke have been tested. Further experimental stroke studies are required to ascertain the kinetics and mechanism of action of rPSG1-Fc in the post-stroke mouse. Studies employing IL-$10^{-/-}$ mice are also required to confirm whether or not this cytokine is the key mediator of rPSG1-Fc-afforded neuroprotection.

6.5 Conclusion

Acute ischaemic stroke remains a major cause of worldwide mortality (2). Previous research suggests regulatory T cells may be one of the most promising avenues for future stroke immunotherapy. The aim of this thesis was to determine the role of

regulatory T cells in ischaemic stroke recovery. This was achieved by exploring the changes in these cells post-brain ischaemia and investigating if, by manipulating either Treg frequency or function with stroke immunotherapies, improvements in functional recovery could be made. A number of novel insights were made. In particular, contributions were made in to the following three areas:

1. The effects of fingolimod on Tregs post-ischaemic stroke.
2. The immunomodulatory and neuroprotective effects of rPSG1-Fc post-stroke.
3. The changes in Treg frequency and function in clinical stroke.

This thesis provides a basis for further study on Tregs in ischaemic stroke. It should be used as a guide for researchers exploring the changes in Tregs or other regulatory populations post-stroke. It also illustrates rigorous methods by which researchers could test future Treg-targeted stroke immunotherapies.

Bibliography:

1. Benjamin EJ, Blaha MJ, Chiuve SE, Cushman M, Das SR, Deo R, et al. Heart Disease and Stroke Statistics-2017 Update: A Report From the American Heart Association. Circulation. 2017;135(10):e146-e603.

2. Katan M, Luft A. Global Burden of Stroke. Semin Neurol. 2018;38(2):208-11.

3. Feigin VL, Brainin M, Norrving B, Martins S, Sacco RL, Hacke W, et al. World Stroke Organization (WSO): Global Stroke Fact Sheet 2022. Int J Stroke. 2022;17(1):18-29.

4. Krishnamurthi RV, Feigin VL, Forouzanfar MH, Mensah GA, Connor M, Bennett DA, et al. Global and regional burden of first-ever ischaemic and haemorrhagic stroke during 1990-2010: findings from the Global Burden of Disease Study 2010. Lancet Glob Health. 2013;1(5):e259-81.

5. Powers WJ, Derdeyn CP, Biller J, Coffey CS, Hoh BL, Jauch EC, et al. 2015 American Heart Association/American Stroke Association Focused Update of the 2013 Guidelines for the Early Management of Patients With Acute Ischemic Stroke Regarding Endovascular Treatment: A Guideline for Healthcare Professionals From the American Heart Association/American Stroke Association. Stroke. 2015;46(10):3020-35.

6. Fischer U, Baumgartner A, Arnold M, Nedeltchev K, Gralla J, De Marchis GM, et al. What is a minor stroke? Stroke. 2010;41(4):661-6.

7. Khatri P, Conaway MR, Johnston KC, Investigators ASAPSA. Ninety-day outcome rates of a prospective cohort of consecutive patients with mild ischemic stroke. Stroke. 2012;43(2):560-2.

8. Mozaffarian D, Benjamin EJ, Go AS, Arnett DK, Blaha MJ, Cushman M, et al. Heart disease and stroke statistics--2015 update: a report from the American Heart Association. Circulation. 2015;131(4):e29-322.

9. Smith S HF, Sexton E, Wiley M, et al. Cost of Stroke in Ireland: Estimating the annual economic cost of stroke and transient ischaemic attack (TIA) in Ireland. In: Foundation IH, editor. 2010.

10. Luengo-Fernandez R, Violato M, Candio P, Leal J. Economic burden of stroke across Europe: A population-based cost analysis. Eur Stroke J. 2020;5(1):17-25.

11. Feigin VL, Nguyen G, Cercy K, Johnson CO, Alam T, Parmar PG, et al. Global, Regional, and Country-Specific Lifetime Risks of Stroke, 1990 and 2016. N Engl J Med. 2018;379(25):2429-37.

12. Ekker MS, Verhoeven JI, Vaartjes I, van Nieuwenhuizen KM, Klijn CJM, de Leeuw FE. Stroke incidence in young adults according to age, subtype, sex, and time trends. Neurology. 2019;92(21):e2444-e54.

13. Boehme AK, Esenwa C, Elkind MS. Stroke Risk Factors, Genetics, and Prevention. Circ Res. 2017;120(3):472-95.

14. Allen CL, Bayraktutan U. Risk factors for ischaemic stroke. Int J Stroke. 2008;3(2):105-16.

15. Goldstein LB, Bushnell CD, Adams RJ, Appel LJ, Braun LT, Chaturvedi S, et al. Guidelines for the primary prevention of stroke: a guideline for healthcare professionals from the American Heart Association/American Stroke Association. Stroke. 2011;42(2):517-84.

16. Soto-Cámara R, González-Bernal JJ, González-Santos J, Aguilar-Parra JM, Trigueros R, López-Liria R. Knowledge on Signs and Risk Factors in Stroke Patients. J Clin Med. 2020;9(8).

17. Chohan SA, Venkatesh PK, How CH. Long-term complications of stroke and secondary prevention: an overview for primary care physicians. Singapore Med J. 2019;60(12):616-20.

18. Albers GW, Bates VE, Clark WM, Bell R, Verro P, Hamilton SA. Intravenous tissue-type plasminogen activator for treatment of acute stroke: the Standard Treatment with Alteplase to Reverse Stroke (STARS) study. JAMA. 2000;283(9):1145-50.

19. Lees KR, Bluhmki E, von Kummer R, Brott TG, Toni D, Grotta JC, et al. Time to treatment with intravenous alteplase and outcome in stroke: an updated pooled analysis of ECASS, ATLANTIS, NINDS, and EPITHET trials. Lancet. 2010;375(9727):1695-703.

20. Messé SR, Khatri P, Reeves MJ, Smith EE, Saver JL, Bhatt DL, et al. Why are acute ischemic stroke patients not receiving IV tPA? Results from a national registry. Neurology. 2016;87(15):1565-74.

21. Marko M, Posekany A, Szabo S, Scharer S, Kiechl S, Knoflach M, et al. Trends of r-tPA (Recombinant Tissue-Type Plasminogen Activator) Treatment and Treatment-Influencing Factors in Acute Ischemic Stroke. Stroke. 2020;51(4):1240-7.

22. Robinson T. Reperfusion in the brain: is time important? The DAWN and DEFUSE-3 trials. Cardiovasc Res. 2018;114(5):e28-e9.

23. Ciccone A, Valvassori L, Nichelatti M, Sgoifo A, Ponzio M, Sterzi R, et al. Endovascular treatment for acute ischemic stroke. N Engl J Med. 2013;368(10):904-13.

24. O'Collins VE, Macleod MR, Donnan GA, Horky LL, van der Worp BH, Howells DW. 1,026 experimental treatments in acute stroke. Ann Neurol. 2006;59(3):467-77.

25. Malone K, Amu S, Moore AC, Waeber C. The immune system and stroke: from current targets to future therapy. Immunol Cell Biol. 2018;97(1):5-6.

26. Traystman RJ. Animal models of focal and global cerebral ischemia. ILAR J. 2003;44(2):85-95.

27. Masopust D, Sivula CP, Jameson SC. Of Mice, Dirty Mice, and Men: Using Mice To Understand Human Immunology. J Immunol. 2017;199(2):383-8.

28. Mhairi Macrae I. New models of focal cerebral ischaemia. Br J Clin Pharmacol. 1992;34(4):302-8.

29. Chung JW, Park SH, Kim N, Kim WJ, Park JH, Ko Y, et al. Trial of ORG 10172 in Acute Stroke Treatment (TOAST) classification and vascular territory of ischemic stroke lesions diagnosed by diffusion-weighted imaging. J Am Heart Assoc. 2014;3(4).

30. Zhang F, Guo RM, Yang M, Wen XH, Shen J. A stable focal cerebral ischemia injury model in adult mice: assessment using 7T MR imaging. AJNR Am J Neuroradiol. 2012;33(5):935-9.

31. Horie N, Maag AL, Hamilton SA, Shichinohe H, Bliss TM, Steinberg GK. Mouse model of focal cerebral ischemia using endothelin-1. J Neurosci Methods. 2008;173(2):286-90.

32. Trotman-Lucas M, Gibson CL. A review of experimental models of focal cerebral ischemia focusing on the middle cerebral artery occlusion model. F1000Res. 2021;10:242.

33. Uzdensky AB. Photothrombotic Stroke as a Model of Ischemic Stroke. Transl Stroke Res. 2018;9(5):437-51.

34. Howells DW, Porritt MJ, Rewell SS, O'Collins V, Sena ES, van der Worp HB, et al. Different strokes for different folks: the rich diversity of animal models of focal cerebral ischemia. J Cereb Blood Flow Metab. 2010;30(8):1412-31.

35. McBride DW, Zhang JH. Precision Stroke Animal Models: the Permanent MCAO Model Should Be the Primary Model, Not Transient MCAO. Transl Stroke Res. 2017.

36. Ma R, Xie Q, Li Y, Chen Z, Ren M, Chen H, et al. Animal models of cerebral ischemia: A review. Biomed Pharmacother. 2020;131:110686.

37. (STAIR) STAIR. Recommendations for standards regarding preclinical neuroprotective and restorative drug development. Stroke. 1999;30(12):2752-8.

38. Llovera G, Roth S, Plesnila N, Veltkamp R, Liesz A. Modeling stroke in mice: permanent coagulation of the distal middle cerebral artery. J Vis Exp. 2014(89):e51729.

39. Wilson EH, Weninger W, Hunter CA. Trafficking of immune cells in the central nervous system. J Clin Invest. 2010;120(5):1368-79.

40. Louveau A, Harris TH, Kipnis J. Revisiting the Mechanisms of CNS Immune Privilege. Trends Immunol. 2015;36(10):569-77.

41. Serlin Y, Shelef I, Knyazer B, Friedman A. Anatomy and physiology of the blood-brain barrier. Semin Cell Dev Biol. 2015;38:2-6.

42. Iadecola C, Anrather J. The immunology of stroke: from mechanisms to translation. Nat Med. 2011;17(7):796-808.

43. Kamel H, Iadecola C. Brain-immune interactions and ischemic stroke: clinical implications. Arch Neurol. 2012;69(5):576-81.

44. Petrovic-Djergovic D, Goonewardena SN, Pinsky DJ. Inflammatory Disequilibrium in Stroke. Circ Res. 2016;119(1):142-58.

45. Fann DY, Lee SY, Manzanero S, Chunduri P, Sobey CG, Arumugam TV. Pathogenesis of acute stroke and the role of inflammasomes. Ageing Res Rev. 2013;12(4):941-66.

46. Vogelgesang A, Becker KJ, Dressel A. Immunological consequences of ischemic stroke. Acta Neurol Scand. 2014;129(1):1-12.

47. Anrather J, Iadecola C. Inflammation and Stroke: An Overview. Neurotherapeutics. 2016;13(4):661-70.

48. Selvaraj UM, Poinsatte K, Torres V, Ortega SB, Stowe AM. Heterogeneity of B Cell Functions in Stroke-Related Risk, Prevention, Injury, and Repair. Neurotherapeutics. 2016;13(4):729-47.

49. Wang X, Xuan W, Zhu ZY, Li Y, Zhu H, Zhu L, et al. The evolving role of neuro-immune interaction in brain repair after cerebral ischemic stroke. CNS Neurosci Ther. 2018;24(12):1100-14.

50. Malone K, Amu S, Moore AC, Waeber C. Immunomodulatory Therapeutic Strategies in Stroke. Front Pharmacol. 2019;10:630.

51. Jander S, Kraemer M, Schroeter M, Witte OW, Stoll G. Lymphocytic infiltration and expression of intercellular adhesion molecule-1 in photochemically induced ischemia of the rat cortex. J Cereb Blood Flow Metab. 1995;15(1):42-51.

52. Stubbe T, Ebner F, Richter D, Engel O, Randolf Engel O, Klehmet J, et al. Regulatory T cells accumulate and proliferate in the ischemic hemisphere for up to 30 days after MCAO. J Cereb Blood Flow Metab. 2013;33(1):37-47.

53. Benakis C, Llovera G, Liesz A. The meningeal and choroidal infiltration routes for leukocytes in stroke. Ther Adv Neurol Disord. 2018;11:1756286418783708.

54. Yilmaz G, Arumugam TV, Stokes KY, Granger DN. Role of T lymphocytes and interferon-gamma in ischemic stroke. Circulation. 2006;113(17):2105-12.

55. Hurn PD, Subramanian S, Parker SM, Afentoulis ME, Kaler LJ, Vandenbark AA, et al. T- and B-cell-deficient mice with experimental stroke have reduced lesion size and inflammation. J Cereb Blood Flow Metab. 2007;27(11):1798-805.

56. Kleinschnitz C, Schwab N, Kraft P, Hagedorn I, Dreykluft A, Schwarz T, et al. Early detrimental T-cell effects in experimental cerebral ischemia are neither related to adaptive immunity nor thrombus formation. Blood. 2010;115(18):3835-42.

57. Gelderblom M, Weymar A, Bernreuther C, Velden J, Arunachalam P, Steinbach K, et al. Neutralization of the IL-17 axis diminishes neutrophil invasion and protects from ischemic stroke. Blood. 2012;120(18):3793-802.

58. Liesz A, Zhou W, Mracskó É, Karcher S, Bauer H, Schwarting S, et al. Inhibition of lymphocyte trafficking shields the brain against deleterious neuroinflammation after stroke. Brain. 2011;134(Pt 3):704-20.

59. Mracsko E, Liesz A, Stojanovic A, Lou WP, Osswald M, Zhou W, et al. Antigen dependently activated cluster of differentiation 8-positive T cells cause perforin-mediated neurotoxicity in experimental stroke. J Neurosci. 2014;34(50):16784-95.

60. Shichita T, Sugiyama Y, Ooboshi H, Sugimori H, Nakagawa R, Takada I, et al. Pivotal role of cerebral interleukin-17-producing gammadeltaT cells in the delayed phase of ischemic brain injury. Nat Med. 2009;15(8):946-50.

61. Jenkins MK, Khoruts A, Ingulli E, Mueller DL, McSorley SJ, Reinhardt RL, et al. In vivo activation of antigen-specific CD4 T cells. Annu Rev Immunol. 2001;19:23-45.

62. Peterfalvi A, Molnar T, Banati M, Pusch G, Miko E, Bogar L, et al. Impaired function of innate T lymphocytes and NK cells in the acute phase of ischemic stroke. Cerebrovasc Dis. 2009;28(5):490-8.

63. Benakis C, Brea D, Caballero S, Faraco G, Moore J, Murphy M, et al. Commensal microbiota affects ischemic stroke outcome by regulating intestinal γδ T cells. Nat Med. 2016;22(5):516-23.

64. Hug A, Dalpke A, Wieczorek N, Giese T, Lorenz A, Auffarth G, et al. Infarct volume is a major determiner of post-stroke immune cell function and susceptibility to infection. Stroke. 2009;40(10):3226-32.

65. Wong CH, Jenne CN, Lee WY, Léger C, Kubes P. Functional innervation of hepatic iNKT cells is immunosuppressive following stroke. Science. 2011;334(6052):101-5.

66. Gelderblom M, Leypoldt F, Steinbach K, Behrens D, Choe CU, Siler DA, et al. Temporal and spatial dynamics of cerebral immune cell accumulation in stroke. Stroke. 2009;40(5):1849-57.

67. Dolati S, Ahmadi M, Khalili M, Taheraghdam AA, Siahmansouri H, Babaloo Z, et al. Peripheral Th17/Treg imbalance in elderly patients with ischemic stroke. Neurol Sci. 2018;39(4):647-54.

68. Zierath D, Schulze J, Kunze A, Drogomiretskiy O, Nhan D, Jaspers B, et al. The immunologic profile of adoptively transferred lymphocytes influences stroke outcome of recipients. J Neuroimmunol. 2013;263(1-2):28-34.

69. Luo Y, Zhou Y, Xiao W, Liang Z, Dai J, Weng X, et al. Interleukin-33 ameliorates ischemic brain injury in experimental stroke through promoting Th2 response and suppressing Th17 response. Brain Res. 2015;1597:86-94.

70. Becker KJ, Kalil AJ, Tanzi P, Zierath DK, Savos AV, Gee JM, et al. Autoimmune responses to the brain after stroke are associated with worse outcome. Stroke. 2011;42(10):2763-9.

71. Planas AM, Gómez-Choco M, Urra X, Gorina R, Caballero M, Chamorro Á. Brain-derived antigens in lymphoid tissue of patients with acute stroke. J Immunol. 2012;188(5):2156-63.

72. Becker KJ, Kindrick DL, Lester MP, Shea C, Ye ZC. Sensitization to brain antigens after stroke is augmented by lipopolysaccharide. J Cereb Blood Flow Metab. 2005;25(12):1634-44.

73. Filiano AJ, Gadani SP, Kipnis J. How and why do T cells and their derived cytokines affect the injured and healthy brain? Nat Rev Neurosci. 2017;18(6):375-84.

74. Baker DE. Natalizumab: overview of its pharmacology and safety. Rev Gastroenterol Disord. 2007;7(1):38-46.

75. Langhauser F, Kraft P, Göb E, Leinweber J, Schuhmann MK, Lorenz K, et al. Blocking of α4 integrin does not protect from acute ischemic stroke in mice. Stroke. 2014;45(6):1799-806.

76. Becker K, Kindrick D, Relton J, Harlan J, Winn R. Antibody to the alpha4 integrin decreases infarct size in transient focal cerebral ischemia in rats. Stroke. 2001;32(1):206-11.

77. Neumann J, Riek-Burchardt M, Herz J, Doeppner TR, König R, Hütten H, et al. Very-late-antigen-4 (VLA-4)-mediated brain invasion by neutrophils leads to interactions with microglia, increased ischemic injury and impaired behavior in experimental stroke. Acta Neuropathol. 2015;129(2):259-77.

78. Relton JK, Sloan KE, Frew EM, Whalley ET, Adams SP, Lobb RR. Inhibition of alpha4 integrin protects against transient focal cerebral ischemia in normotensive and hypertensive rats. Stroke. 2001;32(1):199-205.

79. Heindl S, Ricci A, Carofiglio O, Zhou Q, Arzberger T, Lenart N, et al. Chronic T cell proliferation in brains after stroke could interfere with the efficacy of immunotherapies. J Exp Med. 2021;218(8).

80. Sakaguchi S. Regulatory T cells: key controllers of immunologic self-tolerance. Cell. 2000;101(5):455-8.

81. Chatila TA. Role of regulatory T cells in human diseases. J Allergy Clin Immunol. 2005;116(5):949-59; quiz 60.

82. Battaglia M, Roncarolo MG. Induction of transplantation tolerance via regulatory T cells. Inflamm Allergy Drug Targets. 2006;5(3):157-65.

83. Baecher-Allan C, Anderson DE. Regulatory cells and human cancer. Semin Cancer Biol. 2006;16(2):98-105.

84. Buckner JH, Ziegler SF. Regulating the immune system: the induction of regulatory T cells in the periphery. Arthritis Res Ther. 2004;6(5):215-22.

85. Sakaguchi S, Wing K, Miyara M. Regulatory T cells - a brief history and perspective. Eur J Immunol. 2007;37 Suppl 1:S116-23.

86. Sakaguchi S, Sakaguchi N, Asano M, Itoh M, Toda M. Immunologic self-tolerance maintained by activated T cells expressing IL-2 receptor alpha-chains (CD25). Breakdown of a single mechanism of self-tolerance causes various autoimmune diseases. J Immunol. 1995;155(3):1151-64.

87. Fontenot JD, Gavin MA, Rudensky AY. Foxp3 programs the development and function of CD4+CD25+ regulatory T cells. Nat Immunol. 2003;4(4):330-6.

88. Hori S, Nomura T, Sakaguchi S. Control of regulatory T cell development by the transcription factor Foxp3. Science. 2003;299(5609):1057-61.

89. Barzaghi F, Passerini L, Bacchetta R. Immune dysregulation, polyendocrinopathy, enteropathy, x-linked syndrome: a paradigm of immunodeficiency with autoimmunity. Front Immunol. 2012;3:211.

90. Wang J, Ioan-Facsinay A, van der Voort EI, Huizinga TW, Toes RE. Transient expression of FOXP3 in human activated nonregulatory CD4+ T cells. Eur J Immunol. 2007;37(1):129-38.

91. Santegoets SJ, Dijkgraaf EM, Battaglia A, Beckhove P, Britten CM, Gallimore A, et al. Monitoring regulatory T cells in clinical samples: consensus on an essential marker set and gating strategy for regulatory T cell analysis by flow cytometry. Cancer Immunol Immunother. 2015;64(10):1271-86.

92. Bailey-Bucktrout SL, Bluestone JA. Regulatory T cells: stability revisited. Trends Immunol. 2011;32(7):301-6.

93. Zhou L, Chong MM, Littman DR. Plasticity of CD4+ T cell lineage differentiation. Immunity. 2009;30(5):646-55.

94. Koch MA, Tucker-Heard G, Perdue NR, Killebrew JR, Urdahl KB, Campbell DJ. The transcription factor T-bet controls regulatory T cell homeostasis and function during type 1 inflammation. Nat Immunol. 2009;10(6):595-602.

95. Levine AG, Mendoza A, Hemmers S, Moltedo B, Niec RE, Schizas M, et al. Stability and function of regulatory T cells expressing the transcription factor T-bet. Nature. 2017;546(7658):421-5.

96. Cretney E, Xin A, Shi W, Minnich M, Masson F, Miasari M, et al. The transcription factors Blimp-1 and IRF4 jointly control the differentiation and function of effector regulatory T cells. Nat Immunol. 2011;12(4):304-11.

97. Zheng Y, Chaudhry A, Kas A, deRoos P, Kim JM, Chu TT, et al. Regulatory T-cell suppressor program co-opts transcription factor IRF4 to control T(H)2 responses. Nature. 2009;458(7236):351-6.

98. Chaudhry A, Rudra D, Treuting P, Samstein RM, Liang Y, Kas A, et al. CD4+ regulatory T cells control TH17 responses in a Stat3-dependent manner. Science. 2009;326(5955):986-91.

99. Sefik E, Geva-Zatorsky N, Oh S, Konnikova L, Zemmour D, McGuire AM, et al. MUCOSAL IMMUNOLOGY. Individual intestinal symbionts induce a distinct population of RORγ^+ regulatory T cells. Science. 2015;349(6251):993-7.

100. Chung Y, Tanaka S, Chu F, Nurieva RI, Martinez GJ, Rawal S, et al. Follicular regulatory T cells expressing Foxp3 and Bcl-6 suppress germinal center reactions. Nat Med. 2011;17(8):983-8.

101. Wollenberg I, Agua-Doce A, Hernández A, Almeida C, Oliveira VG, Faro J, et al. Regulation of the germinal center reaction by Foxp3+ follicular regulatory T cells. J Immunol. 2011;187(9):4553-60.

102. Wing JB, Sakaguchi S. Multiple treg suppressive modules and their adaptability. Front Immunol. 2012;3:178.

103. Bluestone JA, Abbas AK. Natural versus adaptive regulatory T cells. Nat Rev Immunol. 2003;3(3):253-7.

104. Caramalho Í, Nunes-Cabaço H, Foxall RB, Sousa AE. Regulatory T-Cell Development in the Human Thymus. Front Immunol. 2015;6:395.

105. Sakaguchi S, Mikami N, Wing JB, Tanaka A, Ichiyama K, Ohkura N. Regulatory T Cells and Human Disease. Annu Rev Immunol. 2020;38:541-66.

106. Josefowicz SZ, Niec RE, Kim HY, Treuting P, Chinen T, Zheng Y, et al. Extrathymically generated regulatory T cells control mucosal TH2 inflammation. Nature. 2012;482(7385):395-9.

107. Piotrowska M, Gliwiński M, Trzonkowski P, Iwaszkiewicz-Grzes D. Regulatory T Cells-Related Genes Are under DNA Methylation Influence. Int J Mol Sci. 2021;22(13).

108. Panduro M, Benoist C, Mathis D. Tissue Tregs. Annu Rev Immunol. 2016;34:609-33.

109. Hong J, Kim BS. Regulatory T Cell-Mediated Tissue Repair. Adv Exp Med Biol. 2018;1064:221-33.

110. Arce-Sillas A, Álvarez-Luquín DD, Tamaya-Domínguez B, Gomez-Fuentes S, Trejo-García A, Melo-Salas M, et al. Regulatory T Cells: Molecular Actions on Effector Cells in Immune Regulation. J Immunol Res. 2016;2016:1720827.

111. Schmidt A, Oberle N, Krammer PH. Molecular mechanisms of treg-mediated T cell suppression. Front Immunol. 2012;3:51.

112. Wing JB, Tanaka A, Sakaguchi S. Human FOXP3 + Regulatory T Cell Heterogeneity and Function in Autoimmunity and Cancer. Immunity. 2019;50(2):302-16.

113. Campbell C, Rudensky A. Roles of Regulatory T Cells in Tissue Pathophysiology and Metabolism. Cell Metab. 2020;31(1):18-25.

114. Dombrowski Y, O'Hagan T, Dittmer M, Penalva R, Mayoral SR, Bankhead P, et al. Regulatory T cells promote myelin regeneration in the central nervous system. Nat Neurosci. 2017;20(5):674-80.

115. Kleinschnitz C, Kraft P, Dreykluft A, Hagedorn I, Göbel K, Schuhmann MK, et al. Regulatory T cells are strong promoters of acute ischemic stroke in mice by inducing dysfunction of the cerebral microvasculature. Blood. 2013;121(4):679-91.

116. Ito M, Komai K, Mise-Omata S, Iizuka-Koga M, Noguchi Y, Kondo T, et al. Brain regulatory T cells suppress astrogliosis and potentiate neurological recovery. Nature. 2019;565(7738):246-50.

117. Ahnstedt H, Patrizz A, Chauhan A, Roy-O'Reilly M, Furr JW, Spychala MS, et al. Sex differences in T cell immune responses, gut permeability and outcome after ischemic stroke in aged mice. Brain Behav Immun. 2020;87:556-67.

118. Liesz A, Kleinschnitz C. Regulatory T Cells in Post-stroke Immune Homeostasis. Transl Stroke Res. 2016;7(4):313-21.

119. Zhou W, Liesz A, Bauer H, Sommer C, Lahrmann B, Valous N, et al. Postischemic brain infiltration of leukocyte subpopulations differs among murine permanent and transient focal cerebral ischemia models. Brain Pathol. 2013;23(1):34-44.

120. Guo S, Luo Y. Brain Foxp3+ regulatory T cells can be expanded by Interleukin-33 in mouse ischemic stroke. Int Immunopharmacol. 2020;81:106027.

121. Ito M, Komai K, Nakamura T, Srirat T, Yoshimura A. Tissue regulatory T cells and neural repair. Int Immunol. 2019;31(6):361-9.

122. Li P, Wang L, Zhou Y, Gan Y, Zhu W, Xia Y, et al. C-C Chemokine Receptor Type 5 (CCR5)-Mediated Docking of Transferred Tregs Protects Against Early Blood-Brain Barrier Disruption After Stroke. J Am Heart Assoc. 2017;6(8).

123. Chen C, Chu SF, Liu DD, Zhang Z, Kong LL, Zhou X, et al. Chemokines play complex roles in cerebral ischemia. Neurochem Int. 2018;112:146-58.

124. Martha SR, Cheng Q, Fraser JF, Gong L, Collier LA, Davis SM, et al. Expression of Cytokines and Chemokines as Predictors of Stroke Outcomes in Acute Ischemic Stroke. Front Neurol. 2019;10:1391.

125. Mirabelli-Badenier M, Braunersreuther V, Viviani GL, Dallegri F, Quercioli A, Veneselli E, et al. CC and CXC chemokines are pivotal mediators of cerebral injury in ischaemic stroke. Thromb Haemost. 2011;105(3):409-20.

126. Lee HT, Liu SP, Lin CH, Lee SW, Hsu CY, Sytwu HK, et al. A Crucial Role of CXCL14 for Promoting Regulatory T Cells Activation in Stroke. Theranostics. 2017;7(4):855-75.

127. Lucaciu A, Kuhn H, Trautmann S, Ferreirós N, Steinmetz H, Pfeilschifter J, et al. A Sphingosine 1-Phosphate Gradient Is Linked to the Cerebral Recruitment of T Helper and Regulatory T Helper Cells during Acute Ischemic Stroke. Int J Mol Sci. 2020;21(17).

128. Liesz A, Zhou W, Na SY, Hämmerling GJ, Garbi N, Karcher S, et al. Boosting regulatory T cells limits neuroinflammation in permanent cortical stroke. J Neurosci. 2013;33(44):17350-62.

129. Li P, Gan Y, Sun BL, Zhang F, Lu B, Gao Y, et al. Adoptive regulatory T-cell therapy protects against cerebral ischemia. Ann Neurol. 2013;74(3):458-71.

130. Liesz A, Hagmann S, Zschoche C, Adamek J, Zhou W, Sun L, et al. The spectrum of systemic immune alterations after murine focal ischemia: immunodepression versus immunomodulation. Stroke. 2009;40(8):2849-58.

131. Offner H, Subramanian S, Parker SM, Wang C, Afentoulis ME, Lewis A, et al. Splenic atrophy in experimental stroke is accompanied by increased regulatory T cells and circulating macrophages. J Immunol. 2006;176(11):6523-31.

132. Lahl K, Sparwasser T. In vivo depletion of FoxP3+ Tregs using the DEREG mouse model. Methods Mol Biol. 2011;707:157-72.

133. Maes W, Verschuere T, Van Hoylandt A, Boon L, Van Gool S. Depletion of regulatory T cells in a mouse experimental glioma model through anti-CD25 treatment results in the infiltration of non-immunosuppressive myeloid cells in the brain. Clin Dev Immunol. 2013;2013:952469.

134. Liesz A, Suri-Payer E, Veltkamp C, Doerr H, Sommer C, Rivest S, et al. Regulatory T cells are key cerebroprotective immunomodulators in acute experimental stroke. Nat Med. 2009;15(2):192-9.

135. Xie L, Sun F, Wang J, Mao X, Yang SH, Su DM, et al. mTOR signaling inhibition modulates macrophage/microglia-mediated neuroinflammation and secondary injury via regulatory T cells after focal ischemia. J Immunol. 2014;192(12):6009-19.

136. Ren X, Akiyoshi K, Vandenbark AA, Hurn PD, Offner H. CD4+FoxP3+ regulatory T-cells in cerebral ischemic stroke. Metab Brain Dis. 2011;26(1):87-90.

137. Li P, Mao L, Zhou G, Leak RK, Sun BL, Chen J, et al. Adoptive regulatory T-cell therapy preserves systemic immune homeostasis after cerebral ischemia. Stroke. 2013;44(12):3509-15.

138. Li P, Mao L, Liu X, Gan Y, Zheng J, Thomson AW, et al. Essential role of program death 1-ligand 1 in regulatory T-cell-afforded protection against blood-brain barrier damage after stroke. Stroke. 2014;45(3):857-64.

139. Brea D, Agulla J, Rodríguez-Yáñez M, Barral D, Ramos-Cabrer P, Campos F, et al. Regulatory T cells modulate inflammation and reduce infarct volume in experimental brain ischaemia. J Cell Mol Med. 2014;18(8):1571-9.

140. Na SY, Mracsko E, Liesz A, Hünig T, Veltkamp R. Amplification of regulatory T cells using a CD28 superagonist reduces brain damage after ischemic stroke in mice. Stroke. 2015;46(1):212-20.

141. Chen Y, Ruetzler C, Pandipati S, Spatz M, McCarron RM, Becker K, et al. Mucosal tolerance to E-selectin provides cell-mediated protection against ischemic brain injury. Proc Natl Acad Sci U S A. 2003;100(25):15107-12.

142. Gee JM, Kalil A, Thullbery M, Becker KJ. Induction of immunologic tolerance to myelin basic protein prevents central nervous system autoimmunity and improves outcome after stroke. Stroke. 2008;39(5):1575-82.

143. Ishibashi S, Maric D, Mou Y, Ohtani R, Ruetzler C, Hallenbeck JM. Mucosal tolerance to E-selectin promotes the survival of newly generated neuroblasts via regulatory T-cell induction after stroke in spontaneously hypertensive rats. J Cereb Blood Flow Metab. 2009;29(3):606-20.

144. Wang J, Xie L, Yang C, Ren C, Zhou K, Wang B, et al. Activated regulatory T cell regulates neural stem cell proliferation in the subventricular zone of normal and ischemic mouse brain through interleukin 10. Front Cell Neurosci. 2015;9:361.

145. Schuhmann MK, Kraft P, Stoll G, Lorenz K, Meuth SG, Wiendl H, et al. CD28 superagonist-mediated boost of regulatory T cells increases thrombo-inflammation and ischemic neurodegeneration during the acute phase of experimental stroke. J Cereb Blood Flow Metab. 2015;35(1):6-10.

146. Lei TY, Ye YZ, Zhu XQ, Smerin D, Gu LJ, Xiong XX, et al. The immune response of T cells and therapeutic targets related to regulating the levels of T helper cells after ischaemic stroke. J Neuroinflammation. 2021;18(1):25.

147. Danese S, Rutella S. The Janus face of CD4+CD25+ regulatory T cells in cancer and autoimmunity. Curr Med Chem. 2007;14(6):649-66.

148. Chu HX, Kim HA, Lee S, Moore JP, Chan CT, Vinh A, et al. Immune cell infiltration in malignant middle cerebral artery infarction: comparison with transient cerebral ischemia. J Cereb Blood Flow Metab. 2014;34(3):450-9.

149. Gauberti M, Martinez de Lizarrondo S, Orset C, Vivien D. Lack of secondary microthrombosis after thrombin-induced stroke in mice and non-human primates. J Thromb Haemost. 2014;12(3):409-14.

150. Bai J, Lyden PD. Revisiting cerebral postischemic reperfusion injury: new insights in understanding reperfusion failure, hemorrhage, and edema. Int J Stroke. 2015;10(2):143-52.

151. Wang HY, Ye JR, Cui LY, Chu SF, Chen NH. Regulatory T cells in ischemic stroke. Acta Pharmacol Sin. 2021.

152. Li S, Huang Y, Liu Y, Rocha M, Li X, Wei P, et al. Change and predictive ability of circulating immunoregulatory lymphocytes in long-term outcomes of acute ischemic stroke. J Cereb Blood Flow Metab. 2021:271678X21995694.

153. Zhang J, Liu G, Chen D, Wang Z, Liu Y, Yu W. The combination of CC chemokine receptor type 5(CCR5) and Treg cells predicts prognosis in patients with ischemic stroke. J Neuroimmunol. 2020;349:577404.

154. Santamaría-Cadavid M, Rodríguez-Castro E, Rodríguez-Yáñez M, Arias-Rivas S, López-Dequidt I, Pérez-Mato M, et al. Regulatory T cells participate in the recovery of ischemic stroke patients. BMC Neurol. 2020;20(1):68.

155. Urra X, Cervera A, Villamor N, Planas AM, Chamorro A. Harms and benefits of lymphocyte subpopulations in patients with acute stroke. Neuroscience. 2009;158(3):1174-83.

156. Miró-Mur F, Laredo C, Renú A, Rudilosso S, Zhao Y, Amaro S, et al. Adrenal hormones and circulating leukocyte subtypes in stroke patients treated with reperfusion therapy. Brain Behav Immun. 2018;70:346-53.

157. Hu Y, Zheng Y, Wu Y, Ni B, Shi S. Imbalance between IL-17A-producing cells and regulatory T cells during ischemic stroke. Mediators Inflamm. 2014;2014:813045.

158. Noh MY, Lee WM, Lee SJ, Kim HY, Kim SH, Kim YS. Regulatory T cells increase after treatment with poly (ADP-ribose) polymerase-1 inhibitor in ischemic stroke patients. Int Immunopharmacol. 2018;60:104-10.

159. Li Q, Wang Y, Yu F, Wang YM, Zhang C, Hu C, et al. Peripheral Th17/Treg imbalance in patients with atherosclerotic cerebral infarction. Int J Clin Exp Pathol. 2013;6(6):1015-27.

160. Mao L, Li P, Zhu W, Cai W, Liu Z, Wang Y, et al. Regulatory T cells ameliorate tissue plasminogen activator-induced brain haemorrhage after stroke. Brain. 2017;140(7):1914-31.

161. Pang X, Qian W. Changes in Regulatory T-Cell Levels in Acute Cerebral Ischemia. J Neurol Surg A Cent Eur Neurosurg. 2017;78(4):374-9.

162. Yan J, Read SJ, Henderson RD, Hull R, O'Sullivan JD, McCombe PA, et al. Frequency and function of regulatory T cells after ischaemic stroke in humans. J Neuroimmunol. 2012;243(1-2):89-94.

163. Yan J, Greer JM, Etherington K, Cadigan GP, Cavanagh H, Henderson RD, et al. Immune activation in the peripheral blood of patients with acute ischemic stroke. J Neuroimmunol. 2009;206(1-2):112-7.

164. Jiang C, Kong W, Wang Y, Ziai W, Yang Q, Zuo F, et al. Changes in the cellular immune system and circulating inflammatory markers of stroke patients. Oncotarget. 2017;8(2):3553-67.

165. Ruhnau J, Schulze J, von Sarnowski B, Heinrich M, Langner S, Pötschke C, et al. Reduced Numbers and Impaired Function of Regulatory T Cells in Peripheral Blood of Ischemic Stroke Patients. Mediators Inflamm. 2016;2016:2974605.

166. Chen S, Wu H, Klebe D, Hong Y, Zhang J, Tang J. Regulatory T cell in stroke: a new paradigm for immune regulation. Clin Dev Immunol. 2013;2013:689827.

167. Garcia JM, Stillings SA, Leclerc JL, Phillips H, Edwards NJ, Robicsek SA, et al. Role of Interleukin-10 in Acute Brain Injuries. Front Neurol. 2017;8:244.

168. Perez-Asensio FJ, Perpiñá U, Planas AM, Pozas E. Interleukin-10 regulates progenitor differentiation and modulates neurogenesis in adult brain. J Cell Sci. 2013;126(Pt 18):4208-19.

169. Pereira L, Font-Nieves M, Van den Haute C, Baekelandt V, Planas AM, Pozas E. IL-10 regulates adult neurogenesis by modulating ERK and STAT3 activity. Front Cell Neurosci. 2015;9:57.

170. Gondek DC, Lu LF, Quezada SA, Sakaguchi S, Noelle RJ. Cutting edge: contact-mediated suppression by CD4+CD25+ regulatory cells involves a granzyme B-dependent, perforin-independent mechanism. J Immunol. 2005;174(4):1783-6.

171. Cao X, Cai SF, Fehniger TA, Song J, Collins LI, Piwnica-Worms DR, et al. Granzyme B and perforin are important for regulatory T cell-mediated suppression of tumor clearance. Immunity. 2007;27(4):635-46.

172. Jiang Y, Chen M, Nie H, Yuan Y. PD-1 and PD-L1 in cancer immunotherapy: clinical implications and future considerations. Hum Vaccin Immunother. 2019;15(5):1111-22.

173. Qin W, Hu L, Zhang X, Jiang S, Li J, Zhang Z, et al. The Diverse Function of PD-1/PD-L Pathway Beyond Cancer. Front Immunol. 2019;10:2298.

174. Bodhankar S, Chen Y, Vandenbark AA, Murphy SJ, Offner H. PD-L1 enhances CNS inflammation and infarct volume following experimental stroke in mice in opposition to PD-1. J Neuroinflammation. 2013;10:111.

175. Krämer TJ, Hack N, Brühl TJ, Menzel L, Hummel R, Griemert EV, et al. Depletion of regulatory T cells increases T cell brain infiltration, reactive astrogliosis, and interferon-γ gene expression in acute experimental traumatic brain injury. J Neuroinflammation. 2019;16(1):163.

176. Zhou K, Zhong Q, Wang YC, Xiong XY, Meng ZY, Zhao T, et al. Regulatory T cells ameliorate intracerebral hemorrhage-induced inflammatory injury by modulating microglia/macrophage polarization through the IL-10/GSK3β/PTEN axis. J Cereb Blood Flow Metab. 2017;37(3):967-79.

177. Manich G, Recasens M, Valente T, Almolda B, González B, Castellano B. Role of the CD200-CD200R Axis During Homeostasis and Neuroinflammation. Neuroscience. 2019;405:118-36.

178. Shi L, Sun Z, Su W, Xu F, Xie D, Zhang Q, et al. Treg cell-derived osteopontin promotes microglia-mediated white matter repair after ischemic stroke. Immunity. 2021;54(7):1527-42.e8.

179. Shu L, Xu CQ, Yan ZY, Yan Y, Jiang SZ, Wang YR. Post-Stroke Microglia Induce Sirtuin2 Expression to Suppress the Anti-inflammatory Function of Infiltrating Regulatory T Cells. Inflammation. 2019;42(6):1968-79.

180. Pekny M, Wilhelmsson U, Pekna M. The dual role of astrocyte activation and reactive gliosis. Neurosci Lett. 2014;565:30-8.

181. Walker LS. Treg and CTLA-4: two intertwining pathways to immune tolerance. J Autoimmun. 2013;45:49-57.

182. Rodríguez-Perea AL, Gutierrez-Vargas J, Cardona-Gómez GP, Guarin CJ, Rojas M, Hernández PA. Atorvastatin Modulates Regulatory T Cells and Attenuates Cerebral Damage in a Model of Transient Middle Cerebral Artery Occlusion in Rats. J Neuroimmune Pharmacol. 2017;12(1):152-62.

183. Borsellino G, Kleinewietfeld M, Di Mitri D, Sternjak A, Diamantini A, Giometto R, et al. Expression of ectonucleotidase CD39 by Foxp3+ Treg cells: hydrolysis of extracellular ATP and immune suppression. Blood. 2007;110(4):1225-32.

184. Zhang H, Xia Y, Ye Q, Yu F, Zhu W, Li P, et al. Expansion of Regulatory T Cells with IL-2/IL-2 Antibody Complex Protects against Transient Ischemic Stroke. J Neurosci. 2018;38(47):10168-79.

185. Eggenhuizen PJ, Ng BH, Ooi JD. Treg Enhancing Therapies to Treat Autoimmune Diseases. Int J Mol Sci. 2020;21(19).

186. Göschl L, Scheinecker C, Bonelli M. Treg cells in autoimmunity: from identification to Treg-based therapies. Semin Immunopathol. 2019;41(3):301-14.

187. Machhi J, Kevadiya BD, Muhammad IK, Herskovitz J, Olson KE, Mosley RL, et al. Harnessing regulatory T cell neuroprotective activities for treatment of neurodegenerative disorders. Mol Neurodegener. 2020;15(1):32.

188. Bluestone JA, Buckner JH, Fitch M, Gitelman SE, Gupta S, Hellerstein MK, et al. Type 1 diabetes immunotherapy using polyclonal regulatory T cells. Sci Transl Med. 2015;7(315):315ra189.

189. Tang Q, Henriksen KJ, Bi M, Finger EB, Szot G, Ye J, et al. In vitro-expanded antigen-specific regulatory T cells suppress autoimmune diabetes. J Exp Med. 2004;199(11):1455-65.

190. Maldini CR, Ellis GI, Riley JL. CAR T cells for infection, autoimmunity and allotransplantation. Nat Rev Immunol. 2018;18(10):605-16.

191. Domogalla MP, Rostan PV, Raker VK, Steinbrink K. Tolerance through Education: How Tolerogenic Dendritic Cells Shape Immunity. Front Immunol. 2017;8:1764.

192. Tang Q. Therapeutic window of interleukin-2 for autoimmune diseases. Diabetes. 2015;64(6):1912-3.

193. Battaglia M, Stabilini A, Roncarolo MG. Rapamycin selectively expands CD4+CD25+FoxP3+ regulatory T cells. Blood. 2005;105(12):4743-8.

194. Serra P, Santamaria P. Antigen-specific therapeutic approaches for autoimmunity. Nat Biotechnol. 2019;37(3):238-51.

195. Neal EG, Acosta SA, Kaneko Y, Ji X, Borlongan CV. Regulatory T-cells within bone marrow-derived stem cells actively confer immunomodulatory and neuroprotective effects against stroke. J Cereb Blood Flow Metab. 2019;39(9):1750-8.

196. Hünig T. The rise and fall of the CD28 superagonist TGN1412 and its return as TAB08: a personal account. FEBS J. 2016;283(18):3325-34.

197. Wang L, Beier UH, Akimova T, Dahiya S, Han R, Samanta A, et al. Histone/protein deacetylase inhibitor therapy for enhancement of Foxp3+ T-regulatory cell function posttransplantation. Am J Transplant. 2018;18(7):1596-603.

198. Bondarev AD, Attwood MM, Jonsson J, Chubarev VN, Tarasov VV, Schiöth HB. Recent developments of HDAC inhibitors: Emerging indications and novel molecules. Br J Clin Pharmacol. 2021;87(12):4577-97.

199. Demyanenko S, Dzreyan V, Sharifulina S. Histone Deacetylases and Their Isoform-Specific Inhibitors in Ischemic Stroke. Biomedicines. 2021;9(10).

200. Hamminger P, Rica R, Ellmeier W. Histone deacetylases as targets in autoimmune and autoinflammatory diseases. Adv Immunol. 2020;147:1-59.

201. Javidi E, Magnus T. Autoimmunity After Ischemic Stroke and Brain Injury. Front Immunol. 2019;10:686.

202. Chen Y, Kuchroo VK, Inobe J, Hafler DA, Weiner HL. Regulatory T cell clones induced by oral tolerance: suppression of autoimmune encephalomyelitis. Science. 1994;265(5176):1237-40.

203. Chen Y, Inobe J, Kuchroo VK, Baron JL, Janeway CA, Weiner HL. Oral tolerance in myelin basic protein T-cell receptor transgenic mice: suppression of

autoimmune encephalomyelitis and dose-dependent induction of regulatory cells. Proc Natl Acad Sci U S A. 1996;93(1):388-91.

204. Wang WZ, Olsson T, Kostulas V, Höjeberg B, Ekre HP, Link H. Myelin antigen reactive T cells in cerebrovascular diseases. Clin Exp Immunol. 1992;88(1):157-62.

205. Jauch EC, Lindsell C, Broderick J, Fagan SC, Tilley BC, Levine SR, et al. Association of serial biochemical markers with acute ischemic stroke: the National Institute of Neurological Disorders and Stroke recombinant tissue plasminogen activator Stroke Study. Stroke. 2006;37(10):2508-13.

206. Zierath D, Thullbery M, Hadwin J, Gee JM, Savos A, Kalil A, et al. CNS immune responses following experimental stroke. Neurocrit Care. 2010;12(2):274-84.

207. Römer C, Engel O, Winek K, Hochmeister S, Zhang T, Royl G, et al. Blocking stroke-induced immunodeficiency increases CNS antigen-specific autoreactivity but does not worsen functional outcome after experimental stroke. J Neurosci. 2015;35(20):7777-94.

208. Frenkel D, Huang Z, Maron R, Koldzic DN, Hancock WW, Moskowitz MA, et al. Nasal vaccination with myelin oligodendrocyte glycoprotein reduces stroke size by inducing IL-10-producing CD4+ T cells. J Immunol. 2003;171(12):6549-55.

209. Wakita H, Ruetzler C, Illoh KO, Chen Y, Takanohashi A, Spatz M, et al. Mucosal tolerization to E-selectin protects against memory dysfunction and white matter damage in a vascular cognitive impairment model. J Cereb Blood Flow Metab. 2008;28(2):341-53.

210. Klehmet J, Hoffmann S, Walter G, Meisel C, Meisel A. Stroke induces specific alteration of T memory compartment controlling auto-reactive CNS antigen-specific T cell responses. J Neurol Sci. 2016;368:77-83.

211. Gee JM, Zierath D, Hadwin J, Savos A, Kalil A, Thullbery M, et al. Long term immunologic consequences of experimental stroke and mucosal tolerance. Exp Transl Stroke Med. 2009;1:3.

212. Liu X, Hu R, Pei L, Si P, Wang C, Tian X, et al. Regulatory T cell is critical for interleukin-33-mediated neuroprotection against stroke. Exp Neurol. 2020;328:113233.

213. Xie D, Liu H, Xu F, Su W, Ye Q, Yu F, et al. IL33 (Interleukin 33)/ST2 (Interleukin 1 Receptor-Like 1) Axis Drives Protective Microglial Responses and Promotes White Matter Integrity After Stroke. Stroke. 2021;52(6):2150-61.

214. Sun Y, Wen Y, Wang L, Wen L, You W, Wei S, et al. Therapeutic Opportunities of Interleukin-33 in the Central Nervous System. Front Immunol. 2021;12:654626.

215. Shevach EM. Application of IL-2 therapy to target T regulatory cell function. Trends Immunol. 2012;33(12):626-32.

216. Webster KE, Walters S, Kohler RE, Mrkvan T, Boyman O, Surh CD, et al. In vivo expansion of T reg cells with IL-2-mAb complexes: induction of resistance to EAE and long-term acceptance of islet allografts without immunosuppression. J Exp Med. 2009;206(4):751-60.

217. Borlongan MC, Kingsbury C, Salazar FE, Toledo ARL, Monroy GR, Sadanandan N, et al. IL-2/IL-2R Antibody Complex Enhances Treg-Induced Neuroprotection by Dampening TNF-α Inflammation in an In Vitro Stroke Model. Neuromolecular Med. 2021;23(4):540-8.

218. Charriaut-Marlangue C, Leconte C, Csaba Z, Chafa L, Pansiot J, Talatizi M, et al. Sex differences in the effects of PARP inhibition on microglial phenotypes following neonatal stroke. Brain Behav Immun. 2018;73:375-89.

219. Luo X, Nie J, Wang S, Chen Z, Chen W, Li D, et al. Poly(ADP-ribosyl)ation of FOXP3 protein mediated by PARP-1 regulates the function of regulatory T cells. J Biol Chem. 2016;291(3):1201.

220. Chen J, Li X, Xu S, Zhang M, Wu Z, Zhang X, et al. Delayed PARP-1 Inhibition Alleviates Post-stroke Inflammation in Male Versus Female Mice: Differences and Similarities. Front Cell Neurosci. 2020;14:77.

221. Liu S, Luo W, Wang Y. Emerging role of PARP-1 and PARthanatos in ischemic stroke. J Neurochem. 2022;160(1):74-87.

222. Fraser H, Safinia N, Grageda N, Thirkell S, Lowe K, Fry LJ, et al. A Rapamycin-Based GMP-Compatible Process for the Isolation and Expansion of Regulatory T Cells for Clinical Trials. Mol Ther Methods Clin Dev. 2018;8:198-209.

223. Gu SC, Wang CD. Early Selective Serotonin Reuptake Inhibitors for Recovery after Stroke: A Meta-Analysis and Trial Sequential Analysis. J Stroke Cerebrovasc Dis. 2018;27(5):1178-89.

224. Xia Y, Cai W, Thomson AW, Hu X. Regulatory T Cell Therapy for Ischemic Stroke: how far from Clinical Translation? Transl Stroke Res. 2016;7(5):415-9.

225. Chun J, Brinkmann V. A mechanistically novel, first oral therapy for multiple sclerosis: the development of fingolimod (FTY720, Gilenya). Discov Med. 2011;12(64):213-28.

226. Brinkmann V, Billich A, Baumruker T, Heining P, Schmouder R, Francis G, et al. Fingolimod (FTY720): discovery and development of an oral drug to treat multiple sclerosis. Nat Rev Drug Discov. 2010;9(11):883-97.

227. Mizuta K, Ohmori M, Miyashita F, Kitoh Y, Fujimura A, Mori M, et al. Effect of pretreatment with FTY720 and cyclosporin on ischaemia-reperfusion injury of the liver in rats. J Pharm Pharmacol. 1999;51(12):1423-8.

228. Awad AS, Ye H, Huang L, Li L, Foss FW, Macdonald TL, et al. Selective sphingosine 1-phosphate 1 receptor activation reduces ischemia-reperfusion injury in mouse kidney. Am J Physiol Renal Physiol. 2006;290(6):F1516-24.

229. Brinkmann V, Davis MD, Heise CE, Albert R, Cottens S, Hof R, et al. The immune modulator FTY720 targets sphingosine 1-phosphate receptors. J Biol Chem. 2002;277(24):21453-7.

230. Strader CR, Pearce CJ, Oberlies NH. Fingolimod (FTY720): a recently approved multiple sclerosis drug based on a fungal secondary metabolite. J Nat Prod. 2011;74(4):900-7.

231. Doggrell SA. Oral fingolimod for relapsing-remitting multiple sclerosis Evaluation of: Kappos L, Radue E-M, O'Connor P, et al. A placebo-controlled trial of oral fingolimod in relapsing multiple sclerosis. N Engl J Med 2010;362:387-401; and Cohen JA, Barkhof F, Comi G, et al. Oral fingolimod or intramuscular interferon for relapsing multiple sclerosis. N Engl J Med 2010;362:402-15. Expert Opin Pharmacother. 2010;11(10):1777-81.

232. Huwiler A, Zangemeister-Wittke U. The sphingosine 1-phosphate receptor modulator fingolimod as a therapeutic agent: Recent findings and new perspectives. Pharmacol Ther. 2018;185:34-49.

233. Li W, Xu H, Testai FD. Mechanism of Action and Clinical Potential of Fingolimod for the Treatment of Stroke. Front Neurol. 2016;7:139.

234. Ward MD, Jones DE, Goldman MD. Overview and safety of fingolimod hydrochloride use in patients with multiple sclerosis. Expert Opin Drug Saf. 2014;13(7):989-98.

235. Wacker BK, Park TS, Gidday JM. Hypoxic preconditioning-induced cerebral ischemic tolerance: role of microvascular sphingosine kinase 2. Stroke. 2009;40(10):3342-8.

236. Matloubian M, Lo CG, Cinamon G, Lesneski MJ, Xu Y, Brinkmann V, et al. Lymphocyte egress from thymus and peripheral lymphoid organs is dependent on S1P receptor 1. Nature. 2004;427(6972):355-60.

237. Sanchez T, Estrada-Hernandez T, Paik JH, Wu MT, Venkataraman K, Brinkmann V, et al. Phosphorylation and action of the immunomodulator FTY720 inhibits vascular endothelial cell growth factor-induced vascular permeability. J Biol Chem. 2003;278(47):47281-90.

238. Xin C, Ren S, Eberhardt W, Pfeilschifter J, Huwiler A. FTY720 suppresses interleukin-1beta-induced secretory phospholipase A2 expression in renal mesangial cells by a transcriptional mechanism. Br J Pharmacol. 2007;150(7):943-50.

239. Gardner NM, Riley RT, Showker JL, Voss KA, Sachs AJ, Maddox JR, et al. Elevated Nuclear and Cytoplasmic FTY720-Phosphate in Mouse Embryonic Fibroblasts Suggests the Potential for Multiple Mechanisms in FTY720-Induced Neural Tube Defects. Toxicol Sci. 2016;150(1):161-8.

240. Hait NC, Wise LE, Allegood JC, O'Brien M, Avni D, Reeves TM, et al. Active, phosphorylated fingolimod inhibits histone deacetylases and facilitates fear extinction memory. Nat Neurosci. 2014;17(7):971-80.

241. Lopes Pinheiro MA, Kooij G, Mizee MR, Kamermans A, Enzmann G, Lyck R, et al. Immune cell trafficking across the barriers of the central nervous system in multiple sclerosis and stroke. Biochim Biophys Acta. 2016;1862(3):461-71.

242. Rommer PS, Sellner J. Repurposing multiple sclerosis drugs: a review of studies in neurological and psychiatric conditions. Drug Discov Today. 2019;24(7):1398-404.

243. Aloizou AM, Siokas V, Pateraki G, Liampas I, Bakirtzis C, Tsouris Z, et al. Thinking outside the Ischemia Box: Advancements in the Use of Multiple Sclerosis Drugs in Ischemic Stroke. J Clin Med. 2021;10(4).

244. Czech B, Pfeilschifter W, Mazaheri-Omrani N, Strobel MA, Kahles T, Neumann-Haefelin T, et al. The immunomodulatory sphingosine 1-phosphate analog FTY720 reduces lesion size and improves neurological outcome in a mouse model of cerebral ischemia. Biochem Biophys Res Commun. 2009;389(2):251-6.

245. Hasegawa Y, Suzuki H, Sozen T, Rolland W, Zhang JH. Activation of sphingosine 1-phosphate receptor-1 by FTY720 is neuroprotective after ischemic stroke in rats. Stroke. 2010;41(2):368-74.

246. Kraft P, Göb E, Schuhmann MK, Göbel K, Deppermann C, Thielmann I, et al. FTY720 ameliorates acute ischemic stroke in mice by reducing thrombo-inflammation but not by direct neuroprotection. Stroke. 2013;44(11):3202-10.

247. Moon E, Han JE, Jeon S, Ryu JH, Choi JW, Chun J. Exogenous S1P Exposure Potentiates Ischemic Stroke Damage That Is Reduced Possibly by Inhibiting S1P Receptor Signaling. Mediators Inflamm. 2015;2015:492659.

248. Nazari M, Keshavarz S, Rafati A, Namavar MR, Haghani M. Fingolimod (FTY720) improves hippocampal synaptic plasticity and memory deficit in rats following focal cerebral ischemia. Brain Res Bull. 2016;124:95-102.

249. Wei Y, Yemisci M, Kim HH, Yung LM, Shin HK, Hwang SK, et al. Fingolimod provides long-term protection in rodent models of cerebral ischemia. Ann Neurol. 2011;69(1):119-29.

250. Wei Y, Yung L, Barfejani A, Waeber C. Delayed treatment with fingolimod improves long-term outcome after stroke. International Journal of Stroke2014.

251. Liu J, Zhang C, Tao W, Liu M. Systematic review and meta-analysis of the efficacy of sphingosine-1-phosphate (S1P) receptor agonist FTY720 (fingolimod) in animal models of stroke. Int J Neurosci. 2013;123(3):163-9.

252. Wang Z, Kawabori M, Houkin K. FTY720 (Fingolimod) Ameliorates Brain Injury through Multiple Mechanisms and is a Strong Candidate for Stroke Treatment. Curr Med Chem. 2020;27(18):2979-93.

253. Liesz A, Sun L, Zhou W, Schwarting S, Mracsko E, Zorn M, et al. FTY720 reduces post-ischemic brain lymphocyte influx but does not improve outcome in permanent murine cerebral ischemia. PLoS One. 2011;6(6):e21312.

254. Brait VH, Tarrasón G, Gavaldà A, Godessart N, Planas AM. Selective Sphingosine 1-Phosphate Receptor 1 Agonist Is Protective Against Ischemia/Reperfusion in Mice. Stroke. 2016;47(12):3053-6.

255. Camp SM, Bittman R, Chiang ET, Moreno-Vinasco L, Mirzapoiazova T, Sammani S, et al. Synthetic analogs of FTY720 [2-amino-2-(2-[4-octylphenyl]ethyl)-1,3-propanediol] differentially regulate pulmonary vascular permeability in vivo and in vitro. J Pharmacol Exp Ther. 2009;331(1):54-64.

256. Prager B, Spampinato SF, Ransohoff RM. Sphingosine 1-phosphate signaling at the blood-brain barrier. Trends Mol Med. 2015;21(6):354-63.

257. Brinkmann V. FTY720 (fingolimod) in Multiple Sclerosis: therapeutic effects in the immune and the central nervous system. Br J Pharmacol. 2009;158(5):1173-82.

258. Hasegawa Y, Suzuki H, Altay O, Rolland W, Zhang JH. Role of the sphingosine metabolism pathway on neurons against experimental cerebral ischemia in rats. Transl Stroke Res. 2013;4(5):524-32.

259. Miron VE, Hall JA, Kennedy TE, Soliven B, Antel JP. Cyclical and dose-dependent responses of adult human mature oligodendrocytes to fingolimod. Am J Pathol. 2008;173(4):1143-52.

260. Miron VE, Jung CG, Kim HJ, Kennedy TE, Soliven B, Antel JP. FTY720 modulates human oligodendrocyte progenitor process extension and survival. Ann Neurol. 2008;63(1):61-71.

261. Miron VE, Ludwin SK, Darlington PJ, Jarjour AA, Soliven B, Kennedy TE, et al. Fingolimod (FTY720) enhances remyelination following demyelination of organotypic cerebellar slices. Am J Pathol. 2010;176(6):2682-94.

262. Das A, Arifuzzaman S, Kim SH, Lee YS, Jung KH, Chai YG. FTY720 (fingolimod) regulates key target genes essential for inflammation in microglial cells as defined by high-resolution mRNA sequencing. Neuropharmacology. 2017;119:1-14.

263. Qin C, Fan WH, Liu Q, Shang K, Murugan M, Wu LJ, et al. Fingolimod Protects Against Ischemic White Matter Damage by Modulating Microglia Toward M2 Polarization via STAT3 Pathway. Stroke. 2017;48(12):3336-46.

264. Shang K, He J, Zou J, Qin C, Lin L, Zhou LQ, et al. Fingolimod promotes angiogenesis and attenuates ischemic brain damage via modulating microglial polarization. Brain Res. 2020;1726:146509.

265. Dang C, Lu Y, Li Q, Wang C, Ma X. Efficacy of the sphingosine-1-phosphate receptor agonist fingolimod in animal models of stroke: an updated meta-analysis. Int J Neurosci. 2020:1-10.

266. Fisher M, Feuerstein G, Howells DW, Hurn PD, Kent TA, Savitz SI, et al. Update of the stroke therapy academic industry roundtable preclinical recommendations. Stroke. 2009;40(6):2244-50.

267. Fu Y, Zhang N, Ren L, Yan Y, Sun N, Li YJ, et al. Impact of an immune modulator fingolimod on acute ischemic stroke. Proc Natl Acad Sci U S A. 2014;111(51):18315-20.

268. Zhu Z, Fu Y, Tian D, Sun N, Han W, Chang G, et al. Combination of the Immune Modulator Fingolimod With Alteplase in Acute Ischemic Stroke: A Pilot Trial. Circulation. 2015;132(12):1104-12.

269. Tian DC, Shi K, Zhu Z, Yao J, Yang X, Su L, et al. Fingolimod enhances the efficacy of delayed alteplase administration in acute ischemic stroke by promoting anterograde reperfusion and retrograde collateral flow. Ann Neurol. 2018;84(5):717-28.

270. Fu Y, Hao J, Zhang N, Ren L, Sun N, Li YJ, et al. Fingolimod for the treatment of intracerebral hemorrhage: a 2-arm proof-of-concept study. JAMA Neurol. 2014;71(9):1092-101.

271. Liantao Z, Jing Z, Lingling L, Hua L. Efficacy of fingolimod combined with alteplase in acute ischemic stroke and rehabilitation nursing. Pak J Pharm Sci. 2019;32(1(Special)):413-9.

272. Haas J, Schwarz A, Korporal-Kunke M, Jarius S, Wiendl H, Kieseier BC, et al. Fingolimod does not impair T-cell release from the thymus and beneficially affects Treg function in patients with multiple sclerosis. Mult Scler. 2015;21(12):1521-32.

273. Liu Y, Jiang J, Xiao H, Wang X, Li Y, Gong Y, et al. The sphingosine-1-phosphate receptor agonist FTY720 and its phosphorylated form affect the function of CD4+CD25+ T cells in vitro. Int J Mol Med. 2012;30(1):211-9.

274. Muls N, Dang HA, Sindic CJ, van Pesch V. Fingolimod increases CD39-expressing regulatory T cells in multiple sclerosis patients. PLoS One. 2014;9(11):e113025.

275. Garris CS, Blaho VA, Hla T, Han MH. Sphingosine-1-phosphate receptor 1 signalling in T cells: trafficking and beyond. Immunology. 2014;142(3):347-53.

276. Wu T, Zhang L, Xu K, Sun C, Lei T, Peng J, et al. Immunosuppressive drugs on inducing Ag-specific CD4(+)CD25(+)Foxp3(+) Treg cells during immune response in vivo. Transpl Immunol. 2012;27(1):30-8.

277. Liu Y, Jiang J, Xiao H, Wang X, Li Y, Gong Y, et al. The sphingosine-1-phosphate receptor agonist FTY720 and its phosphorylated form affect the function of CD4+CD25+ T cells in vitro. Int J Mol Med. 2012;30(1):211-9.

278. Daniel C, Sartory N, Zahn N, Geisslinger G, Radeke HH, Stein JM. FTY720 ameliorates Th1-mediated colitis in mice by directly affecting the functional activity of CD4+CD25+ regulatory T cells. J Immunol. 2007;178(4):2458-68.

279. Kim MG, Lee SY, Ko YS, Lee HY, Jo SK, Cho WY, et al. CD4+ CD25+ regulatory T cells partially mediate the beneficial effects of FTY720, a sphingosine-

1-phosphate analogue, during ischaemia/reperfusion-induced acute kidney injury. Nephrol Dial Transplant. 2011;26(1):111-24.

280. Serpero LD, Filaci G, Parodi A, Battaglia F, Kalli F, Brogi D, et al. Fingolimod modulates peripheral effector and regulatory T cells in MS patients. J Neuroimmune Pharmacol. 2013;8(5):1106-13.

281. Sato DK, Nakashima I, Bar-Or A, Misu T, Suzuki C, Nishiyama S, et al. Changes in Th17 and regulatory T cells after fingolimod initiation to treat multiple sclerosis. J Neuroimmunol. 2014;268(1-2):95-8.

282. Teglund S, Zhou GQ, Hammarström S. Characterization of cDNA encoding novel pregnancy-specific glycoprotein variants. Biochem Biophys Res Commun. 1995;211(2):656-64.

283. Brunkhorst R, Vutukuri R, Pfeilschifter W. Fingolimod for the treatment of neurological diseases-state of play and future perspectives. Front Cell Neurosci. 2014;8:283.

284. Mehling M, Brinkmann V, Antel J, Bar-Or A, Goebels N, Vedrine C, et al. FTY720 therapy exerts differential effects on T cell subsets in multiple sclerosis. Neurology. 2008;71(16):1261-7.

285. Jagger AT, Shimojima Y, J. Goronzy J, M. Weyand C. T regulatory cells and the immune aging process. Gerontology; 2014. p. 130-7.

286. Xue -Mei L, Jie C, Xuan D, Xiao-Xing L, Chun-Lin, Hu, et al. Changes in $CD4^{+}CD25+$ Tregs in the pathogenesis of atherosclerosis in $Apo^{E-/-}$ mice. Experimental Biology and Medicine; 2017. p. 918-25.

287. Carmichael ST. Rodent models of focal stroke: size, mechanism, and purpose. NeuroRx. 2005;2(3):396-409.

288. Percie du Sert N HV, Ahluwalia A, Alam S, Avey MT, Baker M, et al. The ARRIVE guidelines 2.0: Updated guidelines for reporting animal research. PLoS Biol; 2020.

289. Diaz Diaz AC, Malone K, Shearer JA, Moore AC, Waeber C. Histological, behavioural and flow cytometric datasets relating to acute ischaemic stroke in young, aged and ApoE. Data Brief. 2021;36:107146.

290. Lee JA, Spidlen J, Boyce K, Cai J, Crosbie N, Dalphin M, et al. MIFlowCyt: the minimum information about a Flow Cytometry Experiment. Cytometry A. 2008;73(10):926-30.

291. Schneider CA, Rasband WS, Eliceiri KW. NIH Image to ImageJ: 25 years of image analysis. Nat Methods. 2012;9(7):671-5.

292. Sun BL, Wang LH, Yang T, Sun JY, Mao LL, Yang MF, et al. Lymphatic drainage system of the brain: A novel target for intervention of neurological diseases. Prog Neurobiol. 2018;163-164:118-43.

293. Mestas J, Hughes CC. Of mice and not men: differences between mouse and human immunology. J Immunol. 2004;172(5):2731-8.

294. Quirant-Sánchez B, Hervás-García JV, Teniente-Serra A, Brieva L, Moral-Torres E, Cano A, et al. Predicting therapeutic response to fingolimod treatment in multiple sclerosis patients. CNS Neurosci Ther. 2018;24(12):1175-84.

295. Thomas K, Sehr T, Proschmann U, Rodriguez-Leal FA, Haase R, Ziemssen T. Fingolimod additionally acts as immunomodulator focused on the innate immune system beyond its prominent effects on lymphocyte recirculation. J Neuroinflammation. 2017;14(1):41.

296. Takata M, Nakagomi T, Kashiwamura S, Nakano-Doi A, Saino O, Nakagomi N, et al. Glucocorticoid-induced TNF receptor-triggered T cells are key modulators for survival/death of neural stem/progenitor cells induced by ischemic stroke. Cell Death Differ. 2012;19(5):756-67.

297. Gu L, Jian Z, Stary C, Xiong X. T Cells and Cerebral Ischemic Stroke. Neurochem Res. 2015;40(9):1786-91.

298. Chamorro A, Urra X, Planas AM. Infection after acute ischemic stroke: a manifestation of brain-induced immunodepression. Stroke. 2007;38(3):1097-103.

299. Veltkamp R, Gill D. Clinical Trials of Immunomodulation in Ischemic Stroke. Neurotherapeutics. 2016;13(4):791-800.

300. Percie du Sert N, Alfieri A, Allan SM, Carswell HV, Deuchar GA, Farr TD, et al. The IMPROVE Guidelines (Ischaemia Models: Procedural Refinements Of in Vivo Experiments). J Cereb Blood Flow Metab. 2017;37(11):3488-517.

301. Xu X, Li M, Jiang Y. The paradox role of regulatory T cells in ischemic stroke. ScientificWorldJournal. 2013;2013:174373.

302. Macrae IM. Preclinical stroke research--advantages and disadvantages of the most common rodent models of focal ischaemia. Br J Pharmacol. 2011;164(4):1062-78.

303. Dominguez-Villar M, Raddassi K, Danielsen AC, Guarnaccia J, Hafler DA. Fingolimod modulates T cell phenotype and regulatory T cell plasticity in vivo. J Autoimmun. 2019;96:40-9.

304. Izquierdo G, Damas F, Páramo MD, Ruiz-Peña JL, Navarro G. The real-world effectiveness and safety of fingolimod in relapsing-remitting multiple sclerosis patients: An observational study. PLoS One. 2017;12(4):e0176174.

305. Sawicka E, Dubois G, Jarai G, Edwards M, Thomas M, Nicholls A, et al. The sphingosine 1-phosphate receptor agonist FTY720 differentially affects the sequestration of CD4+/CD25+ T-regulatory cells and enhances their functional activity. J Immunol. 2005;175(12):7973-80.

306. Liu G, Yang K, Burns S, Shrestha S, Chi H. The S1P(1)-mTOR axis directs the reciprocal differentiation of T(H)1 and T(reg) cells. Nat Immunol. 2010;11(11):1047-56.

307. Liu G, Burns S, Huang G, Boyd K, Proia RL, Flavell RA, et al. The receptor S1P1 overrides regulatory T cell-mediated immune suppression through Akt-mTOR. Nat Immunol. 2009;10(7):769-77.

308. Tian Y, Liang X, Wu Y. The alternation of autophagy/apoptosis in CD4+CD25+Foxp3+ Tregs on the developmental stages of atherosclerosis. Biomed Pharmacother. 2018;97:1053-60.

309. Chistiakov DA, Sobenin IA, Orekhov AN. Regulatory T cells in atherosclerosis and strategies to induce the endogenous atheroprotective immune response. Immunol Lett. 2013;151(1-2):10-22.

310. Butcher MJ, Filipowicz AR, Waseem TC, McGary CM, Crow KJ, Magilnick N, et al. Atherosclerosis-Driven Treg Plasticity Results in Formation of a Dysfunctional Subset of Plastic IFNγ+ Th1/Tregs. Circ Res. 2016;119(11):1190-203.

311. Huang K, Li SQ, Wang WJ, Liu LS, Jiang YG, Feng PN, et al. Oral FTY720 administration induces immune tolerance and inhibits early development of atherosclerosis in apolipoprotein E-deficient mice. Int J Immunopathol Pharmacol. 2012;25(2):397-406.

312. Commodaro AG, Peron JP, Lopes CT, Arslanian C, Belfort R, Rizzo LV, et al. Evaluation of experimental autoimmune uveitis in mice treated with FTY720. Invest Ophthalmol Vis Sci. 2010;51(5):2568-74.

313. Esposito E, Ahn BJ, Shi J, Nakamura Y, Park JH, Mandeville ET, et al. Brain-to-cervical lymph node signaling after stroke. Nat Commun. 2019;10(1):5306.

314. Tang Q, Bluestone JA. Regulatory T-cell physiology and application to treat autoimmunity. Immunol Rev. 2006;212:217-37.

315. Wang Z, He D, Zeng YY, Zhu L, Yang C, Lu YJ, et al. The spleen may be an important target of stem cell therapy for stroke. J Neuroinflammation. 2019;16(1):20.

316. Urra X, Miró F, Chamorro A, Planas AM. Antigen-specific immune reactions to ischemic stroke. Front Cell Neurosci. 2014;8:278.

317. Cramer JV, Benakis C, Liesz A. T cells in the post-ischemic brain: Troopers or paramedics? J Neuroimmunol. 2019;326:33-7.

318. Yopp AC, Fu S, Honig SM, Randolph GJ, Ding Y, Krieger NR, et al. FTY720-enhanced T cell homing is dependent on CCR2, CCR5, CCR7, and CXCR4: evidence for distinct chemokine compartments. J Immunol. 2004;173(2):855-65.

319. Li LZ, Huang YY, Yang ZH, Zhang SJ, Han ZP, Luo YM. Potential microglia-based interventions for stroke. CNS Neurosci Ther. 2020;26(3):288-96.

320. Santos Samary C, Pelosi P, Leme Silva P, Rieken Macedo Rocco P. Immunomodulation after ischemic stroke: potential mechanisms and implications for therapy. Crit Care. 2016;20(1):391.

321. Pfeilschifter W, Czech-Zechmeister B, Sujak M, Foerch C, Wichelhaus TA, Pfeilschifter J. Treatment with the immunomodulator FTY720 does not promote spontaneous bacterial infections after experimental stroke in mice. Exp Transl Stroke Med. 2011;3:2.

322. Raffin C, Vo LT, Bluestone JA. Treg cell-based therapies: challenges and perspectives. Nat Rev Immunol. 2020;20(3):158-72.

323. Cai Y, Xu TT, Lu CQ, Ma YY, Chang D, Zhang Y, et al. Endogenous Regulatory T Cells Promote M2 Macrophage Phenotype in Diabetic Stroke as Visualized by Optical Imaging. Transl Stroke Res. 2020.

324. Xiong XY, Liu L, Yang QW. Refocusing Neuroprotection in Cerebral Reperfusion Era: New Challenges and Strategies. Front Neurol. 2018;9:249.

325. Naseh M, Vatanparast J, Rafati A, Bayat M, Haghani M. The emerging role of FTY720 as a sphingosine 1-phosphate analog for the treatment of ischemic stroke: The cellular and molecular mechanisms. Brain Behav. 2021;11(6):e02179.

326. Li YJ, Shi SX, Liu Q, Shi FD, Gonzales RJ. Targeted role for sphingosine-1-phosphate receptor 1 in cerebrovascular integrity and inflammation during acute ischemic stroke. Neurosci Lett. 2020;735:135160.

327. Limaye V, Li X, Hahn C, Xia P, Berndt MC, Vadas MA, et al. Sphingosine kinase-1 enhances endothelial cell survival through a PECAM-1-dependent activation of PI-3K/Akt and regulation of Bcl-2 family members. Blood. 2005;105(8):3169-77.

328. Lee JF, Zeng Q, Ozaki H, Wang L, Hand AR, Hla T, et al. Dual roles of tight junction-associated protein, zonula occludens-1, in sphingosine 1-phosphate-mediated endothelial chemotaxis and barrier integrity. J Biol Chem. 2006;281(39):29190-200.

329. Han M, Sun T, Chen H, Wang D. Potential sphingosine-1-phosphate-related therapeutic targets in the treatment of cerebral ischemia reperfusion injury. Life Sci. 2020;249:117542.

330. Malone K, Diaz Diaz A, Shearer J, Moore AC, Waeber C. The Effect of Fingolimod on Regulatory T Cells in a Mouse Model of Brain Ischaemia. Journal of Neuroinflammation; 2021. p. 37.

331. Schaar KL, Brenneman MM, Savitz SI. Functional assessments in the rodent stroke model. Exp Transl Stroke Med. 2010;2(1):13.

332. Pino PA, Cardona AE. Isolation of brain and spinal cord mononuclear cells using percoll gradients. J Vis Exp. 2011(48).

333. Wang H, Wang F, Tao X, Cheng H. Ammonia-containing dimethyl sulfoxide: an improved solvent for the dissolution of formazan crystals in the 3-(4,5-dimethylthiazol-2-yl)-2,5-diphenyl tetrazolium bromide (MTT) assay. Anal Biochem. 2012;421(1):324-6.

334. Yanagawa Y, Masubuchi Y, Chiba K. FTY720, a novel immunosuppressant, induces sequestration of circulating mature lymphocytes by acceleration of lymphocyte homing in rats, III. Increase in frequency of CD62L-positive T cells in Peyer's patches by FTY720-induced lymphocyte homing. Immunology. 1998;95(4):591-4.

335. Diaz Diaz AC, Shearer JA, Malone K, Waeber C. Acute Treatment With Fingolimod Does Not Confer Long-Term Benefit in a Mouse Model of Intracerebral Haemorrhage. Front Pharmacol. 2020;11:613103.

336. Brea D, Poon C, Benakis C, Lubitz G, Murphy M, Iadecola C, et al. Stroke affects intestinal immune cell trafficking to the central nervous system. Brain Behav Immun. 2021;96:295-302.

337. Offner H, Subramanian S, Parker SM, Afentoulis ME, Vandenbark AA, Hurn PD. Experimental stroke induces massive, rapid activation of the peripheral immune system. J Cereb Blood Flow Metab. 2006;26(5):654-65.

338. Zhong L, Xie L, Yang Z, Li L, Song S, Cao D, et al. Prognostic value of S1PR1 and its correlation with immune infiltrates in breast and lung cancers. BMC Cancer. 2020;20(1):766.

339. Xie L, Li W, Hersh J, Liu R, Yang SH. Experimental ischemic stroke induces long-term T cell activation in the brain. J Cereb Blood Flow Metab. 2019;39(11):2268-76.

340. Zhang Q, Liao Y, Liu Z, Dai Y, Li Y, Tang Y. Interleukin-17 and ischaemic stroke. Immunology. 2021;162(2):179-93.

341. Seifert HA, Leonardo CC, Hall AA, Rowe DD, Collier LA, Benkovic SA, et al. The spleen contributes to stroke induced neurodegeneration through interferon gamma signaling. Metab Brain Dis. 2012;27(2):131-41.

342. Luo YT, Liang YF, He H, Zhang MT, Wang R, Li HL. The immunosuppressant fingolimod ameliorates experimental autoimmune myasthenia gravis by regulating T-cell balance and cytokine secretion. Am J Transl Res. 2020;12(6):2600-13.

343. Ghadiri M, Rezk A, Li R, Evans A, Giacomini PS, Barnett MH, et al. Pre-treatment T-cell subsets associate with fingolimod treatment responsiveness in multiple sclerosis. Sci Rep. 2020;10(1):356.

344. Song ZY, Yamasaki R, Kawano Y, Sato S, Masaki K, Yoshimura S, et al. Peripheral blood T cell dynamics predict relapse in multiple sclerosis patients on fingolimod. PLoS One. 2014;10(4):e0124923.

345. Johnson TA, Lapierre Y, Bar-Or A, Antel JP. Distinct properties of circulating CD8+ T cells in FTY720-treated patients with multiple sclerosis. Arch Neurol. 2010;67(12):1449-55.

346. Laribi B, Sahraian MA, Shekarabi M, Emamnejad R, Marzban M, Sadaghiani S, et al. Characterization of CD4+ and CD8+ T Cell Subsets and Interferon Regulatory Factor 4 (IRF4) in MS Patients Treated with Fingolimod (FTY-720): A Follow-up Study. Iran J Allergy Asthma Immunol. 2018;17(4):346-60.

347. Kürtüncü M, Yılmaz V, Akçay H, Türkoğlu R, Altunrende B, Çınar SA, et al. Impact of fingolimod on CD4+ T cell subset and cytokine profile of relapsing remitting multiple sclerosis patients. J Neuroimmunol. 2019;337:577065.

348. Mehling M, Lindberg R, Raulf F, Kuhle J, Hess C, Kappos L, et al. Th17 central memory T cells are reduced by FTY720 in patients with multiple sclerosis. Neurology. 2010;75(5):403-10.

349. Zhou PJ, Wang H, Shi GH, Wang XH, Shen ZJ, Xu D. Immunomodulatory drug FTY720 induces regulatory CD4(+)CD25(+) T cells in vitro. Clin Exp Immunol. 2009;157(1):40-7.

350. Pino M, Paganini S, Deleage C, Padhan K, Harper JL, King CT, et al. Fingolimod retains cytolytic T cells and limits T follicular helper cell infection in lymphoid sites of SIV persistence. PLoS Pathog. 2019;15(10):e1008081.

351. Qiu R, Zhou L, Ma Y, Liang T, Shi L, Long J, et al. Regulatory T Cell Plasticity and Stability and Autoimmune Diseases. Clin Rev Allergy Immunol. 2020;58(1):52-70.

352. Miller DC, Whittington KB, Brand DD, Hasty KA, Rosloniec EF. The CII-specific autoimmune T-cell response develops in the presence of FTY720 but is regulated by enhanced Treg cells that inhibit the development of autoimmune arthritis. Arthritis Res Ther. 2016;18:8.

353. Copsel S, Wolf D, Komanduri KV, Levy RB. The promise of CD4+FoxP3+ regulatory T-cell manipulation in vivo: applications for allogeneic hematopoietic stem cell transplantation. Haematologica. 2019;104(7):1309-21.

354. Yoshida Y, Mikami N, Matsushima Y, Miyawaki M, Endo H, Banno R, et al. Combination treatment with fingolimod and a pathogenic antigen prevents relapse of glucose-6-phosphate isomerase peptide-induced arthritis. Immun Inflamm Dis. 2016;4(3):263-73.

355. Johnson W, Onuma O, Owolabi M, Sachdev S. Stroke: a global response is needed. Bull World Health Organ. 2016;94(9):634-A.

356. Ganesh A, Goyal M. Thrombectomy for Acute Ischemic Stroke: Recent Insights and Future Directions. Curr Neurol Neurosci Rep. 2018;18(9):59.

357. Moore T, Dveksler GS. Pregnancy-specific glycoproteins: complex gene families regulating maternal-fetal interactions. Int J Dev Biol. 2014;58(2-4):273-80.

358. Moore T, Williams JM, Becerra-Rodriguez MA, Dunne M, Kammerer R, Dveksler G. Pregnancy-specific glycoproteins: evolution, expression, functions and disease associations. Reproduction. 2022;163(2):R11-R23.

359. Falcón CR, Martínez FF, Carranza F, Cervi L, Motrán CC. In vivo expression of recombinant pregnancy-specific glycoprotein 1a inhibits the symptoms of collagen-induced arthritis. Am J Reprod Immunol. 2014;72(6):527-33.

360. Masson GM, Anthony F, Wilson MS. Value of Schwangerschaftsprotein 1 (SP1) and pregnancy-associated plasma protein-A (PAPP-A) in the clinical management of threatened abortion. Br J Obstet Gynaecol. 1983;90(2):146-9.

361. Silver RM, Heyborne KD, Leslie KK. Pregnancy specific beta 1 glycoprotein (SP-1) in maternal serum and amniotic fluid; pre-eclampsia, small for gestational age fetus and fetal distress. Placenta. 1993;14(5):583-9.

362. Motrán CC, Diaz FL, Montes CL, Bocco JL, Gruppi A. In vivo expression of recombinant pregnancy-specific glycoprotein 1a induces alternative activation of monocytes and enhances Th2-type immune response. Eur J Immunol. 2003;33(11):3007-16.

363. Motrán CC, Díaz FL, Gruppi A, Slavin D, Chatton B, Bocco JL. Human pregnancy-specific glycoprotein 1a (PSG1a) induces alternative activation in human and mouse monocytes and suppresses the accessory cell-dependent T cell proliferation. J Leukoc Biol. 2002;72(3):512-21.

364. Ha CT, Waterhouse R, Wessells J, Wu JA, Dveksler GS. Binding of pregnancy-specific glycoprotein 17 to CD9 on macrophages induces secretion of IL-10, IL-6, PGE2, and TGF-beta1. J Leukoc Biol. 2005;77(6):948-57.

365. Rayev MB, Litvinova LS, Yurova KA, Dunets NA, Khaziakhmatova OG, Timganova VP, et al. Role of the pregnancy-specific glycoprotein in regulation of the cytokine and chemokine profiles of intact mononuclear cells. Dokl Biol Sci. 2017;475(1):180-2.

366. Bebo BF, Dveksler GS. Evidence that pregnancy specific glycoproteins regulate T-Cell function and inflammatory autoimmune disease during pregnancy. Curr Drug Targets Inflamm Allergy. 2005;4(2):231-7.

367. Wang H, Wang Z, Wu Q, Yuan Y, Cao W, Zhang X. Regulatory T cells in ischemic stroke. CNS Neurosci Ther. 2021;27(6):643-51.

368. Warren J, Im M, Ballesteros A, Ha C, Moore T, Lambert F, et al. Activation of latent transforming growth factor-β1, a conserved function for pregnancy-specific beta 1-glycoproteins. Mol Hum Reprod. 2018;24(12):602-12.

369. Zamorina SA, Litvinova LS, Yurova KA, Dunets NA, Khaziakhmatova OG, Timganova VP, et al. The effect of pregnancy-specific β1-glycoprotein 1 on the transcription factor FOXP3 expression by immunocompetent cells. Dokl Biochem Biophys. 2016;470(1):361-3.

370. Blois SM, Sulkowski G, Tirado-González I, Warren J, Freitag N, Klapp BF, et al. Pregnancy-specific glycoprotein 1 (PSG1) activates TGF-β and prevents dextran sodium sulfate (DSS)-induced colitis in mice. Mucosal Immunol. 2014;7(2):348-58.

371. Jones K, Bryant S, Luo J, Kiesler P, Koontz S, Warren J, et al. Recombinant Pregnancy-Specific Glycoprotein 1 Has a Protective Role in a Murine Model of Acute Graft-versus-Host Disease. Biol Blood Marrow Transplant. 2019;25(2):193-203.

372. Zera KA, Buckwalter MS. T cells direct microglial repair of white matter after stroke. Trends Neurosci. 2021.

373. Ballesteros A, Mentink-Kane MM, Warren J, Kaplan GG, Dveksler GS. Induction and activation of latent transforming growth factor-β1 are carried out by two distinct domains of pregnancy-specific glycoprotein 1 (PSG1). J Biol Chem. 2015;290(7):4422-31.

374. Jones K, Ballesteros A, Mentink-Kane M, Warren J, Rattila S, Malech H, et al. PSG9 Stimulates Increase in FoxP3+ Regulatory T-Cells through the TGF-β1 Pathway. PLoS One. 2016;11(7):e0158050.

375. Martinez FF, Cervi L, Knubel CP, Panzetta-Dutari GM, Motran CC. The role of pregnancy-specific glycoprotein 1a (PSG1a) in regulating the innate and adaptive immune response. Am J Reprod Immunol. 2013;69(4):383-94.

376. Wu Y, Li J, Shou J, Zhang W, Chen C. Diverse functions and mechanisms of regulatory T cell in ischemic stroke. Exp Neurol. 2021;343:113782.

377. Alexander LD, Black SE, Gao F, Szilagyi G, Danells CJ, McIlroy WE. Correlating lesion size and location to deficits after ischemic stroke: the influence of accounting for altered peri-necrotic tissue and incidental silent infarcts. Behav Brain Funct. 2010;6:6.

378. Minnerup J, Wersching H, Brokinkel B, Dziewas R, Heuschmann PU, Nabavi DG, et al. The impact of lesion location and lesion size on poststroke infection frequency. J Neurol Neurosurg Psychiatry. 2010;81(2):198-202.

379. Balkaya MG, Trueman RC, Boltze J, Corbett D, Jolkkonen J. Behavioral outcome measures to improve experimental stroke research. Behav Brain Res. 2018;352:161-71.

380. Martínez FF, Knubel CP, Sánchez MC, Cervi L, Motrán CC. Pregnancy-specific glycoprotein 1a activates dendritic cells to provide signals for Th17-, Th2-, and Treg-cell polarization. Eur J Immunol. 2012;42(6):1573-84.

381. Savage PA, Klawon DEJ, Miller CH. Regulatory T Cell Development. Annu Rev Immunol. 2020;38:421-53.

382. Lee W, Lee GR. Transcriptional regulation and development of regulatory T cells. Exp Mol Med. 2018;50(3):e456.

383. Da Mesquita S, Fu Z, Kipnis J. The Meningeal Lymphatic System: A New Player in Neurophysiology. Neuron. 2018;100(2):375-88.

384. Bolte AC, Lukens JR. Neuroimmune cleanup crews in brain injury. Trends Immunol. 2021;42(6):480-94.

385. Gauberti M, Martinez de Lizarrondo S, Vivien D. Thrombolytic strategies for ischemic stroke in the thrombectomy era. J Thromb Haemost. 2021;19(7):1618-28.

386. Bowler JV, Wade JP, Jones BE, Nijran KS, Steiner TJ. Natural history of the spontaneous reperfusion of human cerebral infarcts as assessed by 99mTc HMPAO SPECT. J Neurol Neurosurg Psychiatry. 1998;64(1):90-7.

387. Datta-Mannan A. Mechanisms Influencing the Pharmacokinetics and Disposition of Monoclonal Antibodies and Peptides. Drug Metab Dispos. 2019;47(10):1100-10.

388. Pérez-de Puig I, Miró F, Salas-Perdomo A, Bonfill-Teixidor E, Ferrer-Ferrer M, Márquez-Kisinousky L, et al. IL-10 deficiency exacerbates the brain inflammatory response to permanent ischemia without preventing resolution of the lesion. J Cereb Blood Flow Metab. 2013;33(12):1955-66.

389. Walsh JT, Zheng J, Smirnov I, Lorenz U, Tung K, Kipnis J. Regulatory T cells in central nervous system injury: a double-edged sword. J Immunol. 2014;193(10):5013-22.

390. Houston A, Williams JM, Rovis TL, Shanley DK, O'Riordan RT, Kiely PA, et al. Pregnancy-specific glycoprotein expression in normal gastrointestinal tract and in tumors detected with novel monoclonal antibodies. MAbs. 2016;8(3):491-500.

391. Zhang D, Ren J, Luo Y, He Q, Zhao R, Chang J, et al. T Cell Response in Ischemic Stroke: From Mechanisms to Translational Insights. Front Immunol. 2021;12:707972.

392. Abu-Raya B, Michalski C, Sadarangani M, Lavoie PM. Maternal Immunological Adaptation During Normal Pregnancy. Front Immunol. 2020;11:575197.

393. Rowe JH, Ertelt JM, Aguilera MN, Farrar MA, Way SS. Foxp3(+) regulatory T cell expansion required for sustaining pregnancy compromises host defense against prenatal bacterial pathogens. Cell Host Microbe. 2011;10(1):54-64.

394. Sporns PB, Fiehler J, Ospel J, Safouris A, Hanning U, Fischer U, et al. Expanding indications for endovascular thrombectomy-how to leave no patient behind. Ther Adv Neurol Disord. 2021;14:1756286421998905.

395. Krishnan S, O'Boyle C, Smith CJ, Hulme S, Allan SM, Grainger JR, et al. A hyperacute immune map of ischaemic stroke patients reveals alterations to circulating innate and adaptive cells. Clin Exp Immunol. 2021;203(3):458-71.

396. Klimiec-Moskal E, Piechota M, Pera J, Weglarczyk K, Slowik A, Siedlar M, et al. The specific ex vivo released cytokine profile is associated with ischemic stroke outcome and improves its prediction. J Neuroinflammation. 2020;17(1):7.

397. Semerano A, Strambo D, Martino G, Comi G, Filippi M, Roveri L, et al. Leukocyte Counts and Ratios Are Predictive of Stroke Outcome and Hemorrhagic Complications Independently of Infections. Front Neurol. 2020;11:201.

398. Yakhkind A, McTaggart RA, Jayaraman MV, Siket MS, Silver B, Yaghi S. Minor Stroke and Transient Ischemic Attack: Research and Practice. Front Neurol. 2016;7:86.

399. Chen C, Ai QD, Chu SF, Zhang Z, Chen NH. NK cells in cerebral ischemia. Biomed Pharmacother. 2019;109:547-54.

400. Chiba T, Umegaki K. Pivotal roles of monocytes/macrophages in stroke. Mediators Inflamm. 2013;2013:759103.

401. Gallizioli M, Miró-Mur F, Otxoa-de-Amezaga A, Cugota R, Salas-Perdomo A, Justicia C, et al. Dendritic Cells and Microglia Have Non-redundant Functions in the Inflamed Brain with Protective Effects of Type 1 cDCs. Cell Rep. 2020;33(3):108291.

402. Chen C, Chencheng Z, Cuiying L, Xiaokun G. Plasmacytoid Dendritic Cells Protect Against Middle Cerebral Artery Occlusion Induced Brain Injury by Priming Regulatory T Cells. Front Cell Neurosci. 2020;14:8.

403. Zhang Y, Wei L, Du Y, Xie Y, Wu W, Yuan Y. Association Between Programed Cell Death-1 and CD4+ T Cell Alterations in Different Phases of Ischemic Stroke Patients. Front Cell Neurosci. 2018;12:170.

404. Ballesteros I, Cuartero M, Pradillo J, Moro M, Lizasoain I. Cytokines and Chemokines in Stroke. Primer on Cerebrovascular Diseases: Academic Press; 2017. p. 280-4.

405. Zhang Y, Liesz A, Li P. Coming to the Rescue: Regulatory T Cells for Promoting Recovery After Ischemic Stroke. Stroke. 2021;52(12):e837-e41.

406. Xiao J, Qiu QW, Qin C, Tao R, Qiao SY, Chen M, et al. Dynamic changes of peripheral blood lymphocyte subsets in acute ischemic stroke and prognostic value. Brain Behav. 2021;11(1):e01919.

407. Wang Y, Liu J, Wang X, Liu Z, Li F, Chen F, et al. Frequencies of circulating B- and T-lymphocytes as indicators for stroke outcomes. Neuropsychiatr Dis Treat. 2017;13:2509-18.

408. Liu Q, Jin WN, Liu Y, Shi K, Sun H, Zhang F, et al. Brain Ischemia Suppresses Immunity in the Periphery and Brain via Different Neurogenic Innervations. Immunity. 2017;46(3):474-87.

409. Rogers SL, Coe CL, Karaszewski JW. Immune consequences of stroke and cerebral palsy in adults. J Neuroimmunol. 1998;91(1-2):113-20.

410. Urra X, Villamor N, Amaro S, Gómez-Choco M, Obach V, Oleaga L, et al. Monocyte subtypes predict clinical course and prognosis in human stroke. J Cereb Blood Flow Metab. 2009;29(5):994-1002.

411. Urra X, Cervera A, Obach V, Climent N, Planas AM, Chamorro A. Monocytes are major players in the prognosis and risk of infection after acute stroke. Stroke. 2009;40(4):1262-8.

412. Kaito M, Araya S, Gondo Y, Fujita M, Minato N, Nakanishi M, et al. Relevance of distinct monocyte subsets to clinical course of ischemic stroke patients. PLoS One. 2013;8(8):e69409.

413. Chu HX, Broughton BR, Kim HA, Lee S, Drummond GR, Sobey CG. Evidence That Ly6C(hi) Monocytes are Protective in Acute Ischemic Stroke by Promoting M2 Macrophage Polarization. Stroke. 2015;46(7):1929-37.

414. ElAli A, Jean LeBlanc N. The Role of Monocytes in Ischemic Stroke Pathobiology: New Avenues to Explore. Front Aging Neurosci. 2016;8:29.

415. Rodríguez-Perea AL, Arcia ED, Rueda CM, Velilla PA. Phenotypical characterization of regulatory T cells in humans and rodents. Clin Exp Immunol. 2016;185(3):281-91.

416. McCoy P. Immunophenotyping Methods & Protocols. Springer Protocols: Humana Press; 2019.

417. Piepke M, Clausen BH, Ludewig P, Vienhues JH, Bedke T, Javidi E, et al. Interleukin-10 improves stroke outcome by controlling the detrimental Interleukin-17A response. J Neuroinflammation. 2021;18(1):265.

418. Tuttolomondo A, Di Raimondo D, di Sciacca R, Pinto A, Licata G. Inflammatory cytokines in acute ischemic stroke. Curr Pharm Des. 2008;14(33):3574-89.

419. Lambertsen KL, Biber K, Finsen B. Inflammatory cytokines in experimental and human stroke. J Cereb Blood Flow Metab. 2012;32(9):1677-98.

420. Li X, Lin S, Chen X, Huang W, Li Q, Zhang H, et al. The Prognostic Value of Serum Cytokines in Patients with Acute Ischemic Stroke. Aging Dis. 2019;10(3):544-56.

421. Kim HM, Shin HY, Jeong HJ, An HJ, Kim NS, Chae HJ, et al. Reduced IL-2 but elevated IL-4, IL-6, and IgE serum levels in patients with cerebral infarction during the acute stage. J Mol Neurosci. 2000;14(3):191-6.

422. Perego C, Fumagalli S, Miteva K, Kallikourdis M, De Simoni MG. Combined Genetic Deletion of IL (Interleukin)-4, IL-5, IL-9, and IL-13 Does Not Affect Ischemic Brain Injury in Mice. Stroke. 2019;50(8):2207-15.

423. Liu X, Liu J, Zhao S, Zhang H, Cai W, Cai M, et al. Interleukin-4 Is Essential for Microglia/Macrophage M2 Polarization and Long-Term Recovery After Cerebral Ischemia. Stroke. 2016;47(2):498-504.

424. Chen X, Zhang J, Song Y, Yang P, Yang Y, Huang Z, et al. Deficiency of anti-inflammatory cytokine IL-4 leads to neural hyperexcitability and aggravates cerebral ischemia-reperfusion injury. Acta Pharm Sin B. 2020;10(9):1634-45.

425. Xu J, Chen Z, Yu F, Liu H, Ma C, Xie D, et al. IL-4/STAT6 signaling facilitates innate hematoma resolution and neurological recovery after hemorrhagic stroke in mice. Proc Natl Acad Sci U S A. 2020;117(51):32679-90.

426. Sheikh AM, Nagai A, Wakabayashi K, Narantuya D, Kobayashi S, Yamaguchi S, et al. Mesenchymal stem cell transplantation modulates neuroinflammation in focal cerebral ischemia: contribution of fractalkine and IL-5. Neurobiol Dis. 2011;41(3):717-24.

427. Tan S, Shan Y, Lin Y, Liao S, Zhang B, Zeng Q, et al. Neutralization of interleukin-9 ameliorates experimental stroke by repairing the blood-brain barrier via down-regulation of astrocyte-derived vascular endothelial growth factor-A. FASEB J. 2019;33(3):4376-87.

428. Zhu H, Hu S, Li Y, Sun Y, Xiong X, Hu X, et al. Interleukins and Ischemic Stroke. Front Immunol. 2022;13:828447.

429. Li T, Liesz A. Immunity in Stroke: The Next Frontier. Thromb Haemost. 2022.

430. Yoshimura A, Ito M. Resolution of inflammation and repair after ischemic brain injury. Neuroimmunology and Neuroinflammation2020. p. 265-76.

431. Schläger C, Körner H, Krueger M, Vidoli S, Haberl M, Mielke D, et al. Effector T-cell trafficking between the leptomeninges and the cerebrospinal fluid. Nature. 2016;530(7590):349-53.

432. Hossmann KA. The two pathophysiologies of focal brain ischemia: implications for translational stroke research. J Cereb Blood Flow Metab. 2012;32(7):1310-6.

433. Chu HX, Kim HAH, Lee S, Moore JP, Chan CT, Vinh A, et al. Immune cell infiltration in malignant middle cerebral artery infarction: comparison with transient cerebral ischemia. J Cerebr Blood F Met. 2014;34(3):450-9.

434. Beuker C, Strecker JK, Rawal R, Schmidt-Pogoda A, Ruck T, Wiendl H, et al. Immune Cell Infiltration into the Brain After Ischemic Stroke in Humans Compared to Mice and Rats: a Systematic Review and Meta-Analysis. Transl Stroke Res. 2021.

435. Zhang SX, Ma XW, Li YF, Lai NL, Huang ZH, Fan K, et al. The Proportion of Regulatory T Cells in Patients with Systemic Lupus Erythematosus: A Meta-Analysis. J Immunol Res. 2018;2018:7103219.

436. Zhang H, Lin S, Chen X, Gu L, Zhu X, Zhang Y, et al. The effect of age, sex and strains on the performance and outcome in animal models of stroke. Neurochem Int. 2019;127:2-11.

437. Li J, McCullough LD. Sex differences in minocycline-induced neuroprotection after experimental stroke. J Cereb Blood Flow Metab. 2009;29(4):670-4.

438. Roy-O'Reilly M, McCullough LD. Age and Sex Are Critical Factors in Ischemic Stroke Pathology. Endocrinology. 2018;159(8):3120-31.

439. Dotson AL, Offner H. Sex differences in the immune response to experimental stroke: Implications for translational research. J Neurosci Res. 2017;95(1-2):437-46.

440. Bravo-Alegria J, McCullough LD, Liu F. Sex differences in stroke across the lifespan: The role of T lymphocytes. Neurochem Int. 2017;107:127-37.

441. Beckmann L, Obst S, Labusek N, Abberger H, Köster C, Klein-Hitpass L, et al. Regulatory T Cells Contribute to Sexual Dimorphism in Neonatal Hypoxic-Ischemic Brain Injury. Stroke. 2022;53(2):381-90.

442. McCann SK, Lawrence CB. Comorbidity and age in the modelling of stroke: are we still failing to consider the characteristics of stroke patients? BMJ Open Sci. 2020;4(1):e100013.

443. Macleod MR, van der Worp HB, Sena ES, Howells DW, Dirnagl U, Donnan GA. Evidence for the efficacy of NXY-059 in experimental focal cerebral ischaemia is confounded by study quality. Stroke. 2008;39(10):2824-9.

444. Ritzel RM, Lai YJ, Crapser JD, Patel AR, Schrecengost A, Grenier JM, et al. Aging alters the immunological response to ischemic stroke. Acta Neuropathol. 2018;136(1):89-110.

445. Sykes GP, Kamtchum-Tatuene J, Falcione S, Zehnder S, Munsterman D, Stamova B, et al. Aging Immune System in Acute Ischemic Stroke: A Transcriptomic Analysis. Stroke. 2021;52(4):1355-61.

446. Ahnstedt H, McCullough LD, Cipolla MJ. The Importance of Considering Sex Differences in Translational Stroke Research. Transl Stroke Res. 2016;7(4):261-73.

447. Spychala MS, Honarpisheh P, McCullough LD. Sex differences in neuroinflammation and neuroprotection in ischemic stroke. J Neurosci Res. 2017;95(1-2):462-71.

448. Sohrabji F, Park MJ, Mahnke AH. Sex differences in stroke therapies. J Neurosci Res. 2017;95(1-2):681-91.

Appendix I: Materials & Reagents

Materials	Catalogue Number (if applicable)	Supplier
Surgical Equipment/Reagents		
Hair Removal Cream	#1117971	Veet
Surgical Instrument Set	-	FST
Stereotaxic Frame	#68038	RWD Life Science
Bipolar Electrocoagulation Forceps	#A842	Symmetry Surgical Inc., USA
Electrosurgical Generator	#A952	Symmetry Surgical Inc., USA
Isoflurane	Merial	Abbeyville Vet
Surgical Gas (70% Nitrogen/30% Oxygen)	-	Irish Oxygen
General Laboratory Materials		
Nitrile Examination Gloves	#SC-359597	Santa Cruz Biotechnology, Inc.
Dissection Kit	#2084002	FST
Pierce Microtissue Grinder Kit	#20017	Pierce Chemical Company, Rockford, Illinois, USA
Plastic Syringe (5ml, 20ml)	#SS05SE1	Terumo
LeurLock Syringe (3ml)	#10608435	ThermoFischer Scientific
LeurLock Syringe (5ml)	#10608435	ThermoFischer Scientific
Microcentrifuge Tubes	#211-0015	VWR

Eppendorf Tubes (5ml)	#30119460	Eppendorf
Eppendorf Tubes (Amber) (5ml)	#30119452	Eppendorf
Cluster Tubes (1.2ml)	#4401	Sigma-Aldrich
Polypropylene Conical Tube (50ml)	#352098	ThermoFischer Scientific
Centrifuge Tube (15ml)	#430791	Sigma-Aldrich
Centrifuge Tubes (50ml)	#430290	Sigma-Aldrich
Pipette Tips (10µl, 200µl, 1000µl)	#70.3010 #70.3030 #70.3060	Sarstedt
EASYstrainer 70 µm sterile cell strainer	#542070	Greiner bio-one
Microtest 96-well Plate V-bottom	#82.1583	Sarstedt
Glass Cover Slips	#631-0121	VWR
Microlance Needles (23-gauge, 25-gauge)	#30060/30070	BD
Plastipak 1mL syringe	#305502	BD
Perfusion Mat Versi-Dry	#62080-00	Nalgene
Serological Pipettes (5ml, 10ml, 25ml, 50ml)	#SP-5/10/25/50	CAPP
Leucosep Tubes (50ml)	#2272906G	Greiner
Vacutainer Plastic K2EDTA 10ml Blood Collection Tubes	#367525	BD
Cryotubes (2ml)	#72379	Sarstedt
Corning CoolCell LX	#CLS4322002	Sigma-Aldrich
Cryosafe Storage Box	#Z756784	Sigma-Aldrich
General Laboratory Reagents		
0.01 mM 2-mercaptoethanol	#M3148	Sigma-Aldrich
10 mM HEPES	#H0887	Sigma-Aldrich
10% Fetal Calf Serum	#F2442	Sigma-Aldrich
Acetone (HPLC Grade)	#179124	Sigma-Aldrich
Ammonium Hydroxide	#221228	Sigma-Aldrich
CD4+CD25+ Regulatory T Cell Isolation Kit	#130091041	Miltenyi Biotec
DMSO	#D8418/D2650	Sigma-Aldrich

Dulbecco's Phosphate Buffered Saline	#D8537	Sigma-Aldrich
Ethanol	#1.00983	Sigma-Aldrich
HALT Protease Inhibitor Cocktail	#78429	ThermoFischer Scientific
Hanks' Balanced Salt Solution	#H6648	Sigma-Aldrich
Lymphoprep	#7811	Stemcell Technologies
MACS Cell Separation LD Columns	#130042901	Miltenyi Biotec
MACS Cell Separation MS Columns	#130042201	Miltenyi Biotec
Methanol (HPLC Grade)	#494291	Sigma-Aldrich
MTT	#M5655	Sigma-Aldrich
Non-essential amino acid solution	#M7145	Sigma-Aldrich
Penicillin/Streptomycin (100U/ml)	#P4458	Sigma-Aldrich
Percoll (pH 8.5-9.5)	#P1644	Sigma-Aldrich
Pierce BCA protein assay	#23227	ThermoFisher Scientific
Recombinant Murine IL-2	#I0523	Sigma-Aldrich
RPMI-1640	#R7658	Sigma-Aldrich
TGFβ 1 Mouse ELISA Kit	#BMS608-4	Invitrogen
Triphenyltetrazolium Chloride	#T8877	Sigma-Aldrich
Trypan Blue Solution	#T8154	Sigma-Aldrich
U-Bottom Suspension Cell Culture Plates	#83.3925.500	Sarstedt
U-PLEX Biomarker Group 1 Assay	K15067L-1	MSD
Drug Molecules/Control		
Fingolimod Hydrochloride	-	Novartis Institutes for Biomedical Research, Basel
Recombinant Pregnancy-Specific Glycoprotein 1-Fc	-	Dr. Tom Moore Lab, School of Biochemistry, UCC
Braun Sodium Chloride Injection BP (0.9% w/v)	#02556	Promed

Antibodies for Human Studies		
Anti-Human CD4 FITC (RPA-T4)	#A42925	Invitrogen
Anti-Human CD8 PE-Cyn5.5 (RPA-T8)	#35008842	Invitrogen
Anti-Human CD3 PE-Cy7 (OKT3)	#25003742	Invitrogen
Anti-Human CD45RA APC (HI100)	#17045842	Invitrogen
Anti-Human CD25 PerCP-eFluor 710 (CD25)	#A42925	Invitrogen
Anti-Human CD127 PE (eBioRDR5)	#A42925	Invitrogen
Anti-Human PD-1 PE-Cyn5 (J105)	#15279942	Invitrogen
Anti-Human CD39 SB600 (EBIOA1)	#63039942	Invitrogen
Anti-Human FoxP3 eFluor 450 (PCH101)	#A42925	Invitrogen
Anti-Human CTLA-4 PE-eFluor 610 (14D3)	#61152942	Invitrogen
Anti-Human Ki67 AF700 (SolA15)	#56569882	Invitrogen
Anti-Human CD45RA PerCP-Cyn5.5 (30-F11)	#45045182	Invitrogen
Anti-Human CD197 PerCP-eFluor710 (3D12)	#46197942	Invitrogen
Anti-Human CD19 AF700 (HIB19)	#56019942	Invitrogen
Anti-Human CD16 APC (CB16)	#17016842	Invitrogen
Anti-Human CD56 PE-Cy5 (CMSSB)	#15056742	Invitrogen
Anti-Human HLA-DR APC-eFluor 780 (LN3)	#47995642	Invitrogen
Anti-Human CD11c PE-eFluor 610 (3.9)	#61011642	Invitrogen
Anti-Human CD123 SB600 (6H6)	#63123942	Invitrogen
Fixable Viability Dye eFluor 455	#65086814	Invitrogen
eBioscience Essential Human Treg Phenotyping Kit	#A42925	Invitrogen
Antibodies for Mouse Studies		
Anti-Mouse CD45 PerCP-CY5.5 (30-F11)	#45045182	Invitrogen
Anti-Mouse CD4 FITC (RM4-5)	#11004282	Invitrogen
Anti-Mouse CD25 APC (PC61.5)	#17025182	Invitrogen
Anti-Mouse Foxp3 PE (FJK-16s)	#12577382	Invitrogen
Anti-Mouse CD8a Pacific Blue (5H10)	#MCD0828	Invitrogen

Anti-Mouse CD3e PE-Cy7 (145-2C11)	#14003182	Invitrogen
Anti-Mouse CD16/32 (93)	#14016181	Invitrogen
Anti-Mouse CD195 PerCP eFluor710 (HM-CCR5 (7A4))	#46195182	Invitrogen
Anti-Mouse CD196 PE-Vio615 (REA277)	#130108396	Miltenyi Biotec
Anti-Mouse CD198 PE-Vio615 (REA921)	#130119922	Miltenyi Biotec
Rat IgG2a κ Iso Control PE (eBR2a)	#12432181A	Invitrogen
Anti-Mouse IFN-γ eFluor610 (XMG1.2)	#61731182	Invitrogen
Anti-Mouse IL-17 PE (TC11-18H10)	#559502	BD
Anti-Mouse IL-10 PerCP-Cy5.5 (JES5-16E3)	#45710182	Invitrogen
Anti-Mouse CD3 (145-2C11)	#14003182	Invitrogen
Anti-Mouse FoxP3 (FJK-16s)	#12577382	Invitrogen
Anti-Mouse ICAM-1 (1A29)	#MA5407	Invitrogen
Anti-Rabbit Iba-1	#019-19741	Wako
Anti-Mouse NeuN	#ab177487	Abcam
Biotinylated Goat Anti-Hamster Secondary Antibody	#PA132045	Invitrogen
Donkey Anti-Rat Secondary Antibody	#A18739	Invitrogen
Goat Anti-Rabbit Biotinylated Secondary Antibody	#ab207995	Abcam
Goat Anti-Rabbit Alexa Fluor 488	#A11008	Invitrogen
Anti-Mouse CD3 (145-2C11)	#14003182	Invitrogen
Anti-Mouse CD28 (37.51)	#14028182	Invitrogen
eBioscience Fixable Viability Dye eFluor 780	#65086514	Invitrogen
Flow Cytometry Reagents		
eBioscience Cell Stimulation Cocktail	#00497593	Invitrogen
eBioscience Mouse Regulatory T Cell Staining Kit #1	#88811140	Invitrogen
eBioscience Red Blood Cell Lysis Buffer (10X)	#00430054	Invitrogen
eBioscience Permeabilization Buffer (10X)	#00833356	Invitrogen

eBioscience Fixation/Permeabilization Concentrate	#00512343	Invitrogen
eBioscience Fixation/Permeabilization Diluent	#00522356	Invitrogen
CountBright Absolute Counting Beads	#C36950	Molecular Probes
CompBeads (Anti-Rat/Anti-Hamster Compensation Particle Set)	#552845	BD
CompBeads (Anti-rat Compensation Particles Set)	#552844	BD
Immunohistochemistry Reagents		
Rabbit Serum	#S-5000	Vector Laboratories
Goat Serum	#S-1000	Vector Laboratories
Avidin/Biotin Blocking Kit	#SP-2001	Vector Laboratories
Hydrogen Peroxide	#H1009	Sigma-Aldrich
Vectastain Avidin-Biotin Complex Kit	#PK-4000	Vector Laboratories
DAB	#SK-4100	Vector Laboratories
HistoChoice	#H2779	Sigma-Aldrich
Permount	#SP15-500	Thermofischer Scientific
Neutral buffered Formalin Solution (10%)	#HT501128	Sigma-Aldrich
Triton X-100	#X100	Sigma-Aldrich
Vectashield	#H 1200	Vector Laboratories
Equipment		
Canon Legria HFR706 Video Camera	#1238C050	Canon
Epson V550 scanner	#B11B210201	Epson
Grant GLS400 Waterbath	-	Grant Instruments

Heated Ultrasonic Cleaning Bath	#FB15046	ThermoFisher Scientific
Heidolph MR 3001 K Hot Plate	-	Sigma-Aldrich
Leica CM 1900UV Cryostat	-	Laboratory Instruments & Supplies
LSR II Flow Cytometer	-	BD
MACS MiniMACS Separator	#130-042-102	Miltenyi Biotec
MACS QuadroMACS Separator	#130-090-976	Miltenyi Biotec
Mars Safety Class 2 Biosafety Cabinet	-	Scanlaf
New Brunswick Galaxy 48R Incubator	-	Mason Technology
Olympus BX51 Microscope	-	Olympus
Precisa XT 120A Weigh Balance	-	Precisa
Rotanta 460R Centrifuge	-	Hettich
Vortex Genie 2	50728002	ThermoFisher Scientific
Software		
FlowJo v10	-	FlowJo LLC
ImageJ	-	National Institutes of Health
GraphPad Prism 8.0	-	GraphPad